DISS. ETH NO. 27496

Identification of Redirected Walking Thresholds in Immersive Virtual Environments

A thesis submitted to attain the degree of

DOCTOR OF SCIENCES of ETH Zurich

(Dr. sc. ETH Zurich)

presented by

ANH NGUYEN

MSc, University of Genova

born on 04.11.1986

from Ho Chi Minh City, Vietnam

accepted on the recommendation of

Prof. Dr. Konrad Wegener, examiner
Prof Dr. Andreas Kunz, co-examiner
Prof. Dr. Peter Brugger, co-examiner

2021

Abstract

Performing real walking in a virtual environment has been consistently shown to invoke a strong sense of presence and allow better way-finding and distance estimation. The biggest problem with real walking in virtual reality is that the virtual environment is most of the time much larger than the available physical space. One possible solution is called *redirected walking* (RDW), where a mismatch between the real and virtual trajectories is introduced. The mismatch could be in terms of linear velocity, angular velocity and heading direction. The focus of this work is on the mismatch in heading direction (also called curvature gain), in which users walk on a different curvature in the virtual environment than in real life.

There is a limit to how much curvature gain can be applied without users noticing it, so-called thresholds. The first part of this work focuses on establishing a threshold identification procedure that is more efficient than the currently widely used one. This proposed procedure consists of an adaptive Bayes method, in conjunction with a true two-alternative forced choice task. Using this procedure, an experiment was conducted to identify their individual thresholds. Results showed that curvature gain thresholds span a wide range, indicating a need for personalized thresholds. Results also showed that men are on average more sensitive to curvature gain than women.

The next part of this work is dedicated to further improving the threshold identification procedure. Relying on the fact that RDW works due to the dominance of the visual sense over other senses, the correlation between curvature gain thresholds and performance in different visual dominance tests was investigated. The selected visual dominance tests were rod-and-frame, sway, vection and blind walking. Results showed that the performance in the rod-and-frame test could be used to partially predict an individual's curvature gain threshold.

RDW is not only perceived differently by individuals, but also in different external conditions. Experiments were conducted to investigate the effect of speed, environment size, feeling of presence and cognitive load on curvature gain thresholds. Using a rhythm to regulate walking speed, a significant impact of speed on thresholds was found. Specifically, users are more sensitive to curvature gain when they walk faster. No significant impact of the environment size (2m wide corridor vs. 10m wide room) was found. It has also been found that there is a negative correlation between the feeling of presence and curvature gain thresholds: users tend to detect redirection better when they have stronger feeling of presence and control over their virtual representation. While users were under the cognitive load of performing a secondary task (seven subtraction task), thresholds were significantly higher.

A new technique to improve RDW was also introduced: a discrete rotation is applied every time users blink. Results show that while a scene can only be rotated 2.4 degrees when eyes are open, it can be rotated significantly more during blinks (9.1 degrees). A computer simulation was carried out in order to investigate if blink redirection technique could be combined with existing RDW techniques to improve redirection efficiency. Simulation results showed that in a sufficiently large tracking space and high enough blink frequency, the reset count and the minimum space requirement for walking without encountering a stop could be significantly reduced by up to 29%.

Finally, in order to improve path prediction accuracy for RDW algorithms, the last part of the thesis explored if humans have a tendency to alternate their walking direction in a maze-like environment, so-called *spontaneous alternation behavior* (SAB). It was found that the probability of a user switching their turning direction is 72%, and 90% if the previous two turns were in the same direction. When users had to perform a secondary task, the alternation rate still remains significantly higher than 50%. A last series of experiments were conducted to investigate whether applying curvature redirection has an effect on SAB rate in a T-maze. In the first scenario, the T-maze is visually curved but curvature gain is applied in the opposite direction such that users ended up walking straight. In the second scenario, the T-maze is visually straight but a curvature gain is applied such that users ended up walking on a curve. Results showed that there is no significant difference in alternation rate in both scenarios.

Zusammenfassung

Grundsätzlich hilft reales Gehen, um sich in einer virtuellen Umgebung zurechtzufinden. Es ruft ein starkes Präsenzgefühl hervor und ermöglicht eine bessere Orientierung und Entfernungsabschätzung in der virtuellen Umgebung. Das grösste Problem beim realen Gehen in der virtuellen Realität besteht darin, dass die virtuelle Umgebung meist viel grösser ist als der verfügbare physische Raum. Eine mögliche Lösung ist das sogenannte *Redirected Walking* (RDW), bei dem gezielt Diskrepanzen zwischen dem realen und virtuellen Laufpfad erzeugt werden. Die Parameter, die dafür manipuliert werden können, sind die Lineargeschwindigkeit, die Drehgeschwindigkeit und die Bewegungsrichtung. Der Schwerpunkt dieser Arbeit liegt auf der Manipulation der Bewegungsrichtung (auch Krümmungsverstärkung genannt), bei der eine Person in der virtuellen Umgebung auf einem anders gekrümmten Pfad läuft als in der Realität.

Die Grenze, ab der ein Anwender die Manipulation bemerkt, ist der Schwellenwert. Der erste Teil dieser Arbeit konzentriert sich auf die Ermittlung eines Verfahrens zur Bestimmung von Schwellenwerten, das effizienter ist als dasjenige, das aktuell am verbreitetsten ist. Das neue Verfahren besteht aus einer adaptiven Bayes-Methode in Verbindung mit einer erzwungenen "ja/nein"-Enschredung (two-alternative forced choice). Mit diesem Verfahren erfolgte ein Experiment, um individuelle Schwellenwerte zu identifizieren. Die gemessenen Schwellenwerte weisen eine breite Streuung auf, was den Bedarf an personalisierten Schwellenwerten erkennen lässt. Die Ergebnisse zeigen auch, dass Männer im Durchschnitt empfindlicher auf die Krümmungsverstärkung reagieren als Frauen.

Der nächste Teil der Arbeit befasst sich mit der Verbesserung der Verfahren, um Schwellwerte zu bestimmen. RDW funktioniert, weil der visuelle Sinn andere Sinne dominiert. Darauf aufbauend wurden Zusammenhänge zwischen Krümmungsverstärkung und visueller Dominanz untersucht. Die ausgewählten visuellen Dominanztests waren Stab-Rahmen-, Body-Sway-, Vektion- und Blind-Walking-Test. Die Ergebnisse zeigen, dass die Leistung im Stab-Rahmen-Test mit der Krümmungsverstärkungsschwelle einer Person korreliert.

RDW wird nicht nur individuell, sondern auch unter verschiedenen äusseren Bedingungen unterschiedlich wahrgenommen. Der Einfluss von Geschwindigkeit, Umgebungsgrösse, Präsenzgefühl und kognitiver Belastung auf die Krümmungsverstärkungsschwelle wurde experimentell untersucht. Wenn die Gehgeschwindigkeit durch einen Rhythmus reguliert wird, zeigt sich ein signifikanter Einfluss der Geschwindigkeit auf die Schwellenwerte. Insbesondere reagieren Testpersonen empfindlicher auf Krümmungsverstärkungen, wenn sie schneller gehen. Frühere Hinweise, dass die Umgebungsgrösse (2 m breiter Ko-

rridor gegenüber 10 m breitem Raum) einen Einfluss auf die Schwellenwerte für die Krümmungsverstärkung haben könn-te, bestätigten sich nicht. Es zeigte sich auch eine negative Korrelation zwischen dem Präsenzgefühl und den Schwellenwerten für die Krümmungsverstärkung. Mit anderen Worten, Testpersonen erkennen die Umleitung tendenziell besser, wenn sie ein stärkeres Präsenzgefühl und eine bessere Kontrolle über die Bewegungen ihrer virtuellen Gestalt haben. Bei allen Experimenten zum Schwellenwert der Krümmungsverstärkung mussten Testpersonen nur eine Aufgabe zur Erkennung von RDW ausführen. Wenn sich die Anwender in einem realistischen Szenario befinden, fokussieren sie sich aber nicht auf die Krümmungsverstärkung. Um diesen Effekt zu simulieren, mussten die Testpersonen während ihres Gehens sieben Subtraktionsaufgaben lösen. Dabei waren die Schwellenwerte signifikant höher, wenn die Testperson eine Subtraktion ausführte.

Im Weiteren wurde das RDW mit einer neuen Technik verbessert: Jedes Mal, wenn eine Testperson blinzelt, wird eine kleine, nicht wahrnehmbare Rotation durchgeführt. Das Experiment zeigte, dass eine Szene bei geöffneten Augen um 2.4 Grad gedreht werden kann, während des Blinzelns jedoch um signifikant höhere 9.1 Grad. Mit einer Computersimulation wurde untersucht, ob mit der Blinzel-Umleitungstechnik die Effizienz von bewährten RDW-Techniken verbessert werden kann. Die Simulationsergebnisse zeigen, dass die Anzahl Notstopps mit anschliessender Richtungsänderung und der minimale Platzbedarf für das Gehen ohne Stopp durch die Kombination beider Techniken um bis zu 29% reduziert werden konnten.

Um die Genauigkeit der Pfadvorhersage für RDW-Algorithmen zu verbessern, wurde im letzten Teil der Arbeit untersucht, ob Menschen die Tendenz haben, ihre Laufrichtung in einer labyrinthartigen Umgebung zu alternieren, das so genannte *spontaneous alternation behavior* (SAB). Das Experiment ergab eine Wahrscheinlichkeit von 72%, dass eine Testperson ihre Drehrichtung beim zweiten Richtungsentscheid ändert, und beim dritten sogar eine von 90%, wenn die beiden vorhergehenden Drehungen in die gleiche Richtung erfolgten. Wenn Testpersonen gleichzeitig eine sekundäre Aufgabe zu erledigen hatten, bleibt die Wechselrate immer noch deutlich höher als 50%. Mit einer weiteren Experimentierreihe wurde untersucht, ob sich die Krümmungsverstärkung auf die SAB-Rate in einem T-Labyrinth auswirkt. Im ersten Szenario ist das T-Labyrinth visuell gekrümmt und die Krümmungsverstärkung erfolgt in die entgegengesetzte Richtung, so dass die Testperson gerade geht. Beim zweiten Szenario ist das T-Labyrinth visuell gerade, mit der Krümmungsverstärkung geht der Anwender entsprechend auf einer Kurve. Die Ergebnisse zeigen, dass es keinen signifikanten Unterschied in der Wechselrate zwischen den beiden Szenarien gibt.

Acknowledgement

First of all, I would like to thank Prof. Konrad Wegener for the opportunity to pursue the doctoral degree at IWF, and the Swiss National Foundation for funding this research.

My sincere gratitude goes to my supervisor, Prof. Andreas Kunz, who has been immensely supportive during and after my time at the ICVR. Moving to Switzerland from Germany and restarting a PhD was difficult, but Prof. Kunz was there to make my transition as smoothly as possible. His door was always open whenever I needed advices, professionally or personally. Living abroad away from my family was tough, but he has always been understanding and accommodating. For that, I am extremely grateful.

I would also like to thank my co-supervisor, Prof. Peter Brugger, for the great collaboration we had. Thank you for the brilliant creative ideas and for the exciting discussions about human behaviors. Your energy and curiosity are an inspiration to me.

I would like to thank Prof. Bigna Lenggenhager for the helpful feedback on all of our study designs and analyses, and particularly the expert knowledge on the sense of agency.

I also enjoyed the short, but successful collaboration with Lukas Imbach and Evdokia Efthymiou. I had a great experience working with them, and had learned a lot from them about sleepwalkers.

I am grateful to Yannick Rothacher for being a great project partner. We had an amazing working relationship, great communication, and his knowledge of study designs and statistics has been essential for the success of our experiments.

I would like to thank my first colleagues at the ICVR, Markus Zank and Ali Alavi for the amazing time we had together, inside and outside the office. I do miss the stimulating discussions we had during lunch and in Bqm. I would like to thank Christian Hirt for the fun conference trips we had. I also enjoyed the random discussions in the LEE L kitchen with many other colleagues outside of ICVR.

I would like to specially thank my grandparents, my aunts and uncles, my parents, and my brother's family for their constant support and encouragement. I am extremely grateful to Myrta and Paul Etter-Haltiner for helping us out in any way they could so that I could meet a paper deadline or focus on writing my thesis. Myrta also helped nicely translating the abstract to German. Finally, I would like to thank my partner Thomas Etter for always being there when I needed a listening ear, for enduring my stress and frustration, and most important of all, for believing in me.

Contents

Abbreviations

1PP   First Person Perspective

2AFC   Two-Alternative Forced Choice

3PP   Third Person Perspective

CAVE   Cave Automatic Virtual Environment

CI   Confidence Interval

CSM   Constant Stimuli Method

DOF   Degree-of-Freedom

HMD   Head-Mounted Display

IMU   Inertial Measurement Unit

MPC   Model Predictive Control

RDW   Redirected Walking

RDT   Redirected Walking Threshold

RNG   Random Number Generation

S2C   Steer-To-Center

S2O   Steer-To-Orbit

SAB   Spontaneous Alternation Behavior

SD   Standard Deviation

SSA   Somatosensory Amplification

SSQ   Simulator Sickness Questionnaire

VE   Virtual Environment

VR   Virtual Reality

<div style="text-align: right; font-size: 4em; font-weight: bold;">1</div>

Introduction

"What is real? How do you define 'real'? If you're talking about what you can feel, what you can smell, what you can taste and see, then 'real' is simply electrical signals interpreted by your brain." - The Matrix (1999) [267]. The idea of constructing a VR is to provide users with the feeling of being there, so-called the feeling of presence, in a responsive virtual world through visual, audio, haptic, or even olfactory interactions. As early as 1950, a device called Sensorama (Figure 1.1) was invented with stereo speakers, a stereoscopic 3D display, fans, smell generators and a vibrating chair with the intention to fully immerse users in the film [107]. While full immersion was achieved, the experience was purely passive, which means there is no motion tracking or interactions, and inputs from the users have no control over the content. In 1968, Ivan Sutherland created the first VR Head-Mounted Display (HMD) with motion tracking using a mechanical system suspended from the ceiling, hence the name Sword of Damocles (Figure 1.2). The system, despite being too cumbersome for users to wear comfortably, has paved the way for today's VR technology.

Virtual reality display technologies today can be broadly divided into two categories: large projection systems and HMDs. Large projection systems consist of a number a projection screens arranged in different configurations such as Cave Automatic Virtual Environment (Figure 1.3) or panoramic displays [50]. Even though these systems provide a wide surrounding field of view and can accommodate a small group of users simultaneously, they are very space inefficient and above all extremely costly. On the other hand, HMDs, with their affordable price, steadily increasing screen resolution, field of view and frame rate, have become the most popular VR display type in both industry and VR research. Virtual reality HMDs nowadays are adopted in many fields such as military training, medical training, architecture exploration, rehabilitation, education, factory planning and simulation, etc. For many of these applications, the most important way of interaction is to be able to navigate in the virtual environment. Various solutions exist for navigation in VR. One classical solution is to use metaphors such as driving a car or flying a plane. With the additional use of haptic devices such as driving or flight simulators, the immersive experience of moving through a virtual environment in a vehicle could be considered a solved problem. Nevertheless, driving or flight simulators are most of the time about training the specific task itself rather than exploring the virtual environment outside of the vehicle. To enable users to explore a virtual environment without using a vehicle metaphor but rather being there "in person", a number of approaches can be used: hand-held input devices, walking-in-place interfaces, or real walking. In this chapter, these aforementioned methods of performing locomotion in a virtual environment will be discussed in details, with a focus on the real walking method, the challenges of implementing real walking

Figure 1.1: *Sensorama: an immersive theater experience*

Source: https://www.vrs.org.uk/virtual-reality/history.html
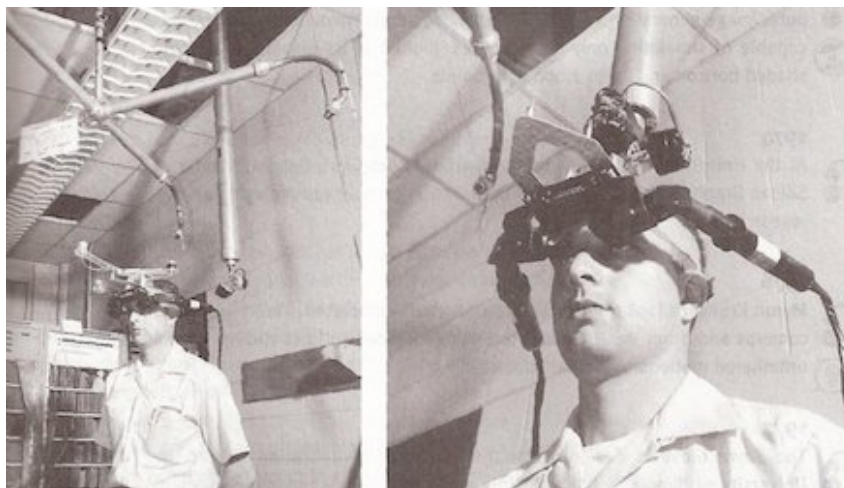
Figure 1.2: *Sword of Damocles: the first VR HMD*

Source: https://www.vrs.org.uk/virtual-reality/history.html

and some existing solutions. Finally, the chapter concludes with the identified research gaps, which will be the main discussion point through out this thesis.

1.1 Locomotion in VR

Before discussing the different locomotion techniques in VR, it is important to first understand which criteria can be used to judge a technique. Generally, locomotion is not a goal itself, but rather a means to perform a specific task in the virtual environment. These tasks can be of three types: exploration, searching, and maneuvering [212]. Exploration tasks require users to roam around the virtual environment often without any explicit goal, but rather to gather information and understand the space and objects in the environment. Searching tasks require users to locate particular objects in the environment, usually without knowing the location of these objects in advance. Finally, maneuvering tasks (for example: walking on a ledge) require small and precise movements. Taking these tasks into account, a locomotion
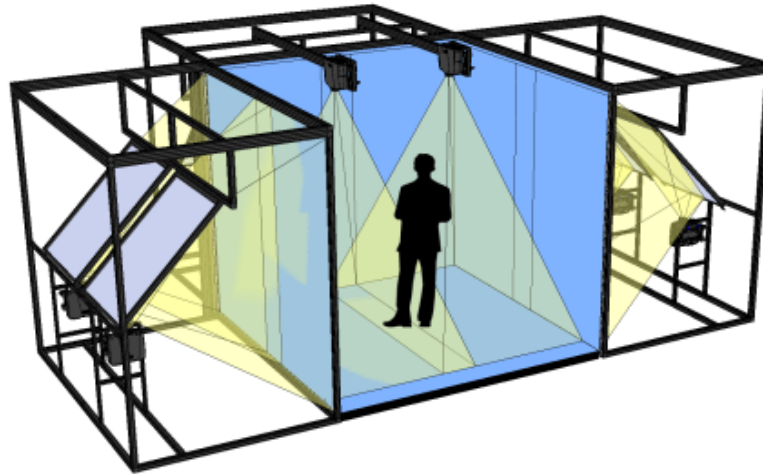
Figure 1.3: *CAVE immersive 3D display*

Source: http://www.visbox.com/products/cave/viscube-c4-t2/

technique should be considered based on the following criteria: how well it aids users in obtaining spatial knowledge (i.e. understanding their position and orientation in space), how fast and accurate users can perform their movement, how comfortable users feel when using the technique over a prolonged period of time (in terms of motion sickness), and most importantly, how much these techniques influence users' feeling of presence in VR.

1.1.1 Hand-held Input Devices

Performing locomotion in a computer-generated virtual environment is not a new topic, particularly in the gaming industry. On a desktop set-up, by simply using common input devices such as the mouse for defining a heading direction, and keyboard for translation (or equivalently on a gamepad), experienced gamers can navigate around a virtual environment and obtain spatial information quite efficiently. However, with an HMD setup, using the mouse and keyboard to control 6-DOF movement can cause significant motion sickness. Therefore, at the current state, most VR set-ups that use common input devices adopt a hybrid solution where rotation is controlled by users' tracked HMD movement, and translation/relocation is performed using a hand-held controller. The simplest technique to achieve relocation in a virtual environment is to use designated controls on the hand-held controller to go forward, backward, and sidewards relative to the heading direction. This way, the user's point of view is "sliding" continuously through the virtual environment. Other techniques that produce similar user movement are route planning, where users select waypoints from an overview map and a continuous path that passes through these points are calculated [25], or LaserGrab, where users select a fixed virtual object and choose how close to that object they want to be through the extension of their arm [289]. Even though less severe, these techniques still suffer the same drawbacks as the full 6-DOF mouse and keyboard control, since too much virtual translational motion without real motion also cause discomfort and motion sickness [149]. To overcome this problem, the user's point of view could be instantaneously moved when a desired position is indicated using a hand-held controller; this navigation technique is called teleport. Teleport has been shown to be much preferred over "sliding", and is one of the most used navigation techniques for room-scale VR nowadays [149]. Even though teleport technique offers considerable advantages in terms

of physical space requirement - users need minimal real space in order to travel infinitely in virtual space and movement speed - users can move around really fast as teleport happens instantaneously regardless of the travel distance, it has been shown that compared to real walking, users using teleport technique do not acquire as good spatial knowledge, and experience lower sense of presence [149, 41].

1.1.2 Walking-in-place

For techniques that use hand-held input devices described in 1.1.1, no body movement (arm swing, stepping) or body displacement in reality is required to initiate movement in VR, resulting in low sense of presence, and in some cases motion sickness. With the aim of improving the matching between body movement in reality and VR, various walking-in-place techniques were created. The simplest form of this type of technique is literally walking-in-place, where users' body parts are tracked and as they step on the spot, movement in VR is performed. Stepping forward, sidewards and backward is controlled using leg movement, speed is controlled using stepping speed and rotation is controlled using torso orientation [248] (Figure 1.4). This approach is quite straightforward to implement, however, since users are only stepping, there is no feedback from the floor for forward movement and therefore does not really provide the sensation of displacement in space. To obtain this forward movement feedback, existing devices that simulate walking such as linear treadmills were the first to be adopted. Despite being simple and readily available, linear treadmills are only one dimensional and do not solve problems such as side stepping, or changing direction. Other solutions, so-called omni-directional treadmills, were created to overcome these limitations. These treadmills can be active, which means they detect users' walking motion and move to negate them such as Torus treadmill [125] (Figure 1.5a), CyberWalk - an improved version of the Torus treadmill [226]; or passive, which means they require users to drive the devices such as VirtuSphere (Figure 1.5b). While these treadmills partially solve the matched body movement problem, walking fast and turning using these devices are still very unnatural and difficult tasks for users [53] [169] [175]. Other more affordable solutions are low friction surfaces such as the Cyberith Virtualizer (Figure 1.6a), where users are required to wear special slippery shoes/socks that allow their feet to slide on the surface. Turning and walking fast on these low friction surfaces is possible, yet the motion is not natural at all. Finally, there are also step-based devices that theoretically allow real, unlimited omni-directional walking. One such device is the CirculaFloor, which consists of floor tiles that move around and re-center the users as they walk, thus keeping the users within certain area of the tracking space (Figure 1.6b). It also allows simulating walking up and down the stairs. As promising as it sounds, the CircularFloor only works if users walk really slowly, therefore unnaturally, and also poses safety concerns in case of mechanical or software failures.

1.1.3 Real Walking

Up to now, no other navigation techniques have been able to compete with real walking in terms of feeling of presence [259, 277]. Users performing real walking are also much better at way finding and distance estimation [200, 220]. The performance in these tasks are especially important for many applications such as architectural exploration, factory planning, military training, education, etc. However, the problem with real walking is that, in these applications, the virtual environment is most of the time much larger than the available tracking space. One approach to tackle this problem is called **flexible spaces** technique [262]. This technique works for a virtual environment that consist of rooms that connect to each other by corridors. In order to fit the larger virtual environment into a smaller physical spaces, virtual rooms that are seemingly next to each other actually overlap. Since the user only sees one room at a time, the room rearrangement can be done while users are in the corridor traveling be-

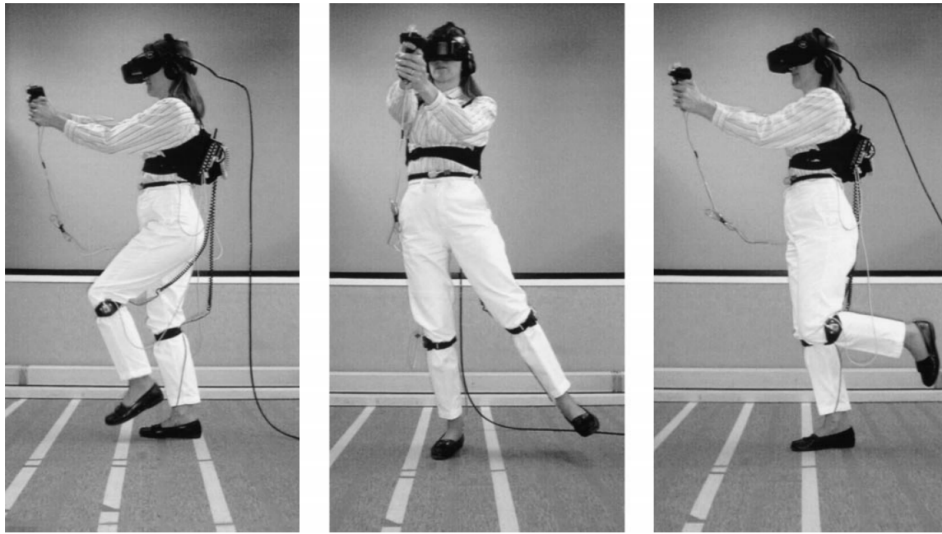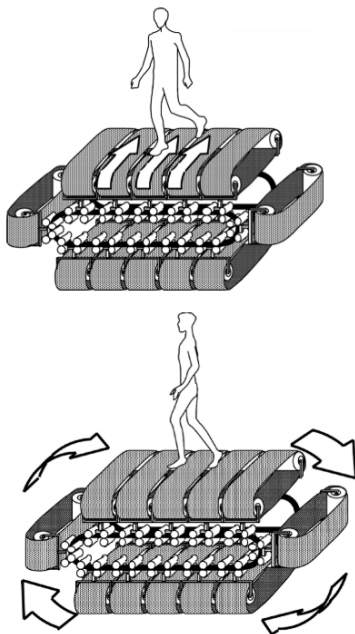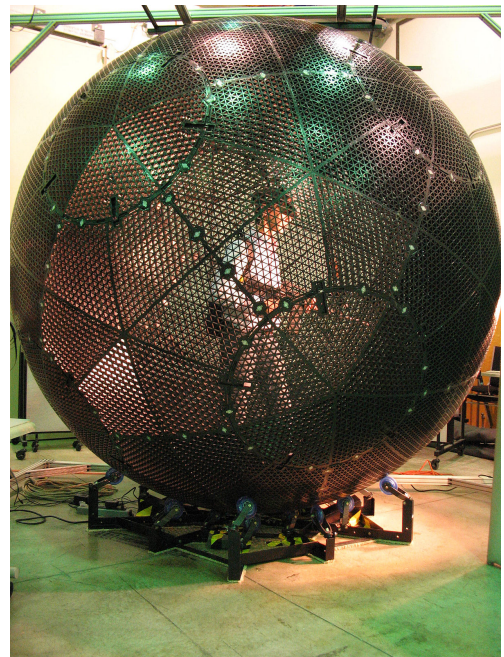**Figure 1.4:** *Stepping in place gesture to move forward, sidewards, and backward in VR [248]. ©1999 IEEE*
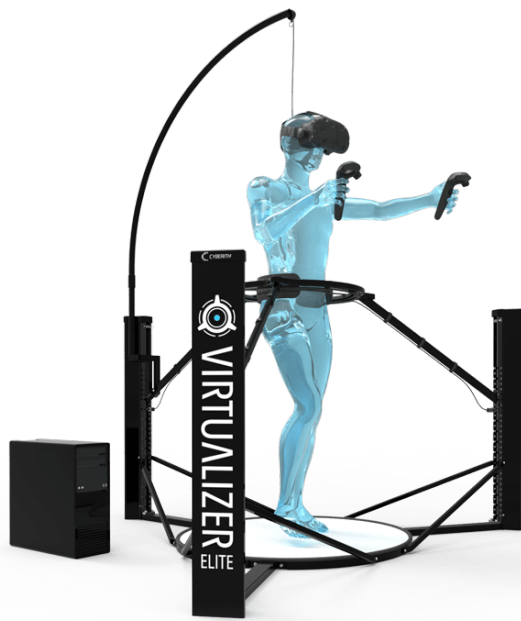

(a) *Torus omni-directional treadmill: (a) user moving in the X direction (b) user moving in the Y direction [226]. ©1999 IEEE*
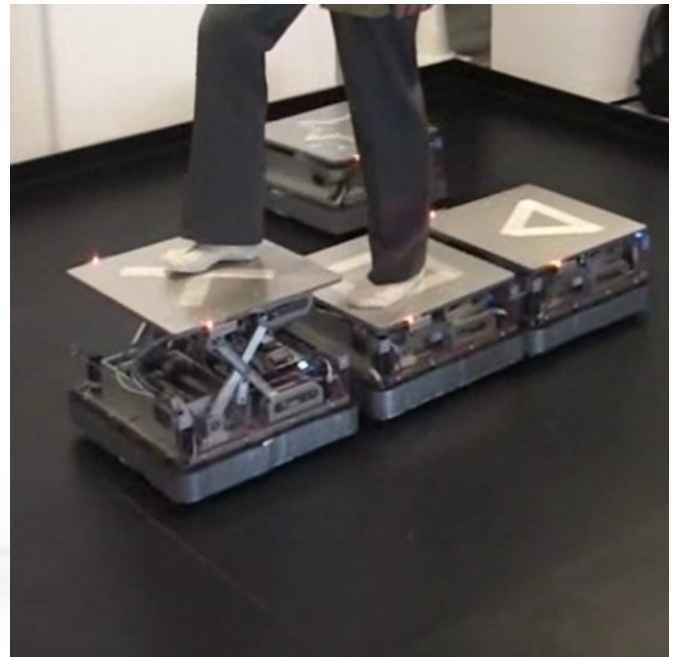

(b) *VirtuSphere - the human "hamster ball" by Paul Monday, licensed under CC BY-SA 4.0*

Figure 1.5: *Active and passive omni-directional treadmills*

(a) Cyberith Virtualizer - an omni-directional treadmill using low-friction surfaces

Source: https://www.cyberith.com/entertainment/

(b) CirculaFloor - robotic floor tiles that shift their positions to keep the users in the center

Source: https://www.youtube.com/watch?v=rYsvB2y2Ero

Figure 1.6: *Low-friction surface and step-based devices*

tween rooms (Figure 1.7). Another approach that is somewhat similar to the flexible spaces approach is called **change blindness**. This approach works based on a perceptual phenomenon that people could miss a major change to the scene when they do not expect it to change. This change could be a small object displacement in the scene, but could be as large as an appearance or disappearance of an object [207]. For example, a change in the scene such as the relocation of a door or an exit behind a user's back could go unnoticed and consequently lead the user to explore a more favorable part of the tracking space [240] (Figure 1.8). However, this approach, together with the flexible spaces approach, share the same drawback that they require the environment to consists of a room-like virtual environment, and they will not work with a generic virtual environment. Another solution to the limited space problem is to warp the larger environment to fit it into a smaller tracking space [242]. Using this approach, the appearance of the virtual environment is noticeably different from the original construct, which potentially leads to misunderstanding spatial information.

For more generic virtual environments, and for keeping the visual appearance of the virtual environment intact, a fourth approach could be applied. This approach is called **redirected walking** (RDW) [206]. Instead of changing the structure of the environment, this approach focuses on manipulating the mapping between the virtual trajectory and the physical trajectory of the user. Since the user's field of view is completely covered by the HMD and therefore visual information comes solely from the virtual environment, it is possible to achieve the manipulation by providing users with conflicting visual and other sensory information. A few examples of RDW techniques are: to continuously rotate the user's point of view as he/she is walking such that he/she will correct for it by walking on a curve - **curvature gain**; to continuously rotate the user's point of view as he/she is rotating such that he/she rotate less or more in reality than in VR - **rotational gain**; or to continuously slow down or speed up the user's point of view as he/she is walking such that he walks faster or slower in reality than in VR - **translational gain**. When

applied within certain thresholds, the manipulation is not noticeable to the users and immersion remains intact. Various research groups have attempted to quantify these thresholds. Steinicke et al. performed a number of comprehensive studies to identify the thresholds of RDW gains (rotational, translational, curvature) and the obtained result has been used in many RDW implementations later [237]. Gerald et al. performed a similar set of experiments as Steinicke et al. and found that while rotational gain and translational gain thresholds approximate the results from Steinicke, there is profound difference in the curvature gain threshold, and discussed that it could be due to a different VR setup or subject groups [29]. Another interesting finding from Bruder et al.'s experiment is that the thresholds notably differ for the case of walking and driving on the wheelchair. This signifies the fact that human perception is extremely complex and supposedly trivial changes in experiment setups could lead to significantly different results. Neth et al. later found that curvature gain threshold depends on walking velocity, specifically that curvature gain threshold increases at a slower speed [187]. Though not formally computed, it was noticed that the RDW thresholds (RDTs) are reduced in an aisle structured environment compared to a virtual forest [113]. However, no formal study exists that investigates how the structure of a VR environment influences RDTs. In summary, the fact that detection threshold results ranges widely across experiments (probably due to factors such as different experiment set-ups, threshold identification methodologies, users etc.) indicates a gap in understanding how RDW works, how to identify RDTs, and the factors that influence RDW.

Other research groups focused on different approaches to improve RDW. One approach is to invent new RDW techniques such as discrete rotation during saccadic eye movement [21]. Using this technique, the scene is instantaneously rotated around the user as he/she performs a rapid eye movement between fixation points, so-called a saccade. Similar to other RDW gains, when these rotations are within certain thresholds, users do not notice them. Another approach is to investigate the use of other sensory information with the prospect of making the "illusion" more believable. One possibility is to combine haptic cues with visual information. This technique is called **unlimited corridor** where users walk and continuously touch a physical curved wall while curvature gain is applied at the same time [167] (Figure 1.9). This set-up is more of an interesting demonstration and proof-of-concept than a practical solution. Rarely in any application users only keep walking straight infinitely or make only 90-degree turns, instead users tend to change their direction stochastically when exploring a virtual environment. Instead of manipulating visual information, RDW can also be achieved by manipulating audio information. It has been shown that it is possible to guide users to walk on a curved path (while thinking they are walking straight) in a darkened virtual room with a sound source that rotates slowly around the user [227]. Some research effort has also been spent on investigating whether the combination of visual and audio information increases the amount of manipulation that can be applied. Results showed that adding audio information does not seem to increase the detection threshold for redirection compared to visual only [193]. However, there are contradicting results indicating that users can be redirected much more using audio only, as compared to a combination of visual and audio [171]. Other approaches focus on improving existing or developing new RDW algorithms that incorporate users' behavior and knowledge of the virtual and real environment better [285], apply existing RDW techniques more efficiently [182], or expand the application of RDW in atypical tracking spaces and for more than one user [9, 249]. Even though commercial off-the-shelf VR systems nowadays can offer from 4m x 4m up to 10m x 10m real tracking space, it is still not large enough for users to walk infinitely without any interruption. Naturally, what cannot be solved with little space can simply be solved with more space [6]. Nevertheless, large empty spaces are generally not available for most research groups and common households. Therefore, constant effort still needs to be made to improve RDW in order to reach the goal of uninterrupted, infinite real walking in a reasonably small tracking space.
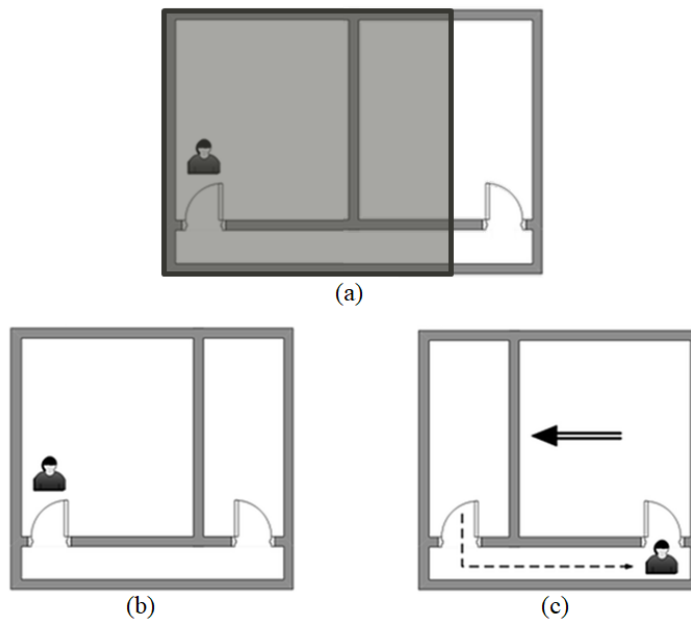
Figure 1.7: *Flexible spaces technique. Reprinted with permission from Springer: Springer Nature [263] ©2015*

(a) Overlay of the real and virtual environments. The real environment (shaded in grey) is smaller than the virtual environment (non-shaded). (b) The user first starts in the room on the left. Once he/she leaves this room and is in the corridor, the appearance of the second room changes. (c) The second room is now seen in full size. If the length of the corridor long enough, the user will not notice that the rooms actually overlap.
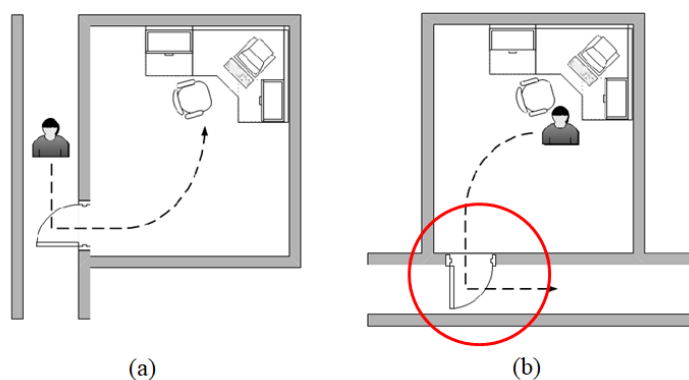
Figure 1.8: *Change blindness technique. Reprinted with permission from Springer: Springer Nature [263] ©2015*

(a) A user comes into the room through the door here on the left (b) Once the user turns away from the door, the position of the door is changed, so he/she walks out of the room through another door without noticing it.

(a)

(b)
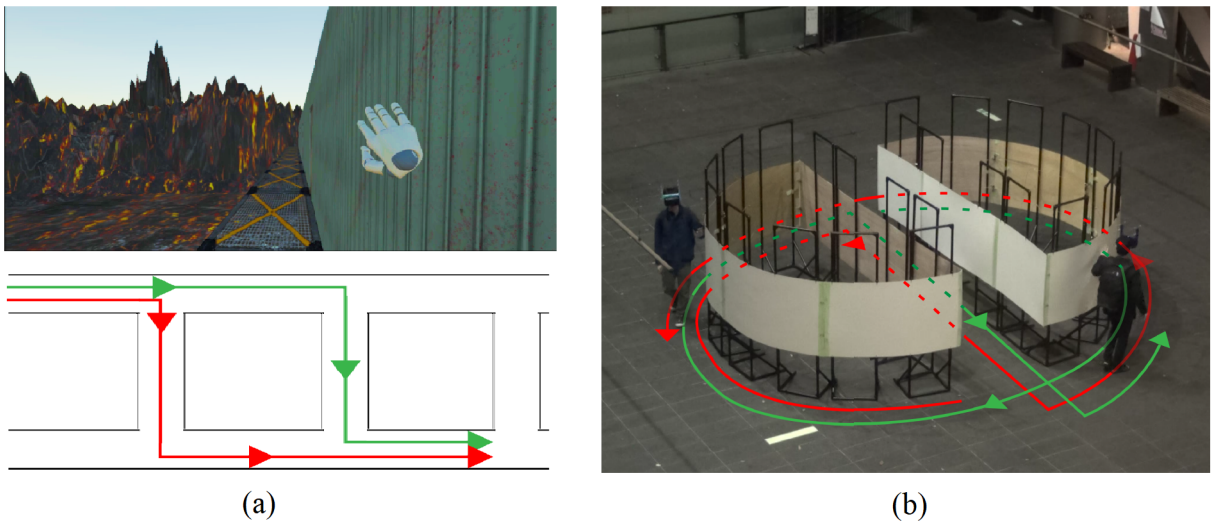
Figure 1.9: *Unlimited corridor technique*

(a) Users' view in VR and their paths (b) Users' paths in reality [167] ©2016 ACM

2

Related Work

2.1 Human Perception during Redirected Walking

During walking, the human brain continuously processes information from different sensory channels such as visual, vestibular and proprioception to estimate where the body is in the world. In order to understand how redirected walking works from the psychological point of view, it is first necessary to understand how these sensory channels work, and how the integration of these different modalities is achieved, especially when they are conflicting with each other.

2.1.1 Visual cues

The movement direction and velocity of the body during walking can be estimated by the movement of features or objects in the scene across the retina, so-called **optical flow** [151]. Each feature's movement in the scene is represented by a movement vector, and the compilation of all movement vectors makes up the optical flow field. There are several types of optical flow: rectilineal, radial and circular. In a rectilineal optical flow field, all movement vectors are parallel and have the same magnitude. This is the result of turning the head around the vertical axis or stepping sidewards (Figure 2.1a). In a radial optical flow field, the vectors radiate from the same point that is called an expansion point. The further from the expansion point a feature is, the larger its movement vector. This optical flow is the result of a forward movement, and the expansion point indicates the heading of the movement (Figure 2.1b). In a circular optical flow field, the movement vectors are tangent to circles of the same center point. The further from the center point a feature is, the larger its movement vector. Tilting the head around the forward axis produces this optical flow (Figure 2.1c). Visual cues are useful for estimating the body's movement in space when the scene has feature points that create a rich enough optical flow [120]. Contrarily, when the scene has no objects or features at all, the body has to rely on other cues.

2.1.2 Vestibular cues

Together with the visual system, the vestibular system contributes to maintaining balance and provides information about the body's orientation in space. The vestibular system consists of two main compo-

(a) Translation optical flow   *(b) Radial optical flow*   *(c) Circular optical flow*
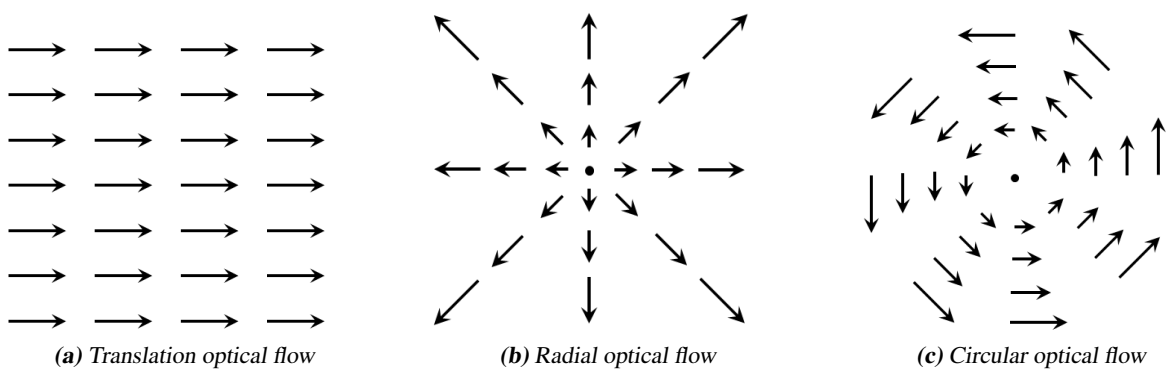
Figure 2.1: *Different types of optical flow*
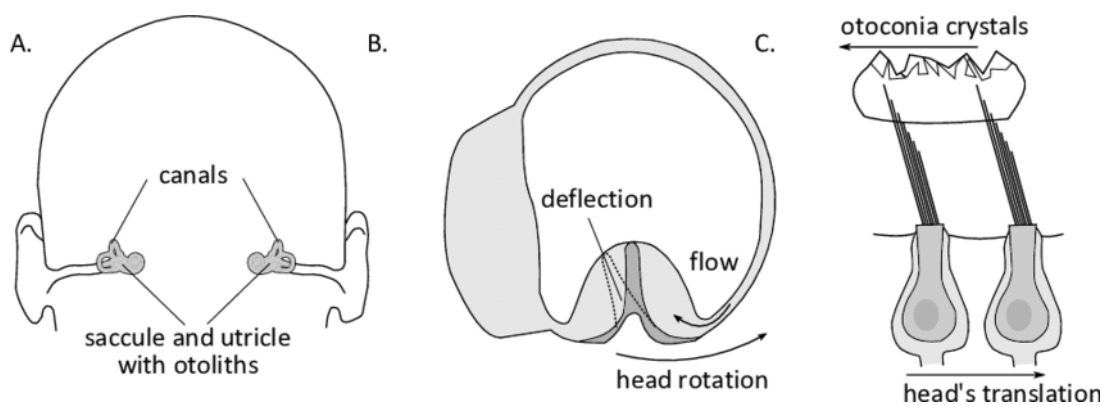
Figure 2.2: *The vestibular system*

Reprinted by permission from Springer: Springer Nature [266] ©2019

nents: the **semicircular canals** and the **otolith organs**. The semicircular canals, as the name implies, are made up of three semicircular canals that are oriented orthogonal to each other and sense rotary acceleration/deceleration in three dimensions: turning the head around the vertical axis, tilting the head to the sides, or tilting the head up and down. Each semicircular canal is filled with a liquid called endolymph, and consists of an enlarged section (the ampula), a thick gelatinous cap (the cupula), within which are many hair cells reside. Whenever the head changes the orientation, the endolymph lags behind due to inertia and pushes the cupula to the same direction as the movement. This in turn stimulates the hair cells to send signals to the central nervous system to indicate that an acceleration has occurred (Figure 2.2). On the other hand, the otolith organs are in charge of sensing linear acceleration/deceleration and gravitational orientation. The otolith organs consist of the utricle and saccule which detect linear movement in the horizontal and vertical planes respectively. The utricle and saccule have similar construct, each consists of hair cells and protein-calcium carbonate crystals called otoconia embedded in a gel-like structure (Figure 2.2). When the head moves, the crystals move and displace the hair cells, indicating a linear acceleration. The ocotonia crystals are also responsible for sensing the direction of gravity.

2.1.3 Proprioceptive and haptic cues

Proprioception refers to the sensation of the body position and configuration. Proprioception is achieved through proprioceptors, which are sensors within muscles, tendons and joints that provide the central nervous system with information about limb velocities, load on limbs, joint angles and joint limits. The

simplest way to understand how proprioception works is to imagine closing one's eyes while lifting one's arm to a certain position, or lifting an object. Here, without any visual information, one would still be able to estimate with certain accuracy where the arm is in space, or how heavy the object is. While walking, proprioceptive information together with the sense of touch (so-called haptic cues) in the soles of the feet are important in understanding the body's configuration as well as its relation to the external space [135]. Imagine again while walking with eyes closed, if there is stronger pressure on the outer part of the left sole and the inner part of the right sole, one should be able to tell that they are leaning towards the left, and potentially make corrections for it if they want to walk straight.

2.1.4 Multi-sensory integration

In order to achieve robust and accurate perception during walking, the integration of multiple sensory channels (visual, vestibular, proprioceptive and haptic) is necessary. Information from multiple sensors has been shown to be combined in the central nervous system in a statistically optimal manner. That is, the estimate of the body's position in the world from multiple sensory cues is the weighted linear combination of the estimates from each cue alone, and the weightings are dynamically adjusted based on the reliability of each cue [77, 72, 142]. More specifically, let μ_v and μ_b be the estimate of the current position using only visual cue and only vestibular cue respectively, and σ_v and σ_b be the variance of these estimates. The visual weighting w_v, vestibular weighting w_b, and the combined estimate of the current position μ using both visual and vestibular cues can be calculated as follows:

$$w_v = \frac{1/\sigma_v^2}{1/\sigma_v^2 + 1/\sigma_b^2} \tag{2.1}$$

$$w_b = \frac{1/\sigma_b^2}{1/\sigma_v^2 + 1/\sigma_b^2} \tag{2.2}$$

$$\mu = w_v\mu_v + w_b\mu_b \tag{2.3}$$

For spatial perception tasks such as walking, visual cues are exceptionally more reliable and precise, resulting in extremely high weighting of visual cues, so-called **visual capture** [76, 279]. In other words, during walking, humans rely almost solely on visual cues unless the quality of visual cues changes (e.g. low light condition, low contrast, etc.). To elaborate further, using hypothetical data, Figure 2.3 demonstrates the impact of cue reliability on the final estimate. In Figure 2.3a, if both cues are equally reliable, the combined estimate is the average of the single-cue estimates. However, if the visual cue is much more reliable than the vestibular cue, the combined estimate is extremely close to the estimate using the visual cue alone (Figure 2.3b). Thanks to visual capture, when there are cue conflicts between visual cues and other cues during walking and if the conflicts are small enough, the human brain will decide to believe what they see. Furthermore, how small the conflicts should be without being detected depends on each person's threshold of when to stop trusting their visual cues. This is how redirected walking works.

2.1.5 Standard Perception Tests

In order to detect how much visual cues dominate other sensory cues during multi-sensory integration, a number of perception tests could be performed. The **rod and frame** test, originally developed by Witkin and Asch in the late 1940s [278], requires a subject to align a rod inside a tilted square frame until it is perceived as vertical (Figure 2.4). The point of the test is that, the visual sensation of the tilted frame influences the subject's perception, resulting in the rod deviating from the true vertical. While it

(a) *Equal weights of vestibular and visual cues*

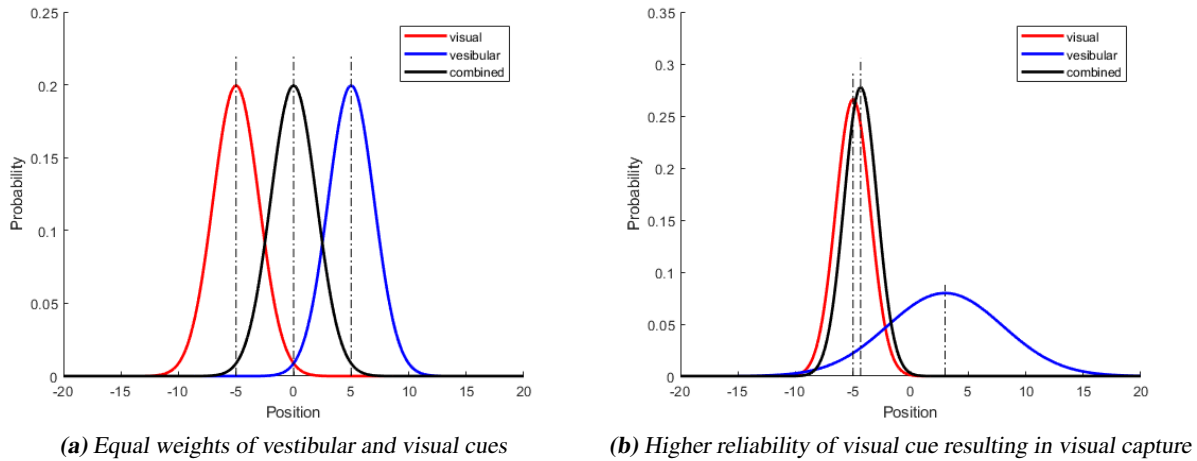**(b)** *Higher reliability of visual cue resulting in visual capture*

Figure 2.3: *Hypothetical data*

was originally created to assess human's sense of space, the rod-and-frame test has become a standard procedure to study interactions between the visual, vestibular and proprioceptive cues [46]. Nowadays, the test is commonly used as a measure of visual dependency, indicating the degree to which a person relies on visual rather than pure postural information to judge the gravitational vertical.

During the visual observation of moving objects, an illusory perception that one's own body is moving, so-called self-motion, could occur, which is called **vection** [100]. One very common occurrence of this phenomenon is when one sits in a stationary train looking out through the window and sees another train moving but for a moment is not able to tell whether one's own train is moving or if it is the other train. This phenomenon happens when there is a conflict between visual and other sensory cues and the visual cues are given more weighting. Depending on the optic flow, vection can be roughly divided into two categories: self-translation and self-rotation. Self-translation, also called linear vection, is similar to the train experience where the optical flow either approaches or precedes and could happen in all three dimensions: left-right, forward-backward, and up-down [255]. Self-rotation could also happen in all three dimensions, but the most convincing illusions occur when the optical flow rotates around the line of sight - roll vection [5] or when the optical flow rotates around a person's vertical axis - circular vection [79] (Figure 2.5). A combination of self-translation and self-rotation also exists, and is called curvilinear vection [255].

Another standard tool that is used in sway analysis and aims at identifying the influence of vision on postural control is called the **Romberg test** [154]. The amount of body sway occurring when a person is trying to stand still reflects their postural stability. Therefore, visual dependency during postural control can be measured by the difference between how much the body sways when the eyes are opened and when the eyes are closed. The ratio of the sway path lengths in the eye opened and eye closed conditions is called the Romberg quotient [216].

Instead of examining how visual dependent a subject is using the aforementioned visual dependency tests, it is possible to also look at how sensitive they are to non-visual cues. High sensitivity to non-visual cues and body awareness may indicate higher non-visual cues weightings. One approach to testing non-visual cues sensitivity is to require subjects to perform certain locomotion tasks with all visual feedback removed. This type of test is called **blind veering test**. Veering refers to the process of deviating from an intended path while walking. Without any visual feedback, it has been shown that humans tend to walk in circle [233]. The blind veering test requires a subject to attempt to walk a straight line without

(a)   *(b)*   *(c)*
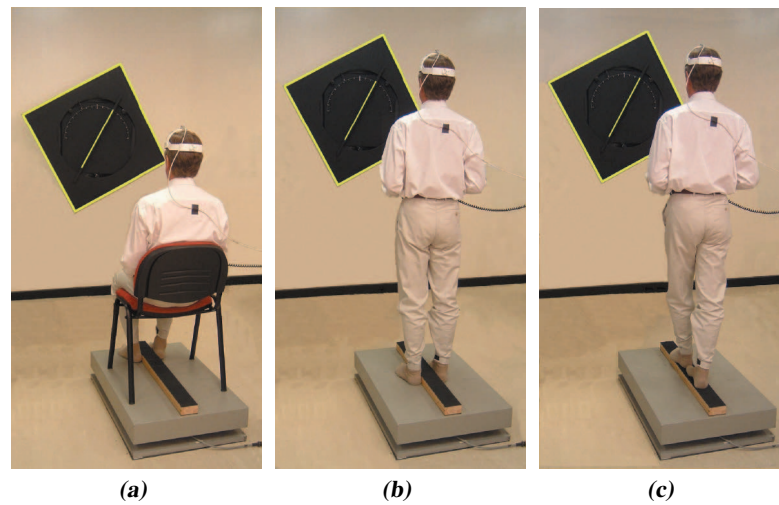
Figure 2.4: *A typical set-up of the rod and frame test: subjects sit (a) or stand (b) looking at a tilted frame and are required to rotate the rod to align it with the gravitational vertical. In this example, an extra condition (c) was added in which the subject is required to stand on a plank where their balance is disturbed. It was shown that while trying to maintain balance, information about one's own orientation is gained, which helps improve their performance in the rod and frame test [26]*

Reprinted with permission from Elsevier [26] ©2004

(a)   *(b)*
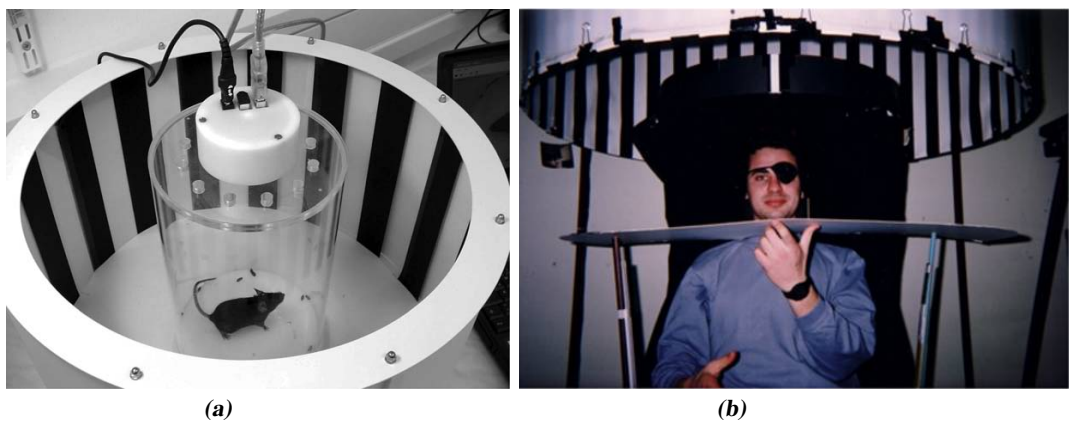
Reprinted with permission from Springer [84] ©2009   *Creative Commons image courtesy of [195] on Frontiers*

Figure 2.5: *Circular vection could be induced by subjecting subjects to a steady optical flow generated by rotating a cylindrical wall with certain patterns. This device is called optokinetic drum, and has been used to study interactions between visual and non-visual cues not only in humans but also in animals such as rats [84] and fishes [222].*
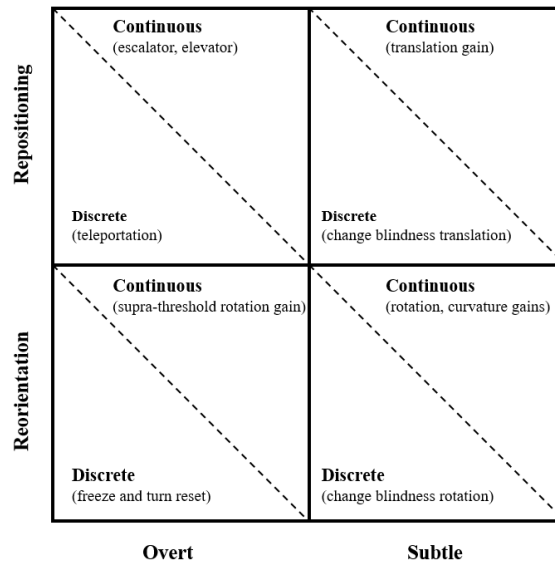
Figure 2.6: *Taxonomy of redirection techniques*

any visual feedback and the lateral deviation from that line is obtained [131].

In contrast to the highly locomotion specific form of body awareness assessed by the blind veering test, a more generic type of body awareness can be measured using **interoception tests**. Interoception describes the perception of the internal state of the body and its visceral organs [90]. The importance of interoception for navigating in virtual environment has been emphasized [247]. Also, a high interoceptive sensitivity has previously been linked to a lower tendency to experience a bodily illusion caused by multi-sensory conflicts [256]. Classically, interoception is measured in cardiac-based tasks. The heartbeat detection task requires a subject to identify whether a series of acoustic signals is synchronous or out-of-sync with their heartbeat.

Finally, sensitivity to non-visual cues can also be subjectively assessed through the use of questionnaires. The **somatosensory amplification** (SSA) scale questionnaire can be used as a qualitative measure to assess a heightened attention to uncomfortable bodily sensations [14].

2.2 Redirected Walking Techniques

In the field of VR research today, redirected walking has a broader meaning than just unnoticeable manipulation, but rather any type of manipulation that distorts the one-to-one mapping between the virtual and real trajectories. Each RDW technique can involve relocation and/or reorientation of a user' point of view, and depending on how it is applied and whether it is noticeable or not, it can be categorized into continuous and discrete, and further divided into overt and subtle [241]. All continuous RDW techniques involve continuously injecting translation and rotation to users' virtual trajectories and discrete RDW techniques refer to the instantaneous relocation or reorientation of users in the virtual environment. A summary of RDW techniques categorization can be seen in Figure 2.6.

2.2.1 Overt Techniques

Overt continuous RDW techniques usually involve the use of metaphors such as seven league boots. Similar to the well known folklore, seven league boots describes a group of techniques where each translational step of the users corresponds to a significantly (and noticeably) larger step in the virtual environment. The simplest implementation of this technique is to linearly scale up users' displacement in all three dimensions: intended heading direction, sidewards swaying and up-down bobbing movement while the user's eye height remains unchanged [273]. However this implementation results in high motion sickness and is not very natural. An improvement to this implementation can be made by simply scaling only the intended direction [119]. Another possible solution to avoid distracting sidewards head movement is to ramp up the highf scale only when user's speed is larger than certain velocity threshold [276]. User's eye height can also be scaled up to mimic a giant exploring a world in miniature [3]. However, it does not improve spatial awareness as compared to unscaled eye height [276]. A combination of one-to-one traveling and scaled traveling can also be applied to maintain navigation and manipulation accuracy within certain part of the virtual environment while enabling fast travel between interactive areas [173]. Overall, the scaling factor can be from a few up to fifty times. Other overt techniques tried to improve the space problem by exploring options in the vertical direction, using metaphors such as virtual escalators or elevators [189, 261]. It has been shown that the elevator metaphor invokes a strong sense of presence and spatial awareness compared to flying or teleporting [261]. Furthermore, overt continuous techniques can also be applied to reorient users by scaling rotational movement. This technique is also called reset [274]. For example, a 180-degree turn in reality could be scaled up to a 360-degree turn in virtual reality. This allows users to face the same direction in virtual reality after the reset even though their current real heading is opposite to their previous real heading. This technique is useful when users end up facing the wall and an automatic reorientation is required without removing the users from the virtual environment.

Overt discrete RDW techniques refers to the instantaneous and perceivable repositioning or reorientation of a user's perspective. The most common overt discrete RDW techniques is teleportation [24]. While users can still walk naturally within a small tracking area, long distance travel could be performed using teleportation [41]. However, since users can perform both natural walking and teleportation, it could happen that after a certain amount of time, they could still end up at the limit of the tracking space. In order to prevent this, an improvement to the classical teleportation technique could be made by using redirected teleporting [161]. During teleportation, redirected teleporting technique also inject a small amount of rotation to the users' current heading, guiding them towards the center of the tracking space. Compared to the classical teleportation technique, redirected teleportation takes more time to complete the same distance. However, more physical tracking space is utitized as users can perform natural walking more often, resulting in higher feeling of presence. Another similar approach to teleportation is by using a metaphor called the jumper metaphor. Here, users can travel through large distance by first indicating a target and then performing a forward jumping motion. A jump animation could be played during the jump to provide optical flow for better spatial awareness [20]. It was found that subjects were equally satisfied with the jumping metaphor and real walking, and found them more preferrable than the classical teleportation. However, subjects were still significantly better in the map drawing task using real walking compared to the other two modes of navigation. The last approach to overt discrete redirection is to use magic metaphors such as portals. Portals were originally used to provide transitions from different locations in the virtual world [83] or from the real world to the virtual world to increase presence [27]. However, portals can also be used to reorient users away from physical boundaries [239]. To achieve this, when users arrive at the physical boundary, they can select a target location and get to that target through a portal. The portal is placed in a way that to walk through it, users have to reorient themselves to a safer part of the tracking space.

In general, overt techniques are quite useful in the sense that they allow users to travel large distances in the virtual environment with much less movement in the physical space. Therefore they do not require a lot of physical space. While some of this techniques can be integrated as a part of the scene, many of these techniques could cause disorientation, discomfort, and potentially motion sickness Furthermore, it has been shown that subtle RDW techniques produce fewer breaks in presence and therefore are generally preferred for a more immersive VR experience [241].

2.2.2 Subtle Techniques

Subtle continuous RDW techniques refer to techniques where translation and/or rotation within certain thresholds are continuously injected into the virtual trajectory such that they are unnoticeable and immersion remains intact [205]. There are three main types of subtle continuous RDW techniques: rotational gain, curvature gain and translational gain [236] (Figure 2.7). Rotational gain g_R is defined as the ratio between the virtual rotation and the real rotation around the yaw axis (the vertical axis) of the user. With a rotational gain larger than one, users rotate faster in the virtual world compared to the real world, and vice versa. Rotational gain is applied when users are rotating on the spot without performing any linear movement. Let ω_v and ω_r be the rotational velocities of a user in virtual reality and in reality, respectively. Rotational gain is calculated as:

$$g_R = \frac{\omega_v}{\omega_r} \tag{2.4}$$

Curvature gain is similar to rotational gain in the sense that rotation around the yaw axis is also injected into users' virtual trajectory but only when users are performing a linear movement. Due to this injected rotation, users subconsciously correct for it by walking on a different curvature in reality compared to the seen curvature in the virtual world. Curvature gain is normally defined as the inverse of the curvature radius that users have to perform in reality such that the virtual trajectory is a straight line. The larger a curvature gain is, the smaller the curvature radius and hence the stronger the manipulation. Curvature gain can be enhanced further by a rotation around the roll axis (the forward axis) of the user to counteract the leaning-in effect of walking on a curve [280]. Let r be the curvature radius of real trajectory, curvature gain g_C is calculated as:

$$g_C = \frac{1}{r} \tag{2.5}$$

Lastly, translational gain is applied during linear movement and is defined as the ratio between virtual travel distance and real travel distance. A translational gain larger than one means users travel faster in the virtual world than in reality, and vice versa. Similar to the seven league boots techniques, sidewards and head bobbing movement during walking need to be taken into account when translational gain is applied in order to ensure subtlety of the technique. One possible method is to calculate the predicted heading direction based on past movement data and apply translational gain only in this direction [224]. In addition to the three aforementioned techniques, there was also effort to create new subtle RDW techniques such as bending gain which is described as the ratio between the seen virtual curvature radius and the performed curvature radius [147]. This technique, however, is not new at all and is only a reformulation of the curvature gain [213]. Moreover, the quantification of bending gains also does not reflect the correct perception of the manipulation because depending on the real curvature radius, the same bending gain value could correspond to different curvature gain values. A formal reformulation of bending gain into an equivalent curvature gain can be found in the Appendix A.5. Additionally, in gaming applications where realistic jumping is a relevant mode of interaction, these subtle RDW techniques can be applied not only during walking but also during jumping to enhance the illusion of jumping further, or higher [106]. Let v_v and v_r be the rotational velocities of a user in virtual reality and in reality,

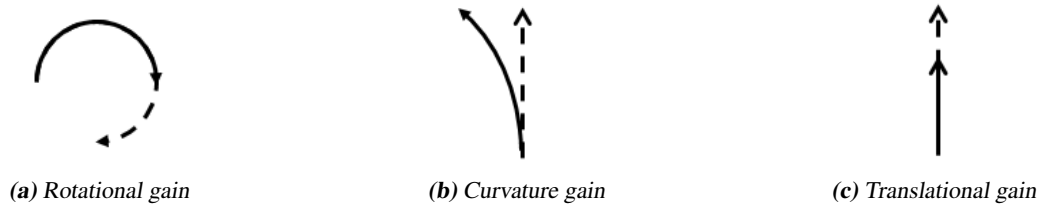*(a) Rotational gain*   *(b) Curvature gain*   *(c) Translational gain*

Figure 2.7: *The three types of continuous RDW techniques. Solid lines represent physical trajectories. Dash lines represent virtual trajectories*

respectively. Translational gain g_T is calculated as:

$$g_T = \frac{v_v}{v_r} \tag{2.6}$$

 While there has been considerable amount of work on subtle continuous RDW techniques, up till now, research on **subtle discrete RDW techniques** has been quite limited. One of the reasons for this is: it is not that easy to apply a sudden jump (rotation or reposition) in the scene without the users noticing it. How can this be made possible? This question can be addressed using the change blindness phenomenon. As previously explained in 1.1.3, change blindness refers to a phenomenon where users do not notice a major change in the environment (appearance, disappearance, or repositioning of one or multiple objects) when these changes happen behind them. The same phenomenon can actually emerge right in front of users' eyes when there is a disruption in the visual input. This is called **visual suppression**, that is, the brain suppresses any change during a interruption of the visual input with the assumption that the surrounding world is stable. Fortunately, this interruption happens very often in humans through saccadic eye movement (fast eye movement between fixation points) and blinking. Profiting from this phenomenon, the first subtle discrete RDT was created that performs rotation and reposition users' perspective during saccadic eye movement. It has been found that a rotation up to 5 degrees around the user's vertical axis and 0.5m translation along the gaze line appeared undetected after saccades with a 15-degree magnitude [21]. It was later found that the same technique can be applied during blinks, with 2 to 5 degrees rotation and 0.04m to 0.09m translation allowable [150]. The limitations of these works are that: first of all, users were told about the manipulation, thus, their eye movements were voluntary and not spontaneous; secondly, in these studies, users were not walking, but only sitting in one place. Therefore, the estimated allowable manipulation is only a conservative one, and not necessarily reflect how much redirection one can use in real applications.

In summary, while subtle continuously RDW techniques have been extensively researched, little knowledge has been acquired about how to apply subtle discrete RDW techniques as well as how much they could contribute to improve the limited space problem.

2.3 Redirected Walking Thresholds

Given that subtle RDW techniques are more preferable over overt ones because a user's feeling of being immersed and present in the virtual environment is not affected, the focus of this thesis is on subtle RDW techniques. In order for the RDW technique to be considered subtle, the manipulation applied has to remain within certain thresholds. This section discusses different methods to identify these thresholds, and factors that have been found to have influence on them.
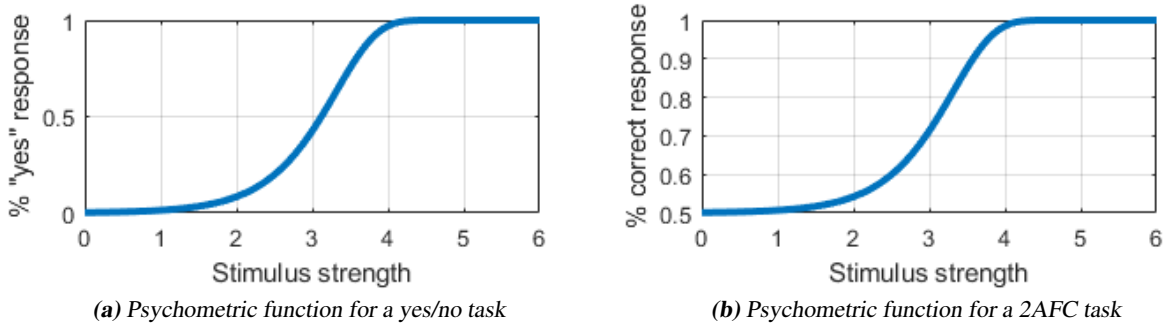
(a) Psychometric function for a yes/no task   *(b) Psychometric function for a 2AFC task*

Figure 2.8: *Psychometric function for different tasks*

2.3.1 Threshold Identification Methods

Threshold identification is the process of identifying how strong a stimulus should be for a user to correctly detect it with a predefined level of chance. In general, there are two types of thresholds: **difference threshold** and **absolute threshold**. Difference threshold, also called just noticeable difference or discrimination threshold, refers to the smallest difference between a stimulus and a reference stimulus that can be correctly detected with a predefined level of chance. Difference threshold is not constant, but in most cases follows Weber's law, in which the difference threshold (ΔI) is proportional to the intensity of the reference stimulus (I) [114].

$$\Delta I = KI \tag{2.7}$$

For example, when trying to distinguish which of two objects is heavier, one may be able to detect a small difference of between two low weight objects. However, the same small difference will not be detected if the two objects in comparison are significantly heavier. Weber's law, however, does not hold for all values of I and starts to break down when I is very small. That is, when I is very small, ΔI approaches zero (K is by definition positive and less than one) but we do not necessarily have the ability to detect it. Weber's law can be adapted to take this limitation into account by adding a constant term I_0.

$$\Delta I = K(I + I_0) \tag{2.8}$$

The term KI_0 is called the absolute threshold, which is the smallest stimulus level that can be perceived/detected correctly a percentage of the time. In the context of redirected walking thresholds (RDTs), what we are interested in is not the difference between the two levels of manipulation, but the absolute amount of manipulation that can be applied without influencing users' sense of presence and immersion. Therefore, the discussion from this point on only focuses on methods to identify absolute thresholds. The general procedure of absolute threshold detection involves the following steps: presenting stimuli to a test subject, collecting his/her responses and establishing a relationship between the stimulus levels and the subject's responses. This relationship is conventionally modelled as a psychometric function, with stimulus level on the x-axis, and the probability of certain response on the y-axis. Variations in the threshold detection procedure result in different psychometric curves. The first variation is called the **yes/no task**, in which only one non-zero stimulus is presented to the subject in each trial and he/she is asked the question: *"Did you detect the stimulus?"*. This yes/no task results in the psychometric function in Figure 2.8a. When the stimulus is very small and close to zero, the probability of the subject detecting it and saying "yes" is close to zero. When the stimulus is very large, and therefore obvious, the probability of the subject detecting it is one. The y-axis of the psychometric function represents the probability of the subject saying "yes" (or "no") and ranges from 0 to 1 (or 1 to 0) with increasing level of stimulus. In a yes/no task, the threshold is commonly defined as the stimulus level at which a subject

says "yes" 50% of the time. The second variation of threshold detection procedures is called the **two-alternative forced-choice task**, or 2AFC in short [75]. In this task, in each trial the subject is presented with not one, but two options either concurrently or sequentially. In one of these options, the stimulus is not presented and the subject is asked: *"In which option was the stimulus presented?"*. This 2AFC task results in the psychometric function shown in Figure 2.8b. The y-axis of the psychometric function in a 2AFC task represents the percentage of correct responses. When the stimulus level is very small and undetectable, the subject has a 50% chance of choosing the right option. When the stimulus level is significantly large, the subject can choose with absolute certainty the option where the stimulus was presented. Therefore, the y-axis ranges from 0.5 to 1 with increasing stimulus level, and the stimulus detection threshold is commonly chosen to be the stimulus level where subjects answer correctly 75% of the time. While in theory, these two variations should return a similar detection threshold value for each subject, in practice, the 2AFC tasks are generally more preferred over the yes/no task owing to the fact that the yes/no task usually contains response biases. For instance, a tendency of a subject to say "yes" whenever he/she is unsure to increase his/her rate of correct detection, or conversely, a tendency of a subject to say "no" when being unsure to reduce his/her rate of false detection [164]. The 2AFC is not without limitation itself, as there is also a risk of interval bias, which means users may answer more correctly when the stimulus is presented in a certain order. However, this bias is not always observed in all experimental settings [282]. Once the type of tasks (yes/no or 2AFC) has been selected, the remaining threshold identification process revolves around identifying the psychometric function. There are two main groups of method to identify the psychometric function: the **constant stimuli method** (CSM) and the **adaptive methods**. The constant stimuli method involves predefining a set of stimulus values (often stimulus values of equal spacing within a certain range) before the experiment and collecting subjects' responses at these stimulus values. The whole psychometric function can then be fitted using these data points. A well-fitted curve requires many stimulus values to be tested, and a sufficiently large number of repetitions per stimulus value. This is most of the time impractical when the time (the amount of time subjects have to spend doing the experiment) and financial (compensation payments for subjects) aspects are taken into account. Moreover, when only the threshold value, i.e. the 0.5 response point for a yes/no task and the 0.75 response point for a 2AFC task, and occasionally the slope of the curve at the threshold value are of interest, spending such effort to identify the whole curve is inefficient. Additionally, a large amount of the collected data is wasted because most of the tested stimulus values are far from the threshold, thus contributing little information about where the threshold is. Adaptive methods overcome this efficiency problem (with the compromise of not identifying the whole psychometric curve, but just the threshold) by adaptively selecting future tested stimulus levels based on subjects' past responses, resulting in presenting stimulus levels that are never too far away from the real threshold. There are two main types of adaptive methods: the staircase method (non-parametric) and the Bayesian method (parametric). The simplest form of a staircase method is a 1-up/1-down staircase in which the stimulus level is increased or decreased with a predefined step size after every incorrect or correct response, respectively. The experiment terminates after a fixed number of stimulus levels have been presented, and the threshold value is computed based on the last few stimulus levels. There are multiple variations of the staircase method depending on which staircase rules are applied (1-, 2-, 3- or more-up/1-, 2-, 3- or more-down), how to select step sizes (relationship between the sizes of the step up and step down), stopping conditions (after fixed number of trials or after fixed number of reversals), how to calculate the final threshold value (how many of the last stimulus levels to take into account), etc. Even though staircase methods are quite straight forward to implement, only a small number of points on the psychometric curve can be estimated with simple staircase rules, e.g. 50% point with a 1-down/1-up staircase, 70.7% point with a 2-down/1-up staircase [89]. Moreover, the staircase methods do not use information from all trials, but only the last few trials to estimate the threshold value, which makes it less efficient and sometimes lead to higher variance in the threshold estimate [4]. Meanwhile, most Bayesian methods assume the shape of the psychometric function (logistic or Weibull function) and sometimes also the slope of the function.

From trial to trial, based on subjects' responses, the posterior probability distribution of the threshold is updated and the psychometric function is shifted along the x-axis to a position that leads to the most likely threshold. This most likely threshold is used as the next tested stimulus level, and the procedure continues until a number of trials has been reached, or the standard deviation of the estimate is lower than a predefined target. While the drawbacks of Bayesian methods are that they are more complex to implement, and assumptions have to be made about the slope of the psychometric functions, they have been shown to be the most efficient when only the threshold value needs to be identified [253]. Similar to the staircase methods, there are many variations of the Bayesian methods differing from each other in terms of assumed function shapes, whether the slope of the function is also identified at the same time as the threshold, stimulus placement strategies, etc. [156, 143, 129, 155, 158]. Nevertheless, a detailed discussion of these different methods is out of this scope. Instead, I will present in detail a Bayesian method called QUEST, chosen for its efficiency over other methods, in a later section [268].

In the context of threshold identification for redirected walking, the first attempt to identify RDTs was by Sharif Razzaque who invented the three basic continuous RDW techniques (without formally name them as curvature, rotational and translational gains) [206, 205]. In his experiments, the 1-up/1-down staircase method was employed in order to reduce experiment time, together with a task in which subjects walked one time through a scene and were asked to detect the direction of their rotation: left or right. Most subsequent RDTs studies employed the classic constant stimuli method, and similar tasks as Razzaque's which they claim to be 2AFC where subjects were asked: "Were you redirected to the left or the right?" or "Did you walk slower or faster?" [236, 70, 237, 290]. While it appears that users were "forced" to choose between two options, they were presented with only one stimulus per trial (i.e. they only walked one time per trial). In fact, this is just a variant of the yes/no task with the question posed differently, and the corresponding psychometric curve is the same as the standard yes/no task. This remark was also made by Grechkin et al., where this method was referred to as pseudo-2AFC [95]. It has been observed in the pilot studies that even though this variation does not have the same type of response bias as the yes/no task, it contains another type of bias where subjects may have a tendency to choose one direction (for example: only "left") when unsure. This behaviour results in the left threshold being a right curvature, which is perceptionally incorrect and can not be used in an RDW application. Despite this limitation, all existing RDW threshold identification studies, except one study by Jerald et al. [128], employed the pseudo-2AFC method. In these studies, only the sample's average thresholds (rather than individual thresholds) were identified, and therefore, the bias was not visible. To overcome this problem, in most of the experiments described in this thesis, the true 2AFC task was employed. Even though adaptive methods have been shown to be more efficient in identifying thresholds very few studies on RDTs apply them. Jerald et al. applied the staircase method to identify rotational gain thresholds following the same procedure as previous NASA experiments [128]. Grechkin et al. performed first an experiment with CSM but later employed Green's maximum likelihood procedure for a second experiment in order to reduce experiment time [97, 95]. Hutton et al. compared the staircase method and a Bayesian method called PEST to identify rotational gain thresholds and found that PEST identified gains that are closer the users' thresholds [117]. A summary of methods used by existing studies can be found in Table 2.1.

2.3.2 Influence Factors

In addition to efforts to understand how much redirection can be applied without users noticing it, there has also been research on which factors influence the perception of RDW. These factors can be roughly divided into two categories: **intrinsic** - factors that are inherent in a user such as their gender, age, experience in VR, etc. and **extrinsic** - external factors such as how the virtual environment is presented,

Author	Gain type	Sample size	Method	Task	Repetition	Stimulus levels	Total trial
[205]	curvature	6	staircase	yes/no	1	20	20
[237]	rotational	12	CSM	pseudo-2AFC	10	10	100
	translational	16	CSM	pseudo-2AFC	8	9	72
	curvature	10	CSM	pseudo-2AFC	n.a.	5	n.a.
[128]	rotational	9	staircase	2AFC	1	148-219	148-219
[236]	rotational	14	CSM	pseudo-2AFC	10	10	100
	translational	15	CSM	pseudo-2AFC	8	9	72
	curvature	12	CSM	pseudo-2AFC	n.a.	5	n.a.
[70]	rotational	10	CSM	pseudo-2AFC	10	9	90
[95]	curvature	18	bayesian	pseudo-2AFC	1	35	35
[290]	translational	24	CSM	pseudo-2AFC	1	11	11
[187]	translational	12	CSM	pseudo-2AFC	10	3	30
[27]	rotational	13	CSM	pseudo-2AFC	10	10	100
	translational	13	CSM	pseudo-2AFC	8	9	72
	curvature	13	CSM	pseudo-2AFC	n.a.	5	n.a.
[196]	rotational	17	CSM	pseudo-2AFC	1	11	11
[145]	translational	20	CSM	pseudo-2AFC	3	9	27
[117]	rotational	20	staircase	yes/no	1	n.a.	n.a.
		20	bayesian	yes/no	1	9	9

Table 2.1: *Summary of existing RDW threshold studies and their study designs*

what task the users are performing, the presence of static and dynamic objects in the scene, etc. It could also be understood that intrinsic factors represent how different individuals process the same external information, and external factors represent the different external information itself. There is so far only one intrinsic factor study, which is on the impact of gender on rotational, translational and curvature gain thresholds [28]. By arguing that men and women have different strategies for spatial recognition and navigation, the authors hypothesized that there may be gender difference in detecting RDW as well. No significant difference in detection threshold between the genders was found in all three types of gains. However, considering their small sample size (7 men and 6 women), the fact which the authors themselves also stated, this results can not be considered conclusive. Since most threshold studies only aimed at identifying an average value to be applied for all users, rather than finding individualized value that fits each user, the focus of research on influence factors so far has been mainly on extrinsic factors. In a study where walking speed was controlled by having the users follow a moving colour-coded target which indicates whether they are walking at the correct speed, it was found that walking speed is negatively correlated with curvature gain thresholds [186]. That is, the faster one walks, the less redirection can be applied before it is noticeable. One drawback of this study is that speed control was performed using a visual task, which may interfere with the main visual task of detecting redirection. In the same experiment, the authors also discussed the potential use of an avatar in the virtual environment as a distraction to inject more redirection, or as a means of controlling users' walking speed. However, no studies have been found to pursue this discussion any further. In an experiment to investigate the performance of different algorithms in a constrained world, it was discovered that in a structured environment (e.g. shop aisles), redirection of the same intensity was detected much more often than in an open environment (e.g. forest) [113]. Nevertheless, this was more of an observation rather than a formal study. Following a similar direction, Paludan et al. investigated the effect of visual density of an environment on rotational gain thresholds [196]. In this study, users' rotational gain thresholds were identified in environments with varying number of objects, which is assumed to correspond to the environment's visual density. No significant difference in thresholds were found between these conditions. Even though not formally investigated in the context of RDW, another aspect of the visual appearance of the virtual environment: the field of view (FOV) could play a role. It has been observed that users seem to detect rotational gains more in small FOV conditions [144]. This could be explained by the fact that the small FOV limits the peripheral optical flow that provides information about rotational speed. This observation was confirmed later by Williams et al, whose results showed that a larger field of view allows a wider range of rotational gain to remain undetected [275]. The existence of a virtual presentation of the user - an avatar - has also been hypothesized to affect the detection thresholds. In one study, the impact of seeing their own feet on translational gain thresholds was investigated [145]. No significant difference in thresholds between the seeing feet and no feet condition was found. In the same study, the authors also compared users' detection thresholds in two different environments: one with detailed ground texture and one without and found a significant difference. The effect of combining different types of RDW gains on thresholds has also been investigated. Grechkin et al. combined curvature gains and translational gains but found no significant effect of this combination on curvature gain thresholds [95]. In another study, the effect of prolonged exposure to curvature gains of the same direction and magnitude on motor behaviour and detection thresholds was investigated [19]. After the users' baseline thresholds were first identified, they were asked to perform 150 walks under the same curvature gain (same magnitude, and always to the left) before their straight walking path behaviour and detection thresholds were measured again. The authors found that after the exposure, users tended to veer more to the right when trying to walk straight, and their left curvature gain thresholds increased. While this is an interesting finding, its application in RDW could be quite limited. First of all, an increase in left curvature gain thresholds led to a decrease in right curvature gain thresholds. That is, one can now be redirected more to the left, but less to the right and the resulted performance may just stay the same. Secondly, the experimental condition of walking 150 walks under the same curvature gains do not generally occur in real applications as redirection direction

changes constantly. Finally, there has also been research on how redirection affects users' performance in various task that require cognitive resources [30]. Results showed that redirection caused performance decline in verbal tasks as well as spatial working memory tasks. Nevertheless, how these tasks affect the detection of redirection was not investigated.

The common limitations among these aforementioned studies are that: first of all, the sample sizes are quite low (6 to 20 users). Moreover, since most of them used CSM as threshold identification method which is less efficient, the number of trials/repetitions are generally not high enough to obtain accurate threshold estimations. Most studies also used a yes/no task which contains response biases. The various sources of noise in the process may have resulted in many potential effects of small to medium effect size not being detected. In summary, while these existing studies are valuable in providing the first glance into how these factors may affect RDTs, their limitations highlight the need for more efficient, yet more accurate methods for individual threshold identification that enable better understanding of the impact of these factors.

2.4 Redirected Walking Algorithms

While the different RDW techniques described in Section 2.2 define the mapping rule between real and virtual trajectories, RDW algorithms decide how much gain, which RDW techniques, and when these RDW techniques are applied in real walking applications.

When the path of users in a virtual environment is predefined, i.e. users need to follow certain paths or reach particular way-points, it is possible to pre-calculate the RDW gains to be applied at every point on the path such that the whole virtual environment is "compressed" to fit into the real physical space. All the calculations can be performed off-line, which reduces computing power requirement, and the amount of redirection applied can be minimized over the whole path to keep presence intact [7]. However, off-line algorithms only work under the assumption that the paths through the virtual environment are predefined and fixed (for example: a tour through a museum) and users strictly keep to the path. Slight deviations from the path can not be corrected in real-time, and may lead to collision with physical boundaries.

Since off-line algorithms are inflexible and not scalable for many types of virtual environments, most existing RDW algorithms are on-line algorithms. These on-line algorithms can be divided into two types: greedy and non-greedy. In greedy algorithms, only the short-term prediction of a user's trajectory is taken into account. Most of the time it is the current position and direction, even though it can also be calculated from past trajectory data [184]. Without the knowledge of a user's future trajectory, a greedy algorithm determines the next redirection action based on what it sees as the current best option, which can be steering the users to the center of a tracking space (steer-to-center), steering the users onto an orbit around the center of the tracking space (steer-to-orbit) or steering the users to predefined targets (steer-to-target) [205, 78]. In case of irregular/non-convex physical spaces such as a living room space where the room center is occupied with obstacles, the best target to steer the user to could be one of the furthest physical boundary points, or onto a precomputed collision-free path [39]. Instead of having pre-calculated targets to steer to, Thomas et al. [249] proposed using artificial potential fields to identify the best steering direction, that is, towards the local minimum. This algorithm could be considered a more generic algorithm that encompasses S2C, when the environment is completely empty, and Chen et al.'s algorithm [39], when there are static obstacles. Artificial potential fields can also be used when moving obstacles such as another user sharing the same tracking space [9]. Steering actions are achieved by applying curvature gains, and when all fails and the users end up facing a physical obstacle, rotation gains can be applied to reset users orientation, a so-called reset action. Greedy algorithms work best with large open space virtual environments where it is difficult to predict far into the future where the

user may go, but may not be optimal when there is more information about the user's future behaviour, the physical space and the virtual environment. This is where non-greedy algorithms come in. In the dynamic path planning for obstacle avoidance algorithm proposed by Sun et al. [243], the possibility of the user being at a position in the virtual environment in the next time step is calculated based on that position visibility to the user and their current virtual position. Using this so-called "importance heat map", together with the map of the physical space (including physical boundaries, static and moving obstacles), a cost function that penalizes close proximity to the physical space can be formulated. The next redirection action is the one that minimizes this cost. In Sun et al.'s work [243], the algorithm only used a subtle discrete RDT that rotates the scene around the users during saccadic eye movements. The algorithm as proposed can not incorporate other continuous RDW techniques. Contrary to Sun et al.'s algorithm [243], the Fully Optimized Redirected walking for Constrained Environment algorithm, in short FORCE, predicts a user's paths further into the future by taking into account the map of the virtual environment [291]. A search tree with all possible redirection actions along these probable paths can be constructed, and the tree branch that ends with the best terminal state is selected. Similar to FORCE, in the model predictive control algorithm (MPC) proposed by Nescher et al. [185], users' possible virtual paths in the next N time steps in the future is also obtained. The difference is that a cost function is defined that penalizes reset action and strong redirection over this next N time steps and the next redirection action is selected to minimize this cost function. In the MPC algorithm, the set of available redirection actions are curvature gains of different magnitude, and rotational gains used for reset. The N time steps into the future prediction in Nescher et al.'s algorithm [185] is made with a simple assumption that until users have taken a specific path, the probability of them taking any available path is equal. For example, up to the intersection point of a T-maze, the chance of a user taking either path is always 50%. Only when the user has chosen a specific path, this probability can get updated. In reality, it is actually possible to make this prediction much earlier before that intersection point by using existing human locomotion models [286, 287], eye tracking information [285], or head orientation and gaze direction [87].

Given a large selection of RDW algorithms, it is important arrive at a common measure to compare their performance. As a reset action involves forcing the users to stop and turn around during their exploration in VR, causing a break in immersion, the number of resets has been used quite often as a performance measure. With number of resets as performance metric, in both simulations and live user studies, it has been shown that S2C is best suited for open virtual environments, whereas S2O performed much better for structured and constrained virtual environments [113]. It was also shown in simulations that an S2C algorithm that uses translational gains together with rotational and curvature gains outperforms the rest (S2C without translational gains, S2O with and without translational gains). When the the physical space is moderately elongated, S2C with translational gains is also most robust [6]. In open spaces with no obstacle, the artificial potential fields algorithm performs equally well as S2C, but it reduces the number of resets by half compared to S2C when obstacles are added [249]. In a live study, it was shown that MPC algorithm reduces the number of resets by 41% compared to S2C in a maze-like environment [185]. Sun et al. [243] proposed a different performance metric called saving error ratio to compare their dynamic path planning algorithm to S2C. First of all, an error area of a path is defined as the area outside of a space or inside an obstacle, and the saving error ratio is the ratio between the virtual path error area and the physical path error area. It has been shown with this metric using simulations that dynamic path planning outperformed S2C. Other metrics have also been used such as total distance to center (the smaller the better) and distance to obstacle (the larger the better). However, from the immersion and presence point of view, the number of resets is the best measure of an algorithm's performance.

In general, although these performance comparisons were carried out in different settings such as type of virtual environments, users' virtual paths, size and shape of the physical space, simulations or live studies, the trend suggests that non-greedy algorithms perform better than greedy algorithms as they incorporate

more information into their planning decision. However, algorithms such as dynamic path planning requires computational power of high end GPUs for the optimization step; and FORCE and MPC require the virtual environments to be generally constrained, and the map of the virtual environments to be discretized, which at the moment cannot be achieved for open unstructured virtual environments [288].

2.5 Spontaneous Alternation Behavior

One behavior that has been consistently observed in many species of animals called spontaneous alternation behavior (SAB) is investigated. SAB refers to an animal's tendency to avoid consecutive repeated choices when exploring a maze. While a large body of research exists on SAB in animals, not much has been done on humans. Therefore, this section is dedicated to investigating whether humans really exhibit SAB (in normal condition as well as in RDW condition) and what their alternation rate is if they do. The results not only allow better understanding of how humans behave, but also contribute to better prediction of users' walking path in RDW applications and further improvement of existing non-greedy RDW algorithms.

SAB refers to an animal's tendency to alternate consecutive directional choices while exploring a maze. First demonstrated in rodents [250], SAB has later been observed in a large number of species across very different taxonomic groups, including vertebrates, invertebrates, and even unicellular organisms [65]. In view of this phylogenetic universality, SAB was designated as "perhaps the most reliable phenomenon in all psychological research" [65]. Despite its reliability, only limited effort has been undertaken to investigate SAB in humans. Before examining the sparse work done in humans in more detail, the extensive body of animal research on the topic is briefly reviewed. Research on animals predominantly aimed to identify the mechanisms underlying SAB. Despite the apparent simplicity of the phenomenon, pinning down the reason why animals alternate has proven most difficult. There are three broad classes of theories accounting for SAB: motor response alternation, stimulus alternation, or spatial direction alternation.

Motor response alternation was historically the earliest approach in explaining SAB, observed most often in insects. Specifically, in a two-alternative forced choice situation, once a motor response is made in one direction, the response in that direction would be inhibited for a certain amount of time. This principle of "reactive inhibition" [232] has been based on findings in simple T-mazes (Figure 2.9a). In T-mazes with a forced 90 degree turn prior to the T-junction, it was shown that invertebrate species alternated directions relative to the orientation of the forced turn [102] (Figure 2.9b). As the distance between the forced and free choice increases, the body asymmetry caused by the previous turn dissipates and SAB is not observed anymore [102] (Figure 2.9b).

Stimulus alternation theories suggest that perceptual factors are driving SAB. Strong support comes from studies using mazes which do not require the animal to perform a motor response on the first trial (thus not causing a body asymmetry) but the animals still alternate with respect to the visual properties of the maze. Dember had rats entering a T-maze with one arm painted white and the other one black (Figure 2.9c) [62]. In the first trial, the entrance to either maze arm was blocked by a glass partitions and the rat could not enter any of the maze arms, hence no motor action was performed. However, the rat was still able to inspect the arms visually. On the second trial, the partitions were removed and the color of one of the arms was changed. The rats entered the arm whose color had changed. This proves that, even in the absence of any motor response, the change in the perceptual characteristics of a maze arm is sufficient to establish a direction preference.

The third class of theories suggests that the absolute spatial direction of a chosen turn is the crucial cue
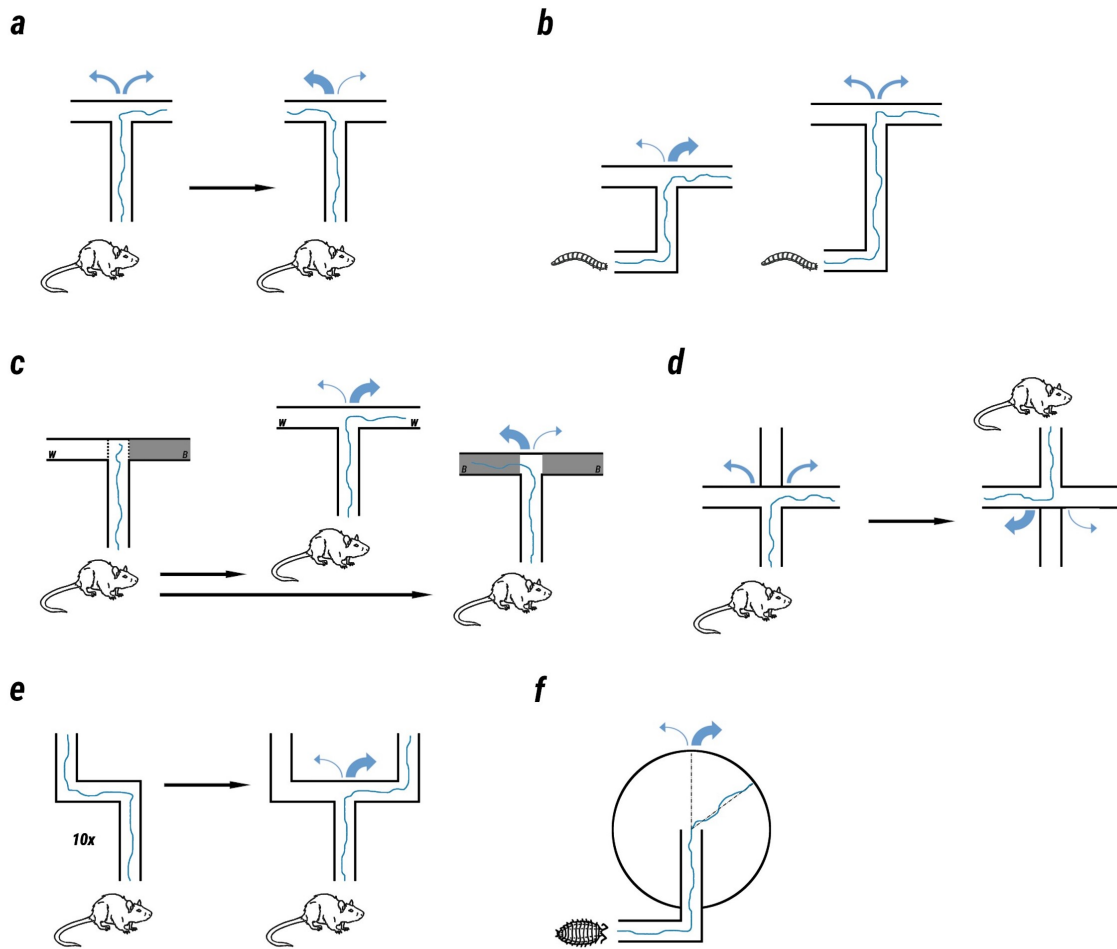
Figure 2.9: *Schematic depiction of maze designs used in studies of SAB in animals. Thin black arrows represent two consecutive trials. The strength of directional preferences at free choice junctions is represented by the thickness of light blue arrows. Sample trajectories through the mazes are indicated. See text for explanation and references. (a)-(b) depict findings supporting response theories of SAB: (a) Classical setup used in the examination of SAB in rodents. During two consecutive trials in a T-maze, in the second trial the direction opposite to the initially chosen direction is preferred. (b) T-mazes used to demonstrate turn alternation at the free choice junction after a 90-degree forced turn, which is diminished by prolongation of the distance between forced and free turn. (c) shows a setup used to support stimulus theories of SAB: A first exposure to a T-maze with a black and a white painted arm after the T-junction allows only visual experience (without motor response) of the corridors due to a glass partition. In subsequent trials the rat shows "stimulus alternation", i.e. a preference for the goal arm, whose colour had been changed. (d)-(e) illustrate findings in support of spatial direction alternation in SAB: (d) shows the use of a cross maze to disentangle response cues and spatial direction cues. After entering a T-maze from one side and choosing a direction at the T-junction, subsequently entering the T-maze from the opposite side leads to a preference of the goal arm pointing in the spatial direction opposite to the one initially chosen, thus involving a repetition of the motor response. (e) Tenfold exposure to a forced left-right turn sequence leading to a right turn preference at a subsequent T-junction. (f) shows the angular deviation from a straight-ahead direction pointing opposite to the direction of a preceding 90 degree forced turn.*

for alternation. *Spatial direction theories* of SAB were typically tested with cross mazes as depicted in Figure 2.9d. In the first trial, the north side of the cross maze was closed, and the animal entered the maze through the south opening. In the second trial, the south side was closed, and the animal entered the maze through the north opening. This setup allows disentangling motor response alternation and spatial direction alternation. Without loss of generality, let's assume that in the first trial, the rat turned to the right. In the second trial, the rat had a stronger tendency to turn to its right again as this would allow it to explore a different spatial direction. In other words, the rat alternated the spatial direction, even though it implied repetition of the previous motor response. Another test that could be used to show spatial direction alternation in rats can be seen in Figure 2.9e. In the first ten trials, the rats were forced to take a left-then-right turn. After these trials they were put in a T maze and they showed a tendency to turn to the right maze arm, which is a repetition of their previous motor response, but allows them to explore another spatial direction [73].

Other theories attempting to explain SAB that rely on concepts of exploratory behavior, curiosity and novelty seeking are reviewed by Montgomery [176], Dember [63] and most comprehensively by Richman [208]. These higher-order theories do not necessarily compete with the response, stimulus or spatial direction alternation theories summarized above. Nevertheless, no single theoretical account of SAB could be favored over others as the manifestation of choice alternation may vary considerably across species [104].

The extensive work done in animals is in contrast to the surprisingly low number of SAB studies in humans, despite multiple implications for psychological research [225]. Up to this point, examinations of SAB tendencies in humans have not managed to move beyond a superficial inspection of the phenomena, solely addressing the question: "Do they or don't they?" Richman et al. and Pate et al. had pre-schoolers crawl twice through a maze constructed out of opaque playground tunnels [208, 198]. They described alternation rates of more than 80%, generally increasing with a child's age. The only study on adult human subjects' SAB in a maze-like situation is by Neiberg et al. [181]. These authors recorded college students' directional choices while they repeatedly walked through a T-shaped corridor. They found an alternation rate of 60%, not significantly different from the chance rate of 50%. Given the impracticality of building life-size mazes for humans, some researchers have studied maze exploration outside the context of walking, requiring subjects to trace mazes drawn on paper [69, 103] or guide a hand-held stylus along small 3D maze models [153]. All these studies, mostly testing young children, reported significant alternation behavior. However, the significance of human alternation behavior extends far beyond issues of directional choices in a maze. Above-chance alternation was also found in more abstract types of "exploration" behavior, e.g. in unreinforced binary guesses of the alternatives "left" and "right" [124], in repeated free choices between objects [127, 204, 265] or among verbal response options [172]. Even more broadly, cognitive biases like the "gambler's fallacy" in Roulette [257] and the "hot hand" in basketball [93] are further illustrations of the pervasiveness of alternation behavior. The fact that alternation of choices is favored over repetitions in these contexts suggested that paradigms of SAB are conceptually equivalent to paradigms which require human subjects to generate random sequences of alternatives [31]. In both contexts, the avoidance of generating an identical response on consecutive trials is the most prominent bias. However, the conceptual equivalence between spontaneous maze alternation and repetition avoidance in subjective randomization has never been empirically tested. Such equivalence would suggest that "movements" in abstract spaces (search in memory, establishing connections in social networks) obey the same laws as locomotion in maze exploration. In addition, it would indicate that SAB in sequential decision making might reflect the primacy of exploration over exploitation in the healthy brain [109], which could make SAB tests candidate instruments to detect both highly functioning cognitive traits [58], but also to uncover early signs of cognitive decline [91].

The lack of classic, locomotion-based SAB experiments in humans may be partly due to the difficulties

posed by the use of walkable mazes. In addition to the significant effort of building a life-size maze, the appearance and properties of the different corridors should either be identical or changeable in a systematic way. Recent advances in VR technology offer a solution to these problems. Using positional tracking combined with HMDs, one can easily build immersive virtual mazes, through which a user can navigate by real walking. By this approach, the features of the maze's appearance, such as structure, texture, brightness and surroundings, can be precisely controlled. The advantages of virtual mazes have long been recognized by behavioral neuro-scientists [246]. Using virtual realizations of the eight-arm radial maze and the Morris water maze, spatial memory was tested in humans using paradigms normally restricted to animal subjects [48, 234]. Furthermore, studies investigating the use of virtual mazes in animal experiments underline the feasibility of translating spatial tasks from the real world to virtual reality [38]. It is not clear whether the lack of an overarching theory of SAB or the increasing use of SAB paradigms for applied purposes (especially in pharmaceutic contexts [115]) has slowed down basic research in the field. In any case, contributions to the very nature of "perhaps the most reliable phenomenon in all psychological research" [65] have undoubtedly become relatively sparse compared to the period between 1940 and the 1970ies.

2.6 Research Gap

2.6.1 Redirected Walking Threshold Identification

Maintaining a user's feeling of presence in the virtual environment is the most important aspect of a VR application. In the context of RDW applications, this means the redirection manipulation should only be applied within certain thresholds such that users do not notice it and their feeling of presence remains intact. Until now, the RDT values found by Steinicke et al. [236] have been used in most RDW applications as the standard gains for all users. While this approach is practical, it raises the question of whether is is the best approach in terms of users' experience in VR and efficiency. More specifically, applying the same threshold value for all users could on one hand risk breaking immersion for more sensitive users, while on the other hand, not take full advantage of strong manipulation for less sensitive users. Due to inefficient and time consuming threshold identification procedures, most existing works reported only the sample average threshold values. Currently, no study exists that investigate whether individual RDTs differ significantly. The first goal of this thesis is therefore to fill this gap. In order to achieve this goal, one straight forward approach would be to use the existing threshold identification procedure that has been established by Steinicke et al. [236] and adopted by many research groups. However, this procedure suffers from bias and demands a large sample size if each subject's threshold is to be identified. As a result, there is a need for fast and new estimation methods of threshold identification, which will be discussed in this thesis.

In addition to potential individual differences, numerous external factors could have an influence on users' perception of redirection. While it has been shown that walking speed negatively correlates with curvature RDTs, the influence of many other external factors has not been investigated. The second goal of this thesis is therefore to investigate the impact of different external factors on curvature RDTs: how the environment looks, what task users are doing, user's perspective, and how much they feel control over the environment. Each of these factors poses unique challenges such as:

- How to quantify and categorize different environments.

- What type of tasks can be used to impose a cognitive load on users.

- How to influence users' feeling of control in VR.

2.6.2 Improving Redirected Walking Using Psychological Factors

While non-greedy algorithms have better performance and require a smaller tracking space for the same virtual environment size, greedy algorithms are simpler, less computational resource demanding to implement, and applicable to all virtual environments. As there are both pros and cons to which type of algorithms to choose, in the context of this thesis, various options to improve both greedy and non-greedy algorithms will be explored.

With better knowledge of how different factors affect users' perception of existing RDW techniques, within limits, maximum possible redirection could be applied without affecting users' experience. From this point, for both greedy and non-greedy algorithms, RDW can only be improved further when new techniques are invented. Very few new techniques have been introduced since Razzaque's introduction of RDW in 2001 [206]. The aim of the second part of this work is therefore to look into psychological factors that have not been "exploited" for RDW.

Another way to improve RDW, specifically non-greedy algorithms, is to gain understanding about users' behavior in VR. The more knowledge about users' behavior there is, the better decisions can be made about which RDW techniques to apply, how much and when to apply these techniques. Until now, predictions of a user's behavior are mostly short-term predictions: based on past head tracking data [183, 184], head orientation [87], eye-tracking data [285] or fitting the path using different locomotion models [286, 287, 110]. Long term prediction, which takes into account the virtual environment structure, so far has been limited to relatively basic assumptions such as: under normal circumstances, users don't walk through virtual obstacles or walls; in a T-maze condition, the probability of turning right or left is 50%; etc. If more knowledge about long term users' behavior is obtained, prediction's accuracy can be improved, consequently enhancing the efficiency of non-greedy algorithms. In this thesis, the aim is to improve state-of-the-art long term predictions based on phenomenon in the field of neuropsychology that has never been explored before such as spontaneous alternation behavior (SAB). Despite being consistently observed in animals, in humans, experiments on SAB have been scarce (mostly performed on children) and it is unclear whether humans exhibit this behavior too. The scarcity of experiment could be mainly due to the fact that it is difficult to construct large adult size mazes in real life. The use of VR in this situation is therefore two-fold. First of all, in VR, mazes can be built in a large enough size, controlled and customized to the experimenter's desire. The virtual environment does not have to be restricted to a maze-like environment, but could also be an open space. It is now possible to really study spontaneous alternation behavior in human adults. Furthermore, as a user's walking trajectory could be manipulated using RDW, the SAB could also be examined further under these conditions. Secondly, in the context of RDW, the knowledge gained from this experiment of humans' behavior could be a solution for the current lack of long term path prediction. The last part of this thesis is therefore dedicated to examining the different aspects of spontaneous alternation behavior through the use of different types of mazes and RDW conditions.

3

Fast Estimation of Personalized Redirected Walking Threshold

3.1 Improving Classical Methods

In the context of identifying redirected walking thresholds, most research groups used the classical constant stimuli method thanks to its simplicity to implement (Table 2.1). However, as previously discussed in Section 2.3.1, the constant stimuli method is not extremely efficient when only the threshold value needs to be identified, resulting in most groups performing not enough repetitions or stimulus levels to save time and cost, and leading to low estimation accuracy. Due to this fact, the results obtained from these studies may still be good enough for estimating the average threshold value of the group when all the data is combined, but not enough to have an accurate estimation of each individual's threshold. Since identifying individual's threshold is important in ensuring that the VR experience maintains undisturbed for each user, closely based on the paper by Watson and Pelli [268], this section aims at describing in detail an alternative to the constant stimuli method: a Bayesian adaptive method called QUEST, which requires fewer trials and provides individual threshold values within certain accuracy.

3.1.1 Assumptions

Similar to other Bayesian adaptive methods, the QUEST method requires certain assumptions regarding the psychometric function to be made.

Assumption 1 *The psychometric function maintains the same shape under all conditions. That is, from condition to condition, the psychometric function could be shifted along the stimulus intensity axis, specified by a parameter T, the threshold, but its shape remains the same.*

This property of the psychometric function has been remarked by many previous authors [178, 98, 219]. With this assumption, it is possible to describe any particular psychometric function $p_T(x)$ where T is the threshold value using a canonical form $\Theta(x)$:

$$p_T(x) = \Theta(x - T) \tag{3.1}$$

The different conditions are the variations in experiment designs such as: the walking speed, the virtual

environment appearance, etc. The first assumption implies that these conditions may result in different threshold values, but the underlying psychometric function assumes the same shape.

Assumption 2 *The threshold T is constant across trials.*
This assumes that there are no learning or adaptation effects involved throughout the experiment. This could be a strong assumption to make as it has been shown that when users are repeatedly redirected to one direction, their thresholds shift towards that same direction, i.e. they become less sensitive to the stimulus [19]. However, the adaptation effects can be counteracted by introducing trials randomly from different conditions (for example: left and right redirection), so-called interleaving. This assumption allows information obtained from all previous trials to be used in estimating the current threshold, as well as selecting the next possible stimulus level.

Assumption 3 *Trials are statistically independent.*
Similar to Assumption 2, users' responses in each trial should not depend on previous trials. This can also be prevented by interleaving trials from different conditions.

3.1.2 Formulation

The QUEST Bayesian adaptive method, as the name implies, employs Bayes theorem in calculating the threshold estimation. The Bayesian theorem describes the probability of an event based on prior information related to that event using the following equation:

$$f_{T|D}(T|D) = \frac{f_T(T)f_{D|T}(D|T)}{f_D(D)} \tag{3.2}$$

whereas:

- $f_T(T)$ is the **prior probability density function** (pdf) of the threshold T. This function defines, for each possible stimulus level, the prior probability of the threshold being at that level. This function is normally obtained from past experiments to indicate a rough estimation of where the threshold could be, and is often a Gaussian distribution, or rectangular distribution. This prior pdf is meant to get the experiment started with an initial guess, but in some case it could create a bias in the estimation of the threshold. In order to avoid this bias, the QUEST method does not include this pdf in the calculation of the final estimate.

- $f_{D|T}(D|T)$ represents the information that is collected throughout the trials. This function describes the **probability of obtaining information** D (a certain response at a stimulus level) given that the threshold T is at a particular stimulus level.

- $f_D(D)$ is the prior pdf of observing the information D. For a particular set of data, $f_D(D)$ is constant and used as a normalizing factor. $f_D(D)$ can be calculated from $f_T(T)$ and $f_{D|T}(D|T)$ using the following equation:

$$f_D(D) = \int_{-\infty}^{\infty} f_T(T)f_{D|T}(D|T)dT \tag{3.3}$$

- $f_{T|D}(T|D)$ is the **posterior pdf** of the threshold T calculated based on the prior pdf and the observed information from the trials. The final threshold estimate is the maximum a posteriori probability estimate, i.e. the mode of the posterior pdf obtained after all trials.

Based on Equations 3.2 and 3.3, the posterior pdf can be calculated using only the product $f_T(T)f_{D|T}(D|T)$ which is the joint probability $f_{(T,D)}(T,D)$. Taking the natural logarithm of this product, the quest func-

tion $Q(T)$ can be obtained:

$$Q(T) = \ln f_T(T) + \ln f_{D|T}(D|T) \tag{3.4}$$

After n number of trials, the obtained information D contains a series of responses, r_i at each stimulus level x_i. Depending on the task used (yes/no or 2AFC), $r_i = 1$ when the response is "yes" or correct (considered as a success S) or $r_i = 0$ when the response is "no" or wrong (considered as a failure F). Since the trials are statistically independent based on Assumption 3, the conditional probability term of Equation 3.4 can be calculated as the product of the conditional probability of each trial:

$$f_{D|T}(D|T) = \prod_{i=1}^{n} p_{r_i|T}(x_i) \tag{3.5}$$

Equation 3.4 then becomes

$$Q(T) = \ln f_T(T) + \ln \prod_{i=1}^{n} p_{r_i|T}(x_i) \tag{3.6}$$

When $r_i = 1$, the conditional probability $p_{r_i|T}(x_i)$ is actually the psychometric function $p_T(x)$. When $r_i = 0$, the conditional probability $p_{r_i|T}(x_i)$ is $1 - p_T(x)$. Based on Equation 3.1, we have:

$$\ln p_T(x) = \ln \Theta(x - T) \tag{3.7}$$
$$\ln(1 - p_T(x)) = \ln(1 - \Theta(x - T)) \tag{3.8}$$

Let us define two auxiliary success and failure functions as:

$$S(x) = \ln \Theta(-x) \tag{3.9}$$
$$F(x) = \ln(1 - \Theta(-x)) \tag{3.10}$$

Equation 3.6 now becomes:

$$Q_i(T) = Q_{i-1}(T) + \begin{cases} S(T - x_i) & \text{if success} \\ F(T - x_i) & \text{if failure} \end{cases} \tag{3.11}$$
$$Q_0(T) = \ln f_T(T) \tag{3.12}$$

Equations 3.11 and 3.12 are all that are required for the QUEST procedure consisting the following steps:

- Step 1: Define a prior probability $f_T(T)$

- Step 2: Construct the success and failure functions $S(x)$ and $F(x)$ based on the canonical form $\Theta(x)$ of the psychometric function

- Step 3: After each trial, if it is a success, shift the success function a distance x_i; otherwise, shift the failure function a distance x_i and add the corresponding function point by point to the previous quest function $Q_i(T)$.

- Repeat Step 3 until the termination condition is met. One natural termination rule could be to stop when the standard deviation of the estimated threshold is smaller than a certain size. Another possible termination condition is to stop the experiment after a fixed number of trials. While this may not be as efficient, it is simpler to implement and more convenient for experiment planning. The standard deviation can still be used in a later analysis to make sure the obtained result is within certain confidence level.

- To calculate the final threshold, the prior pdf needs to be first removed from the quest function to prevent bias: $L_n(T) = Q_n(T) - Q_0(T)$. The final threshold is then the maximum likelihood estimate of the resulted function $L_n(T)$.

3.1.3 Common parameters selection

For the threshold identification experiments in the following sections, the canonical form of the psychometric function is selected to be the Weibull logistic function, as commonly employed by previous threshold experiments [29, 147]:

$$\Theta(x) = 1 - (1 - \gamma)e^{-\beta(x+\epsilon)} \tag{3.13}$$

whereas:

- γ defines the probability of success when no stimulus is present (zero intensity). For a yes/no task, γ is zero, while for a 2AFC task, γ is 0.5.

- β defines the slope of the psychometric function, specifying how sensitive a subject is to changes in stimulus level. β is obtained as an estimation from previous RDW threshold experiments, and is set to be 3.5 in all following experiments.

- δ is the false alarm rate, in all following experiments set to 0.01m.

The prior pdf of the threshold $f_T(T)$ is set to be a rectangular distribution. The range of this distribution is obtained from data from previous experiments or empirically from pilot tests if such experiment has not been previously performed. In each of the following experiments, the tested range will be given. Other QUEST related parameters that are experiment dependent will also be provided in details in the corresponding experiment descriptions.

3.2 Individual differences and impact of gender on curvature redirected walking thresholds

Up to the point of this thesis, all existing RDW applications applied an average threshold value for all users. This approach is not necessarily optimal in terms of maintaining each individual user's sense of immersion and presence (applying a redirection gain too high would cause discomfort to sensitive users) or utilizing RDW algorithms to their best potential (applying too low redirection gain would result in worse performance). However, up to now, no research group has had neither the capacity nor has applied an efficient enough techniques to identify individual threshold with a reasonable sample size. Moreover, gains found from different groups vary significantly: curvature gain threshold ranges from 10.5m to 27m [236, 187]; translational gain threshold ranges from 0.78 to 1.26 [237, 236]; and rotational gain threshold ranges from 0.54 to 1.35 [237, 236, 70, 45]. It is unclear what factors account for these large differences: the variance in experiment designs and methodologies, the different virtual environments, the small sample size, or simply the variance between the different groups of subjects. Using the aforementioned QUEST method, the goal of this section is to efficiently explore how different individual thresholds can be, and consequentially draw conclusion on whether it is worthwhile to identify individual thresholds or an average threshold for all users would be sufficient.

Furthermore, as intrinsic factors have not been much studied previously, this section also investigates the impact of one of the prominent intrinsic factors - gender, on RDTs. Gender was chosen due to the fact that there exists a body of research on gender differences in spatial navigation and perception (which are the relevant components in the context of RDW) that tends to support the hypothesis that gender difference may exist in RDW too. In a large study with 90 men and 104 women, Dabbs et al. [52] found that when giving directions, men tend to use distance and north-south-east-west terms, while women use landmarks and left-right terms. In a study where subjects are required to navigate and find a way out of unfamiliar

virtual mazes, it has been shown that during spatial navigation, women and men activate different parts of the brain, indicating that navigational information may be processed differently [101]. Other studies used the Roelofs illusion to investigate gender difference in the choice of reference frame during goal-directed walking. The Roelofs illusion happens when a small visual target is surrounded by a large frame that is off-centre from the subject's midline. Due to the presence of this frame in the subject's peripheral vision, the perceived location of the visual target appears to be shifted in the opposition direction of the frame. After looking at the offset frame and target for a few seconds, the subjects are required to walk towards the target without vision. Results suggest that women tend to use the offset frame as the fixed frame of reference, while men rely on the egocentric frame as the frame of reference [57, 55, 56, 81]. In the context of RDW, there was one study by Bruder et al. that investigated the effect of gender on RDTs [27]. Although it was found that no gender difference exists in RDTs, it was remarked that the number of subject was too small. In addition, the walking speed was not controlled in their experiment, which may have led to additional noise in the result. Given the well established gender difference in spatial navigation and perception, and the limitations in terms of sample size and controlled factors of the existing RDW study, a larger scale study is performed to investigate the effect of gender on RDTs where walking speed is controlled.

Of the three continuous RDW techniques, translational gain is not often used in RDW algorithms, rotational gain is used only for when a reset action is required, and curvature gain is used in almost all RDW algorithms. Due to time and resource limitation, only curvature gains will be investigated.

3.2.1 Speed Regulation

In an experiment by Neth et al. [187], it has been shown that walking speed has a negative correlation with curvature RDTs. Specifically, subjects tend to notice curvature gains more when they walk faster, and vice versa. This result seems appropriate. Under the application of the same curvature gain magnitude, when subjects walk faster in one direction, it would take a larger momentum to change their current walking direction. This would result in the vestibular system detecting the conflict more easily. However, in that experiment, the subjects' walking speed was controlled by the requirement that they had to follow and maintain constant distance to an object that regulates the speed. Since detecting redirection is an extremely visual task, it is not known how another visual task for speed control distracts the users from the main task of detecting curvature redirection. Therefore, in this thesis, a new method of speed control using audio rhythms is proposed, and this method is subsequently applied to investigate the effect of walking speed on curvature gain thresholds.

By studying the energy expenditure during human walking, Dean derived a relationship between walking speed v (m/s), stepping frequency f (s^{-1}) and height h (m) as follows [59]:

$$v = (\frac{f}{1.57} \cdot \frac{h}{1.72})^2 \tag{3.14}$$

Equation 3.14 is used in the following experiment for generating the aforementioned audio step rhythms.

3.2.2 Curvature Gain Implementation

3.2.3 Experiment Design

In order to remove possible effects of the appearance of the virtual environment on curvature RDTs, the experiment scene is modelled as an empty room with four surrounding walls with no texture, the floor

(a) Top view layout of virtual environ-ment

(b) Virtual view of the subjects before each trial: a virtual room 10m wide, 10m long, and open ceiling. The red target is located in front of the users, at a distance of 7.5m
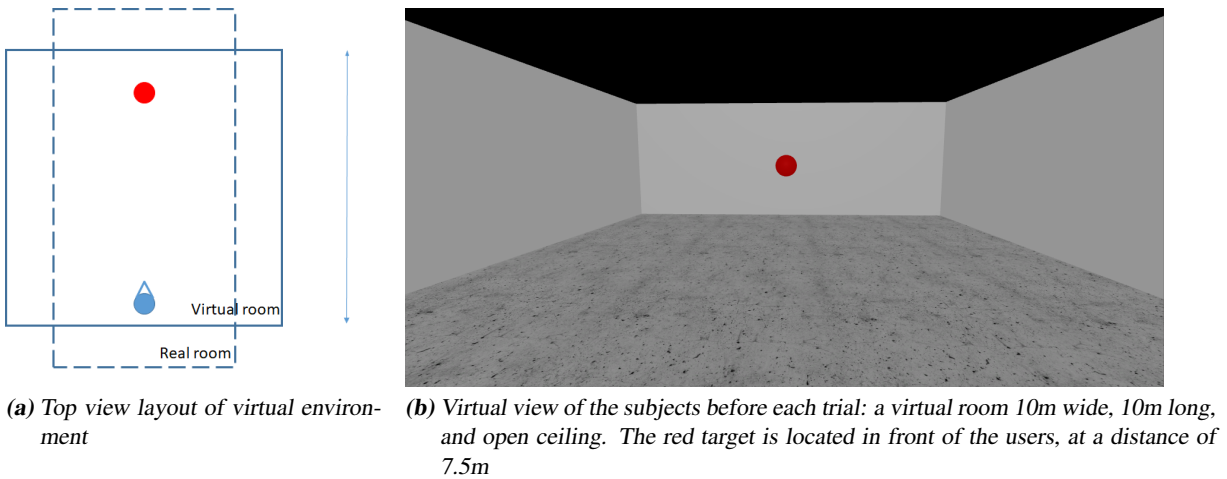
**Figure 3.1:** *Design of the virtual environment*

with sparse concrete texture and a red target located 7.5m from the starting position of the user (Figure 3.1b).

Prior to the experiment, subjects' heights were collected such that their personal step rhythms can be generated. To replicate the conditions of Neth et al.'s experiment, each user has to walk with two speed conditions: 0.75m/s and 1.25m/s regulated by the proposed step rhythms [187]. These two speeds were tested by a number of pilot subjects to make sure it is not too slow or too fast to follow. Only right-handed subjects were recruited in order to eliminate potential differences in redirection perception of subjects with different handedness. Also with the same thought, whether redirection thresholds to the left or right would differ for right-handed subjects were also investigated. Therefore, left and right curvature gain thresholds are separately identified for each user. This results in a total of four threshold values of four psychometric functions to be found per user: two speed conditions × two curvature direction conditions. All four conditions are within-subject conditions, which means every subject performs all four conditions.

To prevent yes/no bias or pseudo yes/no bias commonly present in existing studies, the 2AFC task is used. In each trial, subjects walk to the visual target two times. In only one of the two walks, a curvature gain is applied such that visually (and virtually) the subjects see that they are walking straight, but in reality they are walking on a curve. In the other walk, no redirection is applied. The order of these two walks is randomized between trials. Each of the four tested conditions is handled by a separate "QUEST". The prior probability of each QUEST is set to be a rectangular distribution. In Steinicke et al.'s experiment, curvature gains value ranged from 0.017 (equivalent to a 57.3m radius) to 0.104 (9.55m radius) [236]. Neth et al. tested curvature gain range was from 0 (straight line) to 0.1 (10m radius) [187]. In Grechkin et al. the tested curvature gain range from 0 up to 0.2 (5m radius) [95]. In order to make sure all these extreme cases are included, the range of the rectangular distribution is set to be from 0 to 0.2. To reduce training and adaptation effects, the four QUESTs are interleaved. That is, each QUEST calculates the next curvature gain value to be tested for each condition, resulting in four potential values. The curvature gain value to be presented in the next trial is selected randomly from these four values. Following recommendations by Watson and Pelli, each QUEST stops after 40 trials have been performed, resulting in a total of 160 trials per subject [268]. During the experiment, the process of updating the "QUESTs" with users' responses and computing the next curvature gain value is automated. Users respond to the 2AFC question using a built-in eye tracker (Figure 3.2b).

(a) *Hardware setup*
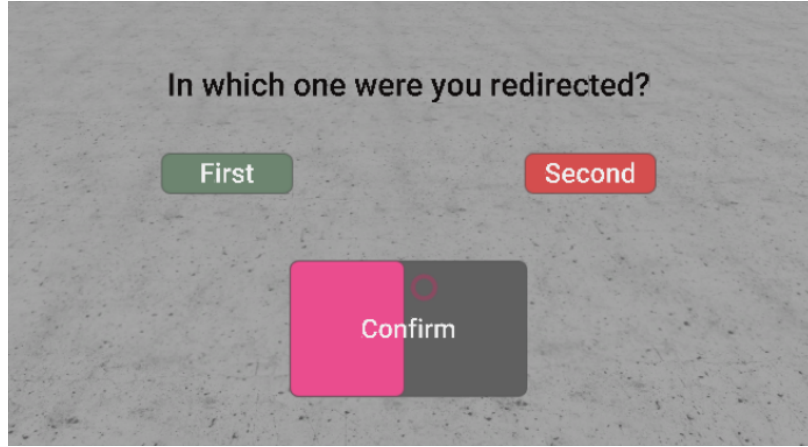
(b) *Question panel shown to users in each trial after the two walks. Users use their eyes to either "First" or "Second" to select, and "Confirm" to finalize the answer.*

Figure 3.2: *Experiment setup*

3.2.4 Experiment Setup

For the experiment, subjects wear an Oculus DK2 with a built-in SMI eye tracker (Figure 3.2a). On top of the headset, an Intersense IS-1200 inside-out optical tracking system is mounted, which provides 6-DOF positional tracking at 180Hz. To prevent the subjects from seeing the floor, which may in turn enable them to "cheat", a shield is added in front of the headset. The virtual environment is optimally designed in Unity to run at the Oculus' maximum frame rate of 75Hz. The whole setup is powered by a backpack-mounted notebook. The available tracking space is 13m x 6.6m. The users also wear noise canceling headphones, on which the step regulating rhythms are played.

3.2.5 Participants and Procedure

A total of 30 subjects (aged from 18-35 (mean=25.1, SD=3.9), 15 men and 16 women, were recruited through the university market place. All subjects were required to be right-handed according to a validated lateral preference inventory [47] (See Appendix A.1), with normal or corrected-to-normal vision (using contact lenses), and have no vestibular dysfunction or injury that affects their balance and walking activities.

The experiment was split into two sessions. In the first session, subjects were informed about the purpose of the experiment and signed the consent forms. They were then informed about the risk of motion sickness and filled out the Kennedy's Simulator Sickness Questionnaire (SSQ) [136]. They also filled out the demographic data form providing their age, gender, handedness, and gaming experience (gaming hours per week). After the forms were completed, subjects were shown different screen shots of the virtual environment and given the following instruction:

"When the program starts, you will see a starting position indicated by a green sphere. Walk to this position into the sphere and an arrow will appear. While inside this sphere, rotate on the spot until you see a tick (Figure 3.3). A scene containing a red target will appear. Wait until you hear the step sound and then start walking in the same frequency as the sound and as naturally as possible towards the target. When you reach the target, a second starting position will appear. Do the same as before and you will see the red target again. Walk to the target again. After you reach the target, a question will appear on the
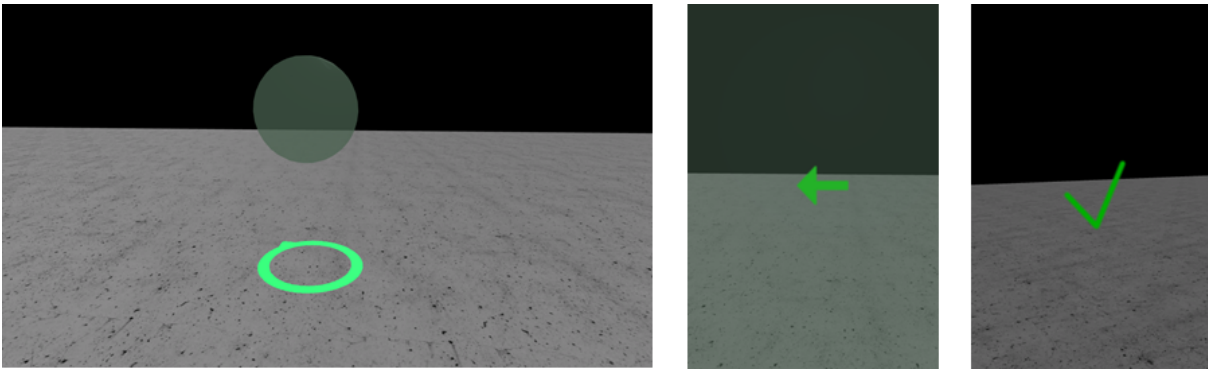
Figure 3.3: *Subjects' virtual view of the starting position and the alignment procedure*

screen asking you: In which walk were you redirected? Select your answer (first or second) by looking at it, and look at the confirm button to confirm (Figure 3.2b). Repeat this until we stop you for a break at about half time. At any moment if you feel uncomfortable or sick, please let us know immediately."

After subjects confirmed that they understood the task, they were given a number of training runs. In these training runs, a curvature gain of 0.2 (corresponding to a 5m radius curve) was used. This value is the upper limit of the tested value range proposed in Section 3.2.3. According to existing research in the field, this amount of curvature gain is perceivable for all subjects. The purpose of using extremely high curvature gain was to ensure that subjects understand how it feels to be redirected. The training runs included both curvature directions and both speed rhythms (in total four conditions). Similar to the main experiment, the training runs were split into two separate blocks: one with 0.75m/s walking speed, and the other 1.25m/s. It was decided before the experiment started, and counter-balanced across subjects that the same number of subjects would perform the slow walking speed block first, and the other would perform the fast walking speed block first. The reason for not interleaving these two blocks was because subjects take certain amount of time to get used to following the speed rhythms. Switching constantly between these two speeds would require them to constantly adjust, which could result in them not following the rhythm very well. Within each block, the left and right curvature redirections were presented in a random order. The training for a condition was considered completed if subjects gave two consecutive correct answers for that condition. If subjects gave an incorrect answer, the number of completed correct runs would be reset back to zero. This procedure aimed to make sure that subjects really understand the task, and to get them familiar with giving the response using the eye-tracker so that they would not accidentally choose the answers they did not mean to choose. After the subjects finished the training runs for one speed condition, the main experiment began. After the first experiment block finished, the training runs for the remaining speed condition followed, and then the second block of experiment started. In all trials, the starting positions were calculated such that subjects would never be close to a wall if they followed the instructions and did not wander off the path towards the target (Figure 3.4). Therefore, an experimenter was always there but there was no need for him/her to walk behind the subjects. Subjects could take a break any time they want, but on average they were stopped after every 20 minutes. At the end of the session, the subjects filled out the SSQ again. The second session was scheduled to be at least 24 hours after the first session. For the second session, subjects came in and continued where they left off without any further instructions, unless they requested. They also filled in the SSQ before and after this session.

Since all camera rotations during curvature redirection are performed around the z-axis, it is sufficient to calculate the starting position and orientation in the xy-plane. Based on Figure 3.5, the starting position S (defined as (x_S, y_S)) and orientation $\vec{h}$ (defined as the angle γ) of the subjects in the beginning of each

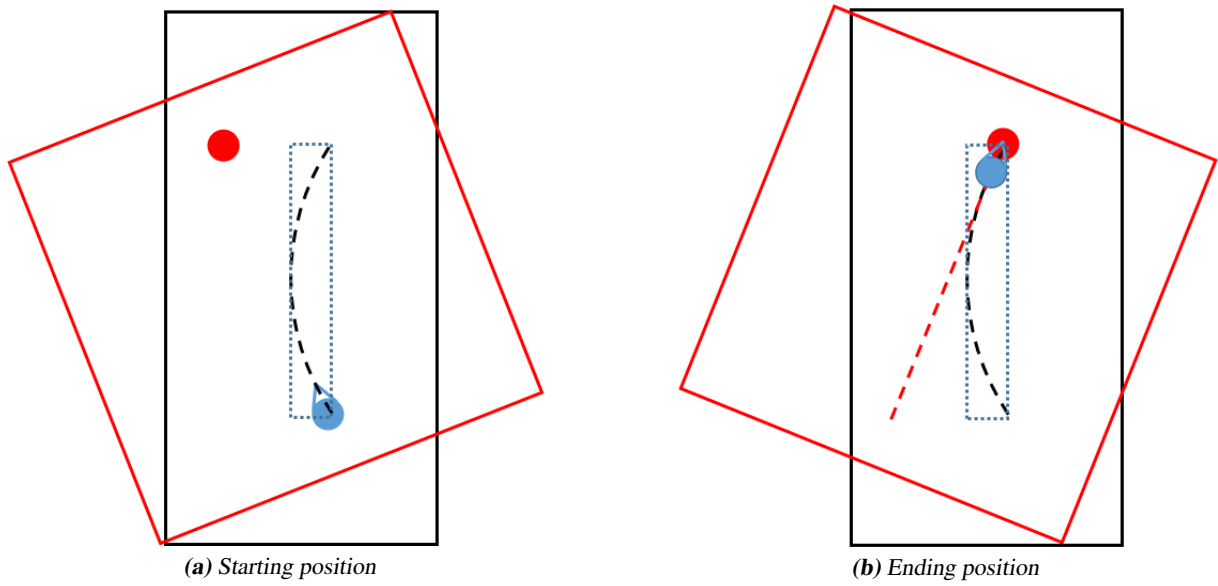*(a) Starting position*   *(b) Ending position*

Figure 3.4: *Subjects' virtual and real paths during a trial. Black and red represent entities in the real world, and virtual world, respectively. The starting position and orientation are selected such that the bounding box of the real path stays in the middle and aligns with the real room. This way, subjects are always in a safe distance from the physical space, provided that they follow the instruction and keep walking towards the red target.*

walk with respect to the real room coordinate system is calculated as follows:

$$x_S = \frac{w + r(1 - \cos(\frac{\alpha}{2}))}{2} \tag{3.15}$$

$$y_S = \frac{h - r\sin(\frac{\alpha}{2})}{2} \tag{3.16}$$

$$\gamma = \frac{\alpha}{2} \tag{3.17}$$

whereas:

- r is the radius of the curve, calculated as the inverse of the current tested curvature gain g_C

$$r = \frac{1}{g_C} \tag{3.18}$$

- α is the angle created by the arc l that has the same length as the distance walked by the subjects (in this experiment $l = 7.5$m). α is calculated as:

$$\alpha = \frac{l}{r} \tag{3.19}$$

3.2.6 Results and Discussion

Out of 61 subjects, one female subject reported motion sickness after 10 minutes and could not continue. 60 remaining subjects could complete the whole experiment. For each subject, the following data was obtained:
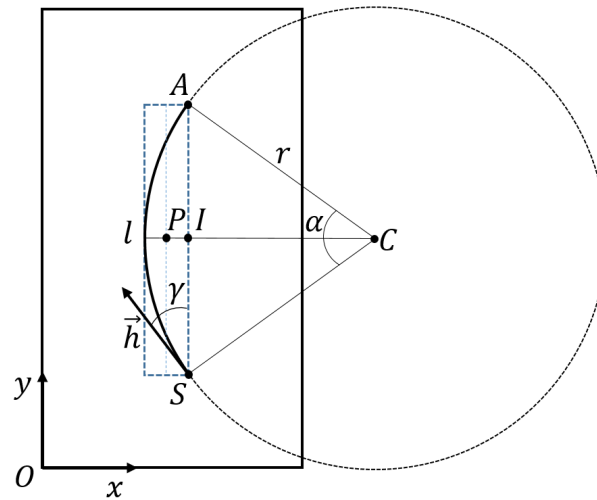
Figure 3.5: *Starting position*

- All positional data during all the straight and curve walks. This type of data was used to calculate subjects' walking speed, path curvature, step length, etc.

- All responses to the curvature redirection to obtain the final identification thresholds.

- Simulator sickness scores before and after each sessions.

- Subjects' demographic data such as age, gender, height and gaming experience.

Speed Following Behaviour

To investigate the effectiveness of regulating speed using step rhythms, subjects' walking speeds in the two speed conditions were calculated. In the slow condition (0.75m/s), the mean speed of all users was 0.9018m/s, SD=0.0814 and significantly different from 0.75m/s; in the fast condition (1.25m/s), the mean speed of all users was 1.1422m/s, SD=0.0834 and significantly different from 1.25m/s. In Figure 5.4, it can be seen that almost all users did not manage to slow down enough for the slow speed, or speed up enough for the fast speed. Users of the same height, and hence same step sound frequency, tend to also have large variation in their speed. It could be possible that users did not synchronize with the step frequency well, and therefore did not reach the desired speed. During the experiment, some users did remark that the slow speed was too slow and not natural. This does not explain why they did not meet the fast speed, as 1.25m/s is close to an average walking speed [177]. A possible explanation for the fast condition could be that users did not feel stable while walking fast in VR, and therefore subconsciously slowed down. Since users' real step frequency unfortunately could not be recorded, it is not possible to understand whether users follow the step rhythms correctly or not, and whether the step frequency equation by Dean could be applied for walking in VR [59].

In order to investigate whether subjects' speed differ in curved and straight walks, or if women and men have different speed following performance, a linear mixed model was used where walking speed is the dependent variable and type of paths (curve or straight), curve direction (left or right), gender, age, height are independent variables. Since multiple data points, specifically four, were collected per subject, subject factor (Id) is also entered into the model as a random factor. The linear mixed model becomes:

$$\text{speed} \sim 1 + \text{path type} + \text{curve direction} + \text{gender} + \text{age} + \text{height} + (1|\text{Id}). \qquad (3.20)$$
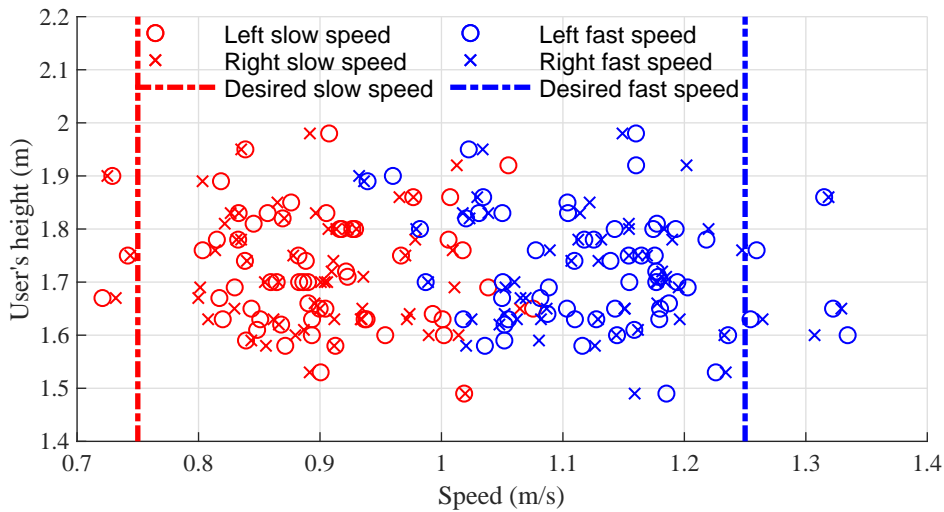
Figure 3.6: *Average speeds of subjects regulated by the step rhythms*

Results from the linear mixed model analysis showed that only the speed condition has a significant effect on walking speed (p< 0.001). This outcome indicates that although the audio step rhythms did not successfully regulate users' speed to the predefined speeds, it is still good enough to produce significantly different walking speeds provided that the difference between the predefined speeds is large enough. Furthermore, while in unregulated conditions, gender significantly affects walking speed, specifically, women tend to walk more slowly than men [177], it was not the case in this experiment. This could imply that the audio step rhythms method managed to override this gender effect, resulting in women and men walking with similar speed. Nevertheless, since it is not possible to pinpoint the reason why users did not reach the predefined speeds, it remains unclear whether regulating speed using audio step rhythms in VR studies is a reliable method and requires further research.

Path Following Behaviour

Before investigating subjects' curvature redirection thresholds, it is first important to look at whether their performed paths have similar curvatures as the desired curved paths defined by the tested curvature gains. In order to achieve this, each user's curved path is fitted with a circular arc based on the method proposed by Kasa [134]. Figure 3.9 shows a typical fitted curved path. It is important to note that the circle fit method was used, and only works well, with the assumption that users performed perfectly circular arcs during the trials. However, this assumption does not always hold true, as users may over-correct in certain parts of their trajectories, while under-correct in other parts in order to finally arrive at the target. In order to check if on average, users performed the desired trajectory, a one sample t-test was performed. Result shows that the ratio of real over desired radius is significantly less than one with mean ratio of 0.95 and standard deviation of 0.17. This indicates that users had some tendency to perform a smaller curve radius than the desired radius. To investigate whether the ratio is influenced by different experiment conditions such as walking speed, curve directions, etc., a linear mixed model was used with ratio as the dependent variable, curve direction (left or right), gain, speed, gender as independent variables and subject as random variable. The linear mixed model becomes:

$$\text{ratio} \sim 1 + \text{speed} + \text{direction} + \text{gain} + \text{gender} + (1|\text{Id}). \tag{3.21}$$

Results showed that, except for gender, the remaining factors have significant impacts on radius ratio. A summary of all significant effects can be seen from Figure 3.7. More specifically, users matched the
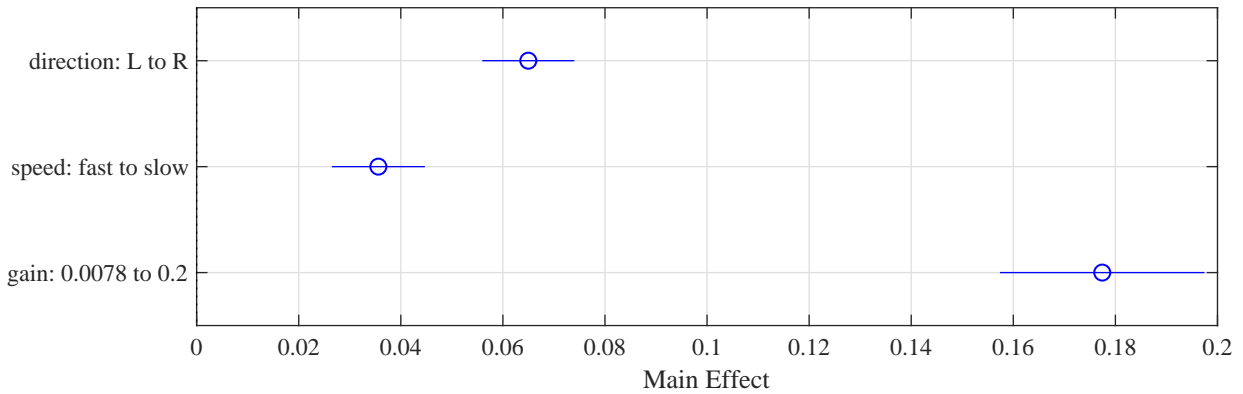
Figure 3.7: *Main effects indicating the average difference in the ratio of real over desired radius between the curvature directions (left or right), walking speed (fast or slow) and gains ranging from 0.0078 to 0.2. Main effects are significant when the 95% confidence interval (indicated by the blue lines) spans an interval that does not include 0*
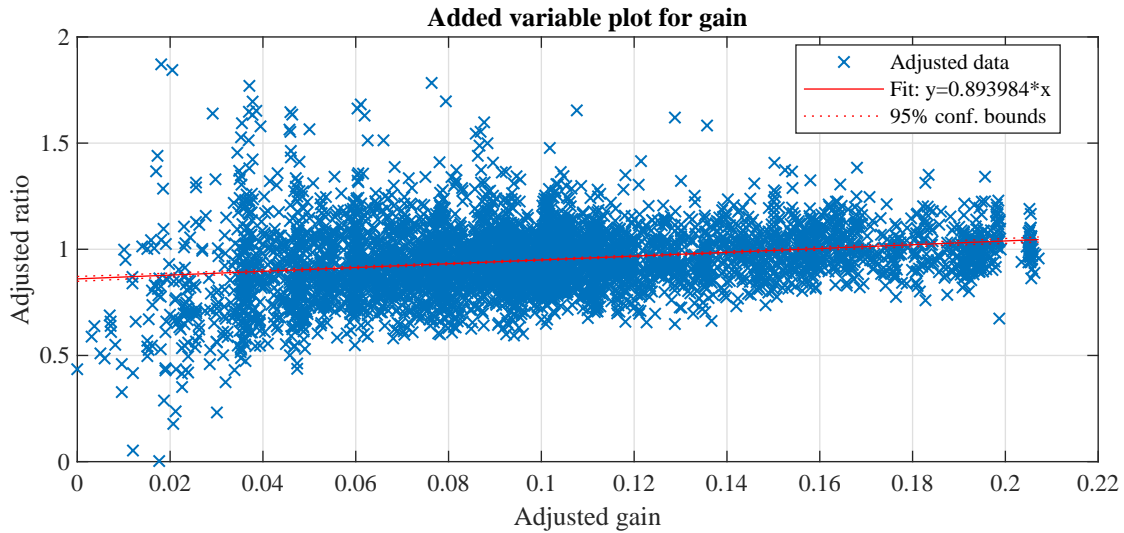

Figure 3.8: *Effect of curvature gain on ratio of real radius over desired radius. The red line indicates the estimated linear correlation between the curvature gains applied and the ratio between the real and desired radius*

desired radius better when they walked to the right than to the left. When they walked slower, the curve radius was closer to the desired radius than when they walked faster. This could be explained by the fact that when users walk slower, they can correct for the deviation introduced by the curvature gain better. However, these two factors have in general much smaller effect sizes in comparison to the effect of curvature gain. It can be seen from Figure 3.7 and 3.8 that users follow the curve much better and with lower variance when the gain is higher, i.e. smaller radius and sharper curve. While this result is intriguing, considering that circle fitting is highly susceptible to noise in trajectories, it could be possible that the estimation of large curve radius is less accurate than small curve radius, resulting in a large effect size of curvature gain. Since this is not a limitation of the circle fitting method itself, but rather solely the nature of real walking trajectories, and on average, the radius ratio is very close to one (0.095), it will be assumed from this point on that users performed trajectories that match the curve radius defined by the tested curvature gains.
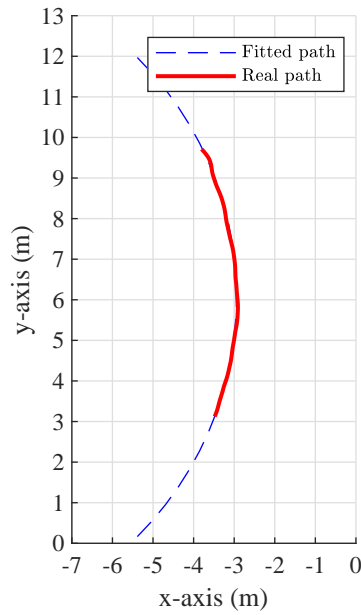
Figure 3.9: *A typical curved path fitted with a circular arc*

Simulation Sickness

Based on the SSQ scores collected before and after each session, two-sample t-tests were conducted. In the first session, there was a significant difference in score for the before (M=4.17, SD=5.89) and after (M=12.39, SD=12.85) conditions with t(118)=-4.5, p=1.6e-5. In the second session, there was also a significant difference in score for the before (M=2.95, SD=4.67) and after (M=8.17, SD=8.99) conditions; t(118)=-3.98, p=1.2e-4. These results suggest that our study has an effect on the SSQ score. However, the average increase of 6.72 in score in both sessions is reasonable, considering the fact that users walked around in the virtual environment for about 40 minutes in each session. Since it has been found in previous literature that women are more susceptible to simulator sickness than men [80], the effect of gender on this increase in SSQ score is investigated using a linear mixed model which includes gender as a fixed factor and subject as a random factor:

$$\text{score increase} \sim 1 + \text{gender} + (1|\text{subject}) \tag{3.22}$$

Results showed no significant effect of gender on the increase in SSQ score.

Identification Thresholds

For each subject, four threshold values were obtained corresponding to two curvature direction and two speed conditions: left slow, left fast, right slow and right fast. The distribution of all 120 obtained threshold values (albeit interdependency between data points since each subject contributes four data points) is shown in Figure 3.10, serving only as an overall picture. In general, there is a high variability in curvature gain thresholds, ranging from 0.0237 (equivalent to a radius of 42.2m) to 0.1994 (equivalent to a radius of 5.2m) and a median of 0.0976 (equivalent to a radius of 10.24m), interquartile range 0.07 to 0.1336. This result confirms that there is significant difference in individual thresholds of curvature gains, and that each user requires their own personalized curvature gains in order to experience VR comfortably.
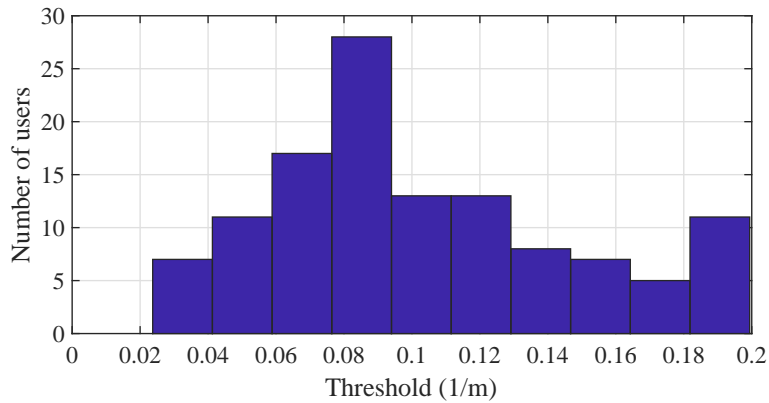
Figure 3.10: *Distribution of all obtained threshold values*

To investigate the effect of gender, speed and curvature direction, a linear mixed model was fitted which includes gender, speed and curvature direction as independent variables and subjects as a random variable. Subjects' gaming experience, calculated as gaming hours per week was also added as an indepedent variable to investigate whether gaming experience influences the ability to detect curvature redirection. The full mixed effect model therefore becomes:

$$\text{threshold} \sim 1 + \text{gender} + \text{speed} + \text{direction} + \text{game hours} + (1|\text{Id}). \tag{3.23}$$

Results showed no significant effect of curvature direction on curvature gain thresholds (p = 0.2), indicating that right-handed subjects tend have equal performance in detecting curvature redirection when the curve is towards either the left or right direction. There is also no significant effect of the number of gaming hours on curvature gain thresholds (p = 0.6), which means gamers do not have an advantage over non-gamers at detecting redirection.

The significant effects on curvature gain thresholds are speed (Figure 3.11a) and gender (Figure 3.11b) with p < 0.001 and p = 0.012 respectively. In Figure 3.11a and 3.11b, the threshold values were adjusted to isolate the effect of the independent variable of interest, while the effects of all other independent variables are averaged. The downward slope in Figure 3.11a indicates that the faster subjects walk, the lower their curvature gain threshold is, i.e. the more sensitive they are to curvature gains. This result agrees with results of the work by Neth et al., despite the fact that they used a visual task to regulate walking speed [187]. Figure 3.11b shows that gender significantly affects curvature gain thresholds, in that men tend to be more sensitive in detecting curvature gain. The average curvature radius threshold for men is 10.7m while it is 8.63m for women. This result is in line with existing findings about gender differences in spatial navigation and perception in that women tend to rely more on visual information during navigation, and also confirms the observed tendency found previously in work by Bruder et al. [27].

In summary, an experiment with 30 subjects was conducted to identify curvature gain thresholds using a within subject design with four conditions: two curvature direction conditions × two speed conditions. Unlike existing studies that employed visual tasks to regulate walking speed, in this experiment an audio task (using step rhythms) was used. It was found that this method was not able to drive subjects to walk at the desired speed, more specifically, subjects tended to walk not slow enough for the slow speed condition, and not fast enough for the fast speed condition. However, for the purpose of the experiment, it was able to regulate significantly different walking speeds. Analysis of subjects' walking trajectories showed that they tend to walk on a slightly tighter radius than the desired one defined by the curvature gain. Due to the limitation of fitting a perfect circle on real trajectories, this difference can be considered
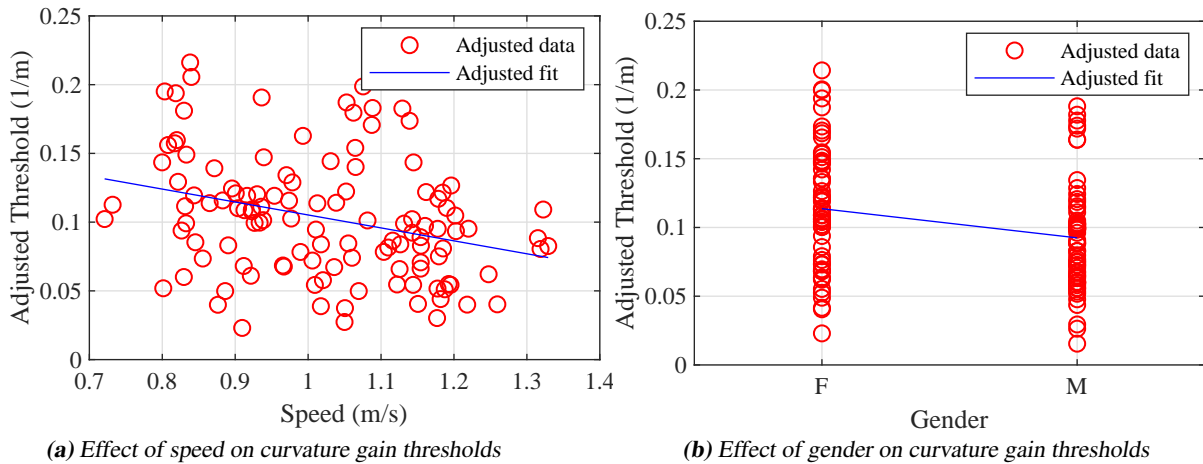
(a) *Effect of speed on curvature gain thresholds*

(b) *Effect of gender on curvature gain thresholds*

Figure 3.11: *Effects of speed and gender on curvature gain thresholds*

negligible. On investigating individual thresholds of curvature gains, it was found that thresholds range widely from 5.2, to 42.2m radius. This wide range of threshold agrees with the initial observation that each user should have their personalized curvature gain when using an RDW application. An applied curvature gain different from the optimal threshold of an individual could result in either a break in presence (if the curvature gain is larger than the individual's threshold) or a suboptimal performance of RDW algorithms (if the curvature gain is smaller than the individual's threshold). It was also found that these thresholds are significantly influenced by how fast the user walk (the faster the speed, the lower the threshold) and gender (men on average notice curvature gain more than women). This finding indicates that during an RDW application, using a constant personalized curvature gain for each user is not sufficient to guarantee optimal sense of presence and performance, the curvature gain also needs to be adapted dynamically to the walking speed.

Despite being much more efficient compared to the classical constant stimuli method, the proposed QUEST method still requires a significant amount of time to identify personalized thresholds. More specifically, each user requires around 20 minutes of walking for the curvature gain threshold to one direction at a predefined speed to be identified, which is generally not practical in real RDW applications. A more efficient method of estimating curvature redirection threshold is therefore desirable, which is the motivation for section 3.3.

3.3 Evaluating Standard Perception Tests for Threshold Estimation [1]

As previously discussed in Chapter 2, during walking, the human brain continuously receives different sensory cues from the visual, vestibular and proprioceptive systems. These different sensory cues are not processed equally, but are weighted according to their reliability. For spatial perception tasks such as estimating spatial orientation and maintaining balance during walking, under good lighting and contrast conditions, visual cues are exceptionally more reliable and precise, and therefore are given extremely high weightings. This process is called visual capture of non-visual senses (also visual dependency). In the context of RDW, a high visual weighting could imply that the user could be more susceptible to visual manipulation, hence have higher RDTs. Conversely, a low visual weighting could mean that the

---

[1]Parts of the section were published in [217]

user could be less susceptible to visual manipulation and more sensitive to vestibular and proprioceptive cues, resulting in lower RDTs.

Given this potential relationship between visual, vestibular and proprioceptive weightings and RDTs, this section is devoted to exploring the use of various perception tests (visual dependence, vestibular and proprioceptive tests) as predictors for RDTs.

3.3.1 Experiment Design and Set-up

In order to investigate which perception tests could be used as a predictor for curvature RDTs, the baseline RDTs of each subject need to be estimated using an established method. Each subject also performed six standard perception tests including: rod and frame, vection, Romberg, blind veering, interoception and the SSA questionnaires. The same subjects from the experiment in Section 3.1 were recruited also for this experiment, and RDTs could be reused as baseline RDTs.

Rod and frame test   In order to perform well in the rod and frame test, i.e. align the rod very closely to the true vertical, the tested subject has to focus on vestibular and proprioceptive cues while ignoring the visual influence of the tilted frame. It is hypothesized that this mechanism is similar to what happens during RDW. That is, subjects also have to focus on postural information while ignoring contradicting visual cues to detect the curved walking trajectory. Therefore, subjects who perform better in the rod and frame test are hypothesized to be less easily "tricked" by redirected walking, hence have a lower RDTs.

Historically, the rod and frame test requires an apparatus that is bulky and complex to use (Figure 3.12a). As it has been shown that performing the rod and frame test using a virtual environment is a valid and reliable method [10], in this experiment, a VR-adapted rod and frame test was implemented. Following the recommendations for a stable measure of visual dependency by Takasaki et al. [245], the experiment consists of 4 different rod and frame orientations ($\pm 20°$ frame angle $\times \pm 18°$ rod angle). Each orientation is repeated 5 times (minimum number of repetitions for a reliable measurement [245]) totalling up to 20 trials per subject. On a black background, the frame was modelled as a white square frame and the rod was composed of a dotted line to prevent the jagged effect that potentially gives the subjects clues about its orientation [66] (Figure 3.13b).

Subjects wear an Oculus DK2 HMD while sitting upright on a chair. On the HMD, they are presented with a virtual environment as shown in Figure 3.13b. While the outer frame is fixed, the rod could be rotated using two joysticks on a game controller. One joystick has a $0.1°$ resolution for fast rotation and the other one has a $0.01°$ resolution for fine tuning. The task given to them is that they have to align the rod in a perfectly vertical orientation. Once they have completed one trial and pressed the confirm button, the next trial automatically starts. The 20 trials are presented in a randomized and balanced order. Subjects can take as much time as they need to finish the task. During each trial of each subject, the angle of the rod with respect to the true vertical was recorded with timestamps.

Vection test   Among the different types of vection, circular vection has the most similar mechanism to curvature redirected walking as they both expose subjects to a visual-vestibular conflict due to the visual rotation of the real/virtual environment around them. The hypothesis is that subjects who are more visually dependent when there are visual-vestibular conflicts and thus more susceptible to vection would also have more difficulties detecting the visual-vestibular mismatch evoked by the rotating virtual environment during curvature RDW, resulting in higher curvature RDTs.
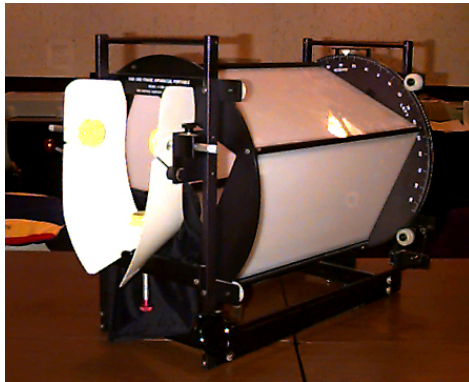
(a) *Original apparatus used for the rod and frame test. Subjects are required to sit straight with the head fixated on head and chin rests while looking at the inside of the apparatus*

Image courtesy of https://www.jasonpatent.com/2009/09/18/eye-of-the-beholder/
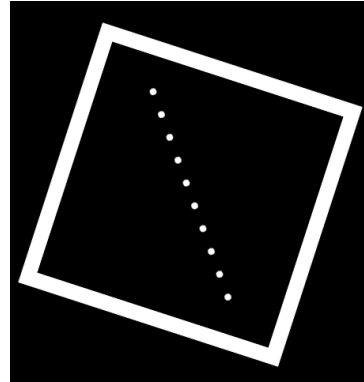
(b) *Virtual environment seen by the subjects performing the rod and frame test*

Figure 3.12: *Rod and frame test implementations - then and now*

The vection test using circular vection is traditionally carried out with an optokinetic drum where subjects sit inside an enclosed drum, and the outside wall containing a pattern is rotated around them (Figure 3.13a). Since it is difficult to procure such a device, many works on vection research had made use of large projection displays [254, 255, 211], or HMDs [42]. It has been shown that the display types (HMDs, stereoscopic projection or 3DTVs) do not matter as long as the field of view (FOV) is matched [210]. Another recent work, however, showed that the Oculus Rift induces stronger sensation of vection, compared to 3DTVs and Google Cardboards, even though it was unclear how the FOV of these displays are compared to each other [42]. Although this experiment was completed before these findings about the use of VR in vection test, it was then already decided that a VR-adapted version of the test should be implemented to keep it consistent with the rod and frame test and to ensure that these tests are easy to perform as a quick estimation of the RDTs.

The subjects were seated upright on an office swivel chair while in the virtual environment, they sat statically in the middle of a drum and observed a pattern of vertical black and white stripes in an Oculus DK2 HMD. Upon button press, the virtual drum started rotating with increasing rotational speed for 6 seconds with an acceleration of $10°/s^2$ and ending up at a constant speed of $60°/s$ (following guidelines from Melcher and Henn [170]). Subjects were asked to focus on the moving surface and report by button press as soon as they felt the sensation of themselves rotating instead of merely looking at a rotating surface. If no such sensation occurred, the simulation would stop after 30 seconds. Following each trial, subjects had to rate the strength of the movement sensation on a scale of 0-100, with 0 denoting no sensation of movement at all, and 100 denoting a sensation indistinguishable from real movement. In total, each subject completed eight trials consisting of four leftward and four rightward rotations presented in a randomized order. In each trial, the vection onset time (the duration from the start of the drum rotation till a subject presses the button indicating a sensation of movement) and the vection strength (a participant's rating of the strength of their sensations of movement) were recorded.

(a) Optokinetic drum used for the vection test. Subjects sit inside the drum with their head fixed and fixate on a point on the rotating wall

Image courtesy of Vestibulo-Oculomotor lab Zürich
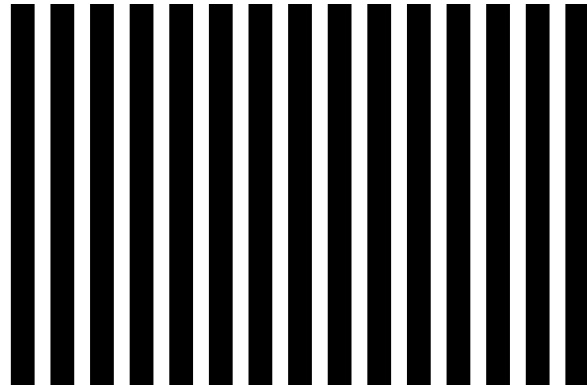
(b) Virtual environment seen by the subjects performing vection test

Figure 3.13: *Vection test implementations*

Romberg test   The amount of body sway occurring when attempting to stand still reflects a person's ability of postural control. Similar to the rationale behind the rod and frame test and the vection susceptibility test, it is hypothesized that participants who are less visual dependent in their postural control would perform better at detecting disruptions in their postural balance due to the curved walking trajectory, despite contradicting visual inputs.

On a Wii balance board, each subject was instructed to stand as still as possible without shoes in a natural, shoulder wide stance, arms hanging down on the side under two conditions [43]. In the first condition, subjects kept their eyes open while fixating on a cross at eye level 40cm in front of them. In the second condition, participants kept their eyes closed. Each condition lasted two minutes. During both conditions, the coordinates of the participants' centre of pressure (COP) were recorded.

Blind veering test   The blind veering test requires a subject to attempt to walk a straight line without any visual feedback and the lateral deviation from that line is obtained [131]. The performance in a blind veering test is a measure of a person's bodily awareness and it is hypothesized that a better performance in the this test predicts lower curvature RDTs.

To quantify a person's blind veering tendency, the procedure described by Kallie et al. was adopted [131]. The same VR set up used for the redirection threshold estimation was employed. Subjects wore an Oculus DK2 HMD and were connected to an Intersense IS-1200 optical tracking system for 6-DOF head position tracking at 180Hz. As shown in Figure 3.14, subjects started at one end of the 13m x 6.6m tracking space and were exposed to a completely dark virtual environment just with a floating red sphere 9.5m in front of them. Subjects were instructed to walk straight towards this sphere. After the subjects crossed the fronto-parallel plane located 1m from the starting position, the red sphere disappeared, leaving the subjects effectively blindfolded. Subjects were beforehand instructed to keep on walking as straight as possible as if the target would still be visible. In each trial, subjects were required to walk until they crossed the fronto-parallel plane located 8m from the starting position, at which point an instruction to stop appeared on the HMD. A shield in front of the HMD was used to ensure that subjects could not get any visual cues from their surroundings. The walking speed of 0.75m/s was controlled by the same
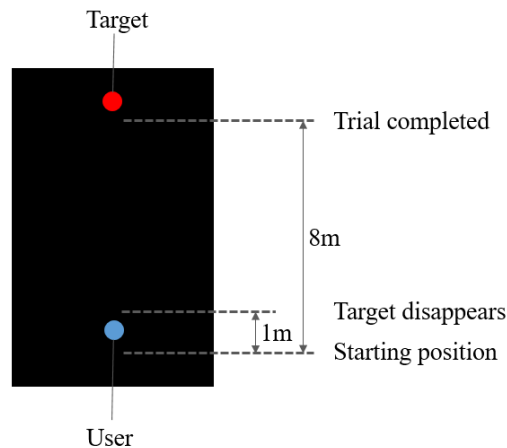
Figure 3.14: *Illustration of the blind veering test. (Drawings are not to scale)*

step rhythms used in the RDTs identification task, to which the subjects were asked to adjust their step frequency. In total, each subject completed 40 trials. During all trials, the walking trajectories of the subjects were recorded.

Interoception test   A subject who performs well in an interoception test is assumed to be more aware of their internal cues, potentially being able to give lower weighting to visual cues when needed. Thus, it is hypothesized that a generic bodily awareness, expressed by a person's interoceptive sensitivity, would facilitate the detection of the body's curved walking trajectory during redirection.

Quantifying interoceptive sensitivity is most commonly done in tasks during which participants are asked to track or detect their own heartbeats. The heartbeat detection task deployed here generally follows the procedures proposed by Kleckner et al. [140]. Subjects were connected to a three-electrode electrocardiogram (ECG) using an e-health sensor platform [1]. The subjects were asked to feel their pulse on the wrist and were presented with the two conditions of the heartbeat detection task. In the synchronous condition, an acoustic signal is played 200ms after an R-spike in the ECG, which has been shown to be perceived as simultaneous with the felt heartbeat in the body [272]. In the asynchronous condition, a delay of 500ms is added between an R-spike in the ECG and the playback of the acoustic signal, which had been shown to be perceived as not synchronous with the felt heartbeat [272]. After subjects had experienced the difference between the two conditions while feeling their pulse, the heartbeat detection task began. While sitting upright on a chair without leaning on the backrest and with the hands placed on the legs (palms facing upwards) the subjects were presented with 10 seconds of either a synchronous or asynchronous playback. Subjects were instructed to feel their heartbeat and to identify whether a synchronous or asynchronous playback had been presented. After the verbal response was given to the experimenter, the next trial was started. In total each participant completed 40 trials balanced for synchronous and asynchronous conditions (in randomized order), with 2 minutes break after 20 trials. The heartbeat detection task was created and presented using the software ExpyVR. Each subject responses (correct or wrong detection) were recorded

Somatosensory amplification   As the somatosensory amplification (SSA) scale questionnaire can be used as a qualitative measure to assess a heightened attention to uncomfortable bodily sensations [14], it is hypothesized that such a heightened attention could be beneficial in detecting potential, uncomfortable bodily sensations triggered by redirection.

Subjects completed the somatosensory amplification (SSA) scale questionnaire which measures heightened attention to uncomfortable bodily sensations [14]. The questionnaire has 10 items scored from 1 to 5 (See Appendix A.2). For each subject, the SSA score was calculated as the sum of the scores for the single items.

3.3.2 Participants and Procedure

The same subjects from the experiment in 3.1 also participated in this experiment. Since their RDTs have been already identified, in this experiment, they only performed the perception tests. In addition to the demographic questionnaires and the simulator sickness questionnaires, subjects also filled out the SSA questionnaire. The experiment was divided into two sessions. In the first session, the participants performed the blind veering test, with the following instruction:

When the program starts, you will see a starting position indicated by a green sphere. Walk to this position into the sphere and an arrow will appear. While inside this sphere, rotate on the spot until you see a tick (Figure 3.3). A completely dark screen containing only a red target will appear. Wait until you hear the step rhythms before you start walking. Try to follow the step rhythms as well as you can. After you have walked a short distance, the red target will disappear. Please do not stop walking when this happens, but try to continue walking naturally and as straight as possible until a stop sign appears on the screen.

The blind veering test consisted of 40 walks per subject, and took about 20 minutes to complete. In the second session, subjects first performed the Romberg test (10 minutes), the rod and frame test (10 minutes), the vection test (5 minutes) and finally the interoception test (20 minutes). Each subject was compensated 15CHF/hour for their participation.

Table 3.1 provides an summary of the perception tasks and their scores that could be potentially used to predict subjects' RDTs. In total, subjects completed the following six tasks: (1) A rod and frame test, which is the classical measurement of visual dependency regarding vestibular and proprioceptive signals; (2) a vection susceptibility measurement, which is an assessment of visual dependency during judgements of illusory self-motion; (3) a Romberg quotient measurement, which determines the visual dependency in postural stability; (4) a blind veering task, which quantifies non-visual, locomotion-related body control; (5) a heartbeat detection task, which scores the participant's interoceptive abilities; and (6) a somatosensory amplification questionnaire, which assesses an increased attention to uncomfortable bodily sensations.

3.3.3 Results and Discussion

In addition to the RDTs of the 60 subjects obtained from the previous experiment, the following data was recorded for each subject:

- The angles of the final rod position with respect to the true vertical in the 20 trials of the rod and frame test

- The vection onset time and the felt vection strength in 8 trials of the vection test

- The sway path length during eye open and eye closed conditions

- The 40 walking trajectories of the blind veering test

- The percentage of correct answers of the interoceptive test
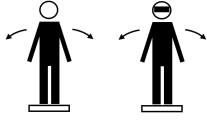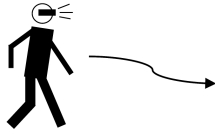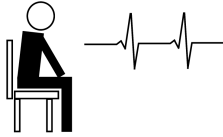
	Task	Score	Description
Visual dependency measures	**Subjective visual vertical (Rod and frame)** [245]: Subjects view a virtual rod surrounded by a tilted frame presented on an HMD. The task is to rotate the rod until it is aligned in a perfectly vertical orientation.	*Mean angle*: relative angular deviation from the true vertical	
	Illusory self motion (Vection) [139]: Subjects observe a white surface with black vertical stripes (on an HMD). The stripes start moving in one lateral direction and subjects (1) indicate the onset of self-motion and (2) rate the intensity of that sensation (on a 100-point scale).	*Mean onset time*: mean duration until a participant indicates a sensation of motion *Mean strength*: mean rated intensity of self-motion	
	Visually-assisted postural stability (Romberg quotient) [154]: Subjects stand on a balance board measuring centre of pressure (COP) coordinates. Standing must be as motionless as possible for two minutes. There are two trials, one with eyes open and one with eyes closed.	*Romberg quotient*: the total sway path length with eyes-closed divided by the total sway path length with eyes-open	
Blind locomotion control and interoceptive awareness	**Blind veering**[131]: Subjects repeatedly walk a given distance blindfolded with the task of walking as straight as possible.	*Mean angle*: mean lateral deviation per step	
	Interoception (heartbeat detection task) [140]: Subjects repeatedly hear series of beep-sounds synchronous or asynchronous with their own heartbeat and must identify synchrony or asynchrony of the playbacks.	*Interoceptive sensitivity*: percentage of correct answers in the heartbeat detection task	
	Somatosensory amplification (SSA)[14]: Subjects complete a 10-item questionnaire assessing an increased attention to uncomfortable bodily sensations.	*SSA score*: Total score in the SSA questionnaire	

Table 3.1: *Summary of the standard perception tests and their scores*

(a)   *(b)*
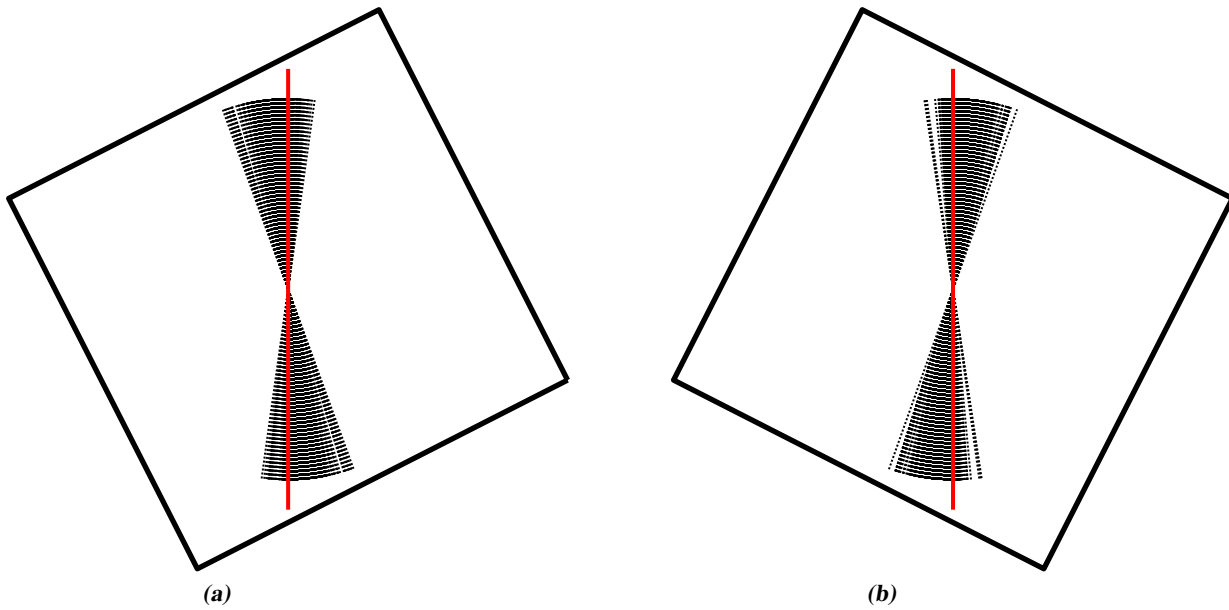
Figure 3.15: *Data collected from all subjects in the rod and frame test. The final rod positions in the corresponding frame conditions are shown separately in (a) and (b). The solid red lines indicate the true vertical*

- The score of the SSA questionnaire

Outliers were removed based on the median absolute deviation for all tests. Data points in each test were classified as outliers if they were located further from the median than three times the median absolute deviation, an approach considered as a very conservative outlier detection measure [159].

Rod and frame test   Figure 3.15 shows data from all subjects in the rod and frame test. It can be clearly seen that the tilted orientation of the frame has an influence on subjects' perception of the true vertical, in that, the final rod position tends to tilt in the same direction as the tilted frame. When taking into account the frame orientation, the mean angle between the final rod position and the true vertical over all subjects is 4.3° with a standard deviation of 4.5°, whereas positive angle indicates final rod position that tilts in the same direction as the frame, and vice versa. The distribution of this data can be found in Figure 3.16a. In the rod and frame test, the extent to which a person's perception of verticality is influenced by a tilted frame is taken as an indicator of their visual dependence. Therefore, based on the 20 trials, the visual independence score for each subject in the rod and frame test is calculated as the mean angle relative to the frame orientation. As numerous previous works had reported a gender difference in the rod and frame test performance, we first looked at the rod and frame score alone without considering the RDTs, and conducted an analysis to investigate if the same result could be reproduced [71, 252, 12, 2]. A significant correlation between rod and frame score and gender was found, in which men were less influenced by the tilted frame than women ($p < 0.005$) (see Figure 3.16b).

As gender and rod and frame score are correlated, in order to investigate whether the measure of visual dependence obtained by the rod and frame test could be used to predict a person's RDTs, a linear mixed model was constructed, in which the RDTs is the dependent variable, curvature direction and the rod and frame test score are independent variables and subjects is a random variable. The model becomes:

$$\text{threshold} \sim 1 + \text{curvature direction} + \text{rod and frame score} + (1|\text{subject}). \tag{3.24}$$

The hypothesis is that, the higher a person scores in the rod and frame test (i.e. the more visual dependent
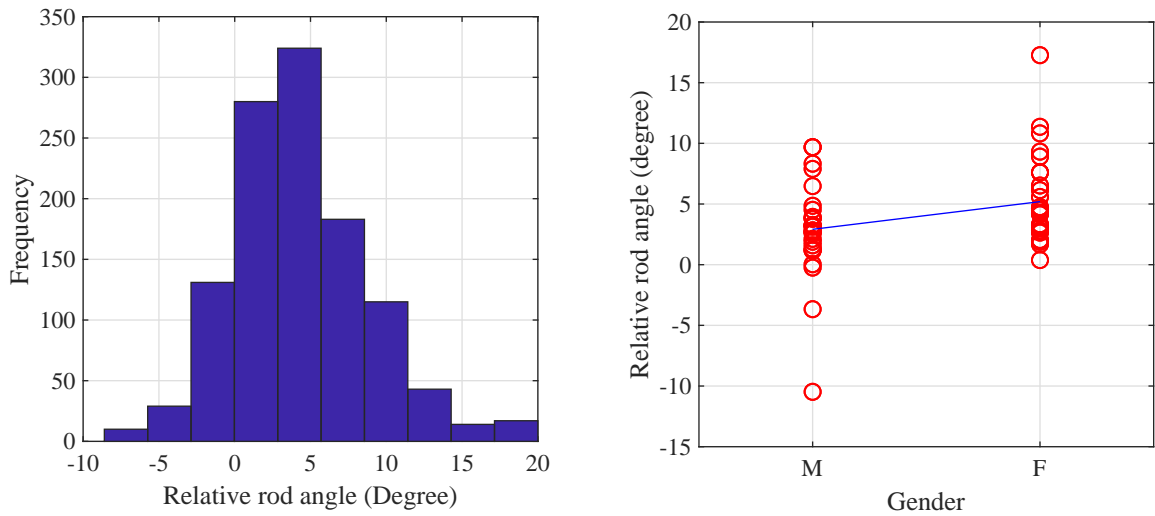
(a) *Distribution of relative angles between the rod and the true vertical, taking into account the frame orientation. Positive values indicate rod position tilting in the same direction as the frame and vice versa*

(b) *Significant effect of gender on the rod and frame score*

Figure 3.16: *Rod and frame score*

they are), the higher their RDTs are. Results showed a significant effect of the rod and frame score on RDTs ($p < 0.001$). As there was no significant effect of the curvature direction on RDTs, we computed the average RDT values from both left and right directions, performed the Pearson's correlation test and obtained a correlation coefficient of 0.37. From Figure 3.17, it can be observed that while there is a relationship between the rod and frame score and RDTs (as indicated by the statistically significant effect), the correlation is not strong (0.37) and therefore it is not possible to use the rod and frame score alone to accurately predict an individual's RDT. However, this result could still be used to provide an estimated range of curvature gains between which an individual's RDT most probably lie. The average of this range could then be used in RDW applications, which could be an improvement to the current practice where the same curvature gain is used for all users. Nevertheless, whether such improvement could be achieved requires further studies and is not in the scope of this work.

Vection test Based on the 8 vection trials, the vection scores for each subject were calculated as the mean of the vection onset time, and the mean of the subjective vection strength. Since vection susceptibility has long been known as a measure of visual dependency in visual-vestibular interactions [139], it is hypothesized that subjects with a low vection susceptibility (i.e. long vection onset time and/or low vection strength) would also show a poor awareness of any imposed redirection while walking. Similar to the rod and frame analysis, before exploring the relationship between vection susceptibility and RDTs, the correlation between vection onset time, vection strength and gender is first investigated using a linear model:

$$\text{vection onset time} \sim 1 + \text{vection onset strength} + \text{gender} \qquad (3.25)$$

Results showed no significant impact of gender on vection onset time. There is, however, a significant impact of vection strength on vection onset time and a medium correlation with correlation coefficient $R = -0.45$ (see Figure 3.18a). The negative correlation between vection onset time and vection strength agrees with the assumption that if a person is more susceptible to vection, they would also tend to experience it stronger. However, there is no significant effect of gender on vection onset time. On one
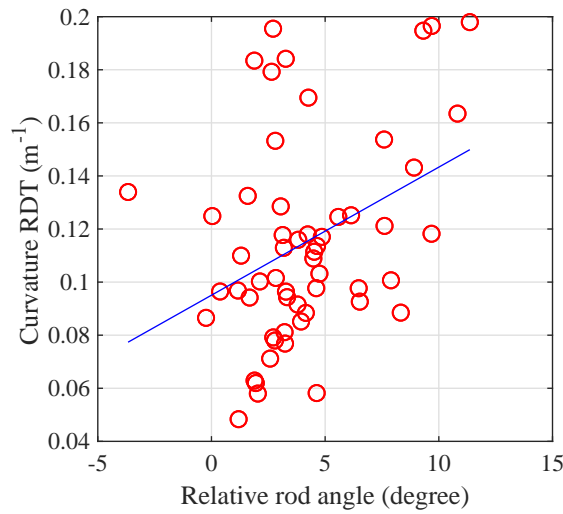
Figure 3.17: *Correlation between the curvature RDTs and rod and frame score*

hand this finding agrees with a more recent study conducted using an immersive virtual optokinetic drum where no gender impact was found [269]. However, it contradicts previous findings about gender effect on vection susceptibility in real optokinetic drums [137, 54, 141]. This result opens up an interesting discussion about whether vection could be induced similarly in a virtual environment as compared to in an optokinetic drum, and if virtual reality technology as of now is good enough for the study of vection. As vection is strongly influenced by the field of view, which is limited in the HMD, it is possible that vection can be much more easily induced in an optokinetic drum than a virtual environment [203, 15]. Additionally, the illusion could be more strongly enforced when there are perception and cognitive cues that indicate the potential of actual motion, i.e. the chair the subjects sit in can be automatically rotated [209]. Having been inside an optokinetic drum personally, I found that the illusion induced in the real drum was so convincing to the point that one would doubt oneself if the chair was really not rotating. The same compelling experience could not be felt in a virtual counterpart. Nevertheless, up to the point of writing this book, no existing work has been done on comparing the experience in a real and virtual optokinetic drum and the discussion provided here remains only a speculation.

Using vection onset time and vection strength as two separate scores, two linear mixed models were constructed with threshold as the dependent variable, vection onset time (or vection strength), gender, and curve direction as independent variables, and subject as random variable:

$$\text{threshold} \sim \text{vection onset time} + \text{gender} + \text{walking speed} + \text{curve direction} + (1|\text{subject}) \quad (3.26)$$

$$\text{threshold} \sim \text{vection strength} + \text{gender} + \text{walking speed} + \text{curve direction} + (1|\text{subject}) \quad (3.27)$$

Results showed a significant effect of gender ($p < 0.001$) and walking speed ($p < 0.001$), which agrees with previous findings in section 3.1 and of vection onset time (p<0.001) but no significant effect of vection strength on RDTs. However, the significant effect of vection onset time on RDTs is in the opposite direction of the original hypothesis: subjects with smaller vection onset time, who accordingly were experiencing the illusion of vection faster, were performing better at detecting redirection in the VE (Figure 3.18b). Note that there was no significant correlation between visual dependency as established by the rod and frame test and the vection onset time. The absence of a correlation between the two measures might be explained by the different natures of the static rod and frame task and the more dynamic vection measurement. The two tests also show clear methodological disparities. In contrast to the rod and frame test, the quantitative measures applied in vection susceptibility tests rely heavily on subjective reporting. In fact, the missing objectivity in vection research is a frequently cited methodological drawback [195].
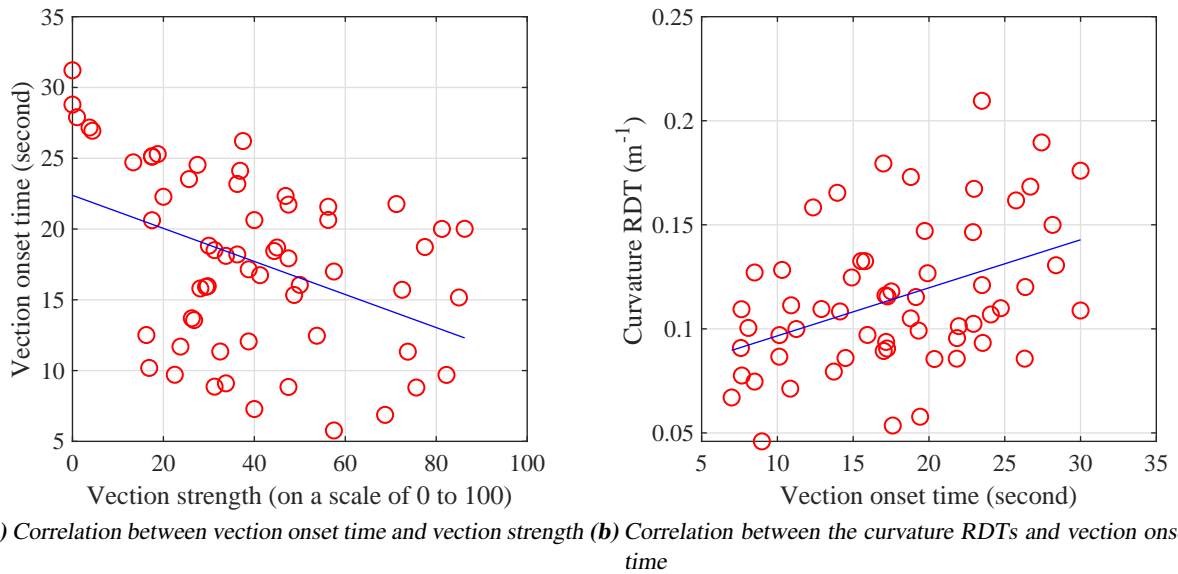
(a) Correlation between vection onset time and vection strength *(b) Correlation between the curvature RDTs and vection onset time*

Figure 3.18: *Vection results*

Considering the highly subjective nature of the vection test, there could be other possible explanations of the observed relation between redirection thresholds and vection onset times. Perhaps subjects with short vection onset times were simply better in experiencing the illusion because of a more rapid visual-vestibular integration. In the VR setting, this integration advantage may have led to a better detection of the redirection manipulation. Nevertheless, it is important to again emphasize that illusions of self motion are not as easily elicited in an HMD than under conditions of full field optic flow observed in an optokinetic drum due to its smaller field of view. Without further investigation into how vection is induced in VR and how different it is compared to an optokinetic drum, it can not be concluded whether the vection test could be effectively used as a tool to predict curvature RDTs.

Romberg test   Using the recorded center of pressure coordinates from the Wii board, the total sway path length was calculated for the eyes open and eyes closed conditions. In order to quantify the influence of vision on sway, the Romberg quotient was calculated for each subject. This is the common measure of visual dependency in sway analysis [154]. The Romberg quotient is derived by dividing the total sway path length with eyes closed by the total sway path length with eyes open. Romberg quotient is in general larger than one, as people most of the time tend to sway more during eye closed condition, resulting in a longer sway path compared to the eyes open condition. In fact, over all 60 subjects, the average Romberg quotient was 1.2, the lowest quotient obtained was 0.91 (Figure 3.19b) and the highest quotient obtained was 2.4 (Figure 3.19b). Again, it is hypothesized that subjects who are less visually dependent in balance control, i.e. whose Romberg quotient is close to 1, are more sensitive to detect being redirected while walking toward a visual target. No gender effect was found and the linear mixed model analysis with RDTs being the dependent variable, Romberg quotient and gender being the independent variables and subject being the random variable showed a significant effect of Romberg quotient on RDTs. However, like in the case of vection, the findings are opposite to the original hypothesis. The higher a subject's Romberg quotient is, i.e. the more they depend on visual cues for balancing, the better they are at detecting redirection (lower RDTs). In order to elucidate the counter-intuitive direction of the observed relationship, the individual Romberg quotients and the sway path length observed under eyes closed and under eyes open conditions were tested for correlation. It was found that the Romberg quotient was highly correlated with the total sway path length in the eye closed condition (R = 0.57, p < 0.001) and
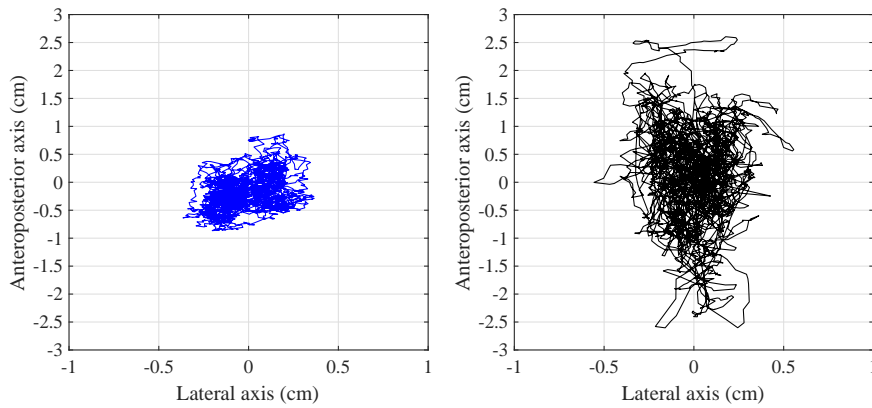
(a) Sway path with open eyes (left) and closed eyes (right) of a subject with Romberg ratio of 2.4
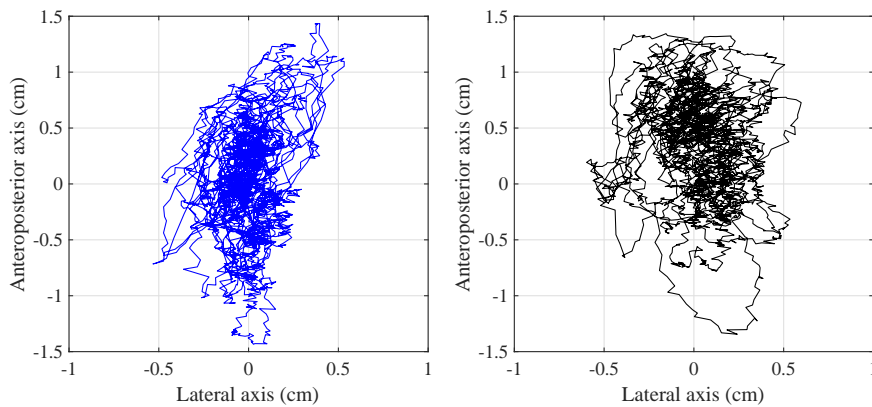
(b) Sway path with open eyes (left) and closed eyes (right) of a subject with Romberg ratio of 0.9

Figure 3.19: *Recorded sway paths*

more weakly correlated with the sway path length in the eye open condition (R = - 0.34, p = 0.008). This raises doubt in traditional interpretations of the Romberg quotient as primarily reflecting the ability to dampen sway by visual information. It rather suggests that the size of the quotient is a more direct function of body sway in the absence of vision. This indicates that a lower postural balance stability is associated with a better ability to detect redirection. One possible explanation for this association is that subjects with relatively poor balance control are also those who are more easily thrown out of balance by even small curvature gains. Even though only post-hoc, this interpretation should be tested in future work by assessing body sway during locomotion in a VE with various forms of redirection. Previous studies have reported correlations between field dependence in the rod and frame test and postural stability. Specifically, reliance on visual cues in the rod and frame test were associated with a worse postural stability in balance tests[121, 122]. No such correlations were found in the present dataset. Also, vection strength has been described as positively correlated with the Romberg quotient [195], but again these two parameters proved to be uncorrelated in the present experiment (see Table 2).

Blind veering test   For the blind veering test, each subject performed 40 walks across the room and their head positions were tracked. Figure 3.20 showed all paths of three different subjects. It can be seen that on average the subject shown in Figure 3.20a had a tendency to veer to the right, the subject in Figure 3.20c walked on average straight ahead, and the subject in Figure 3.20b was an outlier with quite erratic behaviour. Based on this head tracking data, which contains periodic sway movements to the sides, the walking paths of subjects were estimated using the algorithm proposed by Wendt et al.
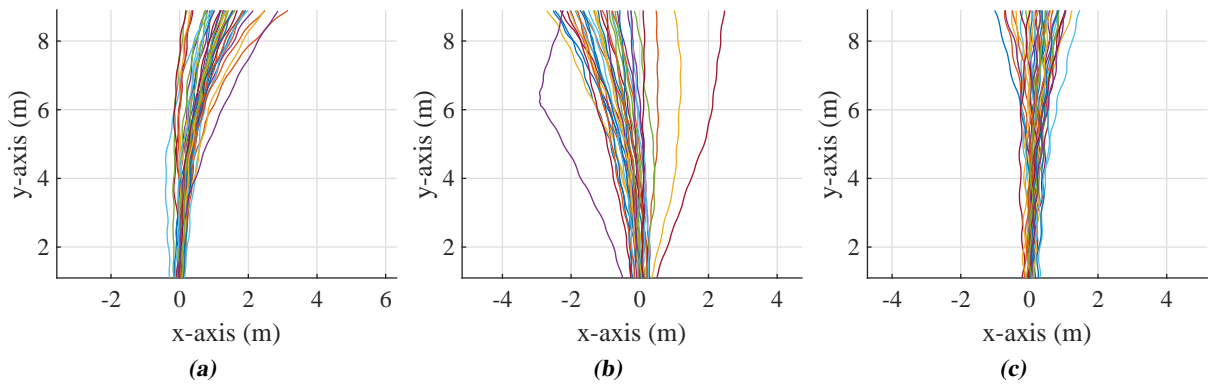
Figure 3.20: *Blind veering paths of three different subjects*

[271]. The intersections between this fitted path and subject real path were then computed, and the steps can be estimated as the lines connecting these intersection points (see Figure 3.21a). Based on the step vectors, the blind veering angle for each step, i.e. the deviation with respect to the preceding step, was calculated and the average angle was obtained for each subject (see Figure 3.21b). This measure reflects how straight a subject walked on average. It is hypothesized that subjects with lower average veering angles would be more aware of their spatial orientation, and hence more sensitive when being redirected onto a curve. Preliminary analysis found that there is no significant effect of gender on the average veering angle, and therefore a linear model was fitted with the average threshold of both left and right curvature direction as the dependent variable, and average blind veering angle and gender as independent variables. Contrary to our hypothesis, results showed no significant effect of average veering angle on RDTs. As the original hypothesis relies on the assumption that if subjects are more sensitive with vestibular and proprioceptive cues during unsighted locomotion, they are more likely to give less weighting to visual cues, our results have shown that this may not be the case. Therefore, one explanation for the lack of significant effect could be that in the presence of visual cues, this sensitivity to vestibular and proprioceptive may be suppressed or not taken into account during the weighting process. In summary, our results showed that a subject's performance in the blind veering test could not be used as a predictor for curvature RDTs.

Interoceptive test and SSA questionnaire The data of four subjects in the interoception test could not be obtained because the heartbeat signal could not be reliably picked up by the electrodes. For each of the remaining 56 subjects, the interoceptive test score was calculated as the percentage of correct answers over 40 trials. It was hypothesized that a better monitoring of one's internal bodily state, i.e. higher percentage of correct answers, would be associated with a better detection of being redirected. However, no significant correlation emerged between subjects' cardiac awareness reflected by the interoceptive test score and their RDTs. From the results obtained, a word of caution is needed about the suitability of the heartbeat detection task for the present context. Although as a group, subjects were able to distinguish between synchronous and asynchronous conditions, performance was not overwhelming (mean success rate: 54.7% against a chance rate of 50%). On an individual basis, only 5 out of 56 subjects achieved a performance statistically better than chance. A less difficult interoceptive task may have produced a different result. In the SSA questionnaire, each subject answered 10 questions about their sensitivity to uncomfortable bodily sensation and their score was calculated as the sum of scores from all 10 questions. Again, the hypothesis was that a high score in this questionnaire, which correspond to subjective higher sensitivity to bodily sensation, predicts a high RDT. Nevertheless, this hypothesis could not be proven, as this score is also uncorrelated to curvature RDTs. Together, these null findings in
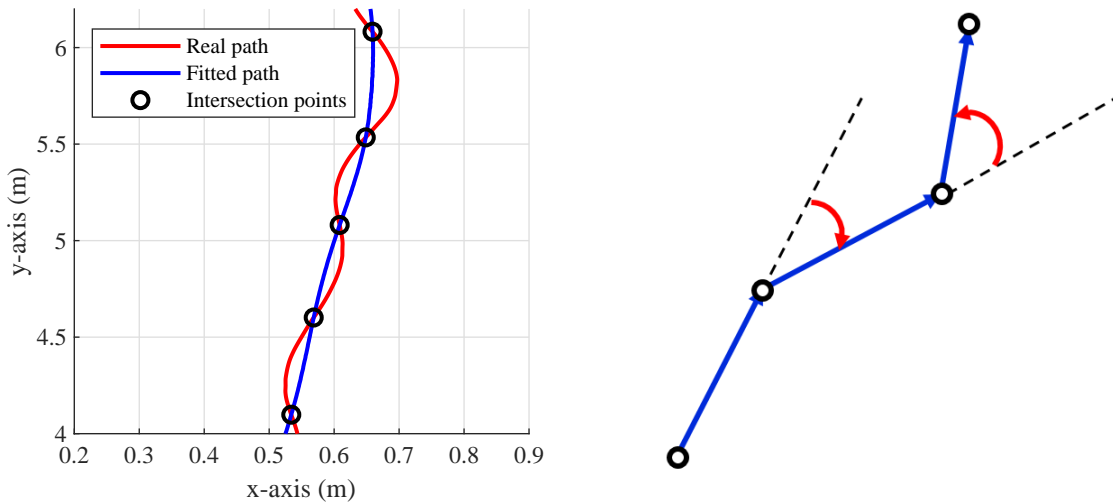
(a) *Fitted path used in the calculation of walking steps and veering angles. Axes are not equally scaled in order to amplify the sidewards sway movements*

(b) *Calculation of veering angle after each step*

Figure 3.21: *Blind veering angle calculation*

cardiac monitoring and questionnaire-based interoceptive sensitivity make it improbable that awareness of gait distortions heavily relies on interoceptive variables.

3.4 Conclusion

In this chapter, a new procedure of threshold identification using a Bayesian adaptive method called QUEST was proposed. This proposed method improved classical methods of constant stimuli methods by only testing at stimulus level close to the threshold, and therefore significantly reduces experiment time. The true two-alternative forced choice task was also proposed, as compared to the pseudo two-alternative forced choice task that has been adopted in many existing studies, but contains inherent bias and can not be used to identify individual thresholds. Instead of the commonly used visual task where subjects are required to maintain a certain distance from a visual target, a non-visual method of regulating walking speed using audio step rhythms was also proposed. Even though this method could be used to produce significantly different walking speeds when the difference between the predefined speeds is large enough, it could not be used to regulate users' speed accurately. Specifically, subjects tended to walk faster when the predefined speed was too slow, and slower when the predefined speed was too fast. It is nevertheless unclear if the visual method of regulating speed has a better performance either, as it was not reported in existing studies. Therefore, speed regulation in VR for RDW studies remains an under-investigated problem and requires further research.

An experiment with 60 subjects was conducted and their individual curvature RDTs were obtained. It was found that there is high variability in individuals' curvature gain thresholds, which confirms the importance of applying an individual curvature gain for each individual user to maximize their VR experience and immersion. There was a significant effect of walking speed on curvature RDTs. Therefore, during an RDW application, it is advisable to adjust the gain dynamically for each subject depending on their walking speed. The obtained results also showed that there is a significant gender difference in detecting redirection and that men are on average more sensitive to curvature redirection than women.

While the efficiency of threshold identification procedure has been increased compared to existing methods by employing the QUEST method, further improvement is still required. In the ideal case, it should take very little time to prepare a user for an RDW application, without having to have them walking back and forth for about 40 minutes in order for their RDTs to be identified. A series of perception tests was therefore proposed as potential tools for this purpose. As RDW works based on the fact that vision dominates when there are conflicts between visual and non-visual information, perception tests that are designed to measure visual dependence and bodily sensitivity were proposed. These tests include rod and frame, vection, Romberg, blind veering, interoception and the somatosensory questionnaires. The same 60 subjects performed these tests in addition to the threshold identification test. Out of these proposed tasks, the most prominent relation to RDTs was found in subjects' adjustments of the visual vertical in the rod and frame task. Even though the correlation between the rod and frame score and RDTs is not a strong correlation, the rod and frame task could still be used as a preliminary tool to indicate the range of curvature gains in which an individual's threshold lies. The average of this range could then be used directly in an RDW application, or the range can be used as the starting range for the QUEST identification method, in which the number of trials could be reduced.

4

Impact of Extrinsic Factors on Redirected Walking Thresholds

The results from Chapter 3 showed that there could be significant differences in an individual's perception of curvature redirected walking, depending on, for example, their gender, walking speed, and their multi-sensor integration process, so-called intrinsic factors. However, an RDW application does not only involve an individual alone, but also consists of different external settings such as different environments, the tasks to be performed, the presence of other agents or users in the scene, etc. This chapter is dedicated to the understanding of how much some of these external factors influence users' perception of redirected walking. The findings of this chapter would augment the knowledge of how to design a virtual environment where higher RDW gains could be applied, and consequently improving usage efficiency of the limited physical tracking space.

4.1 Environment Size [1]

Up to the point of this thesis, limited work has been performed on the effects of environment's design on RDTs. Steinicke et al. performed a threshold identification study where they presented different visual appearances of the environment and applied textures of different visual density to the environment, consequently generating different amount of optical flow [238]. They found that users tend to be less sensitive to RDW when the amount of optical flow is small. However, they remarked that the threshold identification method of a simple up-staircase that was used has drawbacks and is prone to bias. In another study, Paludan et al. varied the number of objects in the scene to investigate the effects of visual density on rotational gain thresholds and could not establish a relationship between visual density and rotational gain thresholds [196]. Considering that high visual density leads to higher optical flow, the two aforementioned studies seem to address the same question about the effects of optical flow on RDTs, but their observations are rather contradictory. Given that there are differences in the design of the environments in the two studies and certain limitations in their threshold identification methods, it is not possible to conclude whether optical flow has an effect on RDTs. While investigating the performance of different RDW algorithms in a constrained world, Hodgson et al. remarked that users tended to notice

---

[1]Parts of the section were published in [191]

(a) 2m room   *(b) 10m room*
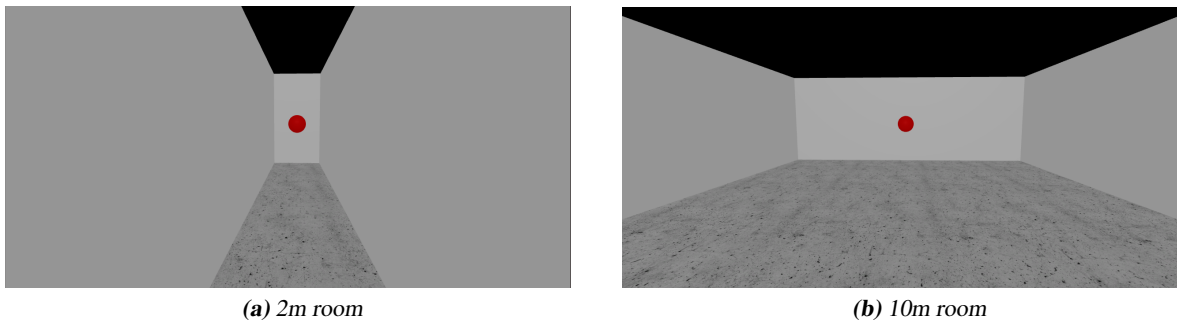
Figure 4.1: *Two different room sizes used in the experiment*

the curvature gains in an aisle more than in a forest [113]. This observation suggests that the dimension of the environment may play a role in the detection of RDW.

Given the aforementioned observations, studies and their limitations in terms of experiment designs and methods, a large scale study was performed to narrow the gap in understanding the effects of environment design on RDTs. While both optical flow and environment size potentially have an effect on RDTs but no formal study has been performed on the environment size, in this experiment, we focus on investigating the effect of size of the environment on RDTs.

4.1.1 Experiment Design

Since factors such as objects and textures could provide optical flow and potentially affect the curvature gain thresholds, two scenes were designed corresponding to two room size conditions to be as plain as possible. Both scenes contain a red target, which is located 7.5m from the starting position of the user, four surrounding walls with simple shading and no texture on the walls. The width of the room in one condition is 10m, while it is 2m in the other condition. In both conditions, the room length is 10m. Figure 4.1 shows the two scenes used in the experiment. Each subject only participates in one room condition, making room size a between-subject variable.

Similar to the set-up in Section 3.1, before the experiment, subjects' heights are collected and their personal step rhythms are generated. For each room condition, each subject has to walk with two speed conditions: 0.75m/s and 1.25m/s regulated by the step rhythms. The left and right thresholds are identified separately for each user, resulting in four threshold values of four psychometric functions to be found per user. Speed and curvature direction are therefore within-subject variables.

Also similar to the description in Section 3.1, using the 2AFC method, in each trial each subject walks to the red target two times. In only one of the two walks, a curvature gain is applied and the order is randomized between trials. Four separate QUESTs handle the four psychometric functions and calculate the next curvature gain value to be tested for each function. These four next values are selected randomly to be presented in the next trial. For each QUEST, 40 trials are required, resulting in a total of 160 trials per subject. During the trials, the whole process of guiding the users to the starting positions, updating the QUESTs with subjects' responses and computing the next curvature gain value is automated and does not involve the experimenter. Subjects respond to the 2AFC question using a built-in eye tracker.

The experiment set-up consists of an Oculus DK2 with a built-in SMI eye tracker and an Intersense IS-1200 inside-out optical tracking system mounted on top, providing 6-DOF positional tracking at 180Hz. A shield is added in front of the headset to prevent users from seeing the floor. The scenes are optimally designed in Unity to run at the HMDs maximum frame rate 75Hz. The whole setup is powered by

a backpack-mounted notebook. The available tracking space is 12m x 6m. Subjects also wore noise cancelling headphones, where the step regulating rhythms are played.

This experiment was combined with the experiment from Section 3.1, which includes 60 subjects (aged from 18-35 (M=25.1, SD=3.9), 30 male and 30 female, right-handed, with normal or corrected-to-normal vision). Thirty subjects performed the task in the 2m room condition, while the other thirty subjects were exposed to the 10m room condition. In each room size condition, there is the same number of female and male subjects.

4.1.2 Results and Discussion

For each subject, four threshold values were obtained corresponding to the two speeds and two curvature directions: left slow, left fast, right slow and right fast. To take into account the known effect of speed (within-subject variable, i.e. each subject performed all speed conditions), gender and room size conditions (between-subject variables, i.e. each subject performed only one room size condition), a linear regression was fitted which includes speed, gender and room size as fixed effects and subjects as a random effect. The full mixed-effect model therefore becomes:

$$\text{threshold} \sim 1 + \text{room size} + \text{speed} + \text{gender} + (1|\text{subject}) \tag{4.1}$$

Results reconfirmed that speed and gender have significant effects on curvature gain RDTs, while room size does not ($p > 0.05$). This result rejected the original hypothesis that room's dimension significantly affects curvature gain thresholds. This also contradicts with the observations by Hodgson et al. that their subjects recognized curvature gains more in the aisle than in the open space [112]. One possible explanation for this finding could be that it is not the room dimension, but the amount of optical flow generated by the scene or the combination of room dimension and optical flow that affect curvature gain thresholds. Since there is no texture on the walls, the amount of optical flow generated in both cases is mostly similar. It could also be possible that there is a small effect that can not be recovered in a between-subject design since there is a high variability in individual thresholds. A within-subject design where each subject's thresholds are measured in both room size conditions could have been more suitable. In summary, it is not possible to reach a conclusion about the effect of room size alone on curvature RDTs and therefore when only plain textures are involved, curvature gains do not need to be adapted for different environment size. However, further investigation should look at the interplay between room size and optical flow and considering the high variability between individuals, a within-subject design should always be preferred.

4.2 Feeling of Presence

Feeling of presence can be referred to as the sensation of being truly immersed the virtual scene. The stronger the feeling of presence, the more difficult it is for users to distinguish between the virtual scene and reality and the more they react to virtual events as if they were real. A typical example of this is: one could see oneself standing on a plank on top of a high building in a virtual environment, and despite knowing that it is not real, it requires immense effort to convince oneself to step forward. Thanks to this strong feeling of presence that VR can induce, a range of interesting applications could be created. VR technology allows life-like but controlled and safe scenarios to be constructed, potentially as a treatment for psychological dispositions. For example, using a confrontational therapy approach, VR has been successfully used to improve anxiety disorders such as acrophobia or fear of spiders [82, 88]. Additionally, VR can be used to provide the possibility to experience an event through another person's perspective,

for example, to help elicit empathy and compassion for disadvantaged society members such as homeless or elderly people [108, 194]. Since feeling of presence is one of the most crucial aspects of VR, in the context of RDW, it is also important to understand whether the feeling of presence has an effect on how a user perceives redirection. The questions being raised here are: does a strong feeling of presence cause a user to be so immersed that they do not notice the manipulation? Or rather reversely, would being more immersed in a virtual environment enable a user to detect a visual-vestibular conflict better? In order to answer these questions, it is necessary to first understand how the feeling of presence could be enhanced (or reduced) in VR.

One potential way to improve the feeling of presence is by allowing the user to see their body presented as a virtual avatar in the virtual environment [230]. In the presence of an avatar, the user could experience a sense of embodiment, which is strongly related to feeling of presence and describes the extent to which a user identifies with their avatar. The sense of embodiment can be separated into three distinct components: a) the sense of self-location: the sensation that one's own body is being located where the virtual body is, b) the sense of agency: the sensation of having motor control over the virtual body, and c) the sense of body ownership: the sensation that the seen virtual body is one's own [138]. Various aspects of this virtual avatar have an influence on the sense of embodiment. For example, it has been shown that the avatar's appearance and level of realism affect the sense of body ownership and how they perceive conflicting cues [166]. More specifically, when the avatar has a more human-like body as compared to a plastic mannequin, subjects had a more convincing illusion that the body was their own, hence, stronger feeling of presence, and the incongruent cues were not detected as incorrect. If this is the case, then it could be hypothesized that a stronger feeling of presence would lead to a higher RDT. Additionally, the congruency between a subject's performed motion and the visual motion seen on the avatar is also an aspect that is relevant to the sense of embodiment. Liang et al. have termed this congruency as visual agency [160]. In other words, when the movement of the observed virtual body corresponds correctly to their own real movement, a person feels that they have control, or visual agency, over that virtual body. It has been shown that visual agency improves the sensation of ownership of a virtual hand in the rubber hand illusion [130, 40] and even could induce a feeling of agency over the body of someone else when that person performs the same body movement as oneself [201].

Another important aspect that contributes to the feeling of presence is the perspective with which the virtual body is viewed. In the first person perspective (1PP), the virtual body is located at the same position as the subject and all spatial tasks such as walking, reaching, etc. are performed with respect to coordinate system centred on the subject's physical body (eco-centric reference frame). In the third person perspective (3PP), the virtual body is located away from the subject and they view the virtual body from above [221], behind [60, 94], or from the side [231]. All spatial tasks are performed with respect to a coordinate system centred on a reference point in an extrapersonal space in world coordinates (allocentric reference frame). It has been shown that subjects felt a stronger sense of body ownership and self-location in the 1PP condition compared to the 3PP condition, but there was no significant difference in the sense of agency [94, 231]. Due to the higher sense of body ownership in the 1PP condition, it has also been shown that subjects reacted more strongly to threat in the 1PP condition [61, 231, 86]. In a drawing task where subjects were asked to draw vertical lines while looking at a virtual hand performing the motion, subjects were more "manipulated" by the deviation from the straight path of the virtual hand in 1PP than in 3PP [35]. It could possibly be inferred that the stronger sense of body ownership in 1PP leads to being more easily "manipulated", which agrees with findings from Maselli et al. as well [166]. In this sense, it could be hypothesized that subjects would have higher RDTs in the 1PP condition compared to the 3PP condition.

All existing works point to the fact that a higher sense of presence could lead to higher RDTs. However, in the context of RDW, little work has been done to investigate this hypothesis. The only exception
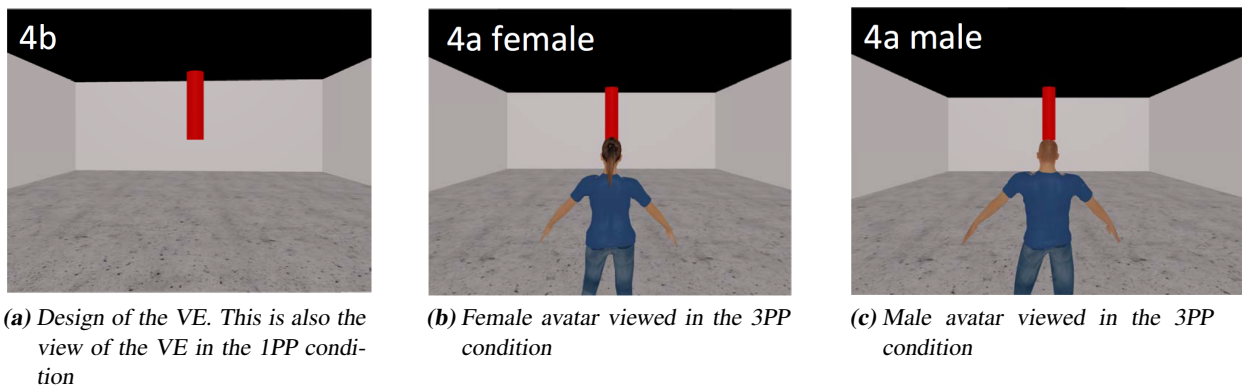
(a) *Design of the VE. This is also the view of the VE in the 1PP condition*

(b) *Female avatar viewed in the 3PP condition*

(c) *Male avatar viewed in the 3PP condition*

Figure 4.2: *Location of the virtual camera in the 1PP and 3PP conditions. The red pillar represents the target. The blue circle represents the virtual avatar's position*

consists of a study by Kruse et al. which investigated the effect of looking at one's feet while walking on the detection threshold of translational gain [145]. The authors found no significant effect of the presence of the feet on translational RDTs. However, it was also found that the presence scores for the with and without avatar conditions were not significantly different, and thus could not reach a conclusion about the effect of sense of presence on RDTs.

In this work, through the use of virtual avatars, the effect of the feeling of presence on curvature gain RDTs is investigated. Based on existing findings about how the feeling of presence is affected by different virtual avatar aspects, the two prominent factors that can be used to regulate the feeling of presence were selected: the congruency between the subject's virtual and real body movements and subject's viewing perspective on the avatar. More particularly, it is hypothesized that the curvature RDTs are higher when the avatar body movement is congruent with the subject's body movement than when it is not; and that the curvature RDTs are higher when the avatar is viewed in 1PP as compared to 3PP.

4.2.1 Experiment Design

In order to limit the effect of other external factors on RDTs, the virtual environment is constructed similarly to the design used in previous experiments. The virtual environment is composed of an empty room of 10m × 10m and a red cylinder used as the target, located 7.5m away from subjects' starting position (Figure 4.2a). Prior to the experiment, subjects's heights were collected and a gender-matched avatar was created for each subject corresponding to their height (see Figures 4.2b and 4.2c).

The experiment consists of two perspective conditions (1PP and 3PP) and two avatar body movement congruency conditions (congruent and incongruent). In the *1PP condition*, the virtual camera is located at the same location as the virtual avatar's head. When the subject looks down, they can see their body located at the same place as their physical body. When no curvature gain is applied, the translation and rotation of the subject's body in reality result in the exact translation and rotation of the avatar body (Figure 4.3a). In the *3PP condition*, the virtual camera is located 2m behind and 1m above the virtual avatar such that the whole avatar's upper body is visible. When no curvature gain is applied, the translation of the subject's body results in the same translation of the avatar body. Originally, the 3PP was designed such that the rotation of the subject's physical body would result only in the rotation of the virtual body and subjects always see the virtual avatar in front of them. However, out of the four pilots subjects, two had no problem completing the whole experiment, while two suffered from severe motion sickness very early on in the 3pp condition. Due to this extreme reaction, the 3PP condition was

(a) 1PP condition *(b) 3PP condition*
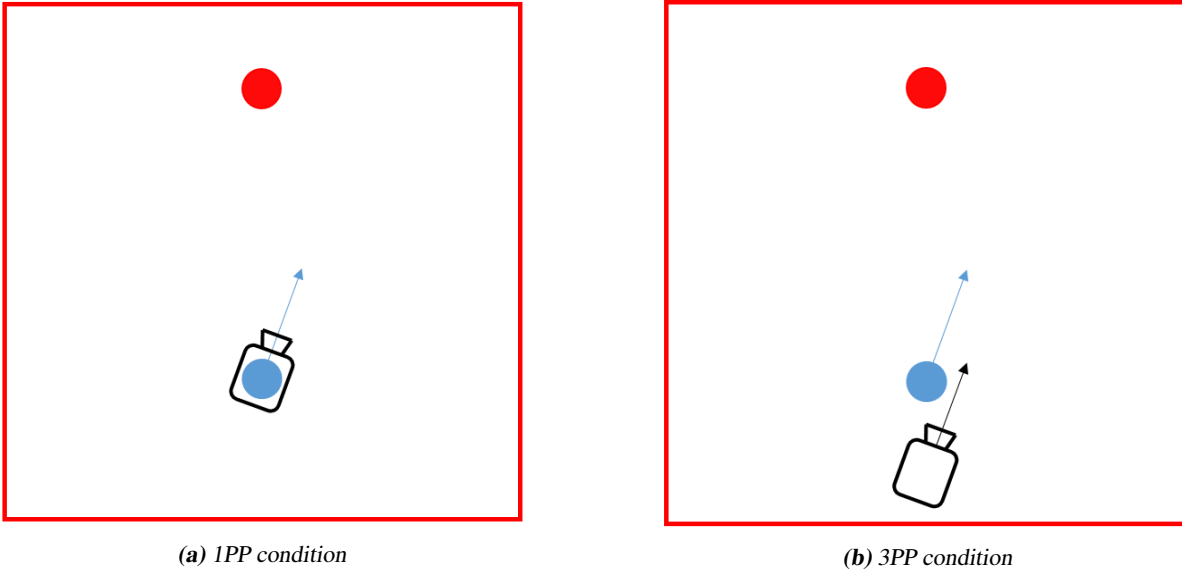
Figure 4.3: *Location of the virtual camera in the 1PP and 3PP conditions. The red circle represents the target. The blue circle represents the avatar's position*

redesigned, and the rotation of the subject's physical body would result in the rotation of both the virtual body and the virtual camera around their own axes (Figure 4.3b). For both conditions, when a curvature gain is applied, the whole environment is rotated around the virtual camera position.

In the *congruent condition*, the avatar body movement follows the subject's physical body movement. In the 1PP condition, this means when subjects bring up their hands in front of their face in real life, they would also see the virtual body's hands. In the 3PP condition, subjects would see the virtual avatar in front of them bringing their hands in front of their face. In the *incongruent condition*, the avatar body movement was pre-animated and does not follow the subjects' physical body movement at all.

The experiment set-up consists of an Oculus DK2 with a built-in SMI eye tracker and an Intersense IS-1200 inside-out optical tracking system mounted on top, providing 6-DOF positional tracking at 180Hz in a tracking space of 13.3m × 6.6m. A shield is added in front of the headset to prevent users from seeing the floor. The scene was optimally designed in Unity to run at the HMD's maximum frame rate 75Hz. In order to track subject's body movement, a Noitom motion capture suit was used (Figure 4.4a). The Noitom motion capture suit consists of 32 motion sensors attached to different body parts, each containing an inertia measuring unit (IMU), to measure the relative positions of head, legs, arms, and fingers with respect to the hip position. Based on the hip sensors, the absolute position of the body in the inertia frame of reference could also be obtained. However, as this absolute position was calculated based on the hip IMU, it suffers significantly from drift, and therefore only the relative positions of the other body parts with respect to the hip was integrated into Unity. The hip position was therefore controlled by the data obtained from the Intersense head tracking (Figure 4.4b), while the rest of the body movement was controlled by the data from the motion suit. Let T_0^{Head} be the transformation matrix from the inertia frame of reference O to subject's head where the Intersense is mounted (obtained from the Intersense tracking data) and T_{Hip}^{Head} be the transformation matrix from the hip frame of reference to the head frame of reference (obtained from the motion suit). The transformation matrix from the inertia frame of reference to the hip T_O^{Hip} can be calculated as:

$$T_O^{Hip} = T_O^{Head} T_{Hip}^{Head^{-1}} \qquad (4.2)$$

(a) *Experiment set-up with the Intersense IS-1200 track-*
ing 6-DOF head position, and the Noitom motion suit
tracking body movement
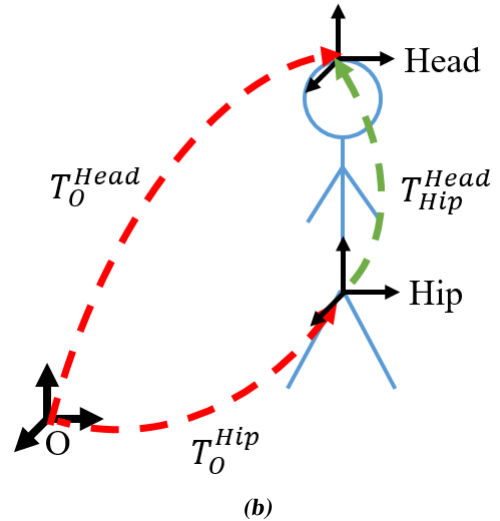
(b)

Figure 4.4

4.2.2 Participants and Procedure

Thirty subjects (aged from 21-34 (M=25.5, SD=3.3), 15 male and 15 female, right-handed, with normal or corrected-to-normal vision) participated in this experiment. None of the subjects had taken part in previous RDTs identification experiments, and therefore were completely naive to the purpose of the experiment. After having signed the consent form and understood the procedure of the experiment, the subject put on the motion suit, the backpack with the attached laptop, and the HMD. Each subject was exposed to three conditions (congruent 1PP, congruent 3PP and incongruent 3PP), performed in three separate blocks. The incongruent 1PP condition was not included as the incongruency cannot be observed while walking in the 1PP condition. The order of all three conditions was randomized for each subject to counteract learning effects. Each block was carried out with the following procedure:

- Pre-experiment questionnaire: subjects filled out the Simulator Sickness Questionnaire (SSQ) in-dicating their subjective physical state before the experiment block.

- Calibration: at the start of each block, subjects performed a number of predefined poses to calibrate the motion suit (Figure 4.5). These poses were shown in the HMD, and subjects performed and held these poses sequentially when a beeping sound was played. Due to the limitation of the IMU-based motion tracking system, tracking quality worsened over time and recalibration had to be performed again every five walks. Each calibration took on average five minutes.

- Familiarization: once the first calibration of the block was completed, subjects would see them-
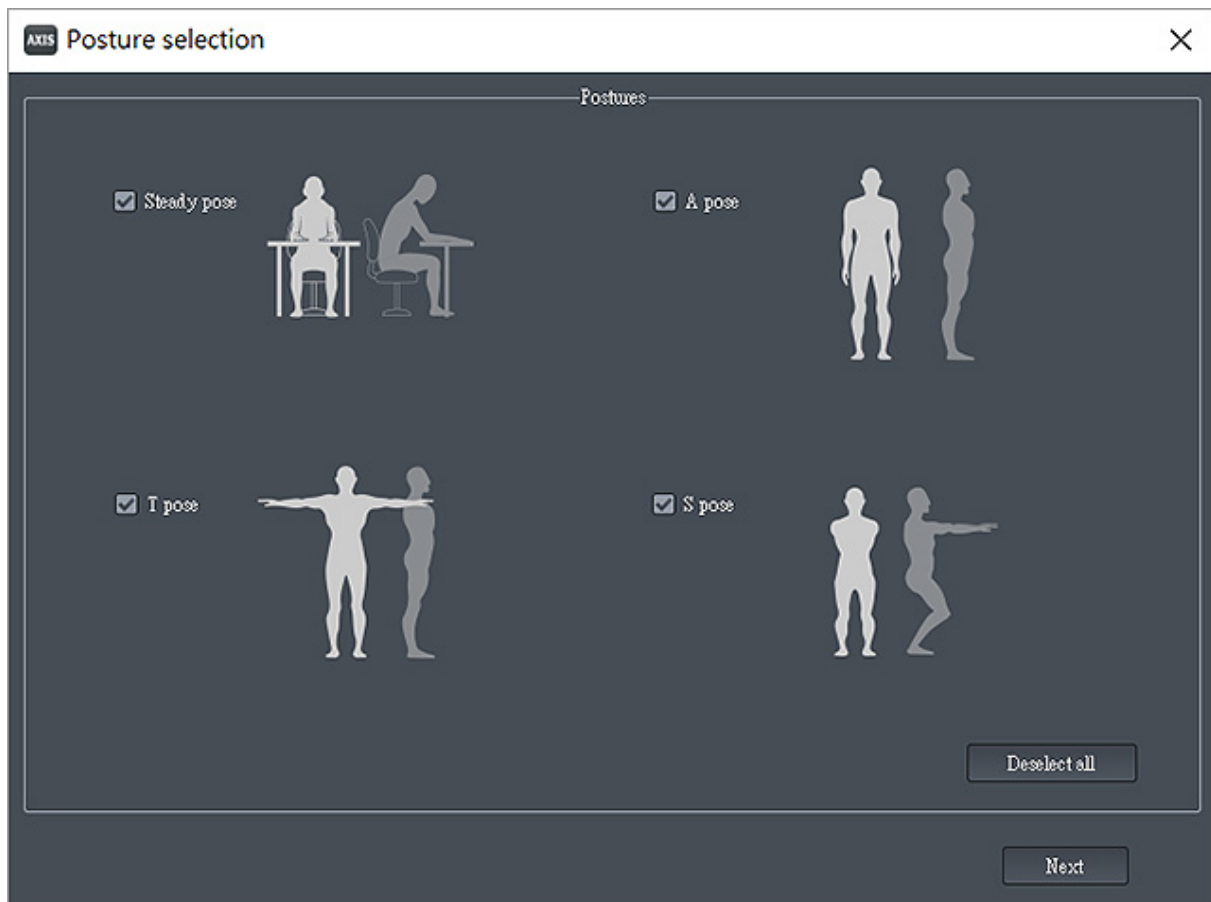
Figure 4.5: *Poses required for the calibration of the motion suit*

Source: https://manual.reallusion.com

selves in an empty room and were asked to look around and familiarize with their virtual body. The purpose of this step is for subjects to establish a sense of ownership and agency over the virtual body that they see (wherever it is possible). While standing on the spot, subjects were asked to raise their arms and legs, and observe the virtual body accordingly. This familiarization process took about 3 minutes.

- Training: once the familiarization phase is over, subjects started the training phase. The purpose of this phase is to familiarize them with the threshold identification procedure, how redirection should feel as well as how to control the virtual avatar while performing locomotion. A strong level of curvature gain was selected (gain = 0.25, equivant to a curve radius of 4m) such that subjects would certainly recognize the manipulation. Subjects could also get used answering the questions using the embedded eye-tracker. The training phase ended once the subject had selected the correct answer three times in a row. This phase lasted about 10 to 15 minutes.

- Experiment: the 2AFC task and the QUEST method were used to identify the RDTs. That is, subjects walked two times to the target, whereas in only one of the walk a curvature gain is applied. Subjects must then select the walk in which they thought redirection happened. Depending on whether this answer is correct or not, the QUEST method adjusts (increases or decreases) the next curvature gain according to Bayes' theorem. Each condition consists of 40 trials and lasts about 25 minutes.

- Post-experiment questionnaires: subjects filled out the SSQ again, indicating their subjective physical state after the experiment block. In order to assess the effectiveness of different perspective and congruency conditions on the feeling of presence, a questionnaire where user could give a subjective rating on the virtual avatar was proposed. The presence questionnaire consists of five 100-point Likert scale questions (from 0 point (strongly disagree) to 100 point (strongly agree)) about different aspects of the virtual avatar:

    - It felt like I was in control of the body I was seeing

    - It felt like the virtual body was my own body

    - It felt as if my body was located where I saw the virtual body to be.

    - It felt as if I had more than one body

    - It felt like I really was in the virtual room.

In addition to subjects' answers at the end of each trial, their position during all walks was also recorded. Moreover, eye gaze direction was also recorded to provide information about where subjects focus on during these walks.

4.2.3 Results and Discussion

For each subject, three threshold values were obtained corresponding to the three conditions: 1PP congruent, 3PP congruent and 3PP incongruent. As it has been shown in previous studies that 3PP helped improve simulator sickness, the difference in SSQ scores before and after each condition was calculated, and a linear mixed model was fitted with the SSQ score difference (only in the congruent conditions) as the dependent variable, perspective and gender as independent variables and subject as a random variable [174]. Contrary to the existing finding by Monteiro et al., result showed no significant effect of gender nor perspective on the SSQ score. One possible explanation for this result is that while subjects' exposure time in VR in Monteiro et al. was much shorter (about 11 minutes per condition), the VR application used was a racing application with fast movement and rich optical flow, which could induce more simulator sickness. On the other hand, the scene in this experiment was designed to be mostly plain, and subjects were allowed to walk at there comfortable speed, which probably helped repressing motion sickness. In fact, the average difference in SSQ score in all condition was 1.9 points, which is equivalent to "feeling a little bit more fatigue". Since this experiment was not specifically designed to investigate the effect of perspective on simulator sickness, no conclusion could be drawn on the lack of significant result.

In order to investigate if the different perspective and congruency conditions had an effect on the feeling of presence, mixed linear model analyses were ran for each component of the presence questionnaire: sense of agency, sense of body ownership, sense of self-location, sense of multiple body and feeling of presence with the score as dependent variable, gender and condition (1PP congruent, 3PP congruent and 3PP incongruent) as independent variables and subject as a random variable.

Agency score. No significant difference was found between 1PP congruent and 3PP congruent or 1PP congruent and 3PP incongruent. This lack of significant difference could be explained by the fact that during the 1PP condition, subjects did not always see the body and therefore did not feel control over the avatar. However, results showed a significant difference in agency score between the 3PP incongruent and 3PP congruent conditions (p=0.045). More specifically, the agency score in the 3PP incongruent condition is on average 16 points lower than in the 3PP congruent condition. The sense of agency describes the feeling of control over the virtual avatar, and therefore this result showed that the use of

animated avatar has achieved the desired effect of lowering subjects' sense of agency over the virtual body.

Body ownership score. There were significant differences in body ownership scores between the congruent conditions and the incongruent condition. Specifically, the body ownership scores in the 1PP congruent and 3PP congruent are 25 points (p<0.001) and 15 points (p=0.03) more than the 3PP incongruent condition, respectively. This result also showed that the use of the animated avatar was effective in creating a significantly difference sense of body ownership between the congruent and incongruent conditions. There was, however, no significant difference in body ownership score between the 1PP and 3PP congruent conditions.

self-location score. There were significant differences in the self-location score between the 1PP condition and the 3PP conditions. The self-location score in the 1PP condition was 21 points higher than the 3PP congruent condition (p=0.028) and 29 points higher than the 3PP incongruent condition (p<0.001). No significant difference was found between the 3PP conditions. This result shows that different perspectives has significant influence on the subjects' feeling that their body is located at same location as the virtual body. For the case of the 3PP congruent condition, subjects feel that they have control over the virtual body, but they themselves are not there where the virtual body is.

Multiple bodies score. Despite subjects not identifying their body to be located at the location of the virtual avatar in the 3PP conditions, their scores in feeling like they have more than one body in the 3PP conditions were significantly higher than the 1PP condition (18.3 points higher, p<0.001 and 19.3 points higher, p<0.001 in the 3PP congruent and incongruent conditions, respectively). This result shows that, to some extent, subjects also felt a sense of ownership over the virtual body that they see in 3PP incongruent condition. This is due to the fact that even though body movement of the avatar was completely different from the subject's body movement, its position and rotation still follow the subject's position and rotation.

Feeling of presence score. The feeling of presence was significantly higher in the 1PP condition compared to the 3PP conditions (10 points higher, p = 0.01 and 11 points higher, p < 0.001 in the 3PP congruent and incongruent condition, respectively). This shows that perspective plays an important role in eliciting the feeling of presence, and agrees with previous study on how users perceive threat to the body more acutely when they view the virtual body in 1PP [166].

In summary, the use of different viewing perspectives and congruency conditions of the avatar has achieved the desired effect of eliciting significant difference in the feeling of agency (congruent vs. incongruent), body ownership, self-location, multiple bodies and feeling of presence (1PP vs. 3PP). The next step is to investigate whether these differences have an effect on how subjects perceive redirected walking. For each of these embodiment scores, a linear mixed model analysis was constructed with RDTs as the dependent variable, gender, walking speed (shown in Section 3.1 to have a significant effect on RDTs) and the embodiment score as independent variables and subject as a random variable. Gender was again shown to have a significant effect on RDTs, in that women on average have higher RDTs than men (p = 0.04). A significant effect of walking speed on RDTs has not been found. This is an interesting result to obtain, as speed has been shown to be a consistent factor that influences RDTs [191, 187]. It is, however, important to note that individual thresholds varies significantly, and since in this experiment speed was not a controlled, within-subject factor, the effect of speed could have been masked by the high variability of RDTs across individuals. Out of all embodiment scores, the agency score was the only factor having significant effect on RDTs (p = 0.03). While existing works lean towards the fact that a strong feeling of presence causes the subject to perceive less cue conflicts [166], the results obtained from this experiment show significant effect in the opposite direction. There is a negative correlation between agency score and RDTs, i.e. in conditions where subjects have stronger feeling of agency over the virtual body, they tend to detect redirection better. This difference could be due to the different nature

of the cue conflicts in existing works and this work. The cue conflicts in existing works involve mainly visual-proprioceptive conflicts in the ego-centric frame, while the cue conflicts in the case of RDW involve mainly visual-vestibular conflicts in the inertia reference frame. The mechanism of detecting these conflicts may be different, and while in one case being immersed may make it harder to detect conflicts, in the other case, being immersed enables users to be more sensitive. Up till now, VR applications in general, and RDW applications particularly, mostly employed the first person perspective. Not much research has been done in this direction, and therefore, the potential of using 3PP in VR applications is yet to be discovered. In this study, the frst step was made in that direction. The fact that the different perspectives did not have a significant effect on RDTs implies that 3PP could in the future replace 1PP in certain RDW applications where better spatial awareness is required [94].

4.3 Cognitive Load

In previous RDTs identification experiments, the only task that was given to subjects was to detect whether redirection was applied. This, however, does not reflect a typical VR application, in which users perform application-specific tasks such as way-finding, performing a procedure, or simply interacting with the virtual environment. The additional cognitive load that is imposed on the users from these tasks may have an effect on how sensitive they are to redirection. This section is dedicated to understanding how RDTs change when users are engaged in another task and what this implies for future RDW applications.

There is a variety of tasks that could be used to impose cognitive load on subjects while walking. These tasks should generally be difficult enough to capture users' attention, but not so difficult that it prevents subjects from performing the primary task successfully. These tasks can be of different types: physical, visual, auditory, verbal, or arithmetic. *Physical tasks* such as carrying a tray with objects on top while walking is an interesting approach [22, 37, 215, 281]. However, when safety and practicality is taken into account, this approach is unsuitable, as well as not realistic, in a VR application. An example of *visual tasks* would be showing subjects a picture before and after performing the primary task and asking them to identify whether the pictures shown were the same of different [284]. In a study in VR, a visual task could also be asking the subject to press a button when an object appears in the field of view [157]. *Auditory tasks* involve asking the subjects to identify the noises (hand clap, door close, dog bark, cat meow, etc.) or voices (man, woman, child) that they hear from a recording [284]. *Verbal tasks* require subjects to name things of the same characteristics such as animals, flowers, men's names or items that start with a particular letter [23, 68, 118, 17, 36]. Meanwhile, *arithmetic tasks* comprise of a wide range of different tasks such as: random digit generation (generate random numbers in a given range), counting backwards, serial 3 or 7 subtraction (e.g. subtracting three or seven from a given number), subtract or add numbers to letter (e.g. k - 1 = j) [235, 283, 105, 229]. Among these many dual tasks, it is to be acknowledged that individual's ability to perform the dual task may differ. Tasks that require mathematical skills such as serial 7 subtractions may require little attention for subjects who are used to working with numbers such as mathematicians, accountants whereas subjects who are not used to doing such tasks might be severely affected. Similarly, a test of verbal fluency could be quite a challenge, resulting in extremely high cognitive load in subjects with language difficulties. However, the task difficulty at the beginning of the experiment should not be the only factor to be considered. Naming words that start with a given letter, or an animal names may be easy in the beginning, but as the test progress may become very challenging. On the other hand, provided that the subjects were given sufficient training and the starting number changes every trial, the attention required to performed serial subtractions could be quite constant over time. Which task to choose for a particular experiment requires careful consideration of all these different aspects. Regardless of the type of dual task chosen, it is also

important to take into account the difference in individual ability, and therefore when the effect of the dual task on a primary task is to be investigated, a within subject would be more appropriate.

Outside the context of RDW and VR, in studies of balance and walking gait, a dual task is very commonly used to assess subjects' motor capabilities, especially in elderly or Parkinson patients [283, 235, 118]. It could be used as a predictor for fall risks among these subjects as the dual task significantly affect their gait and walking stability. However, for healthy adults, it has been consistently shown that the cognitive load induced by the dual task does not change gait characteristics such as stride length and walking stability but only reduce their walking speed [105]. Compared to reality, it has been shown that subjects could perform the serial N subtraction task equally well in VR [163]. Moreover, the dual task has also been used to investigate the impact of cognitive load on spatial orientation [157]. In this study, the primary task involved subjects to point to their original starting position after walking through two different way-points and the dual task required them to perform the visual detection task as fast as possible. It was found that subjects made significantly larger angle error while performing the dual task compared to the single task condition. In another study, subjects walked on a treadmill and their body movement was mapped onto an avatar that is shown on a screen in front of them. The movement of the avatar was either real-time (75ms) or delayed randomly up to 1350ms and subjects had to indicate when they recognized the avatar as themselves. It was shown that when subjects had to perform a the dual task of serial seven subtraction, they had significantly more erroneous self-attribution of the avatar than in the single task condition [132]. The same result was also observed when walking was performed in VR. In this study, subjects were asked to walk a 1.8m long path while watching an avatar on a large projection screen [133]. The avatar body movement followed body movement in real-time, but its path is deviated ± 5 to ± 30 degrees from subjects' real path. Interestingly, even though the experiment was conducted in the field of neuroscience for the understanding of movement kinematics and trajectory formation during goal-directed walking, the manipulation applied to subject's path (albeit measured in deviated angle instead of curve radius) is in fact the same as our RDW technique in third person perspective. Also using the serial seven subtraction as the dual task, this study found that while the dual task did not affect subjects' walking accuracy and trajectories. i.e. they still were able to compensate for the deviation and arrive at the target, it significantly reduced their walking velocity. Furthermore, while performing the dual task, subjects also had significantly lower motor awareness (a measure equivalent to our RDTs) compared to the single task condition.

In the context of VR applications, research has mainly focused on the impact of different factors on the performance of cognitive tasks, rather than vice versa. For example, it has been shown that when subjects see their real body or a full avatar, their performance in a memory task is significantly better than when there is no avatar [197]. Also arriving in a similar conclusion, it was shown that virtual hands displayed at the same location as the real hands significantly improved subjects's working memory [258]. In the field of RDW itself, the only existing study on cognitive load found that RDW significantly affect users' performance in verbal and spatial memory tasks and that the cognitive task significantly increase lateral sway for curvature gain larger than 0.1 [30]. However, as the study was not designed to understand how cognitive load affects RDTs, no conclusion could be drawn.

In this experiment, the aim was to fill in the gap in understanding the effect of cognitive load on curvature RDTs. Considering the consistent finding of reduction in walking speed during the dual task condition, it could be hypothesized that the RDTs would increase when subjects perform the dual task. Whether this hypothesized increase in RDTs is the purely the result of the decrease in walking speed, or the combination effect of the decrease in speed and the extra cognitive load will also be investigated.

4.3.1 Experiment Design

The first step of designing the experiment is to select a dual task that is compatible with the existing RDT identification procedure. As subjects are required to walk back and forth many times for their RDTs to be identified, the selected dual task needs to have the same level of difficulty as the experiment progresses. Taking this criteria into account, since verbal tasks where subjects are required to name items will get increasingly challenging over time, only auditory tasks, visual tasks or arithmetic tasks are suitable. Among these remaining tasks, auditory discrimination tasks would require a lot of audio clips to be pre-generated, and the visual task of detecting objects' abrupt appearance in the field of view would potentially be too disruptive and may cause subjects to stop walking. An arithmetic task, especially the serial N-subtraction that was popular in previous gait studies, which imposes continuous load while not interrupting subjects when they perform the primary task, would be ideal. For this experiment, the serial seven subtraction task was selected. Since three-digit numbers would be too long for subjects to say, the subtraction was performed from two-digits numbers only. In order to ensure that subjects could still make the subtraction until the end of their walks, a large enough two digit number (between 70 and 100) must be randomly selected for each walk.

The virtual environment used in this RDT experiment followed exactly the design of the virtual room used in the experiment in Section 3.1: a virtual room of the size 10m × 10m containing a red target, which the subjects must always walk towards. Unlike previous experiments, the subjects' speed in this experiment was not controlled using step rhythms because that would have been an additional cognitive load that may prevent the subjects from performing the primary task at all. Nevertheless, subjects' trajectories in all trials were recorded, from which the average walking speed could be calculated.

As discussed in the previous section, the ability to perform the dual task could vary significantly between subjects. Therefore, in order to investigate the effect of cognitive load on RDTs using a reasonably small sample size, a within-subject design was selected, in which each subject performs the RDTs identification procedure two times, one with and one without the dual task. Due to the fact that subjects in previous experiments have no significant RDTs in either the left or right direction, in this experiment, it was arbitrarily chosen that redirection was applied to the right direction only. The 2AFC task and the adaptive Bayes method QUEST were again used for the threshold identification procedure. Based on the data from previous experiments which used 40 trials, after about 25 trials the estimated threshold value tended to converge to the final threshold value. As a result, in this experiment, in order to reduce subjects' time in VR, each subject performed only 25 trials per condition.

The experiment set-up consists of an Oculus DK2 with a built-in SMI eye tracker and an Intersense IS-1200 inside-out optical tracking system mounted on top, providing 6-DOF positional tracking at 180Hz in a tracking space of 13.3m × 6.6m. A shield is added in front of the headset to prevent users from seeing the floor. The scene was optimally designed in Unity to run at the HMD's maximum frame rate 75Hz.

4.3.2 Participants and Procedure

Thirty subjects (aged from 20- 46 (M=28.7, SD=7), 15 male and 15 female, right-handed, with normal or corrected-to-normal vision) participated in this experiment. None of the subjects had taken part in previous RDTs identification experiments, and therefore were completely naive to the purpose of the experiment. After having signed the consent form and understood the procedure of the experiment, the experiment began. The single and dual task conditions were administered in two separate blocks. Each block consists of a training phase and an experiment phase.
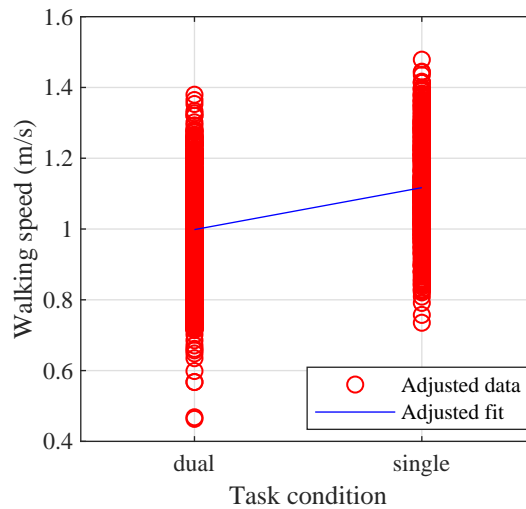
Figure 4.6: *Effect of dual task on subjects' walking speed*

The purpose of the training phase is to familiarize subjects with how redirection should feel, how to perform the dual task while walking and how to answer the questions using the embedded eyetracker. Similar to previous experiments, a strong level of curvature gain was selected (gain = 0.25, equivalent to a radius of 4m) such that the redirection would be obvious. The training phase ended once the subject had selected the correct answer three times in a row. This phase lasted about 10 to 15 minutes.

In the experiment phase, the stimulus levels were adjusted depending on subjects' answers following the QUEST method. At the beginning of each walk in the single task condition, when subjects arrived at the starting position, a black screen appeared and faded out after 2 seconds showing the view of the virtual environment. At the beginning of each walk in the dual task condition, the procedure is the same but a random number would appear on the black screen. As subjects started walking, they also started the subtraction by saying the number that they saw on the screen first. Each condition consists of 25 trials and lasts about 15 minutes. The order of the trials was counter-balanced to take into account learning and adaptation effects.

4.3.3 Results and Discussion

All thirty subjects completed the experiment and no subject reported any discomfort at the end of the experiment. The experiment ran automatically without intervention from the experimenter except for one incident where a subject was so focused on the subtraction task that she closed her eyes but keeping walking and almost collided with the physical boundary. The subject was then reminded that she should focus on reaching the target as the primary task and the experiment could continue smoothly from then on. As predicted, some subjects had difficulties performing the dual task in the training trials and a few needed to count with their fingers. Since the purpose of the dual task was to overload subjects' attention, their performance and accuracy in this dual task was not recorded. However, based on our informal observation, most subjects could perform the subtraction quite accurately. Many previous studies both in VR and in reality have consistently found that for healthy adults, performing a dual task in addition to a walking task decreases their walking speed but does not change they gait characteristics such as stride length, sway amplitude, etc. [229, 105, 235]. However, a study by Bruder et al. found that subjects swayed significantly more during the dual task condition when the gain is higher than 0.1 [30]. Therefore, the first analysis was performed to examine if our results agree with these existing findings. In
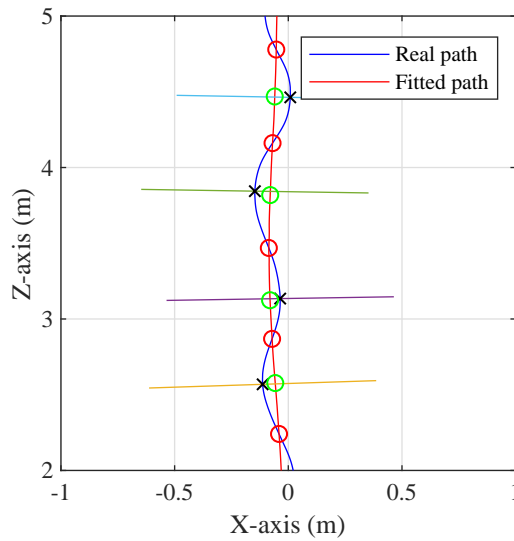
Figure 4.7: *Fitting of a user's walking path and their sway magnitude calculation*

total subjects walked 50 times, each time an average walking speed is obtained, which resulted in 50 data points per subject for each of the thirty subjects. The average speed over all subjects and condition was 1.055m/s (min = 0.75m/s, max = 1.33m/s, sd = 0.14m/s). A linear mixed model was fitted with walking speed as the dependent variable and condition (dual task, single task), gender, applied stimulus during each walk as independent variables and subject as random variable. The linear mixed model becomes:

$$\text{speed} \sim \text{task} + \text{gender} + \text{gain} + (1|\text{subject}) \tag{4.3}$$

It was found that only task condition has a significant effect on the walking speed (p<0.001) (Figure 4.6). This result agrees with numerous findings in previous gait studies of healthy adults that subjects tend to slow down when they have to perform a dual task. In order to investigate if the dual task would also affect head sway magnitude, a similar model was constructed with sway magnitude (instead of speed) as the dependent variable. This sway magnitude was calculated as the average orthogonal distance from the subject's position to the path fitted with the path model proposed by Wendt et al. [270]. An example of how this sway magnitude is calculated can be seen in Figure 4.7. The average sway magnitude over all subjects and conditions was 0.0274m (min = 0.0123m, max = 0.0573m, sd = 0.0087m). Results showed no significant effect of the dual task on swaying magnitude which agrees with other studies on healthy adults, but contradicted to what was found by Bruder et al. Interestingly, there was a significant effect of the applied curvature gain on the sway magnitude during the straight walking trials.

For each of the thirty subjects, two RDT values were found corresponding to the single task and dual task conditions. Thresholds again vary widely across individuals from $0.02m^{-1}$ (equivalent to 50m radius) to $0.27m^{-1}$ (3.7m radius) with a mean of $0.16m^{-1}$ (6.25m radius) and a standard deviation of $0.0616m^{-1}$. The range of thresholds obtained is also similar to results obtained from previous experiments with different groups of subjects. In order to investigate the effect of the dual task on RDTs, a linear mixed model was again fitted with threshold as the dependent variable. From the previous analysis, speed and task condition have been shown to correlate. Therefore, in this analysis, they are added separately to two different linear mixed model. The first model contains walking speed and gender as independent variables, and subject as a random variable:

$$\text{threshold} \sim \text{speed} + \text{gender} + (1|\text{subject}) \tag{4.4}$$

The second model contains task condition (single or dual), gender as independent variables, and subject

(a) *Effect of dual task on curvature gain thresholds*   **(b)** *Effect of gender on curvature gain thresholds*
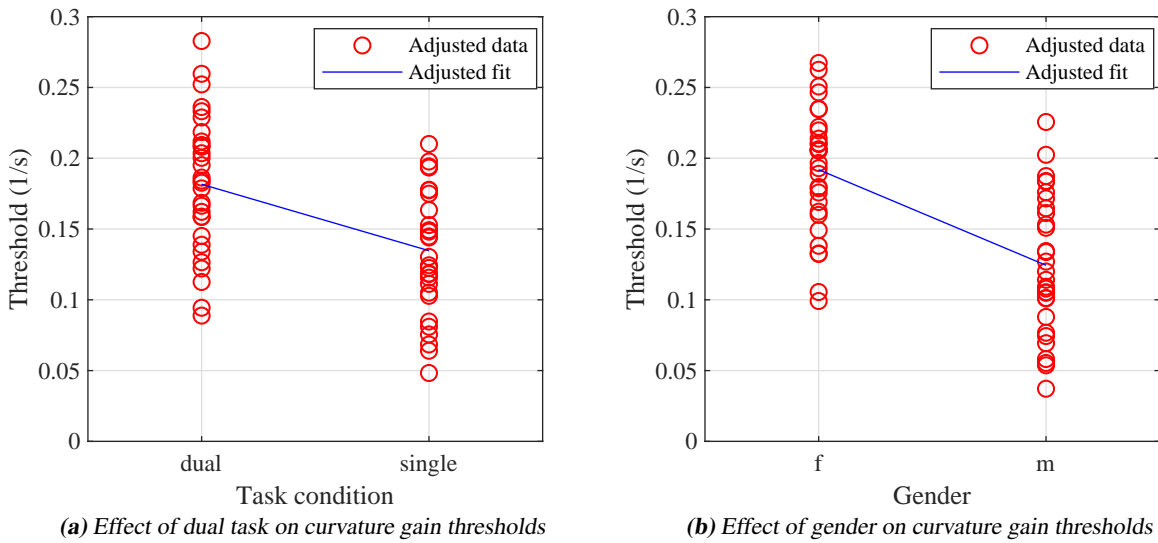
Figure 4.8

as a random variable:

$$\text{threshold} \sim \text{task} + \text{gender} + (1|\text{subject}) \tag{4.5}$$

Results from these two analyses showed that gender is again proven to have a consistent significant effect on RDTs, with men on average have higher RDTs than women ($0.068m^{-1}$ difference with $p = 1.1e-5$) (Figure 4.8b). Surprisingly, there was no significant effect of speed on RDTs. It is important to note that the average speed difference between the two task conditions is about 0.1m/s, which is much lower than the speed difference of 0.25m/s when speed was controlled in the previous experiment. Therefore, a possible explanation for this finding is that the effect of walking speed on RDTs is not strong enough to elicit a significant difference in RDTs when the speed difference is not large enough. Results of the second analysis showed a significant effect of the dual task on RDTs, with the RDTs in the dual task condition is on average $0.04m^{-1}$ higher than the RDTs in the single task condition ($p = 6.4e-5$). This finding confirms the original hypothesis and suggests that results obtained from single task RDT identification paradigm is only a conservative estimate of the thresholds. In reality, when users are performing specific tasks in the virtual environment, a higher gain could very well be applied without them noticing. Future work still remains to understand how much cognitive load different tasks impose on users, how cognitive load changes as users become more proficient in the tasks, and how different levels of cognitive load affect RDTs.

5

Further Improving Redirection

The previous two chapters were dedicated to investigating the perception processes happening during RDW and the factors that have effects on users' RDTs. Based on the results of these previous chapters, it is now understood that RDW gains should be personalized for each individual user such that their feeling of presence remains intact. The obtained understanding about the effects of the design of the environment, perspectives and the main task also allow for designs of VR applications where stronger RDW gains could be applied, thus allowing the exploration of a larger virtual environment given a similar available physical space. Nevertheless, there are always limits to how strong these existing techniques can be applied, and at some point, no matter how complicated the main task of the VR application is, nor how slow the users' speed can be controlled, RDW will be noticed. This leads to the main motivation of this chapter: exploring other aspects of RDW (rather than its thresholds) to improve it further. The two main aspects of RDW that this chapter focuses on are: first, the introduction of new an RDW technique that could be used in conjunction with existing RDW techniques; and second, the understanding of users' path in the environment that could improve current RDW algorithms.

5.1 Subtle Discrete Redirection During Blinks [1]

The first approach to improving RDW is to create new redirection techniques that could be used simultaneously with existing ones without affecting their identification thresholds and thus allowing more redirection to be applied. Depending on how they are applied, existing redirection techniques can be categorized into continuous and discrete, and further divided into overt and subtle [241]. All continuous redirection techniques involve continuously injecting translation and rotation to users' virtual trajectories, resulting in users translating faster or slower in the virtual environment than in real life, rotating faster or slower in the virtual environment than in real life (if the users rotate on the spot and have zero linear velocity) or walking on a different curvature in the virtual environment than in real life (if the users have nonzero linear velocity). *Overt continuous* redirection techniques usually involve the use of metaphors such as seven league boots [119] or virtual elevators and escalators [189]. In *subtle continuous* redirection techniques, the amount of translation and rotation injected (quantified as translation, rotation and curvature gains [236]) is within certain thresholds such that they are unnoticeable and immersion re-

---

[1]Parts of the section were published in [188]

mains intact [205]. Discrete redirection techniques refer to the instantaneous relocation or reorientation of users in the VE. Some examples of *overt discrete* redirection techniques are teleportation [24] and portals [83]. Meanwhile, *subtle discrete* redirection techniques can be performed when users do not notice the relocation and reorientation due to imperfections in human perception such as visual suppression caused by saccadic eye movement or blinking [11, 123, 243, 150].

In general, overt redirection techniques offer a higher range of motion and thus enabling users to travel in a much larger VE. However, it has been shown that subtle redirection techniques produce fewer breaks in presence and therefore are generally preferred for a more immersive VR experience [241]. Among the subtle redirection techniques, most attention has been paid only to continuous redirection techniques including many experiments on detection thresholds and factors that influence them [237, 186, 191]. Furthermore, many existing algorithms that direct users to particular locations in the tracking space such as steer-to-center, steer-to-orbit, steer-to-predefined-target [205] and model predictive control [182] so far employ only continuous redirection techniques. Up till now, research on discrete redirection techniques, especially using eye tracker information (e.g. eye movements, blinks, gazes), is still quite limited.

In this section, a new subtle discrete redirection technique is proposed, which applies discrete rotation of a virtual environment during blinking. An experiment was first conducted to identify how much rotation could be applied during blinking as users walk around in a VE. Based on the obtained results, a series of simulations were run to investigate whether implementing this technique on top of existing continuous redirection techniques would improve the performance of the most common RDW algorithms.

5.1.1 Discrete Redirection Threshold Identification

Blink Physiology

We blink for different reasons, as a reflex to protect our eyes when objects move towards them, during natural breaks in attention such as when a speaker pauses [179], when a movie scene changes [180], or just spontaneously to moisten our corneas. Spontaneous blinks occur 10 to 30 times per minute [244, 67] and last about 100 to 150 ms [260]. During the closing phase of a blink, the eyes move typically downward and nasal-ward and then move back to their previous position when the eyes are open [214]. These eye movements result in gaze direction instabilities and gaze position errors which are then corrected by microsaccades [49]. Due to the inherent gaze position errors, targets could be displaced up to one degree laterally during blink without users noticing and they started to correct their gaze in the direction of the displacement [168]. Furthermore, during blinks the eyelids cover the pupils and prevent light and visual inputs from entering the eyes, resulting in a disruption of the image on the retina. However, this disruption is rarely noticed due to the fact that our brain suppresses visual information during blinks, so-called **visual suppression**. As a result, people sometimes experience temporary blindness to changes happening to the scene such as color change, target appearance/disappearance or target displacement [207]. This phenomenon is called **change blindness**. Due to visual suppression, change blindness does not only occur during spontaneous blinks, but also during reflex and voluntary blinks [165] and saccades (rapid eye movements that abruptly change the fixation point) [18]. Ridder et al. concluded that the same effects responsible for visual suppression during saccades could be in effect during blinks. As blinks last longer than saccades [11], there would be more time to detect when blinks happen. A new approach of applying redirection during blinks is therefore very promising.

While change blindness due to visual suppression is undesirable in tasks that require constant monitoring of visual input such as driving [85], in the context of redirected walking it offers a new possibility for applying discrete RDW techniques. When a blink or saccade occurs, the virtual environment could be

instantaneously reorientated and relocated to direct the users to a desired location without them noticing. Using an electrooculography tracker combined with an HMD, it was found that during a saccade with an amplitude of 15 degrees, the detection threshold is approximately 0.5m for translation along the gaze line and 5 degrees for rotation around the users' vertical axis [21]. In another study, a blink sensor was used with the HTC Vive to identify the detection thresholds for reorientation and repositioning during blinking but no specific threshold values were obtained [123]. A more thorough study was conducted to identify the detection thresholds of scene rotations around users' 3 main axes, and scene translation along users' 3 main axes during blinks [150]. The rotation detection thresholds were found to be about 2 to 5 degrees, and translation detection thresholds 4 to 9 cm. One constraint of all the aforementioned studies is that the users were not performing locomotion when the detection thresholds were identified. Without the additional movements generated during real walking such as head rotation and swaying, which would potentially lead to more sensory noise and make it more difficult to detect scene changes. Moreover, users in these studies were informed to look for changes in the scene as blink or saccade happened. Such instructions may have prompted them to fixate on certain reference points in the environment to detect the scene change better. Therefore, the obtained threshold values from these existing studies are only conservative estimates. To our knowledge, no study has been performed to identify the detection threshold of discrete scene rotation and translation during saccades or blinks when naive users are performing real walking. This has prompted the conduction of this experiment, where the focus is on identifying the detection threshold of scene rotation during blinks as users walk in a virtual environment without knowing the true purpose of the experiment.

Blink Detection

For this experiment, an Oculus DK2 with an integrated SMI eye tracker was used. The eye tracker provides gaze direction, gaze base point and pupil diameters of both eyes, etc. at 60Hz. Whenever the eyes close, the eye tracker loses track of the pupil and returns zero values for the pupil diameters. Figure 5.1a shows a typical pupil diameter signal from the eye tracker. It can be noticed that during blinks both eyes do not close and open at the same time, and there is occasionally spurious noise as shown in Figure 5.1b. It is crucial that blinks are detected reliably and there must be no false positive to ensure that redirection is not applied when eyes are open. Therefore, the following conditions need to be satisfied for an event to be considered a blink: the sum of both pupil diameters must step from nonzero to zero and a new blink only can occur after a timeout period of 1.5 seconds has passed. The timeout period is calculated to be long enough to avoid spurious noise but shorter than the period between blinks, which is about two to three seconds (10-21 times/minute). As an example, using the proposed rules, for each subfigure in Figure 5.1, only two blinks will be detected.

Experiment Design

The goal of this experiment is to identify the detection threshold for scene rotation during blinks as users freely walk around in a VE. In existing redirected walking thresholds studies, the subjects were usually informed about the purpose of the study and questions such as "did you walk to the left of right?" or "in which walk did you walk on a curve?" were posed to collect their responses. The same design cannot be used for this experiment. If the subjects are informed that during blinks the scene will be rotated and asked to identify the rotation direction, they will potentially try to fixate on a reference point and voluntarily blink, without even performing locomotion. The threshold values acquired in that case would be only conservative estimates, and do not necessarily reflect the true values when users are walking and unaware of the manipulation. As a result, the real goal of the study cannot be disclosed. Instead, a cover
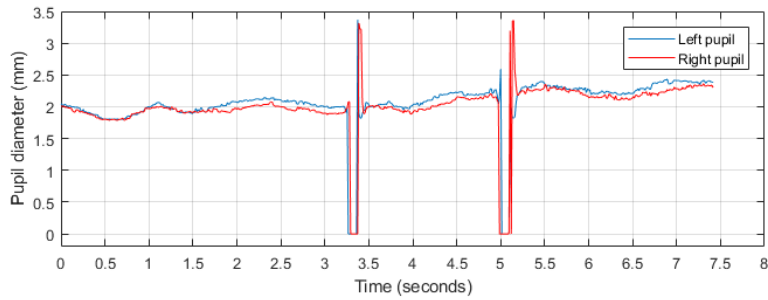
(a) Typical pupil diameter signals
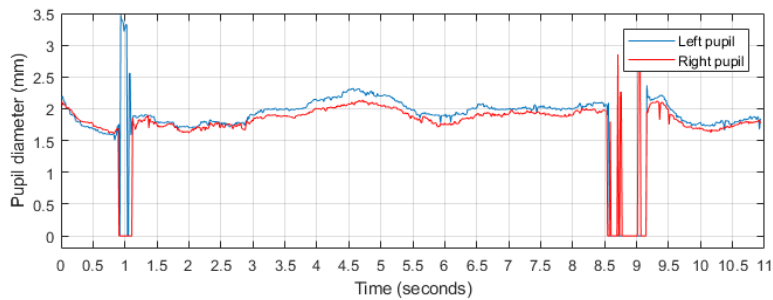
(b) Noisy pupil diameter signals

Figure 5.1: *Recordings of left and right pupils diameter of a participant during walking*

story is given to the subjects that they are testing a new system which may contain some technical bugs and are encouraged to inform the experimenter whenever such a bug occurs. When a subject reports a bug, the experimenter first makes sure that a scene rotation has just been applied and then verifies if the subject has really noticed the rotation rather than something else. When it is confirmed that the subject has noticed the rotation, it will be considered a correct detection response. Otherwise, when a stimulus has been presented without the subject making any comment, it will be considered a no detection response. Depending on the type of responses, the next stimulus level is selected accordingly.

In order to test the hypothesis that larger changes can be introduced during blinks as compared to when eyes are open, each subject is exposed to two conditions for threshold identification: scene rotation during blinks and scene rotation one second after each blink (when eyes are open). The range of tested values for rotation during blinks is 0 to 15 degrees (similar to the range used in [123] and [148]) and 0 to 10 degrees for rotation when eyes are open. In addition, since there may be asymmetry in users' ability to detect scene rotation of different directions, the thresholds for left and right rotations are identified separately. In total, four threshold values are obtained per subject and the identification of these values are handled by four separate interleaving "QUESTs".

The context of this experiment is a virtual forest of 250m x 250m where the subjects are required to walk around to collect targets that have been randomly placed in the environment (Figure 5.2). The virtual forest was created using free Unity assets from Nature Starter Kit 2. The virtual environment is much larger than our available physical space and therefore whenever the subjects come close to the walls they will be prompted to perform a reset. During resets, no scene discrete rotation will occur even if the subjects blink.
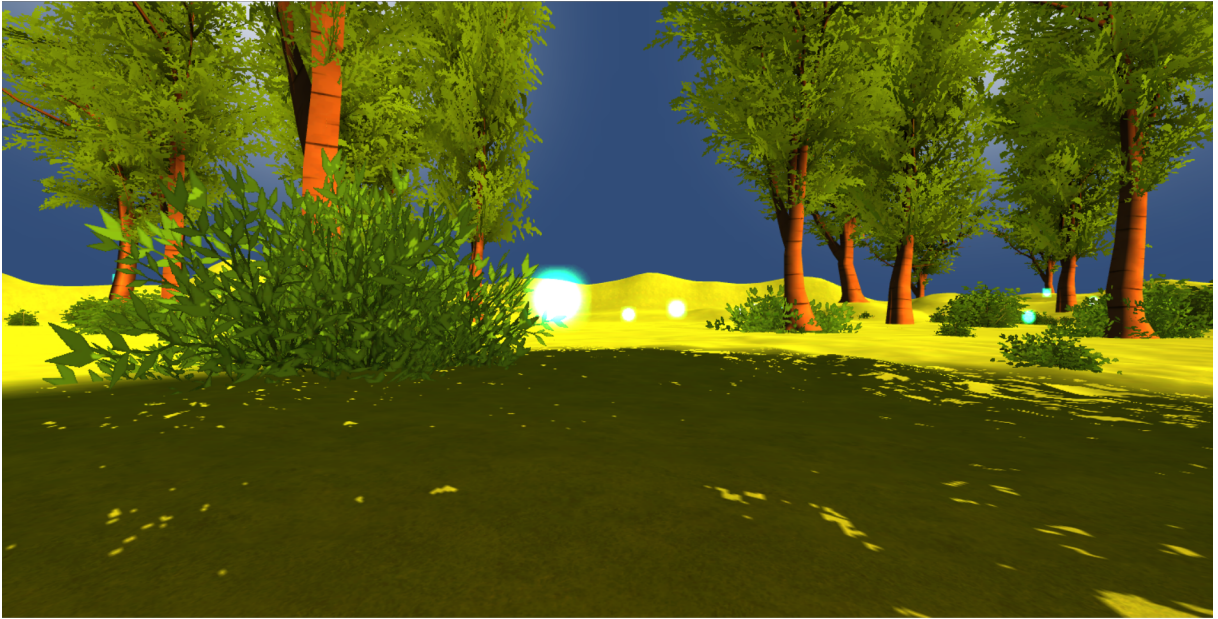
Figure 5.2: *User view of the VE: a forest with randomly placed targets*

Experiment Setup

The experiment setup consists of an Oculus DK2 with a built-in SMI eye tracker and an Intersense IS-1200 inside-out optical tracking system mounted on top, providing 6-DOF positional tracking at 180Hz. The scene is optimally designed in Unity to run at the HMD's maximum frame rate 75Hz. The users also wear noise canceling headphones with microphone to communicate with the experimenter during the study. The whole setup is powered by a backpack-mounted notebook carried by the users. During the study, in addition to users' responses to the scene rotations, their positional tracking and eye tracking data are also recorded. The available tracking space is 13m × 6m.

Pilot Study

A pilot study was conducted to evaluate the experiment design. Five naive subjects (3 men, 2 women, age: 20-29, with normal vision or wearing contact lenses) who were students at the university volunteered to participate in the study. The subjects were first told the cover story, and then the study began. The first pilot subject mentioned to the experimenter each time he noticed a technical "bug" such as: *"the color is weird"*, some things *"seem a bit blurred"*, or *"the scene just glitched"*. However, the next two subjects seemed to be too immersed in the virtual environment and did not mention anything even though the scene rotation was increased up to its predefined maximum of 15 degrees. When asked if they had noticed anything, they replied *"I sometimes saw the scene jump"* and *"I have seen it for a while now but forgot to mention it"*. Since it is crucial that the subject's responses are timely and correctly collected to update the QUESTs, we changed the experiment protocol for the last two pilot subjects and added a training session. In this training session, the subjects were exposed to the same environment but the scene rotation was always 15 degrees. This ensured that the subjects experienced the stimulus and understood what they should point out during the experiment. In addition, keywords were assigned to each "bug" that the subjects discovered in the training session such as: *"blurred"*, *"jump"*, *"color"*, etc. This way, during the experimental session, the subjects only need to use these keywords when they detect a "bug" and do not have to stop and explain in full sentence what just happened. This adjusted protocol worked

well for the last two pilot subjects and was adopted for the main study.

After the experimental session, all pilot subjects were debriefed and asked if they could guess why the technical bugs occurred. All subjects recited the cover story and none of them identified that they were associated with their blinks. This indicates that the cover story is sufficient to conceal the real purpose of the study.

Subjects and Procedure

Fifteen right-handed subjects (10 men and 5 women, age 19 - 29, mean = 23.1, SD = 2.5) who were students and staff of the university volunteered to participate in the main study. The subjects all had normal vision, or wear contact lenses, had no vestibular dysfunction and no injuries that affect their walking.

Before starting the sessions, the subjects were asked to fill in questionnaires regarding their gender, age, handedness, experience in VR and experience in gaming, the pre-exposure simulator sickness questionnaire (SSQ) [137] and then received the description of the experiment. Similar to the pilot study, the same cover story was given to the subjects and once they confirmed that they had understood the task (walk around the forest to collect the targets), the training session began. During the training session, a scene rotation of 15 degrees was applied every time the subjects blinked. The training session ran until the subjects have identified the scene rotation as one "bug" and agreed on a keyword for this "bug". Once the training session ended, which took about 5 to 10 minutes, the experimental session started. During the experimental session, each time the subjects noticed the scene rotation and said the keyword, this indicated a detection response, otherwise a no detection response. These responses were recorded by the experimenter, and the corresponding QUEST was updated automatically. When a scene rotation had occurred but the subject's response had not yet been recorded, no further scene rotation would be applied even if the subjects blinked. Scene rotation was also not applied during blinks during resets. The experimental session ended once 120 scene rotations (4 separate QUESTs x 30 runs per QUEST) have been applied. The duration of the experimental session ranged from 16 to 45 minutes, depending on how often the subject blinked, how much time they spent in resets, etc. Subsequently, the subjects filled the post-exposure SSQ and received step-by-step debriefing about the experiment.

Results and Discussion

Out of 15 subjects, one female subject could not complete the experiment due to motion sickness after about 10 minutes of exposure in the VE. Her threshold data is therefore excluded from the threshold calculation, but the positional and eye tracking data are still included in other analysis. The remaining 14 subjects completed the whole experiment and did not report any significant discomfort. During the debriefing process, when asked about the possible causes of the scene jumps, all subjects attributed the scene jumps to the computer performance, and did not identify that these jumps occurred as they blinked.

From the recorded 6-DOF positional tracking data, subjects' translational and rotational speeds were obtained. On average, subjects walked at 0.66 ± 0.12 m/s during exploration, and rotated at 49.1 ± 14.8 degrees/s during resets. Men and women have almost the same mean translational and rotational speeds and a two-sample t-test shows no significant difference of either speed between the genders (p = 0.81 and 0.88 respectively). Subjects spent on average 25 minutes in the VE, and about 33% of that time performing resets.

Blink frequency varies highly across different subjects. Across all subjects, the average blink frequency
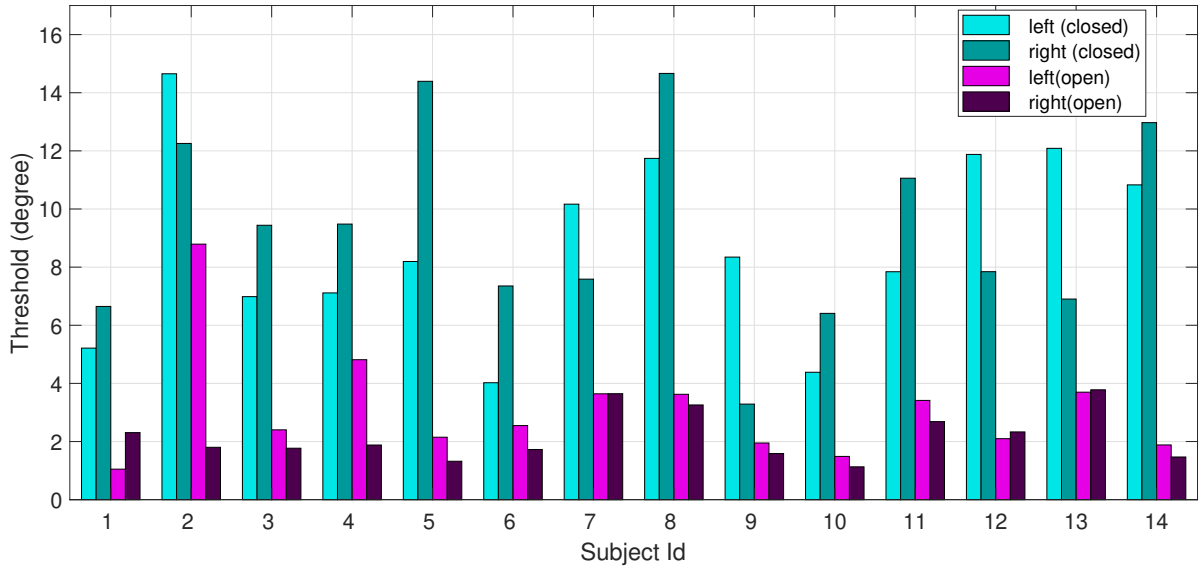
Figure 5.3: *Detection thresholds for scene rotation of all subjects. Green and purple colors represent thresholds during blinks and when eyes are open. Bright and dark colors represent thresholds for left and right rotations.*

is 13 ± 5.5 times/min, which falls within the normal range of 10 - 30 times/min. The lowest blink frequency was 4.78 times/min, and the highest blink frequency was 22 times/min. For men, the mean blink frequency was 11.8 ± 5.1 times/min, whereas it was 15.2 ± 5.9 times/min for women. Although the difference was not statistically significant ($p = 0.277$), the trend agrees with existing results that women tend to perform spontaneous blink more often than men [228]

A two sample t-test was also conducted to compare the SSQ scores before (mean = 11.49, SD = 12.05) and after (mean = 41.14, SD = 38.84) the experiment. There was a significant increase in score in the after condition ($p = 0.01$). More than half of the subjects reported an increase in sweating, general discomfort and nausea. Possible causes of such result could be the high number of resets (on average 90 resets/subject) that subjects had to perform due to the limited room size, the long exposure inside the virtual environment while carrying a heavy backpack or the discrete scene rotations during and after blinks. Nevertheless, it is not possible to pinpoint the exact cause(s) or draw conclusion about the effect of adding discrete scene rotation on simulation sickness based on the obtained data. The usability of this technique in terms of simulation sickness remains to be investigated in more controlled experiments.

For each subject, four detection threshold values corresponding to two rotation directions (left and right) $\times$ two eye states (closed and open) were obtained. A summary of the results can be found in Figure 5.3. In order to investigate the effect of rotation direction and eyes state on detection thresholds, a linear mixed model was fitted which included rotation direction and eyes state as fixed factors, and subjects as a random factor. Gender and gaming experience were also included as fixed factors. Gaming experience is classified as 'low' if playing less than once a month and 'high' if playing more than once a week. As curvature gain thresholds have been consistently shown to correlate with walking speed [186] [191], this effect was also tested by including it in the model. With all the factors defined, the full mixed-effect model becomes:

$$\text{threshold} \sim 1 + \text{rotation direction} + \text{eye state} + \text{gender} + \text{gaming experience} + \text{walking speed} + (1|\text{subject})$$
$$(5.1)$$

Figure 5.4: *Adjusted response plot: Walking speeds vs. Detection thresholds*
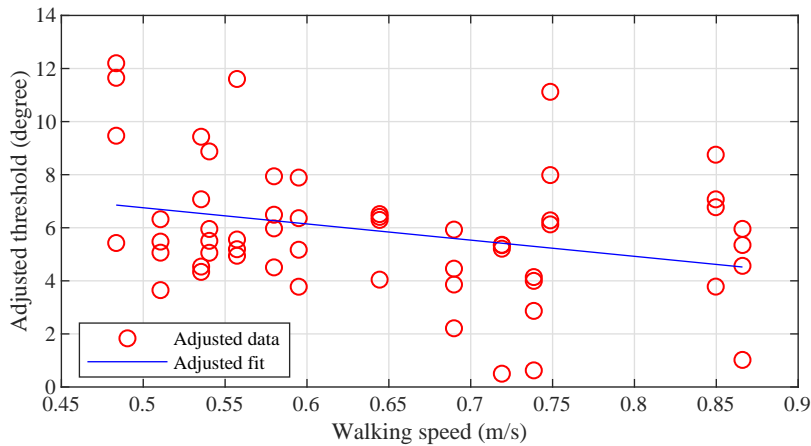
The results show no significant effect of rotation direction ($p = 0.7$), indicating that right-handed subjects tend to perform equally well at detecting discrete scene rotations either to the left or right. There is also no significant effect of gaming experience on the threshold values ($p = 0.44$), which means gamers do not have any advantage over non-gamers at detecting discrete scene rotations. Men and women were equally good at detecting discrete scene rotations as there is no significant effect of gender ($p = 0.73$). While gender difference has been shown to exist in curvature redirection thresholds [191], the mechanism of detecting multi-sensory conflicts introduced by curvature gains could be different from that of detecting discrete scene rotations. Therefore, it is possible that there is no gender difference in detecting scene rotations. However, further research with larger sample size and more even gender ratio is required to confirm this result. The effect of walking speed on detection thresholds is almost significant ($p = 0.07$) with the 95% CI:$[-12.885, 0.68]$. In Figure 5.4, a negative trend could be observed indicating that as walking speed increases, the detection thresholds tend to decrease. Nevertheless, as the experiment was not designed to identify the effect of walking speed on discrete scene rotation thresholds, the range of speed was probably too small (0.48m/s - 0.87m/s) for a significant effect to be detected.

Finally, there is a significant effect of eye state on the threshold values ($p < 0.001$) indicating that larger discrete scene rotations could be applied without being detected during blinks than when eyes are open. This result supports the fact that during blinks, visual suppression causes temporary blindness to changes in the scene that would normally be detected under eyes open condition. Threshold values vary largely across subjects, especially in the during blinks condition (see Figure 5.5). On average, the detection threshold for discrete scene rotation during blinks is 9.1 ± 3.2 degrees and when eyes are open is 2.4 ± 0.97 degrees.

5.1.2 Discrete Redirection in Redirected Walking Algorithms

In order to implement RDW techniques into real walking applications, different algorithms can be used. In classical algorithms such as steer-to-center (S2C), steer-to-orbit (S2O) and steer-to-multiple-targets, fixed targets (or trajectories) are predefined [205]. The algorithms determine the next redirection action that steers users towards these targets based only on the user's current real position and heading. In a dynamic path planning for obstacle avoidance algorithm, the map of the physical space (boundaries, static and moving obstacles) and the user's possible virtual position in the next time step (weighted by visibility and distance to the user's current virtual position) are also taken into account. Based on this, a cost function that penalizes close proximity to the physical space is defined and the next redirection action
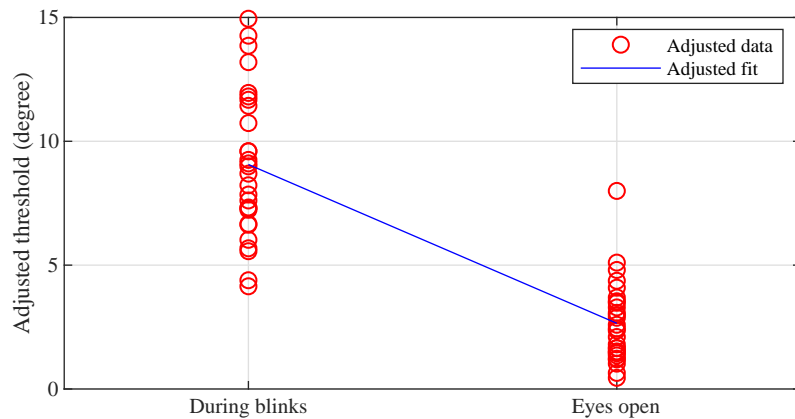
Figure 5.5: *Adjusted response plot: Effect of blinks on discreet scene rotation thresholds*

is the action that minimizes this cost function [243]. In a model predictive control (MPC) algorithm, in addition to the map of the physical space, the map of the virtual environment and the user's possible virtual paths in the next N time steps in the future are also considered. A cost function that penalizes resets (the application of rotational gain to reorient users away from physical boundaries) is defined and the next redirection action is selected to minimize this cost function [182].

Given a wide selection of redirected walking algorithms, research effort has been spent on identifying which algorithm delivers the best performance. Performance of redirected walking algorithms can be measured by the number of times users have to be stopped to perform a reset, causing a break in immersion. It was shown in simulations and live user studies that S2C performs the best in open VEs whereas S2O is most suitable for structured and constrained VEs [113]. S2C algorithm that employs translational gains on top of rotational and curvature gains outperforms the rest (S2C without translational gains, S2O with and without translational gains) and is the most robust when the shape of the physical space is moderately elongated [6]. MPC algorithm was shown to reduce the number of resets by 41% compared to S2C in a maze-like environment [182]. With error saving ratio as a performance metric, dynamic path planning algorithm was shown to outperform S2C [243]. Although these experiments were performed in different settings such as virtual environments, users' virtual paths, size and shape of the physical space, the trend suggests that algorithms such as dynamic path planning and MPC perform better than classical algorithms as they incorporate more information into their planning step. However, dynamic path planning requires computational power of high end GPUs for the optimization step; and MPC requires the virtual environment maps to be formally defined, which at the moment cannot be achieved for open unstructured VEs [288, 6] . Overall, classical algorithms are simpler, less hardware demanding to implement, and more applicable to generic VEs.

Until now, most of the aforementioned algorithms employ only subtle continuous RDW techniques (rotational, curvature and translational gains). In one study where additional rotation was continuously injected during saccades, even at a rate of 0.14 degree/frame it was shown that the algorithm's performance was improved compared to using only rotational and curvature gains [243]. While a higher degree/frame rotation could be achieved using subtle discrete RDW techniques (at least 5 degrees/frame during saccades [21], and 2-5 degrees/frame during blinks [148]), the combination of continuous and discrete RDW techniques has not been much explored. In the second part of this work, using the detection thresholds for discrete scene rotation during blinks obtained in the first experiment, a series of numerical simulations were used to investigate how the combination of discrete RDW techniques during blinks with continuous RDW techniques affect the performance of the classical S2C and S2O algorithms. The aim of the numerical simulations is to provide an estimation of how the incorporation of discrete scene rotation
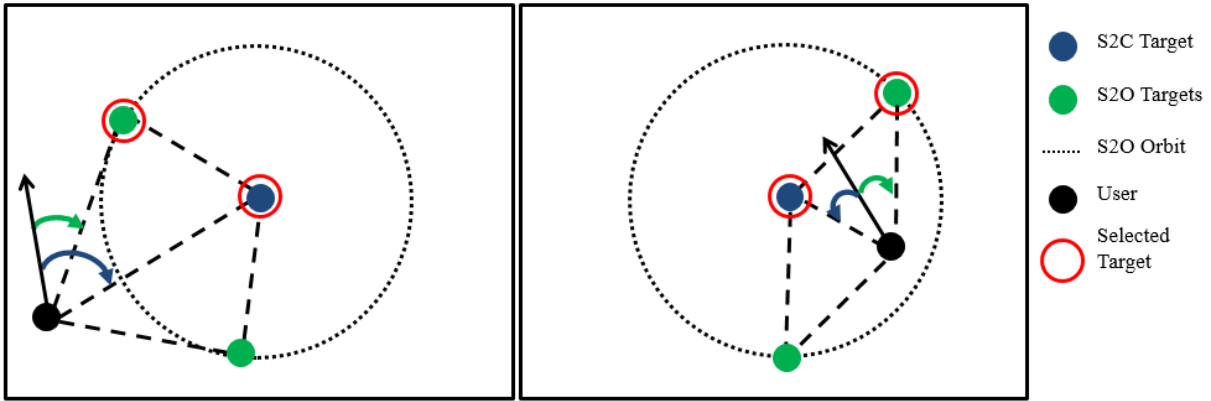
Figure 5.6: *"Steer-to" targets in S2C and S2O algorithms*

during blinks on top of the commonly used rotational and curvature gains affects the performance of classical redirected walking algorithms such as S2C and S2O.

Algorithms

The S2C and S2O algorithms used in our simulations were originally proposed in [205]. Firstly, based on the user's current position, a "steer-to" target can be determined (Figure 5.6). For S2C, the "steer-to" target is always the center of the tracking space. For S2O, two potential targets can be found: if the user is outside the orbit, the two potential targets are tangent points created by tangent lines drawn from the user's position to the orbit; if the user is inside the orbit, the two potential targets are the intersection points between the orbit and the equiangular lines (here defined to be 60 degrees [111]) to either side of the line passing through the user and the center. From these two potential targets, the selected target is the one that requires a smaller angle change from user's current heading (indicated by the blue and green arrows in Figure 5.6). Once a "steer-to" target is defined, the remaining procedure is the same for both algorithms: determining the **continuous rotation θ_{cont}** to be applied each frame and the **discrete rotation θ_{dis}** to be applied during blinks.

Depending on user's current linear and rotational velocity, three types of continuous rotation can be applied to the virtual scene: baseline rotation, rotation from rotational gain and rotation from curvature gain. **Baseline rotation θ_B** is applied when the user is not performing any movement, i.e. his/her linear velocity v_{real} and rotational velocity ω_{real} are below predefined thresholds V_{min} and Ω_{min}, respectively. Baseline rotation θ_B is calculated as follows:

$$\theta_B = \Omega_B \times \Delta t$$

where Ω_B is a predefined baseline rotation rate and Δt is the sampling interval. If the user's rotational velocity ω_{real} is larger than Ω_{min} but there is no linear movement, **rotation from rotational gain θ_R** can be calculated as follows:

$$\theta_R = \min\left(\omega_{real} \times G_R, \Omega_R\right) \times \Delta t$$

where $G_R = \frac{\omega_{virtual}}{\omega_{real}}$ is the predefined rotational gain and Ω_R is the maximum allowable rotation rate when a rotational gain is used. G_R is set to be larger than 1 if the user is rotating towards the target, and smaller than 1 if the user is rotating away from the target. If the user's linear velocity v_{real} is larger than V_{min}, **rotation from curvature gain θ_C** can be calculated as follows:

$$\theta_C = \min\left(\frac{v_{real} \times G_C \times 360}{2 \times \pi}, \Omega_C\right) \times \Delta t$$

where $G_C = \frac{1}{R}$ is the predefined curvature gain with R being the desired curvature radius and Ω_C is the maximum allowable rotation rate when a curvature gain is used. From the three proposed rotations, in order to steer to the target as quickly as possible, the largest rotation is selected:

$$\theta_{max} = \max\left(\theta_B, \theta_R, \theta_C\right)$$

Furthermore, in order to prevent large alternating rotations when the user is almost facing the target, or just walked past the target, the selected rotation θ_{max} can be dampened by two coefficients c_θ and c_d calculated as follows:

$$c_\theta = \begin{cases} \sin(\Delta\theta), & \text{if } |\Delta\theta| \leq \frac{\pi}{2} \\ 1, & \text{otherwise} \end{cases} \tag{5.2}$$

$$c_d = \begin{cases} \frac{d}{D_{min}}, & \text{if } d \leq D_{min} \\ 1, & \text{otherwise} \end{cases} \tag{5.3}$$

where $\Delta\theta$ is the angle between the user's current heading and the target heading, d is the distance from the user to the target, and D_{min} is the predefined distance to the target where dampening starts. The coefficient c_θ ensures that if the user is turning towards the target, the applied rotation becomes smaller as the user's heading converges to the target heading, and the rotation is zero when the user is exactly facing the target. Unlike the algorithm proposed by Razzaque [205], the implementation introduced here will not dampen the rotation by c_θ if the user is facing away from the target. The coefficient c_d ensures that when the user is within a radius of D_{min} to the target. The applied rotation is the smaller the closer the user is to the target, while no rotation is applied if the user is on the target. Finally, to prevent abrupt changes in applied rotations between frames, a smoothing function is applied. The final continuous rotation θ_{cont} to be applied is calculated as follows:

$$\theta_{cont} = (1 - S) \times \theta_{prev} + S \times c_\theta \times c_d \times \theta_{max}$$

where θ_{prev} is the applied rotation in the previous frame and S is the smoothing factor.

Contrary to the continuous rotation that is calculated and applied every frame, discrete rotation is only calculated and applied only when a blink occurs. A maximum rotation Θ_{blink} is defined based on the result of the threshold identification experiment, and depending on the user's current position and heading, the discrete rotation θ_{dis} can be determined:

$$\theta_{dis} = c_\theta \times c_d \times \Theta_{blink}$$

where c_θ and c_d are dampening coefficients that can be obtained from Equations 5.2 and 5.3. A summary of all predefined parameters used in the simulations can be found in Table 5.1.

Simulations Setup

Based on the Redirected Walking Toolkit [6], the S2O and S2C algorithms employing both continuous RDW techniques and discrete RDW techniques as described above were implemented in Unity.

Reset Techniques Reset trigger was implemented to simulate the user reaching the physical boundary where a reset action is required. There exists a reset technique called two-one-turn reset which

Table 5.1: *Predefined parameters*

Parameters	Value	Comments
D_{min} (m)	1	Dampening distance
G_R	0.67; 1.24	Rotational gain *
G_C (1/m)	0.13	Curvature gain (radius $R = 7.5$m) *
Ω_{min} (deg/s)	1.5	Rotation threshold †
Ω_B (deg/s)	0.5	Baseline rotation rate †
Ω_C (deg/s)	15	Max allowable rate for curvature gain †
Ω_R (deg/s)	30	Max allowable rate for rotational gain †
S	0.125	Smoothing factor †
Θ_{blink} (deg)	9	Blink detection threshold
V_{min} (m/s)	0.2	Movement threshold †

* Obtained from [236]
† Similar to [111]

involves users performing a 180-degree turn in reality, while it is a 360-degree turn in the virtual environment [6]. The equivalent rotational gain is always 2, which is larger than the average detection threshold of 1.27 [236]. Moreover, because it is a fixed 180-degree turn in reality, the user's heading after the reset is dependent on his/her heading just before reset, which does not always guarantee that he/she could walk the longest possible distance before encountering a reset again (see Figure 5.7a). In fact, it has been observed in the pilot studies that in some cases the user is stuck walking back and forth in a corner for a long time, resulting in a high variance in reset count. This high variance could potentially mask the effect of adding discrete rotations on the performance of the S2C and S2O algorithms. This limitation could be overcome if regardless of his/her previous heading, the user faces a predefined target in the tracking space after reset. In [199], this target is the center of the tracking space. In this work, we propose that this target could also be the furthest corner of the tracking space. From hereon these reset techniques are referred to as **to-center** reset and **to-corner** reset, respectively. Using these reset techniques, the user has to perform a real rotation of 360 degrees + the smallest angle between his/her heading and the target (center or corner), in the direction of the smallest angle (5.7b and 5.7c). The equivalent rotational gains used by these two techniques are not fixed, and are within thresholds when the angle between the user's heading and target is less than 120 degrees. No previous work has been done to compare these different reset techniques. Therefore, the effects of these reset techniques on the performance of the S2C and S2O algorithms with or withouts discrete rotations during blinks requires further investigation.

Virtual Path Types Since it is not possible to simulate the spontaneous nature of human walking behavior in a VE, in the simulations it is assumed that the user follows certain predefined virtual paths as proposed in [6] including:

- Office: 80 segments of length $l \in \text{unif}(2, 8)$ meters and turning angle between segments $\alpha = 90$ degrees
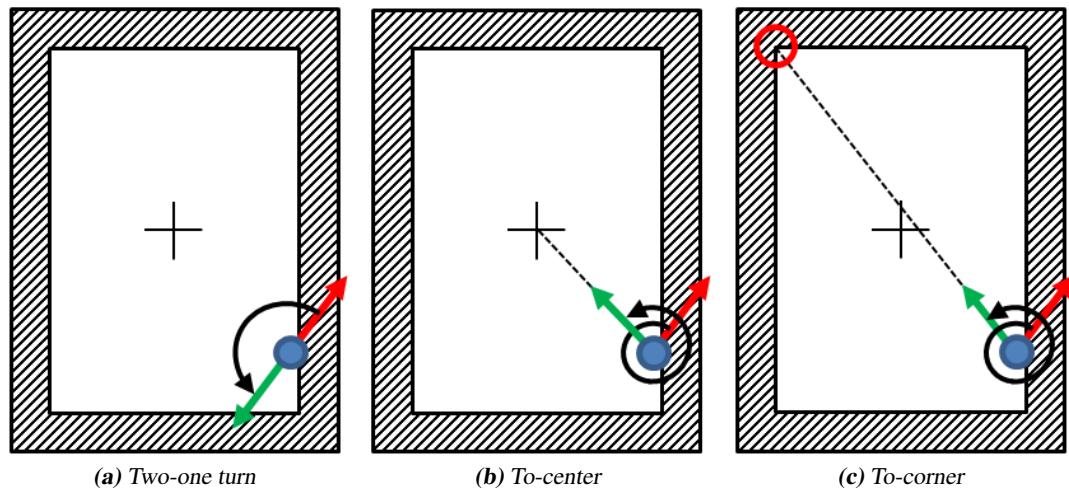
(a) Two-one turn **(b) To-center** **(c) To-corner**

Figure 5.7: *Reset techniques used in the simulations. Red and green arrows indicate user's physical heading before and after resets. Shaded areas indicate safety margin.*

- Small exploration: 100 segments of length $l \in \text{unif}(2, 6)$ meters and turning angle between segments $\alpha \in \text{unif}(-180, 180)$ degrees

- Large exploration: 40 segments of length $l \in \text{unif}(8, 12)$ meters and turning angle between segments $\alpha \in \text{unif}(-180, 180)$ degrees

The expected total path length for all path types is 400m, equivalent to a 10 minute walk of an average user in the VE.

Tracking Space Configurations   It has been shown in previous research that the tracking space size significantly affects the performance of redirected walking algorithms. With a sufficiently large tracking space, e.g. 40m × 40m, there is no difference in performance between any redirected walking algorithm as users can walk infinitely without having to perform any reset [6]. However, in practice, obtaining a space of such size could be challenging. Existing commercial products such as HTC Vive offer a room scale tracking space of up to 4m × 4m, and the HTC Vive Pro promises a tracking space from 6m × 6m up to 10m × 10m. With such limited space, resets are inevitable and the main goal is to improve algorithms' performances to reduce the number of resets.

Simulated Walker   Using the results obtained in Section 5.1.1, the simulated walker was implemented to follow the previously defined virtual paths at a speed of 0.65m/s and rotate during resets at a speed of 50 degrees/s. A safety margin of 1m to the boundaries of the tracking space was set, and resets are triggered once the simulated walker passes this safety margin (Figure 5.7). At the start of each simulation, the simulated walker stands at the center of the tracking space with two possible initial headings: facing forward or a randomly generated direction between 0 and 360 degrees.

The simulated walker was also implemented to raise an event at a predefined frequency, analogous to a blink of a real walker, to trigger a discrete rotation. Since a higher total amount of rotation can be applied if the users blink more frequently, the effect of blink frequencies on the algorithms' performances is also investigated. From Experiment 1, the obtained blink frequency ranged from 4.7 to 22 times/min. Based on existing literature that blinks occur 10-30 times/min [244] [67], this range was extended further and used the following blink frequencies: 5, 10, 15, 20, 25, and 30 times/min in the simulations.

Table 5.2: *S2O orbit radii used in square tracking spaces of different side lengths*

Simulation 1	Length (m)	4	5	6	7	8	9	10
	Radius (m)	0.5	1	1	1.5	2	2.5	3
Simulation 2	Length (m) *	15	20	25	30	35	40	
	Radius (m) *	5	5	5	5	5	5	

* Similar to [6]

Simulation Procedure

Given the aforementioned setups, the following simulations are conducted:

Simulation 1: This first simulation aims at investigating the effects of adding discrete rotations during blinks on top of continuous rotations on the performance of the S2C and S2O algorithms. The simulation is run in tracking space sizes that can potentially be obtained with current typical VR setups (e.g. HTC Vive), ranging from 4m × 4m to 10m × 10m with three reset techniques (two-one turn, to-center and to-corner). The simulated walker setup and virtual path types are as described in Sections 5.1.2 and 5.1.2.

Simulation 2: A second simulation is conducted to determine if adding discrete rotation has an effect on the minimum space required for users to walk without having to perform resets changes. For this simulation, tracking spaces ranging from 15m × 15m to 40m × 40m are used. The simulated walker setup and virtual path types are the same as in Simulation 1.

Considering that there is a safety margin of 1m to the boundaries before a reset is triggered, the S2O orbits have to lie well within this safety margin (with at least 0.5m distance from the wall). The radii of the S2O orbits for different tracking spaces are summarized in Table 5.2. In all simulations, the algorithms' performances are measured by the number of resets.

Results and Discussion

Simulation 1   In this simulation, the simulated walker performed 5 repetitions of 3 types of path (office, small exploration and large exploration), 2 initial headings as described in Section 5.1.2, in 7 tracking space sizes ranging from 4m × 4m to 10m × 10m, 3 reset techniques and 7 blink frequencies: 0, 5, 10, 15, 20, 25 and 30 times/min.

A discrete rotation is applied when a blink happens and the simulated walker is not performing resets. The amount of discrete rotation therefore directly correlates with the blink frequency. In order to investigate the effects additional discrete rotations on the performance of the S2C and S2O algorithms, for each tracking space size a linear model was fitted with blink frequency as a fixed factor. Reset techniques, algorithm types, path types and initial heading were also included as fixed factors to check for possible effects and the final model becomes:

$$\text{reset count} \sim 1 + \text{blink frequency} + \text{reset technique} + \text{algorithm type} + \text{path type} + \text{initial heading} \quad (5.4)$$
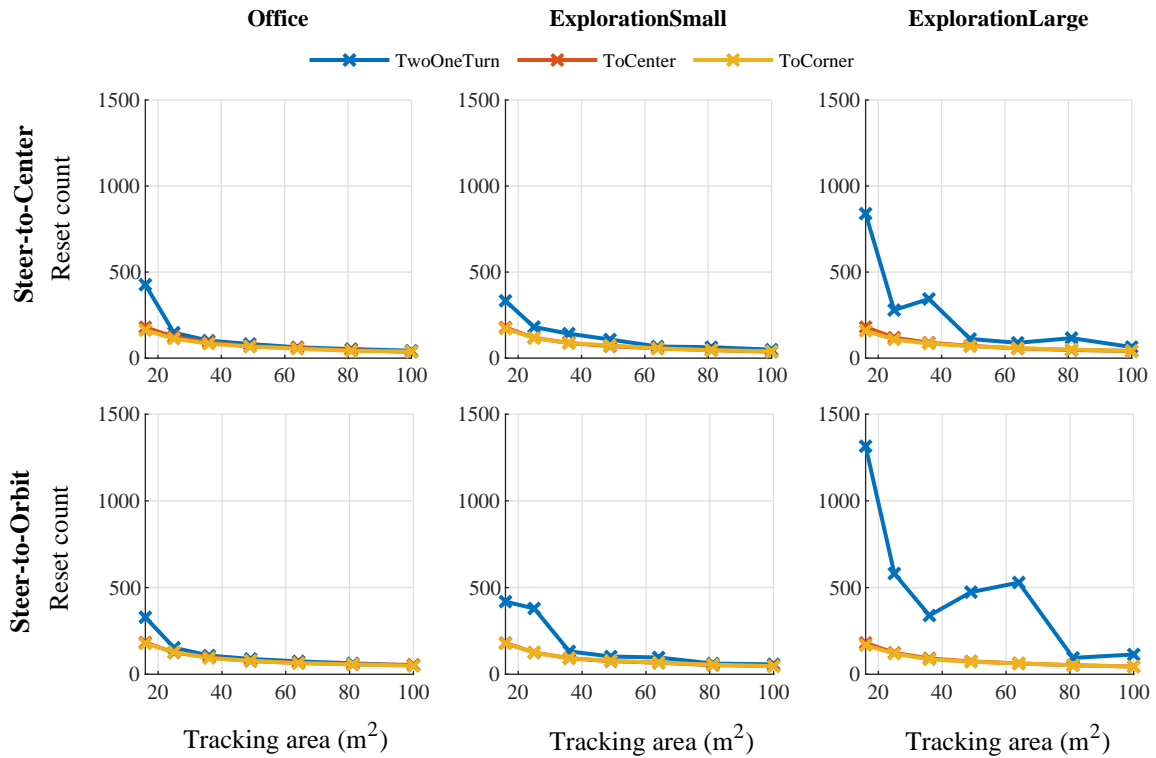
Figure 5.8: *Effects of three reset techniques: two-one turn, to-center and to-corner on the performance of S2C and S2O algorithms using only continuous rotations. The to-center line and the to-corner line mostly overlap in all subplots as large axis limit had to be used to adapt high number of reset in the two-one turn reset condition. Tracking area corresponds to tracking space of 4m × 4m to 10m × 10m.*

For all tracking space sizes, initial heading is the only the factor that does not have a significant effect on the number of resets.

Effect of reset techniques: For all tracking space sizes, results show a significant effect of reset techniques on the number of resets ($p < 0.001$). As shown in Figure 5.8, the number of resets is significantly lower in the to-center and to-corner conditions as compared to the two-one turn condition. In general, the two-one turn reset technique performed much worse when the tracking area is extremely small (4m × 4m and 5m × 5m) and does not perform very well with the large exploration path type even in larger tracking areas. Similar to the observations from the pilot studies, in some cases the simulated walker is stuck walking back and forth in a corner and only got out of the corner when he finishes the current straight segment. The longer the segments are, the longer the simulated walker is potentially stuck in the corner before a direction change and hence the higher number of resets in the large exploration condition. Due to the high variance in reset counts when the two-one turn reset technique is used, the analysis from hereon excludes the two-one turn reset technique. Considering the two remaining reset techniques, their performances only significantly differ for tracking sizes below 6m × 6m, with the to-corner reset technique performing better than the to-center reset technique (on average 3% lower in reset count).

Effect of path types: For tracking spaces below 5m × 5m, the reset count in the large exploration condition is significantly higher than the office and small exploration conditions. This could be explained by the fact that the average segment length of the large exploration condition is 10m, compared to 4m
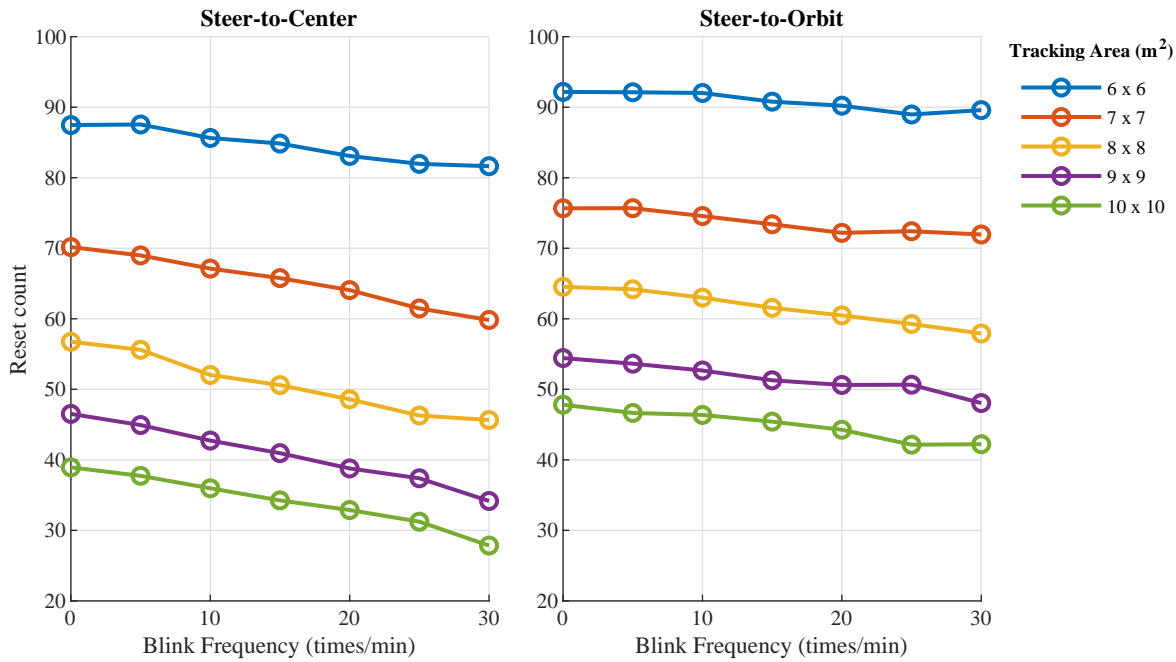
Figure 5.9: *Effects of blink frequency on the performance of S2C and S2O algorithms*

and 5m in the other two conditions. As the applied rotation rate is limited, in a tracking space where the straight segment is significantly longer than the space dimensions, the algorithms will not manage to redirect the user back to the center or orbit, and hence the higher number of resets.

Effect of redirected walking algorithms: For all tracking space sizes, there is a significant effect of redirected walking algorithms on the reset count. It can be seen from Figure 5.9 that on average, the S2C algorithm performs better than the S2O algorithm, which is in line with previous findings [111, 8].

Effect of blink frequencies: Blink frequencies only show significant effects for tracking spaces of 6m × 6m or above, where discrete rotation is applied more often, leading to lower number of resets. In a tracking space of 10m × 10m, if a user blinks only 5 times/min (close to the minimum blink frequency obtained in Section 5.1.1), the reduction in reset count is not statistically significant. However, for the same tracking space size, at a blink frequency of 10 times/min or above, the reduction in reset count is statistically significant. Reset count reduction is 13% at a blink frequency of 15 times/min (close to the average frequency of 13 times/min obtained in Experiment 1), and 29% at a blink frequency of 30 times/min.

Simulation 2

Considering the results from Simulation 1 that incorporating discrete rotation with sufficiently high blink frequency increases the performance of the S2C and S2O algorithms, in this simulation, it is hypothesized that the minimum space required for walking without encountering any reset could also be reduced. The simulation consists of the simulated walker performing 5 repetitions of 3 types of path, 2 initial conditions, 7 blink frequencies ranging from 0 to 30 times/min in interval of 5 times/min, 2 reset techniques and 6 tracking space sizes ranging from 15m × 15m to 40m × 40m. The average reset count can be
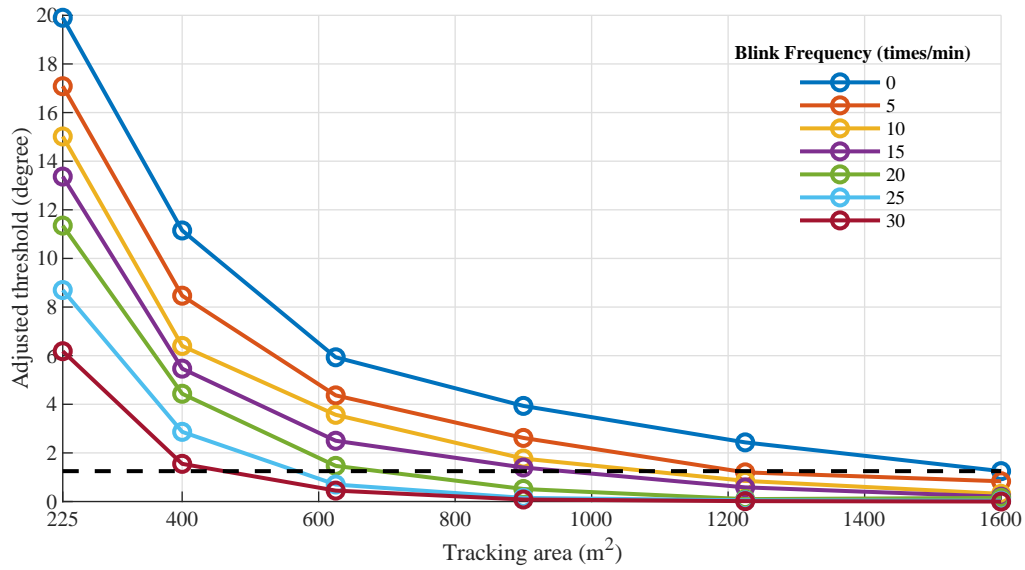
Figure 5.10: *Effects of tracking space size on the performance of S2C algorithm. Tracking area corresponds to tracking space of 15m × 15m to 40m × 40m. Blink frequency of zero means no discrete rotation is applied.*

found in Figure 5.10. It can be seen that in a tracking space of 40m × 40m, using the S2C algorithm with only continuous rotations, users encounter on average only 1.25 resets. If discrete rotation is also applied, the same performance could be achieved in a tracking space of 30m × 30m if the users blink 15 times/min. If the users blink up to 30 times/min, the required space could be reduced further to 20m × 20m.

5.1.3 Conclusion

In this section, a new redirection technique was proposed, in which a scene rotation is discretely applied when users blink. In order to investigate if the technique works, a study was conducted to identify the detection thresholds of the discrete scene rotation during blinks and during eye open conditions. Results showed that right-handed subjects tend to be equally sensitive to either rotation direction, and there is no significant effect of gaming experience or gender on detecting discrete scene rotations. Most importantly, it was found that the detection thresholds are significantly higher during blinks (a scene rotation of 9.1 degrees per blink) as compared to when eyes are open (a scene rotation of 2.4 degrees one second after the eyes are open), indicating the effect of visual suppression and confirming the effectiveness of the proposed technique. From the obtained results, there seems to be a trend that detection thresholds negatively correlate with walking speed. However, the validation of this trend remains to be investigated in future experiments. While it is possible to apply blink redirections and other redirection techniques simultaneously, it would be interesting to know how the thresholds for blink redirections are affected in the presence of other techniques. Since the modes of application of the two types of technique is different: blink redirections are applied discretely and curvature, rotational and translation gains are applied continuously, a hypothesis could be made that the perception thresholds for each technique would be unaffected by the others and can be superposed. To test this hypothesis, a new multi-dimensional threshold identification protocol must be devised such that the thresholds for both discrete and continuous techniques can be identified at the same time. This would also be a topic for future investigation.

Two new reset techniques were also proposed that direct users to the furthest corner or the center of the

(a) T-maze   *(b) Forced maze*

Figure 5.11: *Types of mazes*

tracking space instead of a fixed rotational gain reset. Computer simulations were run to investigate the effectiveness of the proposed reset techniques, and if the blink redirection technique improves common RDW algorithms when it is applied in conjunction with existing subtle continuous redirection techniques. Results showed that the to-center and to-corner reset techniques give better performance than the two-one turn reset techniques. Results also showed that given a sufficiently large tracking space and high enough blink frequency, the reset count and the minimum space required for walking without encountering a stop and reset could be significantly reduced (potentially up to 29%). Future work therefore involves identifying factors that induce more frequent blinks in a virtual environment.

5.2 Spontaneous Alternation Behavior [2]

In this section, a series of experiments are proposed, aiming at picking up the thread and initiate the systematic investigation of human SAB. By bringing the traditional paradigm of SAB into VR, the most basic question is raised: "Do human alternate?" (Experiment 1). Secondly, the different factors that potentially affect this behavior such as cognitive load (Experiment 2), visual and/or bodily change of direction (Experiment 3) are explored. Concurrently, the relationship between the tendency to avoid repetition in a random number generation task [33] with the tendency to alternate direction during walking is also investigated. The possibility that the mental task could be used as a predictor for users' behavior is also explored. Furthermore, Experiment 4 is conducted to explore if the alternation behavior also exists when the environment is not constrained by binary choices, but rather an open, unconstrained environment where the number of choices is infinite.

5.2.1 Experiment 1 - SAB in humans

Experiment Design

In most existing SAB experiments in walking humans, the classical T-maze is used (Figure 5.11a) [198, 153]. That is, subjects are required to walk two times through the same T-maze, and SAB is quantified as the percent of times the subjects select a different arm of the T-maze in the second walk. This quantity is called the *alternation rate*. Another possible maze design for an SAB experiment in humans is an extended forced maze (or triple T-maze), where subjects perform a forced turn before the free turns at the following T-junctions (Figure 5.11b). In this type of maze, the alternation rate can be calculated as the conditional probability of alternation given the direction of the previous turn(s). While both designs are suitable for investigating the existence of SAB, the triple T-maze was selected over the classical T-maze as the environment is more similar to a natural setting. Moreover, a triple T-maze also offers the

---

[2]Parts of the section were published in [190, 218]
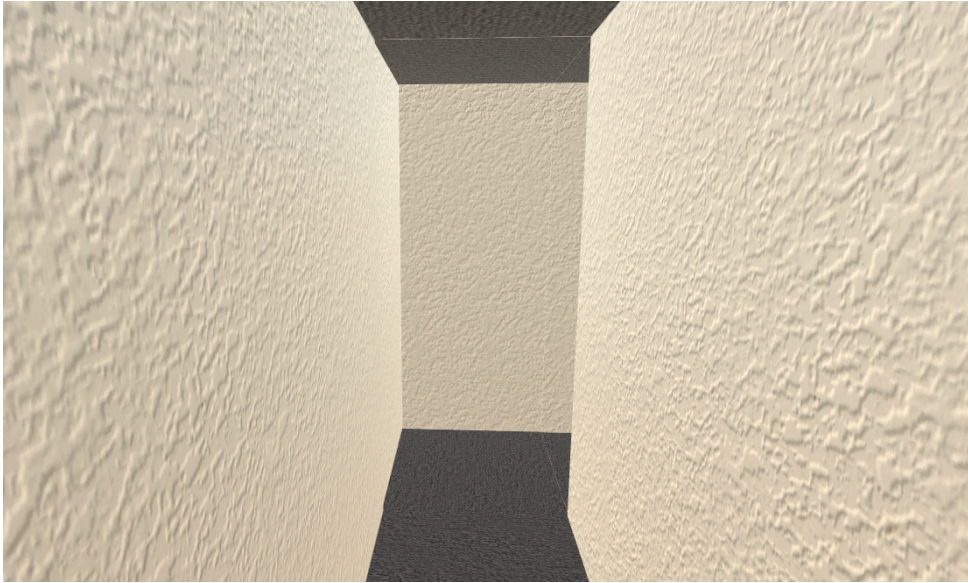
Figure 5.12: *Maze view from the starting position, before the forced turn*

possibility to observe whether users maintain or change their alternation rate as they walk further into the maze.

The final maze design consists of an initial 90° forced turn, which is followed by three consecutive T-junctions (Figure 5.11b). Unit pieces of the maze such as straight, corner and T-joint are first modeled in Blender and then imported and assembled in Unity. The maze walls have a generic plaster texture (Figure 5.12), and lights are placed in the environment such that when the subjects are at the T-intersections, both choices look completely identical. The distance between each turn is 1.5m. Due to limited lab space, the complete maze can not all fit in. As a result, only parts of the environment are shown at a time depending on the position of the subjects (Figure 5.13). This approach is similar to the flexible spaces approach introduced in [262]. Step regulating sound is played during the subjects' walk in the maze to ensure a walking speed of 0.75m/s for all subjects. The height information of subjects was collected before the experiment day, and the step sound prepared in advance using the formula in [59]. Even though it was found in previous experiments that this method did not accurately regulate users' walking speed, the main aim in this particular case is to ensure subjects walk continuously through the maze without stopping.

The experiment setup consists of an Oculus DK2 and an Intersense IS-1200 optical tracking system mounted on top, providing 6-DOF positional tracking at 180Hz. The scene is optimally designed in Unity to run at the HMD's maximum frame rate 75Hz. The whole setup is powered by a backpack-mounted notebook. The available tracking space is 13.3m × 6.6m.

Participants and procedure

Sixty subjects (aged from 18-35 (mean=25.2, SD=3.8), 30 male and 30 female, right-handed, with normal or corrected-to-normal vision) were recruited through the university market place. The SAB experiment lasted about 15 minutes including instructions and setup time. The subjects were not informed about the purpose of the experiment. The direction of the initial forced turn was balanced across subjects. Before starting the experiment, subjects were shown screen shots of different parts of the experiment and were given this instruction: *"When the program starts, you will see a starting position. Walk to this po-*

(a) Start of the maze   (b) Middle of the maze   (c) End of the maze
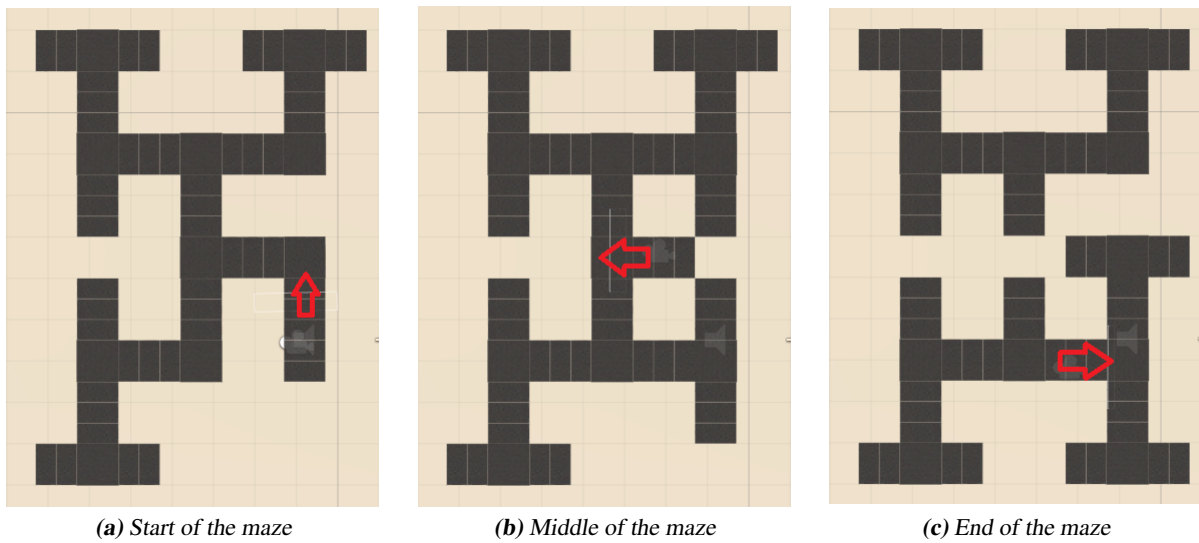
Figure 5.13: *Visibility of different maze parts depending on the position of the subject*

The red arrow indicates the current position and orientation of the subject

sition. A maze will appear (Figure 5.12) and you will hear ongoing step sounds. Please follow this step rhythm while walking through the maze without stopping. You can freely explore the maze as you want." After signing the consent form, subjects put on the backpack and started walking. An experimenter walked right behind the subjects to prevent them from colliding with the physical walls in the event that they would not follow the path of the VR maze. After the subjects completed the experiment, they were asked: *"Did you use any strategy or plan where to go? Or were you just walking spontaneously?"* Their answer to this question determined whether their data would be used for the analysis. Subjects were paid 15CHF/hour for their contribution.

Results

When being asked if they used any strategy for the maze, out of 60 subjects, 11 subjects (8 male and 3 female) answered similar to one of the following ways: *"I was trying to see if I can walk in a circle"*, *"I deliberately changed directions so that I can walk further"*, or *"I decided to always turn left"*. The data from these subjects were not included in the analysis. The remaining 49 subjects answered that they were walking spontaneously without any planning.

The three consecutive direction choices per subject were scored either as alternations or repetitions based on the prior direction choice, or in the case of the first junction, based on the direction of the forced turn. This resulted in three binary data points per subject. There are eight different possibilities for an outcome of a subject (000, 001, 010, 100, 011, 101, 110, 111; 1 = Alternation, 0 = Repetition). The frequencies of those eight outcomes were counted and the overall distribution of walking patterns is presented in Figure 5.14. Using a chi-squared goodness of fit test, this distribution was shown to be significantly different from what would be expected if the subjects had alternated at a chance level ($\chi^2 = 34.76$, $p < 0.001$). To estimate an overall alternation rate while incorporating the threefold contribution to the dataset by each subject, a logistic regression was fitted to the data, which included subjects as a random factor. The linear model is as follows:

$$\text{Alternation} \sim 1 + (1|\text{Subject}) \tag{5.5}$$

	$P(R|FL)$	$P(L|FR)$	$P(X|FY)$	$P(X|Y)$	$P(X|YY)$
Male (N=22)	0.82 (11)	0.64 (11)	0.73* (22)	0.73* (22)	0.93* (14)
Female (N=27)	0.75 (12)	0.80* (15)	0.78* (27)	0.72* (27)	0.92* (13)
Total (N=49)	0.78* (23)	0.73* (26)	0.76* (49)	0.72* (49)	0.93* (27)

Table 5.3: *Summary of spontaneous alternation rates expressed as conditional probabilities given the prior turn direction(s). $P(R|FL)$ and $P(L|FR)$ are the alternation rates after the first forced left and right turn respectively. $P(X|FY)$ is the alternation rate right after the primary forced turn regardless of direction. $P(X|Y)$ and $P(X|YY)$ are the overall estimated alternation rates after 1 and 2 turns in the same direction respectively. Number of subjects is indicated in brackets. (Stars indicate significant differences to $p = 0.5$, α = 0.05)*

Based on the formula of the logistic regression, let $P(X|Y)$ be the probability of alternation (and $P(Y|Y)$ be the probability of repetition), the estimated intercept a of this linear model is calculated as:

$$a = log(\frac{P(X|Y)}{1 - P(X|Y)}) \tag{5.6}$$

. By looking at the intercept's confidence interval, it was tested whether the intercept is significantly different from zero, which corresponds to an alternation rate of 50% ($log(\frac{0.5}{0.5}) = 0$). The logistic regression showed an overall estimated alternation rate of 72%, which was shown to be significantly different from a 50% alternation rate (95% confidence interval: 0.65 - 0.79). In order to examine effects of gender and the sequential position of the junction (first, second or third junction) a second logistic regression was fitted, which included gender and junction position as fixed effects. The linear model is as follows:

$$Alternation \sim 1 + Gender + Junction\ Position + (1|Subject) \tag{5.7}$$

The statistical significance of the effects gender and junction position were tested using likelihood ratio tests by comparing the full model to a reduced model missing the factor of interest respectively. The likelihood ratio tests however showed no significant effects of either gender nor junction position (gender: $\chi^2 = 0.02$, $p = 0.88$; junction position: $\chi^2 = 0.20$, $p = 0.65$). To specifically test the alternation rate right after the primary forced turn regardless of direction (defined as $P(X|FY)$) against a rate of 50%, a binomial test was conducted. Results showed that subjects alternated with a rate of 76% , which is significantly different from what would be expected by chance ($p < 0.001$ (two-sided)). Finally we also performed a binomial test on whether the alternation rate after two consecutive turns in the same direction (defined as $P(X|YY)$) is significantly higher than 50%. The alternation rate following such two consecutive turns was 93%, which is significantly different from what would be expected by chance (p < 0.001 (two-sided)). An overview of alternation rates can be found in Table 5.3. All tests were performed using the statistical software R [34] [16] with a significance level of $\alpha = 0.05$.

Discussion

The results indicate that in a maze-like VE, walking subjects alternate directions with a rate around 72%. This alternation rate was shown to be independent of gender and sequential junction position, where the latter finding suggests that the alternation behavior does not decay or increase over time. The finding seems to be comparable to alternation rates found when humans are navigating through a stylus maze as
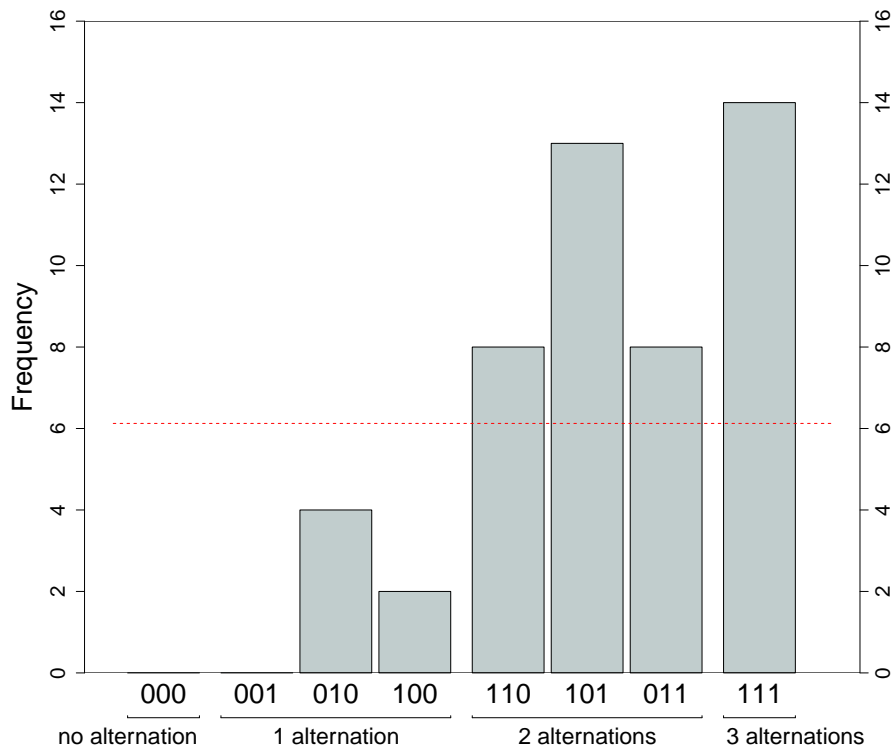
Figure 5.14: *Distribution of the frequencies of the eigth possible maze trajectories (1=Alternation, 0=Repetition). The dashed red line indicates the frequencies expected by an alternation rate of 50%.*

in [153] and surpasses the alternation rate so far found in walking humans [181]. Additionally, it was shown that a forced turn, in which subjects don't make a direction decision themselves, still resulted in an alternation rate of 76%. This finding suggests that in the context of SAB it does not seem to make a difference for humans whether a turn direction is self-chosen or imposed. When looking at the distribution of the eight possible maze trajectories in Figure 5.14, a clear shift towards trajectories with two or three alternations can be observed, whereby all trajectories with one or no alternations occurred less than what would have been expected with a 50% alternation rate. Finally, when looking at junctions after two consecutive left or right turns, subjects changed direction with an even higher rate of 93%. In general, the positive finding of alternation behavior in walking humans shows potential that this can be used to increase the efficiency of redirected walking using the MPC algorithm. However, how much of an enhancement the inclusion of an SAB rate would bring is still not clear and requires further investigation. Moreover, while the alternation behavior seemed stable in the experiment setting, it remains to be investigated how SAB can change in slightly different contexts. Effort was taken to exclude other factors that might possibly influence alternation behavior as much as possible for this study: The subjects were not given any specific task, for example finding a way out of the maze; All junctions were created to be completely equal in terms of visual appearances including brightness. When considering more realistic VEs that might come up in real applications, these factors are not suppressed as they were in this experiment. In a virtual supermarket for example, whose aisles and corridors approximatively resemble a maze-like structure, users might be driven in their walking trajectories by many more factors than just an internal tendency to alternate turn directions. Such factors might be the effort of a user to find a specific article, the visual appearance of certain aisles, and other structural characteristics of the supermarket. Another point that should be addressed is that the distances between T-junctions in the maze were uniform and relatively short (1.5m). In previous studies with humans, the distance between junctions has been shown to significantly influence alternation rates; longer distances between turns lead

to lower alternation rates [153]. Finally, only a first level alternation analysis was presented, which assumes that alternation is only dependent on the immediately previous turn. A more in-depth analysis might be required to understand whether earlier turns also have an effect on the current turning choice. and may reveal more complex alternation patterns. One example could be a tendency to systematically alternate alternations themselves, which would favor trajectories like (0,1,0) and (1,0,1). Indeed the distribution in Figure 5.14 might indicate such a trend.

Conclusion

In this experiment, the existence of SAB in human adults during walking in a virtual maze was investigated. Across the extend forced maze, the average alternation rate with respect to the immediately preceding turn was 72%, and the alternation rate with respect to the previous two turns in the same direction was 93%. This result shows that humans do in fact exhibit SAB. It would also be interesting to see if the behavior is affected when RDW techniques are applied. More specifically, a curvature gain, which forces the user onto a curved path through the insertion of a small rotation of the virtual scene, might influence the alternation rate in maze-like scenarios. This topic will be addressed in Experiment 3. It should be pointed out that the experiment was focused on testing SAB in a relative simple setting, without defined tasks, or other factors such as visual information (brightness, moving objects, etc.) and auditory information. The presence of these factors could significantly affect the alternation rate, and therefore requires further research. This point will be discussed in Experiment 3. Finally, the alternation rate obtained could be used to update existing prediction models, thus enhancing the efficiency of the MPC planner. However, how much performance improvement could be achieved is not yet known, and will require further implementation and benchmarking.

5.2.2 Common setup in Experiment 2, 3 and 4

Participants   The following three experiments were carried out with the same group of subjects containing 288 healthy, right-handed subjects, within the age range of 18-40 years (144 men and 144 women). Handedness was assessed with a shortened version of the Edinburgh Handedness Inventory [264] See Appendix A.3. Exclusion criteria included any history of neurological, vestibular or psychiatric disorder. Any injuries affecting the natural gait of subjects also led to an exclusion from the study. Subjects were informed about the exclusion criteria beforehand and asked to only apply if no criteria are violated. Subjects were mainly recruited using the online forum "Marktplatz" of the University of Zurich (UZH) and via mailing lists of the psychology department of the UZH. Reimbursement for participation was 10 Swiss francs for an approximate duration of 20 minutes. subjects were asked to sign an informed consent form prior to starting the experiment. All experimental procedures had been approved by the Cantonal Ethics Committee of Zurich and were carried out in accordance with the ethical standards of the Declaration of Helsinki.

General experiment procedure   The session consisted of three experiments, each including a specific type of virtual maze. The details of each experiment will be discussed in following sections. Each participant took part in all three experiments, performing in total six walks through the different virtual mazes. To counteract possible order effects between trials, the order of the six walks was randomized and balanced across subjects. One constraint in the randomization was that two walks of the same experiment are never conducted right after each other (see Appendix A.4) for a full description of the randomization scheme). The three experiment lasted a duration of two months for the recruitment and testing of all subjects.

Subjects wore an Oculus DK2 HMD with an InterSense IS-1200 optical tracking system mounted on top for 6-DOF head position tracking at 180 Hz in a 13.3 m x 6.6 m tracking area. The virtual maze environments were generated in Unity, which ran on a laptop carried by subjects on their back during the experiment (Figure 5.15a). Before each walk through the maze, a starting position and orientation was shown through the HMD and the trial started once the subjects had reached the indicated starting position and orientation. The procedure was fully automated and did not require the involvement of the experimenter. The experimenter viewed the same virtual scene as the subjects through a separate display and only interfered when technical problems would arise. Subjects were not informed about the actual focus of the study and were only instructed that they will be exposed to maze-like virtual environments, in which they are invited to freely move around. The only limitations to their exploration were 1) subjects should not turn around (180 degree turn) when walking in a corridor, and 2) when coming across open spaces, subjects can walk around in theses spaces but not go back into the corridor they came from. After completing all trials, subjects were asked whether they had followed a specific strategy to navigate through the VEs and, if yes, to characterize this strategy. The answers to this question were considered for a potential explorative analysis, examining differences between individuals, who adhered to specific navigation strategies, and subjects walking without strategy.

General pre-processing and statistical procedures Based on the head tracking recordings, the walking trajectories throughout the mazes were calculated for each subject. There was no outlier removal in the collected data. If at any point technical issues arose during an experiment interfering with the experiment's procedure or data logging, the subject was excluded from the experiment in which the issue emerged, and replaced by a new subject. Issues rated as interfering with the experiment's procedure included any type of freezing of the displayed virtual environment or any other distortion of the presented virtual environment. Technical issues were recognized by the experimenter, who monitored the procedure of all experiments on a separate display. In case of a subject wanting to stop the experiment due to motion sickness or any other discomfort, they were excluded from all experiments independent of how many walks had already been completed.

All statistical analyses were performed with the statistics software R, using a significance level of p= 0.02. For each tested value, the associated 98% confidence interval is reported. Analyses involving mixed-effects models were performed with the R packages "lme4" and "lmerTest" [16]. Confidence intervals for coefficients in mixed-effects models were based on parametric bootstrapping.

5.2.3 Experiment 2 - SAB under cognitive load and its relation to random number generation

Experiment 1 aimed at investigating if SAB exists in humans under the most simplified scenario: performing locomotion without any specific goal nor additional task. This is most often not the case in typical VR applications. In this experiment, the aim was to investigate how being "cognitively occupied" with a generic dual task affects SAB in humans. Results in Experiment 1 showed that alternation at a junction is dependent on the choice in the previous trial and gives thus testimony to the fact that this choice is somehow remembered (physiologically or cognitively). Even though there have been observations that performing a dual task diminishes repetition avoidance in humans attempting to generate random numbers [31], the role of cognitive load in human SAB has never been empirically investigated. Theories suggesting that SAB happens because the previous choice is remembered [146] would predict alternation rates to decrease under additional cognitive load because of its detrimental effect on remembering the previous turn.

Figure 5.15: *Depiction of a participant and schematic drawings of the virtual mazes. (a) Participant wearing an Oculus DK2 and a laptop running the VR simulation on the back. The HMD is equipped with a shield to prevent visual feedback from the ground. (b) The triple T-maze of experiment 1. Scored responses are indicated at the three T-junctions. (c) The three curved T-mazes of experiment 2. The blue lines represent the physical trajectories, which are not congruent with the maze outlines due to the applied redirected walking (curvature gain) in the "visual" and "physical" conditions. (d) The open maze of experiment 3. The reverse turning angle is indicated for a fictional walking pathway (blue line) at a specified distance from the corridor exit.*

Experiment design

In this experiment, the effect of cognitive load on SAB in the same triple T-maze used in Experiment 1 is investigated (Figure 5.15b). Assuming that memory is an integral component of human SAB, it was hypothesized that an increase in cognitive load leads to reduced alternation rates.

As a dual task, an auditory Stroop task was selected, in which the subjects (while walking) repeatedly heard the words "Frau"/"woman" and "Mann"/"man" spoken by either a woman or a man [99]. Thus, voice and word were either congruent or incongruent. Subjects had to indicate the gender of the speaker for each presentation. The auditory Stroop task was chosen because of the task's lack of a spatial component. More conventional dual tasks, such as the serial-7 or serial-3 subtraction tasks used in Section 4.3, are known for their potential to introduce a spatial bias, due to the internal representation of numbers on a mental number line expanding from left to right [162]. Such implicit spatial bias could interfere with the alternation of turn directions in the maze. In addition to the absence of a spatial bias, the auditory Stroop task has been shown to reliably engage walking humans' working memory [202].

Before the virtual maze experiment, subjects' repetition avoidance was assessed in a Mental Dice Task [92]. The Mental Dice Task is a random number generation task that requires the paced naming of the digits from 1 to 6 in a sequence mimicking consecutive rolls of a fair dice as closely as possible. The assessment of repetition behaviour with the Mental Dice Task allowed the notion of a conceptual equivalence of response alternation in random number generation and SAB in maze exploration [31]. This was more than just a superficial correlation analysis; any association between the avoidance of repetition on a highly cognitive level [32] and that on the level of effector physiology [33] might point to some fundamentals in the control of the serial order of behaviour [152].

Power analysis

The assumed parameters used for the power analysis were taken from Experiment 1. In this experiment, the overall significant alternation rate of 72% in the control condition in a sample size of 60 subjects. The random effect of subjects was estimated to entail a standard deviation of $5e - 8$. A power analysis, incorporating this random effect and an assumed alternation rate of 72%, revealed a necessary sample size of 28 subjects to detect an alternation rate in the control condition different from chance with a power of 90%. An additional power analysis was performed to investigate the sample size necessary to detect a difference of alternation rates between the two conditions (with and without dual task). Because there is no data on the effect of a dual task on alternation rates in walking humans, it is reasonable to rely on dual task experiments from general alternation experiments to estimate expected effect sizes. However, despite a variety of dual task experiments in random number generation, the translation of effects to SAB rates is difficult to achieve. In random number generation, the randomness of the produced sequence, which consists of more than just two possible elements (usually the numbers 1-9), is scored as a mathematical index or an entropy value, which does not correspond directly to an alternation rate. What remains is to fall back on animal experiments. Although in the animal literature on SAB classical dual task paradigms have not been employed, there are studies in which visual cues from a maze were gradually removed, making it more difficult for the animal to remember them in upcoming trials. Gerbils alternated in a standard T-maze with a rate of 72% [64], an alternation rate comparable to the one found in humans walking in Experiment 1. When removing internal cues from the maze, leaving only spatial orientation, alternation rates of gerbils dropped to 55%. Removing all possible cues from a maze resulted in an alternation rate of 50% [64]. Based on these results, it could be concluded that a decrease in alternation of 15% is a reasonable estimate of the dual-task effect on human alternation rates. Using this decrease as the assumed effect size results in an alternation rate of 57% in the dual task condition.

The power analysis revealed a necessary sample size of 135 to detect the assumed alternation decrease with a power of 90%. For the correlation test between the subjects' number of digit repetitions (Mental Dice Task), the power analysis (assuming a medium effect of correlation between the two variables of 0.3 [44]) indicated a needed sample size of 139 to reach a power of 90%.

Procedure

Prior to walking in the mazes, subjects completed a training session to familiarize themselves with the dual task. While sitting, they were presented with five audio playbacks of the auditory Stroop task, to which they had to verbally react appropriately. Subjects were informed that at one point during the experiment, they would have to react to audio playbacks in the fashion just trained. In addition, subjects performed the Mental Dice Task while sitting, without being immersed in a virtual environment. In this task, subjects were asked to generate a random number sequence with digits ranging from 1 to 6, mimicking the rolls of a fair dice. In total, 66 numbers were generated with a 1Hz frequency. The timely generation of new numbers was dictated by a metronome. The random number sequences were recorded following the procedure described by Geisseler et al. [92].

Subjects then performed two walks through the maze, once with and once without performing a dual task. The direction of the initial forced turn was randomized and counterbalanced over subjects. The audio Stroop task was prepared in advance with English and German, and subjects could select which language they prefer to perform the task in. The audio was recorded from computer generated male and female voices, using three different artificial voices for each gender. Subjects were asked to verbally report the gender of the speakers. Starting with the first step into the maze, new audio playbacks were presented in time intervals of two seconds. Subjects were instructed to react as fast and accurately as possible. Correctness of the responses were scored, but we did not intend to analyze this variable any further, as the main purpose of this task was to introduce cognitive load. In the control condition, subjects walked through the maze without hearing any audio playbacks.

Results

Similar to Experiment 1, the decisions at the three junctions of the maze were scored as a repetition or alternation in relation to the chosen turn direction in the immediately preceding turn. The direction decision at the first junction was evaluated in relation to the direction of the initial forced turn. It could be hypothesized that subjects would significantly alternate direction choices in the control condition and that in the dual task condition this alternation rate would be decreased. To test these hypotheses, an overall alternation rate was calculated for the control condition. This was achieved by fitting a mixed-effects logistic regression model to the alternation responses of the subjects in the control condition, only including subjects as a random intercept:

$$\text{Alternation} \sim 1 + (1|\text{subject}) \tag{5.8}$$

The intercept of this fit was tested against a value of zero, which is identical to testing the overall alternation rate against an alternation rate of 50%. The estimated intercept a of the logistic regression is equal to:

$$a = \log(\frac{P(alternation)}{(1 - P(alternation))}) \tag{5.9}$$

Therefore an intercept of zero corresponds to an alternation rate of 0.5, since $\log(\frac{0.5}{0.5}) = 0$. This analysis additionally served as a replication of Experiment 1, in which a significant overall alternation rate of
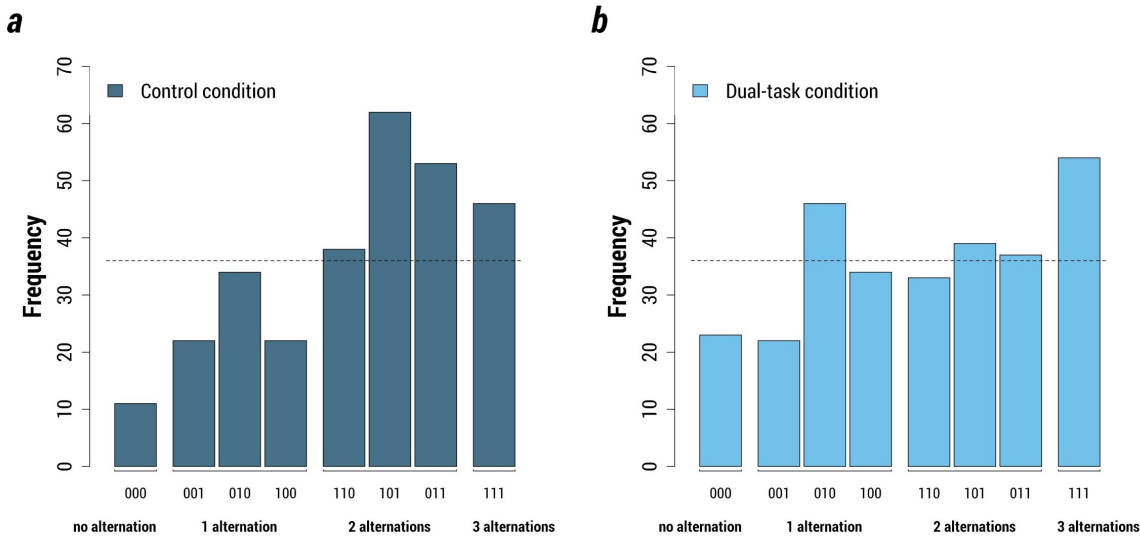
Figure 5.16: *Histograms of the different alternation patterns exhibited in the triple T-maze. The three traversed T-junctions are scored as 0 for repetition of direction and as 1 for alternation. The eight possible pathways range from no alternation at all (000) to the maximum of three alternations (111). The frequencies for the possible trajectories are shown for the control condition (a) and the dual task condition (b).*

72% was observed. Subsequently, a mixed-effects logistic regression model was fitted to the entire data, including alternation rate as the dependent variable, condition (two-level factor, with or without dual-task) as a independent variable and subjects as a random intercept:

$$\text{Alternation} \sim 1 + \text{condition} + (1|\text{subject}) \qquad (5.10)$$

The coefficient of the condition factor was tested against a value of zero. In the control condition, subjects showed an overall alternation rate of 60.4%, significantly higher than the chance rate of 50% ($p = 1.21E - 9$, 98%-CI: [56.6%, 64.3%]). In the dual task condition, the alternation rate was 55.8%, which is significantly higher than the chance rate of 50% ($p = 0.0007$, 98%-CI: [52.5%, 59.1%]). The difference in alternation rate between the control and dual task conditions, however, was not significant ($p = 0.051$, 98%-CI: [-0.418, 0.038]). Subjects' alternation tendencies in the triple T-maze can be seen in Figure 5.16.

There was no significant left or right turn preference in subjects (right turning rate of 48.1%, $p = 0.112$). There was no significant gender effect in alternation behavior ($p = 0.845$) nor in side preference ($p = 0.194$). In the junction immediately after the initial forced turn in the triple T-maze, subjects alternated with a significant rate of 58.3% in the control condition ($p = 0.006$, 98%-CI: [51.3%, 65.1%]) and a non-significant rate of 55.6% in the dual task condition ($p = 0.068$, 98%-CI: [84.5%, 62.4%]). After turning two times in the same direction (left-left or right-right) subjects alternated the direction at the subsequent junction with a significant rate of 73% in the control condition ($p = 3.34e - 11$, 98%-CI: [65.2%, 80.0%], n = 204) and a significant rate of 60.7% in the dual-task condition ($p = 0.003$, 98%-CI: [52.3%, 68.7%], n = 201). Comparing these two alternation rates using a two-proportion z-test indicated a significant difference between them ($\chi^2 = 6.42$, df = 1, $p = 0.011$). Subjects' digit repetitions of the Mental Dice Task did not significantly correlate with the individual alternation tendency in the triple

T-maze (p = 0.117).

Discussion

In this experiment, the aim was to investigate the effect of cognitive load on SAB in walking humans. In the control condition, subjects showed an overall significant tendency to alternate direction choices with a rate of 60.4%. Although this is evidence for the presence of SAB in walking humans, the found alternation rate was smaller than expected. In Experiment 1 (with a sample size of 60 subjects), an overall alternation rate of 72% was found using the same virtual maze. These two experiments have used a very similar population to draw subjects from and the instructions to subjects were identical. The only difference between the two experiments was the omission of step rhythm in the second experiment. This design decision was made due to the fact that the dual task was an audio task and could not be played at the same time as the step rhythms. It could be speculated that the step rhythms caused subjects to perform the task in a more automatic and intuition-driven manner, and thus resulting in a higher alternation rate. Nevertheless, given the much larger sample size of the current study, the results presented here possibly provide a more precise estimate of alternation rates representative of human subject populations.

The dual task condition, in which subjects traversed the triple T-maze while performing an auditory Stroop task, only showed a trend in reducing alternation behavior. It had been hypothesized that, due to the detrimental effect of the dual task on remembering the previous turn, subjects would show less alternation. This expectation was based on the suggested role of memory in SAB [146]. Given the non-significant result, however, it remains unknown how dual task conditions influence alternation behaviour. Based on the obtained data we can only declare that if increased cognitive load does reduce alternation behavior, the effect is likely to be small. One possible explanation, accounting for the absence of a significant effect, is that the auditory Stroop task was not difficult enough to impair subjects' attention sufficiently. Although subjects often reported being completely unaware of where they had walked to in the dual-task condition, using an even more engaging task could help reveal the hypothesized effect. Other ways to improve the power of the experiment would be the increase of the sample size or the use of a larger maze to achieve a more precise estimate of individual alternation rates. The only significant result when comparing the alternation rates between the control and dual task conditions is at junctions prior to which subjects had turned in the same direction twice (left-left or right-right). Possibly, the generally higher alternation rates due to the stronger repetitions of direction facilitated the exposure of the dual task effect.

Given these results, the next question would be: what do these results mean in the context of RDW? As the alternation rates are significantly higher than 50% in both the control and dual task conditions, it could be assumed that this behavior will persist in a generic VR application (rather than in an experiment setting). However, it should be brought to attention that depending on the specific task required by the VR application, users' behavior may be completely different. Therefore, further investigation of the behavior in specific settings should be carried out to achieve more applicable alternation rates.

5.2.4 Experiment 3 - SAB during RDW

The previous experiment described SAB in humans in settings where the mapping between the real and virtual environments is identity. During redirected walking, the mapping between the real and virtual environments is manipulated, and therefore the visual information and motor information are not matching anymore. The question addressed in this section is: how does this affect SAB behavior? In the case of users seeing that they walk on a curve 90 degrees to the right, thus equivalent to a right turn, but in

reality are physically walking straight, will they alternate? Or reversely, if a user sees that they walk straight, but in reality is physically walking on a curve 90 degrees to the right, will they alternate? The answers to these question may help estimate the real alternation rate that could potentially be used for RDW algorithms.

These scenarios can be implemented by combining curvature gains with curved or straight T-mazes. A subject can experience the following conditions:

- *Physical* condition: users walk on a curve but see a straight T-maze (Figure 5.15c)

- *Visual* condition: users walk straight but see a curved T-maze (Figure 5.15c)

- *Congruent* condition: users walk on a curved and see a curved T-maze (Figure 5.15c)

To determine the expected effect sizes for the power analysis, the alternation rate in the congruent condition had to be estimated first. The most closely comparable data to alternation behavior in a curved T-maze are from Experiment 1, in which subjects showed an alternation rate of 72% in response to the primary forced turn. However, a sharp 90 degree turn as in Experiment 1 might differ from a smooth, curved 90 degree turn in terms of the elicited alternation response. To get a more appropriate estimate of the alternation rate, a pilot study was conducted including 60 subjects, who walked through the curved T-maze in the congruent condition. The results of the pilot study indicated an alternation rate in the curved maze of only 60% (one-sided binomial test: $p = 0.0775$). A power analysis for a one-sided binomial test (based on the discrete binomial distribution) revealed a necessary sample size of 282 subjects to distinguish the assumed alternation rate of 60% from chance with a power of 90%.

To estimate the difference between alternation rates in the congruent and the physical condition, a further pilot study was conducted. 30 subjects completed the T-maze in the physical condition (using a curvature gain of 0.2). The subjects showed an alternation rate of 40% (95% CI: 0.23 - 0.59) which is not significantly different from chance. Regarding alternation behavior in the visual condition, there is no pilot data available, and no previous study has investigated comparable effects in humans. Analogous to the estimation of the effect of a dual task in experiment 1, an increase of 15% should be a reasonable effect size estimation. Such an increase would assume an alternation rate of 75% in the visual condition. A power analysis, incorporating the assumed alternation rates in the three conditions (visual, physical, congruent) and the random effect of subjects taken from Experiment 1, revealed a necessary sample size of 170 subjects to distinguish a difference between the congruent condition and the physical condition with a power of 90%. For the distinction of the alternation behavior between the congruent and the visual condition, a sample size of 265 was revealed to be necessary.

The results from the aforementioned pilot studies on the physical and congruent conditions suggested that the physical component of the forced turn is detrimental to alternation rates in humans. More specifically, the alternation rate in the physical condition was 40%, compared to 60% in the congruent condition. This could possibly because of the additional effort to change the current turning direction of the curved pathway prior to the T-junction. On the other hand, it was expected that the visual representation of the forced turn to be causing a higher alternation rate in the visual condition. This expectation is based on previous studies, which emphasized the predominant visual component of animals' and specifically primates' SAB [62, 126]. Therefore, it was hypothesized that an increased alternation rate in the visual condition relative to the congruent condition and a decreased alternation rate in the physical condition relative to the congruent condition. Further, it was hypothesized that subjects show significant alternation in the congruent condition.

Experiment design

This experiment consisted of one walk through each of the three curved T-mazes (Figure 5.15c). Using redirected walking (curvature gain), the subjects' walking trajectories were manipulated while walking through the T-mazes in the physical and visual conditions. In the physical condition, a curvature gain of 0.25 (equivalent to a radius of 4m) was applied to force subjects onto a curved walking trajectory while passing through the visually straight passage leading up to the T-junction. The gain intensity of 0.25 lies above the detection thresholds for curvature gains reported in the literature [96, 186, 217, 236, 192]. Thus, the curved walking was expected to be physically perceived as such by the subjects. The curvature gain was applied until subjects had reached the T-junction. In the visual condition, a curvature gain of the same intensity was applied in the opposite direction of the curved turn to force subjects into a straight walking trajectory while passing through the visually curved corridor leading up to the T-junction. In the congruent condition, no curvature gain was applied, which led to subjects walking the curved turn congruent with their visual experience of the maze. The mazes and applied curvature gains were designed in a way that the radius (4 m) and length (6.28 m) of the walked or visually perceived curvatures were equal in the physical, visual and congruent conditions and that at the T junction, the subject would be facing exactly 90 degree away from their original orientation (visually or physically). The width of the corridors in the mazes was 1.5m. Subjects were not informed about the redirection before the experiment. The directions of the forced turns of each T-maze (left or right) and the order of the conditions were randomized and counterbalanced over subjects.

Results

The chosen directions in the T-mazes were scored as alternations or repetitions in relation to the direction of the preceding curved turn. It was hypothesized that subjects show significant alternation in the congruent condition. Furthermore, it was hypothesized that compared to the congruent condition, alternation rates would decrease in the physical condition while the visual condition would lead to an increase in alternation rates. To test these hypotheses, in a first step the alternation behavior of all subjects in the congruent condition was tested against an alternation rate of 50% using a one-sided binomial test. To compare this alternation rate with the two other conditions, a mixed-effects logistic regression model was fitted using alternation behavior as the target variable, condition (three level factor, physical/visual/-congruent) as a predictor, and subjects as a random intercept:

$$\text{Alternation} \sim 1 + \text{condition} + (1|\text{subject}) \tag{5.11}$$

Using the congruent condition as the reference, the differences to the other two conditions are expressed by the two respective condition-factor coefficients, which were tested against a value of zero. In the congruent condition, subjects alternated with a rate of 61%, which was significantly higher than 50% (p = 0.0002, (one-sided) 98%-CI: [54.6%, 100%]). In the visual and physical condition, subjects alternated with a similar rate of 55.9%, which was not significantly different from chance (p = 0.052, 98%-CI: [48.9%, 62.8%]). In the subsequent mixed-effects logistic regression analysis, compared to the congruent condition, the decrease in alternation rate of the visual and physical conditions was non-significant (p = 0.234, 98%-CI: [-0.603, 0.184]; p = 0.234, 98%-CI: [-0.608, 0.190], respectively).

Additionally, subjects did not show any significant left or right turn bias (right turning rate of 52%, p = 0.248). There was no significant gender effect in alternation behavior (p = 0.634) nor in side preference (p = 0.634).

Discussion

In the congruent condition, subjects physically and visually experienced a curved forced turn before arriving at the T-junction. At the T-junction, subjects alternated direction with a significant rate of 61%. This suggests that walking adults alternate directions at similar rates independent of whether the forced turn prior to a T-junction is a curved, gradual turn as in the congruent condition of this experiment, or an abrupt 90 degree turn as in Experiment 2 (alternation rate of 60.4%). The finding is insofar notable as the classical study of SAB is restricted to sudden, abrupt turns. Showing alternation for a more drawn-out, continuous rotation provides an insight into the flexibility of SAB in humans. Despite the tendency to alternate directions in the congruent condition, neither the exclusively visual nor the exclusively physical condition showed the hypothesized effect on alternation rates. It had been hypothesized that there would be an increase of alternation in the visual condition and a decrease of alternation in the physical condition. The results, however, showed an identical, non-significant decrease in both conditions. Furthermore, the alternation rates in both conditions were shown to be not significantly different from 50%. Therefore, it remains unclear whether an exposure exclusively to the visual or physical component of a forced turn is sufficient to evoke any kind of alternation response. Although of speculative nature, one possible interpretation of this finding is that both the physical and visual component of a turn are necessary to trigger an alternation response.

These results may mean "bad news" for RDW. The fact that both the physical and visual conditions do not show an alternation rate different from chance means it is just equivalent to a simple straight T-maze. Nevertheless, it is not clear how the alternation rate changes when subjects walk further into a maze such as the triple T-maze in Experiment 1 and 2. As a virtual environment is not normally restricted to a single T-junction, it would be interesting to investigate users' walking behaviors under the application of curvature gains in varying directions and observe how that affects subsequent alternation rates.

5.2.5 Experiment 4 - SAB in an open space

While it has been shown that humans exhibit SAB in T-mazes, it has never been tested whether human SAB exist outside the maze. Examining SAB in other types of maze architectures presents a crucial step in understanding SAB's generalizability and flexibility in human walking. In the context of RDW, it means that the environment does not necessarily have to be restricted to mazes but path prediction can potentially be made also in an open space environment.

In this experiment, the existence of SAB beyond its classic, corridor-based framework was investigated. In insects, isopods and myriapods, SAB has been observed in a modified paradigm where the animals deviate from a straight locomotor path at the exit of a maze. This deviation points opposite to the direction of the previously traversed forced turn (Figure 2.9f) [13]. In this setting, SAB is not expressed as a binomial variable ("alternation" or "repetition") but as a continuous variable (the angle of deviation from the straight path in the opposite direction of the previous turn, also dubbed the "reverse turning" angle). Similar to the alternation rate, this angle decreases with increasing walking distance between forced turn and the maze exit [116]. Using a continuous variable as a measure of SAB is statistically more powerful [51] and could therefore allow identifying smaller effect sizes. On the basis of work in arthropods [13], it was hypothesized that reverse turning to occur also in human subjects.

Experiment design

The virtual environment, modeled after mazes used in lower arthropods, consisted of an initial 90 degree forced turn that leads into an open area (hence the "open maze", see Figure 5.15 d). First, subjects passed through a 4.5m long corridor to reach the initial 90 degree forced turn. After making the forced turn, subjects walked straight for another 2.5m before finding themselves in front of an open space. The open space was only limited by walls running perpendicular to the corridor walls, preventing the subjects from walking behind the level of the corridor exit Apart from these walls, the open space was empty and seemingly infinite, showing only the horizon when looking forward into the open space. Subjects were free to walk in any direction desired, except for walking back into the corridor (as instructed before the experiment). Subjects were stopped as soon as they had passed a distance of three meters from the corridor exit. In the case of a participant stopping in the open space, asking where they are supposed to go, the experimenter instructed the subject to *"just walk a bit further wherever you want to go"*.

Since no prior experiment has tested a similar paradigm in humans, a pilot study was performed to test the experiment's feasibility and to estimate the expected effect size. Thirty healthy subjects were sent through the virtual open maze, counterbalanced for left and right directed initial forced turns. The reverse turning angles showed a sample standard deviation of 26.2 degrees and a mean value of 7.6 degrees (one-sided t-test: t = 2.23, p = 0.0147). Assuming that these results represent the true parameters, a power analysis revealed a necessary sample size of 137 subjects to detect a mean reverse turning angle greater than zero with a power of 90% using a one-sided t-test. In the main experiment, the direction of the forced turn (left/right) was counterbalanced among subjects in a randomized order, leading to half of the 288 subjects completing the open maze with an initial forced right turn, while the other half completed the open maze with an initial forced left turn. We hypothesized that subjects also alternate in this setting, which means they would deviate from the straight line in the direction opposite to the previous forced turn.

Results

The outcome variable of this experiment was the reverse turning angle, which expresses the deviation in the open space relative to the direction of the prior forced turn (Figure 5.15d). Positive angles denote directions opposite to the forced turn direction and therefore an alternation, while negative angles denote a repetition of direction in the open space. To test our hypothesis that subjects generally alternate their chosen direction in the open space, the mean of all reverse turning angles was tested in a one-sample t-test against a value of zero in a one-sided fashion. In the case of reverse turning angles not following a normal distribution (tested by Kolmogorow-Smirnow test and inspection of the normal qq-plot), a one-sample Wilcoxon signed rank test would be applied as a non-parametric alternative to the one-sample t-test. Results showed that the mean reverse turning angle was 1.46 degrees (SD = 20.2 degrees), not significantly larger than zero (t = 1.23, p = 0.11, (one-sided) 98%-CI: [-0.99, Inf]), which disproved our original hypothesis.

Subjects' digit repetitions in the Mental Dice Task were not significantly correlated with the reverse turning angles measured in Experiment 3 (p = 0.211, 98%-CI: [-0.064, 0.209], see Figure 5.17). Subjects' random number generation (RNG) index for the Mental Dice Task was also calculated. The RNG index is a widely used measure of non-randomness in random number generation tasks [74, 251] and partially depends on the number of repetitive responses. Subjects' RNG-indices were not significantly correlated with the reverse turning angles (p = 0.109, 98%-CI: [-0.229, 0.043]). Subjects did not show a general left or right turn bias (mean right-turning angle 1.76 degrees, p = 0.139). There was no significant gender difference in alternation behavior (t = 1.37, p = 0.171) nor in side preferences (t = 1.078, p = 0.282).
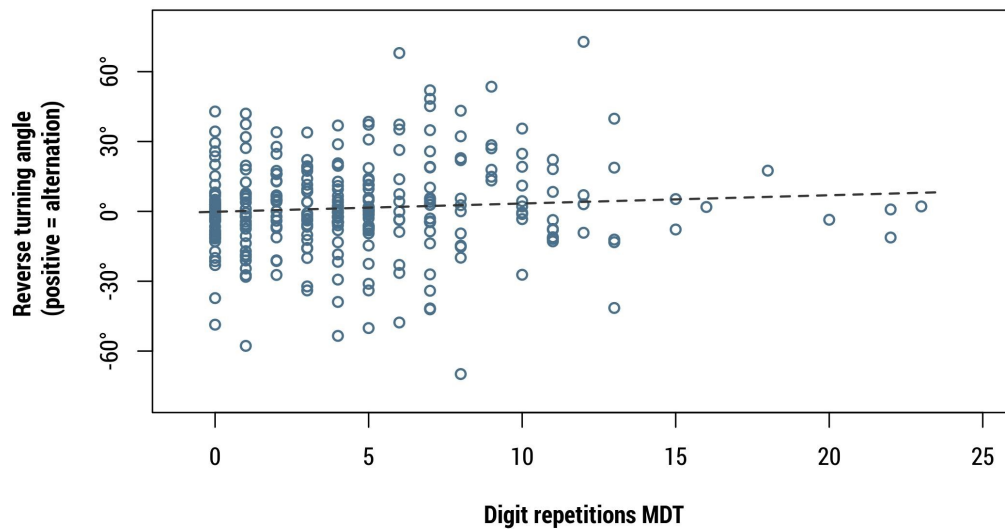
Figure 5.17: *Scatterplot of digit repetitions in the Mental Dice Task versus the reverse turning angles of experiment 3 at three meters from the corridor exit. The regression line (dotted) is shown in grey.*

In Figure 5.18, mean reverse turning angles are plotted against the distance in the open space from the corridor exit.

Discussion

In this experiment, it had been hypothesized an alternation of direction based on comparable experiments performed on arthropod species [13]. However, subjects did not show a significant tendency to alternate their chosen direction in the open area relative to the initial forced turn. As visible in Figure 5.18, the mean reverse turning angle at a distance of three meters lies very close to zero (mean value of 1.46 degrees). The curve shown in Figure 5.18 seems to be slightly U-shaped. Whether this shape is simply due to random noise or whether it expresses a specific walking pattern cannot be determined based on the obtained data. One limitation in the open maze was that the trajectories of subjects were only tracked for a maximum radius of three meters after the maze exit. The limited tracking distance was due to the dimensions of the available tracking space. Whether an extended tracking of subjects would have revealed a clearer alternation pattern is impossible to say based on the results. Often, however, subjects followed the trajectory they were on when leaving the corridor and continued walking straight into the open area. The non-significant finding stands in contrast to the result of the performed pilot experiment, in which a significant mean reverse turning angle of 7.6 degrees was found (using a sample of 30 subjects). Again, the much larger sample size of the present investigation makes the estimates presented here more trustworthy and representative of the studied population. Finally, the tested correlation between digit repetitions in the Mental Dice Task and the reverse turning angles was not significant (Figure 5.18).
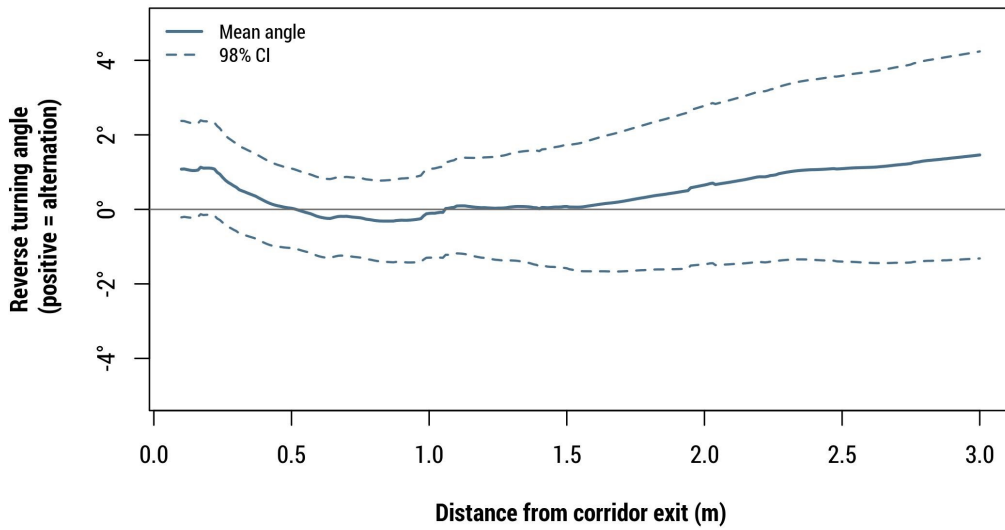
Figure 5.18: *The mean reverse turning angle is plotted against the distance from the corridor exit in the open maze*

The 98% confidence interval is represented as dashed lines. .

5.2.6 Conclusion

In summary, the presented series of experiments confirmed a general bias in humans to alternate directional choices in corridor-based virtual environments. This bias is weak compared to the vertebrate alternation bias commonly observed during real locomotion [65]. Moreover, it seems to be restricted to the classic setting of T-junctions and does not extend to a more unrestricted directional choice in an open area, which makes it less useful for RDW application. Nevertheless, the present study hopefully will serve as a springboard to future investigations of locomotor sequential biases in walking adults. While SAB has been probed under rather restricted, artificial circumstances, future investigators may wish to study it under more natural conditions of veering and turning [223, 233]. Especially when facing much larger environments, or when pursuing ecologically relevant tasks such as finding a specific location, predictive walking patterns such as SAB may be more prevalent.

6

Conclusion and Outlook

This work was dedicated to gaining in-depth understanding about how RDW works, the various factors which influence the perception of RDW, and develop additional techniques which further improve RDW's efficiency, focusing mainly on curvature gains. The procedure for identifying RDTs and average RDTs for the three gains (curvature, rotation, and translation) had been established by Steinicke et al. and used by many follow-up work. While originally intending to adopt this pre-established procedure for this work, it was later found out that this procedure has a number of limitations: it requires a long experiment time if the individual threshold is to be identified, and it is only a pseudo two-alternative forced choice (2AFC) method and therefore still suffers from yes-no bias. The first part of this thesis was therefore dedicated to establishing a new procedure in which these issues were addressed. To reduce the experiment time, instead of using the constant-stimuli method, which tests users at all threshold values within a predefined range, an adaptive method called QUEST was used. Similar to other adaptive methods, the QUEST method quickly narrows down the range in which the users' threshold lies and tests intensively within this range. To address the inherent bias of the pseudo 2AFC method, the true 2AFC method was used, in which for each trial, the users had to walk two times to the target and in only one walk curvature gain was applied. This proposed procedure was then used to conduct the first experiment to identify individual thresholds. Results showed that individual curvature RDTs span a wide range from 0.0237 (equivalent to a radius of 42.2m) to 0.1994 (equivalent to a radius of 5.2m). Results also showed that there is a significant impact of gender on RDTs, specifically, men are on average more sensitive to RDW than women. A previous study from Steinicke et al. found an average curvature gain of 0.133 (equivalent to a radius of 7.5m) and this value had since been used in many work as the standard curvature gain for all users. However, according to the findings from the first experiment, this average value is far from ideal when individual thresholds are concerned: it is too strong for sensitive users which may cause a break in presence, and not strong enough for other users, which means RDW is not utilized to its full potential.

Even though the proposed procedure is more efficient than existing methods, it is still quite time consuming. On average, at least 20 minutes were required to identify curvature RDTs in one direction for each user. A closer look at how different individuals are in perceiving RDW could help better identifying their RDTs. While it has always been assumed that RDW works due to the dominance of the visual sense over other senses, the relation between visual dominance and RDTs has never been explored. The next part of the thesis was therefore dedicated to investigating if the measurement of visual dominance obtained in various perception tests is correlated with the RDTs identified using the previously proposed

methods. The hypothesis was: the more visual-dominant a user is, the higher their RDT is. The visual dominance tests selected were: rod-and-frame, sway, vection and blind walking tests. Only a significant correlation was found between the rod-and-frame test score and the RDTs. However, the correlation was not strong enough to allow an accurate prediction of RDTs. Nevertheless, it could be used to identify a narrower range of where a user's RDT could be, and consequently allows a faster RDT identification process using the previously proposed method. Whether this approach would result in accurate RDTs and a more efficient procedure remains to be explored in future work.

Not only is RDW perceived differently by individuals (intrinsic factors), it is also perceived differently in different external conditions (extrinsic factors). An extrinsic factor that has been shown to influence the perception of curvature RDW is walking velocity: the slower a user walks, the harder it is for them to detect curvature gain. As the visual tasks used in previous studies to regulate users' walking speed could have a confounding influence on the perception of RDW, a new method which uses auditory step rhythms was proposed. It was found that this method could not accurately regulate users' walking speed, specifically, users did not walk slow enough in the slow speed condition, and not fast enough in the fast speed condition. Nevertheless, the speed difference between the speed conditions were large enough and results reconfirmed the significant impact of speed on RDTs. Even though the auditory step rhythms did not successfully regulate the walking speed accurately, it is unclear if the visual method performs better. A formal investigation into methods of regulating walking speed in VR could be an interesting topic for the future.

Other factors such as corridor size and environment visual density have only been informally observed to have an effect on RDTs of curvature gains, but never formally studied. Inspired by these observations, an experiment was conducted to identify the impact of environment size on curvature RDTs. The observations in previous studies could not be confirmed as no significant impact of the environment size was found on RDTs. However, in retrospect, there were certain limitations to the design of this experiment. First of all, a between-subject design was used. With a limited sample size of 30 subjects, it may not have had enough power to detect the potential effect of the environment size. Secondly, the walls of the environment in both conditions were plain and without texture. While this design was originally meant to isolate the impact of size from the impact of visual density, it created two conditions with little difference in optical flow. A worthwhile further investigation would be on the impact of visual density alone, as well as the interaction between the environment size and visual density on the detection of curvature RDTs. Since RDTs ranges widely between individuals, it would also be best to use a within-subjects design when the sample size is relatively small.

Feeling of presence refers to the sensation of being truly immersed in the virtual scene. The stronger the feeling of presence, the more difficult it is for a user to distinguish between the virtual and real worlds. Even though feeling of presence is one of the most crucial aspects of VR, in the context of RDW, little work has been done to investigate the impact of feeling of presence on RDTs. In this thesis, through the use of different viewing perspectives of a virtual avatar (first person vs. third person), and the varying congruency between the avatar's movement and users' body movement (congruent vs. incongruent), the impact of feeling of presence on curvature gain RDTs was investigated. Results showed a negative correlation between the feeling of presence (in terms of agency score) and RDTs, in other words, users tend to detect RDW better when they have stronger feeling of presence and control over the virtual avatar. This result has certain implications for future RDW applications: in order to apply the maximum possible curvature gains, it is necessary to ensure that users experience a strong feeling of presence. This is particularly important when a virtual representation of the user is viewed in third person perspective, the virtual avatar movement needs to be congruent with the real body movement.

Until the end of this thesis, all existing RDTs experiments required users to perform only one main task of detecting RDW. This, however, does not reflect a realistic scenario as users normally perform

other tasks in a VR applications. Therefore, the existing RDTs obtained in previous studies may only be conservative estimates. The next part of the thesis focused on investigating the impact of performing another task on the detection of curvature gains. For this experiment, the same procedure of RDTs identification was used, but in addition to the task of detecting in which walk users were redirected, they were also required to perform a seven subtraction task simultaneously. It was found that RDTs were significantly higher when users performed an additional task. This result indicates that a much higher curvature gain can potentially be applied outside of the experiment setting. Interesting questions still remain for future work: How much cognitive load different tasks impose on users? How much cognitive load is enough to elicit higher RDTs? And finally, how much cognitive load is too much such that users could no longer adapt their path to the applied curvature gains?

While understanding the impact of different factors on the perception of curvature gains allows designing VR applications with higher unnoticeable gains, there are always limits to how strong a gain could be applied without users noticing it. To improve RDW further, a new RDW technique was introduced: applying discrete rotation every time users blink. An experiment was conducted to investigate if this technique is feasible. Results show that a scene can be rotated significantly more during blinks (9.1 degrees) as compared to when users' eyes are open (2.4 degrees). In order to investigate if the newly proposed technique could be combined with existing RDW techniques to improve redirection efficiency, a computer simulation was carried out. Results showed that given a sufficiently large tracking space and high enough blink frequency, the reset count and the minimum space required for walking without encountering a stop and reset could be significantly reduced (potentially up to 29%). It is, however, important to note that there was certain simplification in the simulation setup that does not accurately reflect reality: the simulated walker predefined path does not simulate the natural head bobbing motion during walking, which could affect how the algorithms calculate the next applicable gains. Realistic walking paths, or even live user study would provide a better estimate of the effect of using the new technique on the efficiency of greedy algorithms such as steer-to-center. An investigation into how this new technique affects the performance of non-greedy algorithms such as model predictive control would also be interesting. Furthermore, the hypothesis is that the application of discrete redirection during blink can be superposed to the application of curvature, rotation or translation gains due to the different nature of the techniques: discrete versus continuous. In order to prove this hypothesis, a new multi-dimensional threshold identification protocol must be devised such that the thresholds for both discrete and continuous techniques can be identified at the same time. This would also be a topic for future investigation. Another interesting topic could also involve identifying factors that induce more frequent blinks in a virtual environment, which allows more chances to perform discrete rotation.

The last part of the thesis is dedicated to understanding walking behavior in humans. The idea is that: the more information is known about where users will be going, the better it is to apply the correct redirection action that keeps the users within the physical space. Inspired by a phenomenon called spontaneous alternation behavior that has been consistently observed in many animal species, this part of the thesis explored if humans also have a tendency to alternate their walking direction in a maze-like environment. It was shown that the probability of a user switching their turning direction is 72%, and 90% if the previous two turns were in the same direction. In a second experiment, the effect of performing a secondary task on the alternation behavior in the same maze-line environment was investigated. The alternation rate in the dual task condition remains significantly higher than 50%, and not significantly different from the control condition. While the fact that SAB still persists in the dual task condition could be considered good news for RDW applications, similar questions on the effect of dual task could be raised as future work: how to measure the cognitive load imposed by the different tasks, and how much cognitive load is enough to cause a significant change in SAB. A last series of experiments were conducted to investigate whether SAB was "triggered" by the visual alternation of direction (with the use of a visually curved T-maze in combination with a curvature gain in the opposite direction such that users

ended up walking straight) or the bodily alternation of direction (with the use of a visually straight T-maze in combination with a curvature gain such that users ended up walking on a curve). Results showed no significant alternation rate in either conditions. It is important to note that the maze design in these last experiments consists of smooth turns that results in a 90 degree change in direction, as compared to a sharp 90 degree turn in the first experiment. It is therefore unclear whether redirection would affect SAB in sharp turn conditions. It is also interesting to see if continuous application of redirection in the same direction would also affect SAB. And finally, a formal study is still required to investigate whether the prediction of users' path based on SAB would improve the efficiency of non-greedy algorithms.

6

Bibliography

[1] "My signals - e-health sensor platform," http://www.my-signals.com/, accessed: 2020-12-14.

[2] R. Abdul Razzak, J. Bagust, S. Docherty, Z. Hasan, Y. Irshad, and A. Rabiah, "Menstrual phase influences gender differences in visual dependence: A study with a computerised Rod and Frame Test," *Journal of Cognitive Psychology*, vol. 27, no. 1, pp. 80–88, 2015.

[3] P. Abtahi, M. Gonzalez-Franco, E. Ofek, and A. Steed, "I'm a Giant: Walking in Large Virtual Environments at High Speed Gains," pp. 1–13, 2019.

[4] R. Alcalá-Quintana and M. A. García-Pérez, "A comparison of fixed-step-size and Bayesian staircases for sensory threshold estimation." *Spatial vision*, vol. 20, no. 3, pp. 197–218, 2007.

[5] R. S. Allison, I. P. Howard, and J. E. Zacher, "Effect of field size, head motion, and rotational velocity on roll vection and illusory self-tilt in a tumbling room," *Perception*, vol. 28, no. 3, pp. 299–306, 1999.

[6] M. Azmandian, T. Grechkin, M. Bolas, and E. Suma, "The Redirected Walking Toolkit: A Unified Development and Deployment Platform for Exploring Large Virtual Environments," *Everyday VR Workshop, IEEE VR*, pp. 9–14, 2016.

[7] M. Azmandian, R. Yahata, M. Bolas, and E. Suma, "An Enhanced Steering Algorithm for Redirected Walking in Virtual Environments," *2014 IEEE Virtual Reality (VR)*, pp. 65–66, 2014.

[8] M. Azmandian, T. Grechkin, M. Bolas, and E. Suma, "Physical Space Requirements for Redirected Walking: How Size and Shape Affect Performance," *Proceedings of the 25th International Conference on Artificial Reality and Telexistence and 20th Eurographics Symposium on Virtual Environments*, pp. 93–100, 2015.

[9] E. R. Bachmann, E. Hodgson, C. Hoffbauer, and J. Messinger, "Multi-User Redirected Walking and Resetting Using Artificial Potential Fields," *IEEE Transactions on Visualization and Computer Graphics*, vol. 25, no. 5, pp. 2022–2031, 2019.

[10] J. Bagust, G. D. Rix, and H. C. Hurst, "Use of a Computer Rod and Frame (CRAF) Test to Assess Errors in the Perception of Visual Vertical in a Clinical Setting - A Pilot Study," *Clinical Chiropractic*, vol. 8, no. 3, pp. 134–139, 2005.

[11] R. W. Baloh, A. W. Sills, W. E. Kumley, and V. Honrubia, "Quantitative Measurement of Saccade Amplitude, Duration, and Velocity," *Neurology*, vol. 25, no. 11, pp. 1065–1070, 1975.

[12] M. Barnett-Cowan, R. T. Dyde, C. Thompson, and L. R. Harris, "Multisensory Determinants of Orientation Perception: Task-Specific Sex Differences," *European Journal of Neuroscience*, vol. 31, no. 10, pp. 1899–1907, 2010.

[13] F. H. Barnwell, "An Angle Sense in the Orientation of a Millipede," *The Biological Bulletin*, vol. 128, no. 1, pp. 33–50, 1965.

[14] A. J. Barsky, G. Wyshak, and G. L. Klerman, "The Somatosensory Amplification Scale and Its Relationship to Hypochondriasis," *Journal of Psychiatric Research*, vol. 24, no. 4, pp. 323–334, 1990.

[15] O. Basting, A. Fuhrmann, and S. M. Grünvogel, "The Effectiveness of Changing the Field of View in a HMD on the Perceived Self-Motion," *2017 IEEE Symposium on 3D User Interfaces, 3DUI 2017 - Proceedings*, pp. 225–226, 2017.

[16] D. Bates, M. Mächler, B. M. Bolker, and S. C. Walker, "Fitting Linear Mixed-Effects Models Using lme4," *Journal of Statistical Software*, vol. 67, no. 1, 2015.

[17] O. Beauchet, V. Dubost, R. Gonthier, and R. W. Kressig, "Dual-Task-Related Gait Changes in Transitionally Frail Older Adults: The Type of the Walking-Associated Cognitive Task Matters," *Gerontology*, vol. 51, no. 1, pp. 48–52, 2005.

[18] W. H. Bidder II and A. Tomlinson, "A Comparison of Saccadic and Blink Suppression in Normal Observers," *Vision Res*, vol. 37, no. 22, pp. 3171–3179, 1997.

[19] L. Bölling, N. Stein, F. Steinicke, and M. Lappe, "Shrinking Circles: Adaptation to Increased Curvature Gain in Redirected Walking," *IEEE Transactions on Visualization and Computer Graphics*, vol. 25, no. 5, pp. 2032–2039, 2019.

[20] B. Bolte, G. Bruder, and F. Steinicke, "The Jumper Metaphor: An Effective Navigation Technique for Immersive Display Setups," *Proceedings of Virtual Reality International Conference (VRIC)*, no. April, pp. 6–8, 2011.

[21] B. Bolte and M. Lappe, "Subliminal Reorientation and Repositioning in Immersive Virtual Environments using Saccadic Suppression," *IEEE Transactions on Visualization and Computer Graphics*, vol. 21, no. 4, pp. 545–552, 2015.

[22] J. M. Bond and M. Morn's, "Goal-Directed Secondary Motor Tasks: Their Effects on Gait in Subjects With Parkinson Disease," *Archives of Physical Medicine and Rehabilitation*, vol. 81, no. 1, pp. 110–116, 2000.

[23] A. Bootsma-van der Wiel, J. Gussekloo, A. J. De Craen, E. Van Exel, B. R. Bloem, and R. G. Westendorp, "Walking and Talking as Predictors of Falls in the General Population: The Leiden 85-Plus Study," *Journal of the American Geriatrics Society*, vol. 51, no. 10, pp. 1466–1471, 2003.

[24] D. a. Bowman, D. Koller, and L. F. Hodges, "Travel in Immersive Virtual Environments: An Evaluation Motion Control Techniques of Viewpoint," *IEEE Virtual Reality Annual Symposium*, pp. 45–52, 1997.

[25] D. A. Bowman, E. T. Davis, L. F. Hodges, and A. N. Badre, "Maintaining Spatial Orientation during Travel in an Immersive Virtual Environment," *Presence*, vol. 8, no. 6, pp. 618—-631, 1999.

[26] A. Bray, A. Subanandan, B. Isableu, T. Ohlmann, J. F. Golding, and M. A. Gresty, "We Are Most Aware of Our Place in the World When About to Fall," *Current Biology*, vol. 14, no. 15, pp. 609–610, 2004.

[27] G. Bruder, F. Steinicke, and K. H. Hinrichs, "Arch-Explore: A Natural User Interface for Immersive Architectural Walkthroughs," *3DUI - IEEE Symposium on 3D User Interfaces 2009 - Proceedings*, pp. 75–82, 2009.

[28] G. Bruder, F. Steinicke, K. H. Hinrichs, H. Frenz, and M. Lappe, "Impact of Gender on Discrimination between Real and Virtual Stimuli," *Workshop on Perceptual Illusions in Virtual Environments*, pp. 10–15, 2009.

[29] G. Bruder, V. Interrante, L. Phillips, and F. Steinicke, "Redirecting Walking and Driving for Natural Navigation in Immersive Virtual Environments," *IEEE Transactions on Visualization and Computer Graphics*, vol. 18, no. 4, pp. 538–545, 2012.

[30] G. Bruder, P. Lubos, S. Member, and F. Steinicke, "Cognitive Resource Demands of Redirected Walking," *IEEE Transactions on Visualization and Computer Graphics*, vol. 21, no. 4, pp. 539–544, 2015.

[31] P. Brugger, "Variables That Influence the Generation of Random Sequences: An Update," *Perceptual and motor skills*, vol. 84, no. 2, pp. 627–661, 1997.

[32] P. Brugger, T. Landis, and M. Regard, "A 'Sheep-Goat Effect' in Repetition Avoidance: Extra-Sensory Perception as an Effect of Subjective Probability?" *British Journal of Psychology*, vol. 81, no. 4, pp. 455–468, 1990.

[33] P. Brugger, E. Macas, and J. Ihlemann, "Do Sperm Cells Remember?" *Behavioural Brain Research*, vol. 136, no. 1, pp. 325–328, 2002.

[34] A. Bunn and M. Korpela, "An Introduction to dplR," Tech. Rep., 2020.

[35] D. Burin, K. Kilteni, M. Rabuffetti, M. Slater, and L. Pia, "Body Ownership Increases the Interference Between Observed and Executed Movements," *PLoS ONE*, pp. 1–16, 2019.

[36] R. Camicioli, B. S. Oken, G. Sexton, J. A. Kaye, and J. G. Nutt, "Verbal Fluency Task Affects Gait in Parkinson's Disease With Motor Freezing," *Journal of Geriatric Psychiatry and Neurology*, 1998.

[37] C. G. Canning, "The Effect of Directing Attention During Walking Under Dual-Task Conditions in Parkinson's Disease," *Parkinsonism and Related Disorders*, vol. 11, no. 2, pp. 95–99, 2005.

[38] G. Chen, J. A. King, Y. Lu, F. Cacucci, and N. Burgess, "Spatial Cell Firing During Virtual Navigation of Open Arenas by Head-Restrained Mice," *eLife*, vol. 7, pp. 1–20, 2018.

[39] H. Chen, S. Chen, and E. S. Rosenberg, "Redirected Walking Strategies in Irregularly Shaped and Dynamic Physical Environments," no. March, 2018.

[40] W.-Y. Chen, H.-C. Huang, Y.-T. Lee, and C. Liang, "Body Ownership and the Four-Hand Illusion," *Scientific Reports*, vol. 8, no. 1, p. 2153, dec 2018.

[41] L. A. Cherep, J. W. Kelly, A. Ostrander, and S. B. Gilbert, "Spatial Cognitive Implications of Teleporting Through Virtual Environments," *Journal of Experimental Psychology: Applied*, no. June, 2019.

[42] M. Chessa, G. Maiello, A. Borsari, and P. J. Bex, "The Perceptual Quality of the Oculus Rift for

Immersive Virtual Reality," *Human-Computer Interaction*, vol. 34, no. 1, pp. 51–82, 2019.

[43] R. A. Clark, A. L. Bryant, Y. Pua, P. McCrory, K. Bennell, and M. Hunt, "Validity and Reliability of the Nintendo Wii Balance Board for Assessment of Standing Balance," *Gait and Posture*, vol. 31, no. 3, pp. 307–310, 2010.

[44] J. Cohen, *Statistical Power Analysis for the Behavioral Sciences*, 2nd ed.   New York, New York, USA: Lawrence Erlbaum Associates, 1997.

[45] B. J. Congdon and A. Steed, "Sensitivity to Rate of Change in Gains Applied by Redirected Walking," *Virtual Reality Software and Technology Symposium*, 2019.

[46] J. E. Corbett and J. T. Enns, "Observer Pitch and Roll Influence: The Rod and Frame Illusion," *Psychonomic Bulletin and Review*, vol. 13, no. 1, pp. 160–165, 2006.

[47] S. Coren, "The Lateral Preference Inventory for Measurement of Handedness, Footedness, Eyedness, and Earedness: Norms for Young Adults," *Bulletin of the Psychonomic Society*, vol. 31, no. 1, pp. 1–3, 1993.

[48] B. R. Cornwell, L. L. Johnson, T. Holroyd, F. W. Carver, and C. Grillon, "Human Hippocampal and Parahippocampal Theta During Goal-Directed Spatial Navigation Predicts Performance on a Virtual Morris Water Maze," *Journal of Neuroscience*, vol. 28, no. 23, pp. 5983–5990, 2008.

[49] F. M. Costela, J. Otero-Millan, M. B. McCamy, S. L. Macknik, X. G. Troncoso, A. N. Jazi, S. M. Crook, and S. Martinez-Conde, "Fixational Eye Movement Correction of Blink-Induced Gaze Position Errors," *PLoS ONE*, vol. 9, no. 10, 2014.

[50] C. Cruz-neira, D. J. Sandin, and T. A. Defanti, "Surround-Screen Projection-Based Virtual Reality: The Design and Implementation of the CAVE."

[51] T. J. Czaczkes, "Using T- and Y-Mazes in Myrmecology and Elsewhere: A Practical Guide," *Insectes Sociaux*, vol. 65, no. 2, pp. 213–224, 2018.

[52] J. M. Dabbs, E. L. Chang, R. A. Strong, and R. Milun, "Spatial Ability, Navigation Strategy, and Geographic Knowledge Among Men and Women," *Evolution and Human Behavior*, vol. 19, no. 2, pp. 89–98, 1998.

[53] R. Darken, W. Cockayne, and D. Carmein, "The Omni-Directional Treadmill: A Locomotion Device for Virtual Worlds," *Proceedings of the 10th Annual ACM Symposium on User Interface Software and Technology*, pp. 213–221, 1997.

[54] C. L. Darlington and P. F. Smith, "Further Evidence for Gender Differences in Circularvection," *Journal of Vestibular Research*, vol. 8, no. 2, pp. 151–153, 1998.

[55] P. Dassonville and J. K. Bala, "Perception, Action, and Roelofs Effect: A Mere Illusion of Dissociation," *PLoS Biology*, vol. 2, no. 11, 2004.

[56] P. Dassonville, J. K. Bala, D. D. De Grave, E. Brenner, and J. B. Smeets, "Are the original Roelofs effect and the induced Roelofs effect confounded by the same expansion of remembered space? (multiple letter)," *Vision Research*, vol. 44, no. 10, pp. 1025–1029, 2004.

[57] P. Dassonville, B. Bridgeman, J. K. Bala, P. Thiem, and A. Sampanes, "The Induced Roelofs Effect: Two Visual Systems or the Shift of a Single Reference Frame?" *Vision Research*, vol. 44, no. 6, pp. 603–611, 2004.

[58] Ö. de Manzano and F. Ullén, "Goal-Independent Mechanisms for Free Response Generation:

Creative and Pseudo-Random Performance Share Neural Substrates," *NeuroImage*, vol. 59, no. 1, pp. 772–780, 2012.

[59] G. A. Dean, "An Analysis of the Energy Expenditure in Level and Grade Walking," *Ergonomics*, vol. 8, no. 1, pp. 31–47, 1965.

[60] H. G. Debarba, E. Molla, B. Herbelin, and R. Boulic, "Characterizing Embodied Interaction in First and Third Person Perspective Viewpoints," in *2015 IEEE Symposium on 3D User Interfaces (3DUI).* IEEE, mar 2015, pp. 67–72.

[61] H. G. Debarba, S. Bovet, R. Salomon, O. Blanke, B. Herbelin, and R. Boulic, "Characterizing first and third person viewpoints and their alternation for embodied interaction in virtual reality," *PLoS ONE*, vol. 12, no. 12, pp. 1–19, 2017.

[62] W. N. Dember, "Response by the Rat to Environmental Change," *Journal of Comparative and Physiological Psychology*, vol. 49, no. 1, pp. 93–95, 1956.

[63] W. N. Dember and R. W. Earl, "Analysis of Exploratory, Manipulatory, and Curiosity Behaviors," *Psychological Review*, vol. 64, no. 2, pp. 91–96, 1957.

[64] W. N. Dember and R. Kleinman, "Cues for Spontaneous Alternation by Gerbils," vol. 1, no. 4, pp. 287–289, 1973.

[65] W. N. Dember and C. L. Richman, "Spontaneous Alternation Behavior," *Spontaneous Alternation Behavior*, 1989.

[66] S. Docherty and J. Bagust, "From Line to Dots: An Improved Computerised Rod and Frame System for Testing Subjective Visual Vertical and Horizontal," *BMC Research Notes*, vol. 3, 2010.

[67] M. J. Doughty, "Further Assessment of Gender- and Blink Pattern-Related Differences in the Spontaneous Eyeblink Activity in Primary Gaze in Young Adult Humans," *Optometry and Vision Science*, vol. 79, no. 7, pp. 439–447, 2002.

[68] V. Dubost, R. W. Kressig, R. Gonthier, F. R. Herrmann, K. Aminian, B. Najafi, and O. Beauchet, "Relationships Between Dual-Task Related Changes in Stride Velocity and Stride Time Variability in Healthy Older Adults," *Human Movement Science*, vol. 25, no. 3, pp. 372–382, 2006.

[69] N. Ellis and M. Arnoult, "Novelty as a determinant of spontaneous alternation in children," *Psychonomic Science*, vol. 2, no. 1-12, pp. 163–164, 1965.

[70] D. Engel, C. Curio, L. Tcheang, B. J. Mohler, H. Bulthoff, and H, "A psychophysically calibrated controller for navigating through large environments in a limited free-walking space." in *ACM Symposium on Virtual Reality Software and Technology*, 2008, pp. 157–164.

[71] L. K. Epting and W. H. Overman, "Sex-Sensitive Tasks in Men and Women: A Search for Performance Fluctuations Across the Menstrual Cycle," *Behavioral Neuroscience*, vol. 112, no. 6, pp. 1304–1317, 1998.

[72] M. O. Ernst and M. S. Banks, "Humans Integrate Visual and Haptic Information in a Statistically Optimal Fashion," *Nature*, vol. 415, no. January, pp. 429–433, 2002.

[73] W. K. Estes and M. S. Schoeeeijcr, "Analysis of Variables Influencing Alternation After Forced Trials," *Journal of Comparative and Physiological Psychology*, vol. 5, no. 48, p. 357, 1955.

[74] F. J. Evans, "Monitoring Attention Deployment By Random Number Generation," *Bulletin of the Psychonomic Society*, vol. 12, no. 1, pp. 35–38, 1978.

[75] G. T. Fechner, "Elements of Psychophysics," no. 1912, pp. 66–75, 1965.

[76] C. R. Fetsch, A. H. Turner, G. C. DeAngelis, and D. E. Angelaki, "Dynamic Re-Weighting of Visual and Vestibular Cues During Self- Motion Perception," *European Journal of Neuroscience*, vol. 2, no. 49, pp. 507–510, 2009.

[77] C. R. Fetsch, G. C. DeAngelis, and D. E. Angelaki, "Visual-Vestibular Cue Integration for Heading Perception: Applications of Optimal Cue Integration Theory," *European Journal of Neuroscience*, vol. 31, no. 10, pp. 1721–1729, 2010.

[78] T. Field and P. Vamplew, "Generalised Algorithms for Redirected Walking in Virtual Environments," *AISAT2004 International Conference on Artificial Intelligence in Science and Technology*, vol. 65, no. 11, pp. 1357–1366, 2004.

[79] M. H. Fischer, "Optokinetisch ausgeloste Bewegungswahrnehmungen und optokinetischer Nystagmus," *Journal of Psychological Neurology*, no. 41, pp. 273–308, 1930.

[80] M. B. Flanagan, J. G. May, and T. G. Dobie, "Sex Differences in Tolerance to Visually-Induced Motion Sickness," *Aviation Space and Environmental Medicine*, vol. 76, no. 7 I, pp. 642–646, 2005.

[81] F. C. Fortenbaugh, S. Chaudhury, J. C. Hicks, L. Hao, and K. A. Turano, "Gender Differences in Cue Preference During Path Integration in Virtual Environments," *ACM Transactions on Applied Perception*, vol. 4, no. 1, pp. 6–es, 2007.

[82] D. Freeman, P. Haselton, J. Freeman, B. Spanlang, S. Kishore, E. Albery, M. Denne, P. Brown, M. Slater, and A. Nickless, "Automated Psychological Therapy Using Immersive Virtual Reality for Treatment of Fear of Heights: A Single-Blind, Parallel-Group, Randomised Controlled Trial," *The Lancet Psychiatry*, vol. 5, no. 8, pp. 625–632, 2018.

[83] S. Freitag, D. Rausch, and T. Kuhlen, "Reorientation in Virtual Environments Using Interactive Portals," *IEEE Symposium on 3D User Interfaces 2014, 3DUI 2014 - Proceedings*, pp. 119–122, 2014.

[84] V. Gailus-Durner, H. Fuchs, T. Adler, A. A. Pimentel, L. Becker, I. Bolle, J. Calzada-Wack, C. Dalke, N. Ehrhardt, B. Ferwagner *et al.*, *Systemic first-line phenotyping.* Springer, 2009.

[85] A. Galpin, G. Underwood, and D. Crundall, "Change Blindness in Driving Scenes," *Transportation Research Part F: Traffic Psychology and Behaviour*, vol. 12, no. 2, pp. 179–185, 2009.

[86] H. Galvan Debarba, S. Bovet, R. Salomon, O. Blanke, B. Herbelin, and R. Boulic, "Characterizing first and third person viewpoints and their alternation for embodied interaction in virtual reality," *PLOS ONE*, vol. 12, no. 12, p. e0190109, dec 2017.

[87] J. Gandrud and V. Interrante, "Predicting Destination Using Head Orientation and Gaze Direction During Locomotion in Vr," pp. 31–38, 2016.

[88] A. Garcia-Palacios, H. Hoffman, A. Carlin, T. A. Furness, and C. Botella, "Virtual Reality in the Treatment of Spider Phobia: A Controlled Study," *Behaviour Research and Therapy*, vol. 40, no. 9, pp. 983–993, 2002.

[89] M. A. García-Pérez, "Forced-Choice Staircases With Fixed Step Sizes: Asymptotic and Small-Sample Properties," *Vision Research*, vol. 38, no. 12, pp. 1861–1881, 1998.

[90] S. N. Garfinkel, A. K. Seth, A. B. Barrett, K. Suzuki, and H. D. Critchley, "Knowing Your Own Heart: Distinguishing Interoceptive Accuracy From Interoceptive Awareness," *Biological Psy-*

chology, vol. 104, pp. 65–74, 2015.

[91] N. Gauvrit, H. Zenil, F. Soler-Toscano, J. P. Delahaye, and P. Brugger, "Human Behavioral Complexity Peaks at Age 25," *PLoS Computational Biology*, vol. 13, no. 4, 2017.

[92] O. Geisseler, T. Pflugshaupt, A. Buchmann, L. Bezzola, K. Reuter, B. Schuknecht, D. Weller, M. Linnebank, and P. Brugger, "Random Number Generation Deficits in Patients With Multiple Sclerosis: Characteristics and Neural Correlates," *Cortex*, vol. 82, pp. 237–243, 2016.

[93] T. Gilovich, R. Vallone, and A. Tversky, "The Hot Hand in Basketball: On the Misperception of Random Sequences," *Cognitive Psychology*, vol. 17, no. 3, pp. 295–314, 1985.

[94] G. Gorisse, O. Christmann, E. A. Amato, and S. Richir, "First- and Third-Person Perspectives in Immersive Virtual Environments: Presence and Performance Analysis of Embodied Users," *Frontiers in Robotics and AI*, vol. 4, no. July, pp. 1–12, 2017.

[95] T. Grechkin and J. Thomas, "Revisiting Detection Thresholds for Redirected Walking : Combining Translation and Curvature Gains," pp. 113–120, 2016.

[96] T. Grechkin, M. Azmandian, M. Bolas, and E. Suma, "Automated Path Prediction for Redirected Walking Using Navigation Meshes," *IEEE Symposium on 3D User Interfaces*, pp. 63–66, 2016.

[97] D. M. Green, "A Maximum-Likelihood Method for Estimating Thresholds in a Yes-No Task," vol. 93, no. April 1993, 1992.

[98] D. M. Green and R. D. Luce, "Parallel Psychometric Functions From a Set of Independent Detectors," *Psychological Review*, vol. 82, no. 6, pp. 483–486, 1975.

[99] E. J. Green and P. J. Barber, "An Auditory Stroop Effect With Judgments of Speaker Gender," *Perception & Psychophysics*, vol. 30, no. 5, pp. 459–466, 1981.

[100] C. R. Griffith, "The Perceptions and Mechanisms of Vestibular Equilibration," *Psychological Bulletin*, vol. 29, no. 4, pp. 279–303, 1932.

[101] G. Grön, A. P. Wunderlich, M. Spitzer, R. Tomczak, and M. W. Riepe, "Brain Activation During Human Navigation: Gender-Different Neural Networks as Substrate of Performance," *Nature Neuroscience*, vol. 3, no. 4, pp. 404–408, 2000.

[102] J. H. Grosslight and W. Ticknor, "Variability and Reactive Inhibition in the Meal Worm as a Function of Determined Turning Sequences," *Journal of Comparative and Physiological Psychology*, vol. 46, no. 1, pp. 35–38, 1953.

[103] L. Harris, "Variability in Maze Drawings of Young Children : Effects of Stimulus Change and Chronological Age," *Psychonomic Science*, vol. 23, no. 4, pp. 305–307, 1971.

[104] A. W. Harvey and N. K. Bovell, "Spontaneous Alternation Behavior in Paramecium," *Learning and Behavior*, vol. 34, no. 4, pp. 361–365, 2006.

[105] J. M. Hausdorff, "Stride-to-Stride Variability While Backward Counting Among Healthy Young Adults," vol. 9, pp. 1–9, 2005.

[106] D. Hayashi, "Redirected Jumping : Imperceptibly Manipulating Jump Motions in Virtual Reality," in *Proc. IEEEE VR2019*, 2019.

[107] M. L. Helig, "Sensorama Simulator," p. 15, 1962.

[108] F. Herrera, J. Bailenson, E. Weisz, E. Ogle, and J. Zak, "Building long-term empathy: A large-

scale comparison of traditional and virtual reality perspective-taking," *PLoS ONE*, vol. 13, no. 10, 2018.

[109] T. T. Hills, P. M. Todd, D. Lazer, A. D. Redish, I. D. Couzin, M. Bateson, R. Cools, R. Dukas, L. A. Giraldeau, M. W. Macy, S. E. Page, R. M. Shiffrin, D. W. Stephens, and J. W. Wolfe, "Exploration versus Exploitation in Space, Mind, and Society," *Trends in Cognitive Sciences*, vol. 19, no. 1, pp. 46–54, 2015.

[110] C. Hirt, M. Zank, and A. Kunz, "Short-term Path Prediction for Virtual Open Spaces," *IEEE Conference on Virtual Reality and 3D User Interfaces (VR)*, pp. 978–979, 2019.

[111] E. Hodgson and E. Bachmann, "Comparing four approaches to generalized redirected walking: simulation and live user data." *IEEE transactions on visualization and computer graphics*, vol. 19, no. 4, pp. 634–43, 2013.

[112] E. Hodgson, E. Bachmann, and D. Waller, "Redirected Walking to Explore Virtual Environments," *ACM Transactions on Applied Perception*, vol. 8, no. 4, pp. 1–22, 2011.

[113] E. Hodgson, E. Bachmann, and T. Thrash, "Performance of Redirected Walking Algorithms in a Constrained Virtual World," *IEEE Transactions on Visualization and Computer Graphics*, vol. 20, no. 4, pp. 579–587, 2014.

[114] A. S. Householder and G. Young, "Weber Laws, the Weber Law, and Psychophysical Analysis," *Psychometrika*, vol. 5, no. 3, pp. 183–193, 1940.

[115] R. N. Hughes, "The Value of Spontaneous Alternation Behavior (Sab) as a Test of Retention in Pharmacological Investigations of Memory," *Neuroscience and Biobehavioral Reviews*, vol. 28, no. 5, pp. 497–505, 2004.

[116] R. N. Hughes, "An Intra-Species Demonstration of the Independence of Distance and Time in Turn Alternation of the Terrestrial Isopod, Porcellio Scaber," *Behavioural Processes*, vol. 78, no. 1, pp. 38–43, 2008.

[117] C. Hutton, S. Ziccardi, J. Medina, and E. S. Rosenberg, "Individualized Calibration of Rotation Gain Thresholds for Redirected Walking," pp. 61–64, 2018.

[118] M. Iersel, "The interplay between gait and cognitive function in elderly people," 2007.

[119] V. Interrante, B. Ries, and L. Anderson, "Seven League Boots: A New Metaphor for Augmented Locomotion Through Moderately Large Scale Immersive Virtual Environments," *IEEE Symposium on 3D User Interfaces 2007 - Proceedings, 3DUI 2007*, pp. 167–170, 2007.

[120] V. Interrante, B. Ries, J. Lindquist, and Lee Anderson, "Elucidating Factors that can Facilitate Veridical Spatial Perception in Immersive Virtual Environments," *2007 IEEE Virtual Reality Conference*, pp. 11–18, 2007.

[121] B. Isableu, T. Ohlmann, J. Crémieux, and B. Amblard, "Selection of Spatial Frame of Reference and Postural Control Variability," *Experimental Brain Research*, vol. 114, no. 3, pp. 584–589, 1997.

[122] B. Isableu, T. Ohlmann, J. Crémieux, and B. Amblard, "How Dynamic Visual Field Dependence-Independence Interacts With the Visual Contribution to Postural Control," *Human Movement Science*, vol. 17, no. 3, pp. 367–391, 1998.

[123] V. Ivleva, G. Zachman, and M. Bhatt, "Redirected Walking in Virtual Reality During Eye Blinking," p. 113, 2016.

[124] S. Iwahara and T. Sugimura, "Studies on Shifts of Discrimination Learning: I. The Number of Trials during Prior Learning," *Japanese Journal of Educational Psychology*, vol. 4, no. 2, 1958.

[125] H. Iwata, "Torus Treadmill: Realizing Locomotion in VEs," *IEEE Computer Graphics and Applications*, vol. 19, no. 6, pp. 30–35, 1999.

[126] A. Izumi, J. Tsuchida, and C. Yamaguchi, "Spontaneous Alternation Behavior in Common Marmosets (Callithrix Jacchus)," *Journal of Comparative Psychology*, vol. 127, no. 1, pp. 76–81, 2013.

[127] W. E. Jeffrey and L. B. Cohen, "Response Tendencies of Children in a Two-Choice Situation," *Journal of Experimental Child Psychology*, vol. 2, no. 3, pp. 248–254, 1965.

[128] J. Jerald, T. C. Peck, F. Steinicke, and M. C. Whitton, "Sensitivity to Scene Motion for Phases of Head Yaws," *Review Literature And Arts Of The Americas*, vol. 126, no. 7, pp. 155–162, 2008.

[129] C. Kaernbach, "Adaptive Threshold Estimation With Unforced-Choice Tasks," *Perception & psychophysics*, vol. 63, no. 8, pp. 1377–88, 2001.

[130] A. Kalckert and H. H. Ehrsson, "Moving a Rubber Hand That Feels Like Your Own: A Dissociation of Ownership and Agency," *Frontiers in Human Neuroscience*, vol. 6, no. March, pp. 1–14, 2012.

[131] C. S. Kallie, P. R. Schrater, and G. E. Legge, "Variability in Stepping Direction Explains the Veering Behavior of Blind Walkers," *J Exp Psychol Hum Percept Perform*, vol. 33, no. 1, pp. 183–200, 2007.

[132] O. A. Kannape and O. Blanke, "Self in Motion: Sensorimotor and Cognitive Mechanisms in Gait Agency," *Journal of Neurophysiology*, vol. 110, no. 8, pp. 1837–1847, 2013.

[133] O. A. Kannape, A. Barré, K. Aminian, and O. Blanke, "Cognitive loading affects motor awareness and movement kinematics but not locomotor trajectories during goal-directed walking in a virtual reality environment," *PLoS ONE*, vol. 9, no. 1, pp. 1–11, 2014.

[134] I. Kasa, "A Circle Fitting Procedure and its Error Analysis," *IEEE Transactions on Instrumentation and Measurement*, vol. IM-25, no. 1, pp. 8–14, 1976.

[135] A. Kavounoudias and C. A. R. Roll, "The Plantar Sole Is a Dynamometric Map for Human Balance Control," *Cognitive Neuroscience*, vol. 9, no. 14, pp. 3247–3252, 1998.

[136] R. S. Kennedy, N. E. Lane, S. Kevin, and M. G. Lilienthal, "The International Journal of Aviation Psychology Simulator Sickness Questionnaire : An Enhanced Method for Quantifying Simulator Sickness," *The International Journal of Aviation Psychology*, vol. 3, no. 3, pp. 203–220, 1993.

[137] R. S. Kennedy, L. J. Hettinger, D. L. Harm, J. M. Ordy, and W. P. Dunlap, "Psychophysical Scaling of Circular Vection (CV) Produced by Optokinetic (Okn) Motion: Individual Differences and Effects of Practice," *Journal of vestibular research : equilibrium & orientation*, vol. 6, no. 5, pp. 331–41, 1996.

[138] K. Kilteni, R. Groten, and M. Slater, "The Sense of Embodiment in Virtual Reality," *Presence: Teleoperators and Virtual Environments*, vol. 21, no. 4, pp. 373–387, nov 2012.

[139] J. Kim, C. Y. L. Chung, S. Nakamura, S. Palmisano, and S. K. Khuu, "The Oculus Rift: A Cost-Effective Tool for Studying Visual-Vestibular Interactions in Self-Motion Perception," *Frontiers in Psychology*, vol. 6, no. MAR, pp. 1–7, 2015.

[140] I. R. Kleckner, J. B. Wormwood, W. K. Simmons, L. F. Barrett, and K. S. Quigley, "Methodological Recommendations for a Heartbeat Detection-Based Measure of Interoceptive Sensitivity," *Psychophysiology*, vol. 52, no. 11, pp. 1432–1440, 2015.

[141] S. Klosterhalfen, E. R. Muth, S. Kellermann, K. Meissner, and P. Enck, "Nausea Induced by Vection Drum: Contributions of Body Position, Visual Pattern, and Gender," *Aviation Space and Environmental Medicine*, vol. 79, no. 4, pp. 384–389, 2008.

[142] D. C. Knill, "Robust Cue Integration: A Bayesian Model and Evidence From Cue-Conflict Studies With Stereoscopic and Figure Cues to Slant," *Journal of Vision*, vol. 7, no. 7, p. 5, 2007.

[143] L. L. Kontsevich and C. W. Tyler, "Bayesian adaptive estimation of psychometric slope and threshold," *Vision Research*, vol. 39, no. 16, pp. 2729–2737, 1999.

[144] R. Kopper, C. Stinson, and D. A. Bowman, "Towards an Understanding of the Effects of Amplified Head Rotations," *Proceedings of the Workshop on Perceptual Illusions in Virtual Environments*, no. February 2015, pp. 10–15, 2011.

[145] L. Kruse, E. Langbehn, and F. Steinicke, "I Can See on my Feet While Walking : Sensitivity to Translation Gains with Visible Feet," *IEEE Virtual Reality*, pp. 305–312, 2018.

[146] R. Lalonde, "The Neurobiological Basis of Spontaneous Alternation," *Neuroscience and Biobehavioral Reviews*, vol. 26, no. 1, pp. 91–104, 2002.

[147] E. Langbehn, P. Lubos, G. Bruder, and F. Steinicke, "Bending the Curve: Sensitivity to Bending of Curved Paths and Application in Room-Scale VR," vol. 23, no. 4, pp. 1349–1358, 2017.

[148] E. Langbehn, E. Harting, and F. Steinicke, "Shadow-Avatars: A Visualization Method to Avoid Collisions of Physically Co-Located Users in Room-Scale VR," *Proceedings of IEEE Workshop on Everyday Virtual Reality (WEVR)*, 2018.

[149] E. Langbehn, P. Lubos, and F. Steinicke, "Evaluation of locomotion techniques for room-scale vr: Joystick, teleportation, and redirected walking," *Proceedings of the Virtual Reality International Conference - Laval Virtual*, 2018.

[150] E. Langbehn, F. Steinicke, M. Lappe, G. F. Welch, and G. Bruder, "In the Blink of an Eye – Leveraging Blink-Induced Suppression for Imperceptible Position and Orientation Redirection in Virtual Reality," in *ACM Transactions on Graphics*, vol. 37, no. 4, 2018.

[151] M. Lappe, F. Bremmer, and A. Van den Berg, "Perception of self-motion from visual flow," *Trends in Cognitive Sciences*, vol. 3, no. 9, pp. 329–336, 1999.

[152] K. Lashley, "The Problem of Serial Order in Behavior," *Cerebral mechanisms in behavior*, no. 7, pp. 112–147, 1951.

[153] R. H. Lawless and R. D. Engstrand, "Alternation in the Human Stylus Maze: Time and Distance Factors," *The Psychological Record*, vol. 10, pp. 101–105, 1960.

[154] T. T. Lê and Z. Kapoula, "Role of Ocular Convergence in the Romberg Quotient," *Gait and Posture*, vol. 27, no. 3, pp. 493–500, 2008.

[155] M. R. Leek, "Adaptive procedures in psychophysical research," *Perception & Psychophysics*, vol. 63, no. 8, pp. 1279–1292, 2001.

[156] M. R. Leek, T. E. Hanna, and L. Marshall, "Estimation of Psychometric Functions From Adaptive Tracking Procedures," *Perception & Psychophysics*, vol. 51, no. 3, pp. 247–256, 1992.

[157] P. Legkov and P. König, "Dual Task based Cognitive Stress Induction and its Influence on Path Integration," 2017.

[158] L. A. Lesmes, Z.-L. Lu, J. Baek, N. Tran, B. A. Dosher, and T. D. Albright, "Developing Bayesian Adaptive Methods for Estimating Sensitivity Thresholds (d') in Yes-No and Forced-Choice Tasks," *Frontiers in Psychology*, vol. 6, no. August, pp. 1–24, 2015.

[159] C. Leys, C. Ley, O. Klein, P. Bernard, and L. Licata, "Detecting Outliers: Do Not Use Standard Deviation Around the Mean, Use Absolute Deviation Around the Median," *Journal of Experimental Social Psychology*, vol. 49, no. 4, pp. 764–766, 2013.

[160] C. Liang, S.-Y. Chang, W.-Y. Chen, H.-C. Huang, and Y.-T. Lee, "Body Ownership and Experiential Ownership in the Self-Touching Illusion," *Frontiers in Psychology*, vol. 5, no. 12, pp. 270–274, jan 2015.

[161] J. Liu, H. Parekh, M. Al-Zayer, and E. Folmer, "Increasing Walking in VR using Redirected Teleportation," pp. 521–529, 2018.

[162] T. Loetscher and P. Brugger, "Exploring Number Space by Random Digit Generation," *Experimental Brain Research*, vol. 180, no. 4, pp. 655–665, 2007.

[163] T. Luong, N. Martin, and L. Anatole, "Studying the Mental Effort in Virtual Versus Real Environments," in *IEEE Conference on Virtual Reality and 3D User Interfaces (VR)*, Osaka, Japan, 2019, pp. 809–816.

[164] N. A. Macmillan and C. D. Creelman, "Response Bias: Characteristics of Detection Theory, Threshold Theory, and "Nonparametric" Indexes," *Psychological Bulletin*, vol. 107, no. 3, pp. 401–413, 1990.

[165] K. A. Manning, , L. A. Riggs, , and J. K. Komenda, "Reflex Eyeblinks and Visual Suppression," *Perception & Psychophysics*, vol. 34, no. 3, pp. 250–256, 1983.

[166] A. Maselli and M. Slater, "The building blocks of the full body ownership illusion," *Frontiers in Human Neuroscience*, vol. 7, no. March, pp. 1–15, 2013.

[167] K. Matsumoto, Y. Ban, T. Narumi, Y. Yanase, T. Tanikawa, and M. Hirose, "Unlimited Corridor : Redirected Walking Techniques using Visuo Haptic Interaction," in *ACM SIGGRAPH 2016 Emerging Technologies*, 2016, pp. 16–17.

[168] G. W. Maus, M. Duyck, M. Lisi, T. Collins, D. Whitney, and P. Cavanagh, "Target Displacements during Eye Blinks Trigger Automatic Recalibration of Gaze Direction," *Current Biology*, vol. 27, no. 3, pp. 445–450, 2017.

[169] E. Medina, R. Fruland, and S. Weghorst, "Virtusphere: Walking in a Human Size VR "Hamster Ball"," *Proceedings of the Human Factors and Ergonomics Society Annual Meeting*, vol. 52, no. 27, pp. 2102–2106, 2008.

[170] G. Melcher and V. Henn, "The Latency of Circular Vection During Different Accelerations of the Optokinetic Stimulus," *Perception & Psychophysics*, vol. 30, no. 6, pp. 552–556, 1981.

[171] F. Meyer, M. Nogalski, and W. Fohl, "Detection Thresholds in Audio-Visual Redirected Walking," 2016.

[172] F. D. Miller, J. D.-W. Tu, G. H. Moffat, and S. Manley, "Children's Response Alternation as a Function of Stimulus Duration, Intertrial Interval, and Trials," *Psychonomic Science*, vol. 15, no. 4, pp. 199–200, 1969.

[173] R. A. Montano Murillo, E. Gatti, M. Oliver Segovia, M. Obrist, J. P. Molina Masso, and D. Martinez Plasencia, "Navifields: Relevance Fields for Adaptive VR Navigation," *Proceedings of the 30th Annual ACM Symposium on User Interface Software and Technology - UIST '17*, no. October, pp. 747–758, 2017.

[174] D. Monteiro, H. N. Liang, W. Xu, M. Brucker, V. Nanjappan, and Y. Yue, "Evaluating Enjoyment, Presence, and Emulator Sickness in vr Games Based on First- and Third- Person Viewing Perspectives," *Computer Animation and Virtual Worlds*, vol. 29, no. 3-4, pp. 1–12, 2018.

[175] P. Monteiro, D. Carvalho, M. Melo, F. Branco, and M. Bessa, "Application of the Steering Law to Virtual Reality Walking Navigation Interfaces," *Computers and Graphics (Pergamon)*, vol. 77, pp. 80–87, 2018.

[176] K. A. Y. C. Montgomery, "Exploratory Behavior and its Relation to Spontaneous Alternation in a Series of Maze Exposures," *Journal of Comparative and Physiological Psychology*, vol. 1, no. 45, pp. 50–57, 1952.

[177] J. Montufar, J. Arango, M. Porter, and S. Nakagawa, "Pedestrians' Normal Walking Speed and Speed When Crossing a Street," *Transportation Research Record: Journal of the Transportation Research Board*, vol. 2002, no. 1, pp. 90–97, 2007.

[178] J. Nachmias, "On the Psychometric Function for Contrast Detection," *Vision Research*, vol. 21, no. 2, pp. 215–223, 1981.

[179] T. Nakano and S. Kitazawa, "Eyeblink Entrainment at Breakpoints of Speech," *Experimental Brain Research*, vol. 205, no. 4, pp. 577–581, sep 2010.

[180] T. Nakano, Y. Yamamoto, K. Kitajo, T. Takahashi, and S. Kitazawa, "Synchronization of Spontaneous Eyeblinks While Viewing Video Stories," *Proceedings of the Royal Society B: Biological Sciences*, vol. 276, no. 1673, pp. 3635–3644, 2009.

[181] A. Neiberg, J. Dale, and D. Grainger, "Alternation of Stimulus and Response in Three Species," *Psychonomic Science*, vol. 18, no. 3, pp. 183–184, 1970.

[182] T. Nescher, Y. Huang, and A. Kunz, "Planning Redirection Techniques for Optimal Free Walking Experience Using Model Predictive Control," *3D User Interfaces (3DUI), . . .* , 2014.

[183] T. Nescher and A. Kunz, "Analysis of Short Term Path Prediction of Human Locomotion for Augmented and Virtual Reality Applications," *Proceedings of the 2012 International Conference on Cyberworlds, Cyberworlds 2012*, pp. 15–22, 2012.

[184] T. Nescher and A. Kunz, "Using Head Tracking Data for Robust Short Term Path Prediction of Human Locomotion," *Lecture Notes in Computer Science*, vol. 7848, pp. 172–191, 2013.

[185] T. Nescher and A. Kunz, "Planning redirection techniques for optimal free walking experience using model predictive control," in *2014 IEEE Symposium on 3D User Interfaces (3DUI)*. IEEE, mar 2014, pp. 111–118.

[186] C. Neth, J. Souman, D. Engel, U. Kloos, H. Bülthoff, and B. Mohler, "Velocity-Dependent Curvature Gain and Avatar Use for Redirected Walking," *Virtual Reality*, vol. 12, pp. 1–2, 2010.

[187] C. T. Neth, J. L. Souman, D. Engel, U. Kloos, H. H. Bülthoff, and B. J. Mohler, "Velocity-Dependent Dynamic Curvature Gain for Redirected Walking," *IEEE Transactions on Visualization and Computer Graphics*, vol. 18, no. 7, pp. 1041–1052, 2012.

[188] A. Nguyen and A. Kunz, "Discrete Scene Rotation During Blinks and Its Effect on Redirected

Walking Algorithms," *Proceedings of the ACM Symposium on Virtual Reality Software and Technology, VRST*, 2018.

[189] A. Nguyen, F. Cervellati, and A. Kunz, "Gain Compensation in Redirected Walking," 2017.

[190] A. Nguyen, Y. Rothacher, P. Brugger, B. Lenggenhager, and A. Kunz, "Spontaneous Alternation Behavior in Humans," *Proceedings of the 23rd ACM Symposium on Virtual Reality Software and Technology*, 2017.

[191] A. Nguyen, Y. Rothacher, A. Kunz, P. Brugger, and B. Lenggenhager, "Effect of Environment Size on Curvature Redirected Walking Thresholds," *25th IEEE Conference on Virtual Reality and 3D User Interfaces, VR 2018 - Proceedings*, pp. 645–646, 2018.

[192] A. Nguyen, Y. Rothacher, B. Lenggenhager, P. Brugger, and A. Kunz, "Individual Differences and Impact of Gender on Curvature Redirection Thresholds," *Proceedings - SAP 2018: ACM Symposium on Applied Perception*, 2018.

[193] N. C. Nilsson, E. Suma, R. Nordahl, M. Bolas, and S. Serafin, "Estimation of Detection Thresholds for Audiovisual Rotation Gains," *Proceedings - IEEE Virtual Reality*, vol. 2016-July, pp. 241–242, 2016.

[194] S. Y. Oh, J. Bailenson, E. Weisz, and J. Zaki, "Virtually Old: Embodied Perspective Taking and the Reduction of Ageism Under Threat," *Computers in Human Behavior*, vol. 60, pp. 398–410, 2016.

[195] S. Palmisano, R. S. Allison, M. M. Schira, and R. J. Barry, "Future Challenges for Vection Research: Definitions, Functional Significance, Measures, and Neural Bases," *Frontiers in Psychology*, vol. 6, no. FEB, pp. 1–15, 2015.

[196] A. Paludan, J. Elbaek, M. Mortensen, M. Zobbe, N. C. Nilsson, R. Nordahl, L. Reng, and S. Serafin, "Disguising Rotational Gain for Redirected Walking in Virtual Reality: Effect of Visual Density," *Proceedings - IEEE Virtual Reality*, vol. 2016-July, pp. 259–260, 2016.

[197] Y. Pan and A. Steed, "Avatar Type Affects Performance of Cognitive Tasks in Virtual Reality," in *Virtual Reality Software and Technology Symposium*, 2019.

[198] J. L. Pate and G. L. Belle, "Alternation Behavior of Children in a Cross-Maze," *Psychonomic Science*, vol. 23, no. 6, pp. 431–432, 1971.

[199] T. C. Peck, H. Fuchs, and M. C. Whitton, "Improved Redirection With Distractors: A Large-Scale-Real-Walking Locomotion Interface and Its Effect on Navigation in Virtual Environments," *Proceedings - IEEE Virtual Reality*, pp. 35–38, 2010.

[200] T. C. Peck, H. Fuchs, and M. C. Whitton, "An Evaluation of Navigational Ability Comparing Redirected Free Exploration With Distractors to Walking-in-Place and Joystick Locomotion Interfaces," *Proceedings - IEEE Virtual Reality*, pp. 55–62, 2011.

[201] V. I. Petkova and H. H. Ehrsson, "If I were you: Perceptual illusion of body swapping," *PLoS ONE*, vol. 3, no. 12, 2008.

[202] P. Plummer-D'Amato, B. Brancato, M. Dantowitz, S. Birken, C. Bonke, and E. Furey, "Effects of Gait and Cognitive Task Difficulty on Cognitive-Motor Interference in Aging," *Journal of Aging Research*, vol. 2012, 2012.

[203] R. B. Post, "Circular Vection Is Independent of Stimulus Eccentricity," *Perception*, vol. 17, no. 6, pp. 737–744, 1988.

[204] F. M. Rabinowitzt, D. B. Kronfield, and J. C. Campione, "Stimulus Alternation and Continuous Short-Term Memory in Young Children," *Psychonomic Science*, vol. 22, no. 2, pp. 99–100, 1971.

[205] S. Razzaque, "Redirected Walking," Ph.D. dissertation, 2005.

[206] S. Razzaque, Z. Kohn, and M. C. Whitton, "Redirected Walking," *Proceedings of EUROGRAPHICS*, pp. 289–294, 2001.

[207] J. K. O. Regan, J. J. Clark, and R. A. Rensink, "Picture Changes During Blinks : Looking Without Seeing and Seeing Without Looking," vol. 7, pp. 191–211, 2000.

[208] C. L. Richman, W. N. Dember, and P. Kim, "Spontaneous Alternation Behavior in Animals: A Review," *Current Psychological Research & Reviews*, vol. 5, no. 4, pp. 358–391, 1986.

[209] B. E. Riecke, "Cognitive and Higher-Level Contributions to Illusory Self-Motion Perception ("Vection") : Does the Possibility of Actual Motion Affect Vection?" *The Japanese Journal of Psychonomic Science*, vol. 28, no. 1, pp. 135–139, 2009.

[210] B. E. Riecke and J. D. Jordan, "Comparing the Effectiveness of Different Displays in Enhancing Illusions of Self-Movement (Vection)," *Frontiers in Psychology*, vol. 6, no. JUN, pp. 1–16, 2015.

[211] B. E. Riecke, J. Schulte-Pelkum, H. H. Bülthoff, and M. von der Heyde, "Cognitive Factors Can Influence Self-Motion Perception (Vection) in Virtual Reality," *ACM Transactions on Applied Perception*, vol. 3, no. 3, pp. 194–216, 2006.

[212] B. E. Riecke, J. J. LaViola, and E. Kruijff, "3D User Interfaces for Virtual Reality and Games: 3D Selection, Manipulation, and Spatial Navigation," in *Proceedings of ACM SIGGRAPH 2018 Courses*. ACM, 2018.

[213] M. Rietzler, J. Gugenheimer, T. Hirzle, M. Deubzer, E. Langbehn, and E. Rukzio, "Rethinking Redirected Walking: On the Use of Curvature Gains beyond Perceptual Limitations and Revisiting Bending Gains," *Proceedings of the 2018 IEEE International Symposium on Mixed and Augmented Reality, ISMAR 2018*, pp. 115–122, 2019.

[214] L. A. Riggs, J. P. Kelly, K. A. Manning, and R. K. Moore, "Blink-Related Eye Movements," *Investigative Ophthalmology & Visual Science*, pp. 334–342, 1987.

[215] L. Rochester, V. Hetherington, D. Jones, A. Nieuwboer, A. M. Willems, G. Kwakkel, and E. Van Wegen, "The Effect of External Rhythmic Cues (Auditory and Visual) on Walking During a Functional Task in Homes of People With Parkinson's Disease," *Archives of Physical Medicine and Rehabilitation*, vol. 86, no. 5, pp. 999–1006, 2005.

[216] Romberg Moritz Heinrich, *The Manual of the Nervous Diseases of Man*, 1853.

[217] Y. Rothacher, A. Nguyen, B. Lenggenhager, and A. Kunz, "Visual Capture of Gait During Redirected Walking," *Scientific Reports*, no. November, pp. 1–13, 2018.

[218] Y. Rothacher, A. Nguyen, B. Lenggenhager, A. Kunz, and P. Brugger, "Walking Through Virtual Mazes: Spontaneous Alternation Behaviour in Human Adults," *Cortex*, vol. 127, pp. 1–16, 2020.

[219] J. A. Roufs, "Dynamic Properties of Vision-VI. Stochastic Threshold Fluctuations and Their Effect on Flash-to-Flicker Sensitivity Ratio," *Vision Research*, vol. 14, no. 9, pp. 871–888, 1974.

[220] R. A. Ruddle, E. Volkova, and H. H. Bülthoff, "Walking Improves Your Cognitive Map in Environments That Are Large-Scale and Large in Extent," *ACM Transactions on Computer-Human Interaction*, vol. 18, no. 2, 2011.

[221] P. Salamin, T. Tadi, O. Blanke, F. Vexo, and D. Thalmann, "Quantifying effects of exposure to the third and first-person perspectives in virtual-reality-based training," *IEEE Transactions on Learning Technologies*, vol. 3, no. 3, pp. 272–276, 2010.

[222] M. Santon, T. A. Münch, and N. K. Michiels, "The Contrast Sensitivity Function of a Small Cryptobenthic Marine Fish," *Journal of Vision*, vol. 19, no. 2, 2019.

[223] A. A. Schaeffer, "Spiral Movement in Man," *Journal of Morphology*, vol. 45, no. 1, pp. 293–398, 1928.

[224] S. Schaller, "Velocity Gains for Real Walking in Virtual Environments," Semester's Thesis, ETH Zurich, 2016.

[225] D. P. Schultz, *Psychological Bulletin*, no. 6.

[226] M. Schwaiger, T. Thümmel, and H. Ulbrich, "Cyberwalk: An Advanced Prototype of a Belt Array Platform," *HAVE 2007 - The 6th IEEE International Workshop on Haptic, Audio and Visual Environments and Games, Proceedings*, no. October, pp. 50–55, 2007.

[227] S. Serafin, N. C. Nilsson, E. Sikstrom, A. D. Goetzen, and R. Nordahl, "Estimation of Detection Thresholds for Acoustic Based Redirected Walking Techniques," 2013, pp. 161–162.

[228] C. Sforza, M. Rango, D. Galante, N. Bresolin, and V. F. Ferrario, "Spontaneous Blinking in Healthy Persons: An Optoelectronic Study of Eyelid Motion," *Ophthalmic and Physiological Optics*, vol. 28, no. 4, pp. 345–353, 2008.

[229] P. L. Sheridan, J. Solomont, N. Kowall, and J. M. Hausdorff, "Influence of Executive Function on Locomotor Function: Divided Attention Increases Gait Variability in Alzheimer's Disease," *Journal of the American Geriatrics Society*, pp. 1633–1637.

[230] M. Slater and M. Usoh, "Body Centred Interaction in Immersive Virtual Environments," *Artificial Life and Virtual Reality*, pp. 125–148.

[231] M. Slater, B. Spanlang, M. V. Sanchez-Vives, and O. Blanke, "First person experience of body transfer in virtual reality," *PLoS ONE*, vol. 5, no. 5, p. e10564, may 2010.

[232] R. L. Solomon, "The Influence of Work on Behavior," *Psychological Bulletin*, vol. 45, no. 1, pp. 1–40, 1948.

[233] J. L. Souman, I. Frissen, M. N. Sreenivasa, and M. O. Ernst, "Walking Straight into Circles," *Current Biology*, vol. 19, no. 18, pp. 1538–1542, 2009.

[234] E. A. Spieker, R. S. Astur, J. T. West, J. A. Griego, and L. M. Rowland, "Spatial memory deficits in a virtual reality eight-arm radial maze in schizophrenia," *Schizophrenia Research*, vol. 135, no. 1-3, pp. 84–89, 2012.

[235] S. Springer, N. Giladi, C. Peretz, G. Yogev, E. S. Simon, and J. M. Hausdorff, "Dual-tasking effects on gait variability: The role of aging, falls, and executive function," *Movement Disorders*, vol. 21, no. 7, pp. 950–957, 2006.

[236] F. Steinicke, G. Bruder, J. Jerald, H. Frenz, and M. Lappe, "Estimation of Detection Thresholds for Redirected Walking Thechniques." *IEEE Transactions on Visualization and Computer Graphics*, vol. 16, no. 1, pp. 17–27, 2010.

[237] F. Steinicke, G. Bruder, J. Jerald, H. Frenz, and M. Lappe, "Analyses of Human Sensitivity to Redirected Walking," in *Proceedings of the 15th Symposium on Virtual Reality Software and Tech-*

nology, 2008, pp. 149–156.

[238] F. Steinicke, G. Bruder, T. Ropinski, and K. Hinrichs, "Moving Towards Generally Applicable Redirected Walking," *Proceedings of the 10th Virtual Reality International Conference ({VRIC} 2008)*, pp. 15–24, 2008.

[239] F. Steinicke, G. Bruder, K. Hinrichs, and A. Steed, "Gradual Transitions and Their Effects on Presence and Distance Estimation," *Computers and Graphics (Pergamon)*, vol. 34, no. 1, pp. 26–33, 2010.

[240] E. A. Suma, S. Clark, D. Krum, S. Finkelstein, M. Bolas, and Z. Warte, "Leveraging Change Blindness for Redirection in Virtual Environments," in *2011 IEEE Virtual Reality Conference*, 2011, pp. 159–166.

[241] E. A. Suma, G. Bruder, F. Steinicke, D. M. Krum, and M. Bolas, "A Taxonomy for Deploying Redirection Techniques in Immersive Virtual Environments," *Proceedings - IEEE Virtual Reality*, pp. 43–46, 2012.

[242] Q. Sun, L.-Y. Wei, and A. Kaufman, "Mapping Virtual and Physical Reality," *ACM Transactions on Graphics*, vol. 35, no. 4, pp. 1–12, 2016.

[243] Q. Sun, A. Kaufman, A. Patney, L.-Y. Wei, O. Shapira, J. Lu, P. Asente, S. Zhu, M. Mcguire, and D. Luebke, "Towards Virtual Reality Infinite Walking: Dynamic Saccadic Redirection," *ACM Transactions on Graphics*, vol. 37, no. 4, pp. 1–13, 2018.

[244] W. S. Sun, R. S. Baker, J. C. Chuke, B. R. Rouholiman, S. A. Hasan, W. Gaza, M. W. Stava, and J. D. Porter, "Age-Related Changes in Human Blinks: Passive and Active Changes in Eyelid Kinematics," *Investigative Ophthalmology and Visual Science*, vol. 38, no. 1, pp. 92–99, 1997.

[245] H. Takasaki, J. Treleaven, V. Johnston, and G. Jull, "Minimum Repetitions for Stable Measures of Visual Dependency Using the Dot Version of the Computer-Based Rod-Frame Test," *Manual Therapy*, vol. 17, no. 5, pp. 466–469, 2012.

[246] M. J. Tarr and W. H. Warren, "Virtual Reality in Behavioral Neuroscience and Beyond," *Nature Neuroscience*, vol. 5, no. 11s, pp. 1089–1092, 2002.

[247] L. Tcheang, H. H. Bülthoff, and N. Burgess, "Visual Influence on Path Integration in Darkness Indicates a Multimodal Representation of Large-Scale Space," *Proceedings of the National Academy of Sciences of the United States of America*, vol. 108, no. 3, pp. 1152–1157, 2011.

[248] J. N. Templeman, P. S. Denbrook, and L. E. Sibert, "Virtual Locomotion: Walking in Place through Virtual Environments," vol. 8, no. 6, pp. 598–617, 1999.

[249] J. Thomas and E. S. Rosenberg, "A General Reactive Algorithm for Redirected Walking using Artificial Potential Functions," *Proc. IEEEE VR2019*, 2019.

[250] E. C. Tolman, "Purpose and Cognition: The Determiners of Animal Learning," *Psychological Review*, vol. 32, no. 4, pp. 285–297, 1925.

[251] J. N. Towse and D. Neil, "Analyzing Human Random Generation Behavior: A Review of Methods Used and a Computer Program for Describing Performance," *Behavior Research Methods, Instruments, and Computers*, vol. 30, no. 4, pp. 583–591, 1998.

[252] L. Tremblay, D. Elliott, and J. L. Starkes, "Gender differences in perception of self-orientation: Software or hardware?" *Perception*, vol. 33, no. 3, pp. 329–337, 2004.

[253] B. Treutwein, "Adaptive Psychophysical Procedures," *Vision Research*, vol. 35, no. 17, pp. 2503–2522, 1995.

[254] L. C. Trutoiu, S. D. Marin, B. J. Mohler, and C. Fennema, "Orthographic and Perspective Projection Influences Linear Vection in Large Screen Virtual Environments," *ACM International Conference Proceeding Series*, vol. 253, p. 145, 2007.

[255] L. C. Trutoiu, B. J. Mohler, J. Schulte-Pelkum, and H. H. Bülthoff, "Circular, Linear, and Curvilinear Vection in a Large-Screen Virtual Environment With Floor Projection," *Computers and Graphics (Pergamon)*, vol. 33, no. 1, pp. 47–58, 2009.

[256] M. Tsakiris, A. Tajadura-Jiménez, and M. Costantini, "Just a Heartbeat Away From One's Body:Interoceptive Sensitivity Predicts Malleability of Body-Representations," *Proceedings of the Royal Society B: Biological Sciences*, vol. 278, no. 1717, pp. 2470–2476, 2011.

[257] G. Tune, "Response Preferences: A Review of Some Relevant Literature," *Psychological Bulletin*, vol. 61, no. 4, pp. 286–302, 1964.

[258] A. Tutar and T. Peck, "Working Memory Load Performance Based on Collocation of Virtual and Physical Hands," in *IEEE Conference on Virtual Reality and 3D User Interfaces (VR)*, 2019.

[259] M. Usoh, K. Arthur, M. C. Whitton, R. Bastos, A. Steed, M. Slater, and F. P. Brooks, "Walking > Walking-in-Place > Flying, in Virtual Environments," *Proceedings of the 26th annual conference on Computer graphics and interactive techniques - SIGGRAPH '99*, pp. 359–364, 1999.

[260] F. VanderWerf, P. Brassinga, D. Reits, M. Aramideh, and B. Ongerboer de Visser, "Eyelid Movements: Behavioral Studies of Blinking in Humans Under Different Stimulus Conditions," *Journal of Neurophysiology*, vol. 89, no. 5, pp. 2784–2796, 2003.

[261] K. Vasylevska and H. Kaufmann, "Influence of Vertical Navigation Metaphors on Presence," *Challenging Presence - Proceedings of 15th International Conference on Presence (ISPR 2014)*, pp. 205–212, 2014.

[262] K. Vasylevska, H. Kaufmann, M. Bolas, and E. A. Suma, "Flexible Spaces: Dynamic Layout Generation for Infinite Walking in Virtual Environments," *IEEE Symposium on 3D User Interface 2013, 3DUI 2013 - Proceedings*, pp. 39–42, 2013.

[263] K. Vasylevska, I. Podkosova, and H. Kaufmann, "Walking in Virtual Reality : Flexible Spaces and Other Techniques," pp. 1–17, 2014.

[264] J. F. Veale, "Edinburgh Handedness Inventory - Short Form: A revised version based on confirmatory factor analysis," *Laterality*, vol. 19, no. 2, pp. 164–177, 2014.

[265] S. P. Vecera, M. K. Rothbart, and M. I. Posner, "Development of Spontaneous Alternation in Infancy," *Journal of Cognitive Neuroscience*, vol. 3, no. 4, pp. 351–354, 1991.

[266] G. Venture, J.-P. Laumond, and B. Watier, *Biomechanics of Anthropomorphic Systems*, 2019, vol. 124.

[267] L. Wachowski and L. Wachowski, *The Matrix*, 1999.

[268] A. B. Watson and D. G. Pelli, "Quest: A Bayesian Adaptive Psychometric Method," *Perception & Psychophysics*, vol. 33, no. 2, pp. 113–120, 1983.

[269] M. Wei, J. Luo, H. Luo, and R. Song, "The Effect of Gender on Vection Perception and Postural Responses Induced by Immersive Virtual Rotation Drum," *International IEEE/EMBS Conference*

on Neural Engineering, NER, pp. 473–476, 2017.

[270] J. D. Wendt, M. C. Whitton, and F. P. Brooks, "GUD WIP: Gait-Understanding-Driven Walking-in-Place," *Proceedings - IEEE Virtual Reality*, no. m, pp. 51–58, 2010.

[271] J. D. Wendt, M. C. Whitton, D. Adalsteinsson, and F. P. Brooks, "Reliable Forward Walking Parameters From Head-Track Data Alone," *Proceedings - IEEE Virtual Reality*, pp. 81–82, 2012.

[272] S. Wiens and S. N. Palmer, "Quadratic Trend Analysis and Heartbeat Detection," *Biological Psychology*, vol. 58, no. 2, pp. 159–175, 2001.

[273] B. Williams, G. Narasimham, T. P. McNamara, T. H. Carr, J. J. Rieser, and B. Bodenheimer, "Updating Orientation in Large Virtual Environments Using Scaled Translational Gain," *Proceedings of the 3rd Symposium on Applied Perception in Graphics and Visualization*, p. 21–28, 2006.

[274] B. Williams, G. Narasimham, B. Rump, T. P. McNamara, T. H. Carr, J. Rieser, and B. Bodenheimer, "Exploring Large Virtual Environments With an HMD When Physical Space Is Limited," *Proceedings of the 4th symposium on Applied perception in graphics and visualization - APGV '07*, vol. 1, no. 212, p. 41, 2007.

[275] N. Williams and T. C. Peck, "Estimation of Rotation Gain Thresholds for Redirected Walking Considering FOV and Gender," vol. 25, no. 11, pp. 1229–1230, 2019.

[276] B. Williams-Sanders, T. Carr, G. Narasimham, T. McNamara, J. Rieser, and B. Bodenheimer, "Scaling gain and eyeheight while locomoting in a large ve 123," *International Conference on Human-Computer Interaction*, pp. 277–298, 2019.

[277] P. T. Wilson, W. Kalescky, and A. Maclaughlin, "VR locomotion : Walking > Walking in Place > Arm Swinging," in *Proceedings of the 15th ACM SIGGRAPH Conference on Virtual-Reality Continuum and Its Applications in Industry*, no. December 2016.   ACM, 2016.

[278] H. A. Witkin and S. E. Asch, "Studies in Space Orientation. IV. Further Experiments on Perception of the Upright With Displaced Visual Fields," *Journal of Experimental Psychology*, vol. 38, no. 6, pp. 762–782, 1948.

[279] I. B. Witten and E. I. Knudsen, "Why Seeing Is Believing: Merging Auditory and Visual Worlds," *Neuron*, vol. 48, no. 3, pp. 489–496, 2005.

[280] T. Yamamoto, J. Shimatani, I. Ohashi, K. Matsumoto, T. Narumi, T. Tanikawa, and M. Hirose, "Mobius Walker: Pitch and Roll Redirected Walking," no. December, pp. 1–2, 2017.

[281] Y. R. Yang, Y. C. Chen, C. S. Lee, S. J. Cheng, and R. Y. Wang, "Dual-Task-Related Gait Changes in Individuals With Stroke," *Gait and Posture*, vol. 25, no. 2, pp. 185–190, 2007.

[282] Y. Yeshurun, M. Carrasco, and L. T. Maloney, "Bias and Sensitivity in Two-Interval Forced Choice Procedures: Tests of the Difference Model," *Vision Research*, vol. 48, no. 17, pp. 1837–1851, 2008.

[283] G. Yogev, N. Giladi, C. Peretz, S. Springer, E. S. Simon, and J. M. Hausdorff, "Dual Tasking, Gait Rhythmicity, and Parkinson's Disease: Which Aspects of Gait Are Attention Demanding?" *European Journal of Neuroscience*, vol. 22, no. 5, pp. 1248–1256, 2005.

[284] G. Yogev-Seligmann, J. M. Hausdorff, and N. Giladi, "The Role of Executive Function and Attention in Gait," *Movement Disorders*, vol. 23, no. 3, pp. 329–342, 2008.

[285] M. Zank and A. Kunz, "Eye Tracking for Locomotion Prediction in Redirected Walking," in *IEEE*

Symposium on 3D User Interfaces, 2016, pp. 49–58.

[286] M. Zank and A. Kunz, "Using Locomotion Models for Estimating Walking Targets in Immersive Virtual Environments," *Proceedings - 2015 International Conference on Cyberworlds, CW 2015*, pp. 229–236, 2016.

[287] M. Zank and A. Kunz, "Where Are You Going? Using Human Locomotion Models for Target Estimation," *Visual Computer*, vol. 32, no. 10, pp. 1323–1335, 2016.

[288] M. Zank and A. Kunz, "Optimized Graph Extraction and Locomotion Prediction for Redirected Walking," in *IEEE Symposium on 3D User Interfaces*, no. 1, 2017, pp. 120–129.

[289] R. Zeleznik, J. LaViola, D. Acevedo Feliz, and D. Keefe, "Pop Through Button Devices for VE Navigation and Interaction," *Proceedings IEEE Virtual Reality*, pp. 127–134.

[290] R. Zhang and S. a. Kuhl, "Human Sensitivity to Dynamic Translational Gains in Head-Mounted Displays," *Proceedings of the ACM Symposium on Applied Perception - SAP '13*, p. 71, 2013.

[291] M. A. Zmuda, J. L. Wonser, E. R. Bachmann, and E. Hodgson, "Optimizing Constrained-Environment Redirected Walking Instructions Using Search Techniques," *IEEE Transactions on Visualization and Computer Graphics*, vol. 19, no. 11, pp. 1872–1884, 2013.

A

Appendix

A Appendix

A.1 The Lateral Preference Inventory [1]

Simply read each of the questions below. Decide which hand, foot, etc. you use for each activity and then put a check mark next to the answer that describes you the best. If you are unsure of any answer, try to act out the action.

1. With which hand do you draw? __ Left __ Right __ Either
2. Which hand would you use to throw a ball to hit a target? __ Left __ Right __ Either
3. In which hand would you use an eraser on paper? __ Left __ Right __ Either
4. Which hand removes the top card when you are dealing from a deck? __ Left __ Right __ Either
5. With which foot would you kick a ball to hit a target? __ Left __ Right __ Either
6. If you wanted to pick up a pebble with your toes, which foot would you use? __ Left __ Right __ Either
7. Which foot would you use to step on a bug? __ Left __ Right __ Either
8. If you had to step up onto a chair, which foot would you place on the chair first? __ Left __ Right __ Either
9. Which eye would you use to look through a telescope? __ Left __ Right __ Either
10. If you had to look into a dark bottle to see how full it was, which eye would you use? __ Left __ Right __ Either
11. Which eye would you use to peep through a keyhole? __ Left __ Right __ Either
12. Which eye would you use to sight down a rifle? __ Left __ Right __ Either
13. If you wanted to listen in on a conversation going on behind a closed door, which ear would you place against the door? __ Left __ Right __ Either
14. Into which ear would you place the earphone of a transistor radio? __ Left __ Right __ Either
15. If you wanted to hear someone's heartbeat which ear would you place against their chest? __ Left __ Right __ Either
16. Imagine a small box resting on a table. This box contains a small clock. Which ear would you press against the box to find out if the clock was ticking? __ Left __ Right __ Either

Scoring Instructions:

Items 1–4 are handedness, 5–8 are footedness, 9–12 are eyedness, and 13–16 are earedness. For each 4-item subscale, compute (R–L), where R is the number of "right" responses and L is the number of "left" responses.

143

A.2 Somatosensory Amplification Questionnaire [2]

Please answer to the following questions on the ordinal scale from 1-5.

Somatosensory Amplification

No.	Questions	Strongly Disagree 1	2	3	4	Strongly Agree 5
1	When someone else coughs, it makes me cough too.	☐	☐	☐	☐	☐
2	I can't stand smoke, smog, or pollutants in the air.	☐	☐	☐	☐	☐
3	I am often aware of various things happening within my body.	☐	☐	☐	☐	☐
4	When I bruise myself, it stays noticeable for a long time.	☐	☐	☐	☐	☐
5	Sudden loud noises really bother me.	☐	☐	☐	☐	☐
6	I can sometimes hear my pulse or my heartbeat throbbing in my ear.	☐	☐	☐	☐	☐
7	I hate to be too hot or too cold.	☐	☐	☐	☐	☐
8	I am quick to sense the hunger contractions in my stomach.	☐	☐	☐	☐	☐
9	Even something minor, like an insect bite or a splinter, really bothers me.	☐	☐	☐	☐	☐
10	I have a low tolerance for pain.	☐	☐	☐	☐	☐

---

[2]Reproduced with permission [14] ©Elsevier

A.3 Edinburgh Handedness Inventory - Short Form[3]

Please indicate your preferences in the use of hands in the following activities or objects:

	Always right	Usually right	Both equally	Usually left	Always left
Writing					
Throwing					
Toothbrush					
Spoon					

Scoring:

For each item: Always right = 100; Usually right = 50; Both equally = 0; Usually left = -50; Always
left = -100

To calculate the Laterality Quotient add the scores for the four items in the scale and divide this by four:

Writing score	
Throwing score	
Toothbrush score	
Spoon score	
Total	
Total ÷ 4 (Laterality Quotient)	

Classification:	Laterality Quotient score:
Left handers	-100 to -61
Mixed handers	-60 to 60
Right handers	61 to 100

---

[3][264] ©Taylor & Francis

A.4 Randomization Scheme of SAB trials [4]

In total there are six trials for each participant to complete: one walk in Experiment 4, two walks in Experiment 2 and three walks in Experiment 3. The main constraint to the randomization of the order of trials is that there are never two trials of the same experiment directly after each other. To this end the six trials have been divided into two groups, group 1 containing the three trials of Experiment 3 and group 2 containing the two trials of Experiment 2 and the one trial of Experiment 4. On this group level, half of the participants follows the order "1,2,1,2,1,2", while the other half follows the order "2,1,2,1,2,1" for the completion of the six trials. For the order "1,2,1,2,1,2", the three trials of each group can be permutated into six different sequences, which leads to 6 x 6 = 36 possible sequences in total (e.g. exp3a, exp2b, exp3c, exp1, exp3b, exp2a). This is doubled when adding the 36 possibilities of the order "2,1,2,1,2,1", leading to an absolute total of 72 possible trial sequences. We chose the number of subjects to be 288, since this value lies above the required sample sizes based on the power analyses and is dividable by 72, allowing each of the 72 possible trial sequences to appear equally often.

In a second step the order of left and right forced turns was randomized over participants. In Experiment 4 there are two possible configurations for the forced turn since there is only one trial ("L", "R"). In Experiment 2 there are four different configurations of forced turns possible since there are two trials ("L,L" , "L,R" , "R,L" , "R,R"). And in Experiment 3 there are eight different configurations possible due to the three trials. Since 288 is dividable by 8 (and therefore also by 4 and 2), the different forced turn configurations appear equally often for each experiment. Starting with the first participant, the forced turn configurations for each experiment were assigned randomly using sampling without replacement from all possible configurations and starting again once all configurations were used up (after two participants for Experiment 2, four participants for Experiment 3 and eight participants for Experiment 4).

A.5 Conversion of Bending Gains to Curvature Gains

The bending gain, proposed by Langbehn et al., claimed to be a new redirection technique in which the users walk on a different curvature radius in real life compared to virtual reality [147] (Figures A.1a and A.2a). Let r_v and r_r be the curvature radii of the real and virtual paths, respectively, the bending gain is quantified as:

$$g_B = \frac{r_v}{r_r} \tag{A.1}$$

Meanwhile, curvature gain is quantified as:

$$g_C = \frac{1}{r_r} \tag{A.2}$$

One way to interpret curvature gain is that: while users walk the same path length in reality and in VR, for each 1m the users walk, the difference between the real and virtual headings is $\frac{1}{r_r}$ radian, which is also the value of the curvature gain. When interpreted in this sense, for each 1m of path length under a particular bending gain g_B, an equivalent curvature gain $\tilde{g}_C$ can be calculated as:

$$\tilde{g}_C = \frac{1}{r_r} - \frac{1}{r_v} \tag{A.3}$$

Replacing r_v as $g_B r_r$ from Equation A.5, we obtain:

$$\tilde{g}_C = \frac{g_B - 1}{g_B r_r} \tag{A.4}$$

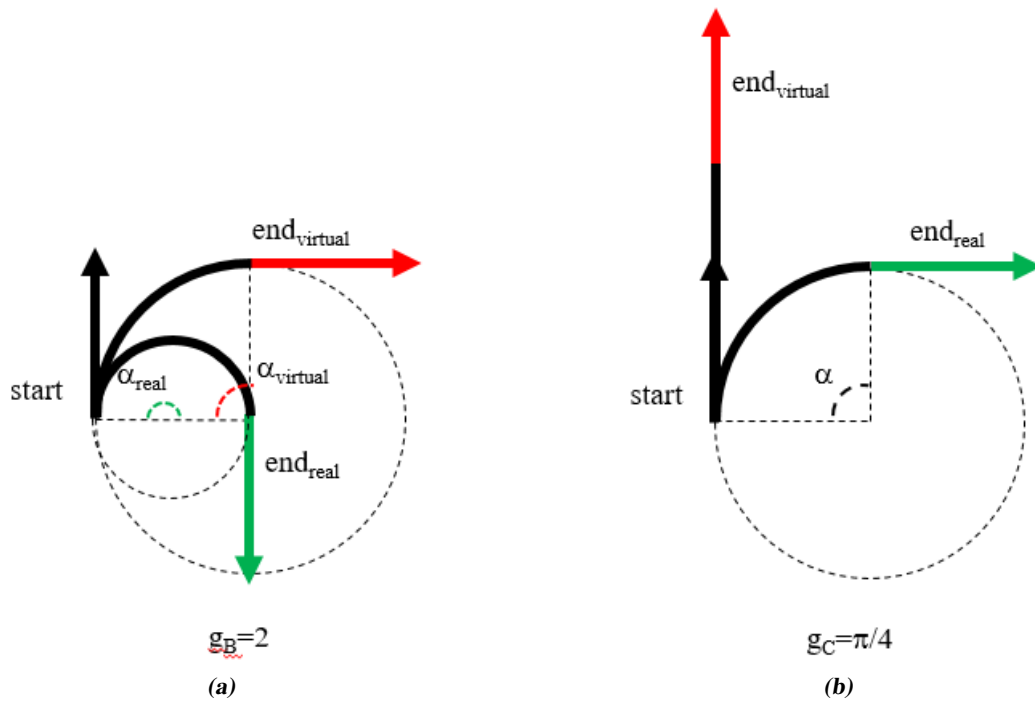[4]Supplementary material from Rothacher et al. [218] ©ScienceDirect

Figure A.1: *Bending gain $g_B = 2$ with real radius $r_r = \frac{\pi}{8}$ and the equivalent curvature gain*

From Equation A.5, it can be seen that for a particular value of bending gain g_B, different value of equivalent curvature gain can be obtained depending on the predefined real walking radius. In other words, one bending gain value does not map to one fixed heading difference, and will be perceived differently depending on the the predefined real walking radius. Figures A.1 and A.2 illustrate how the same bending gain could lead to perceptually different manipulation.

end$_{\text{virtual}}$

end$_{\text{real}}$

start

α_{real}

α_{virtual}

$g_B{=}2$

(a)

end$_{\text{virtual}}$

end$_{\text{real}}$
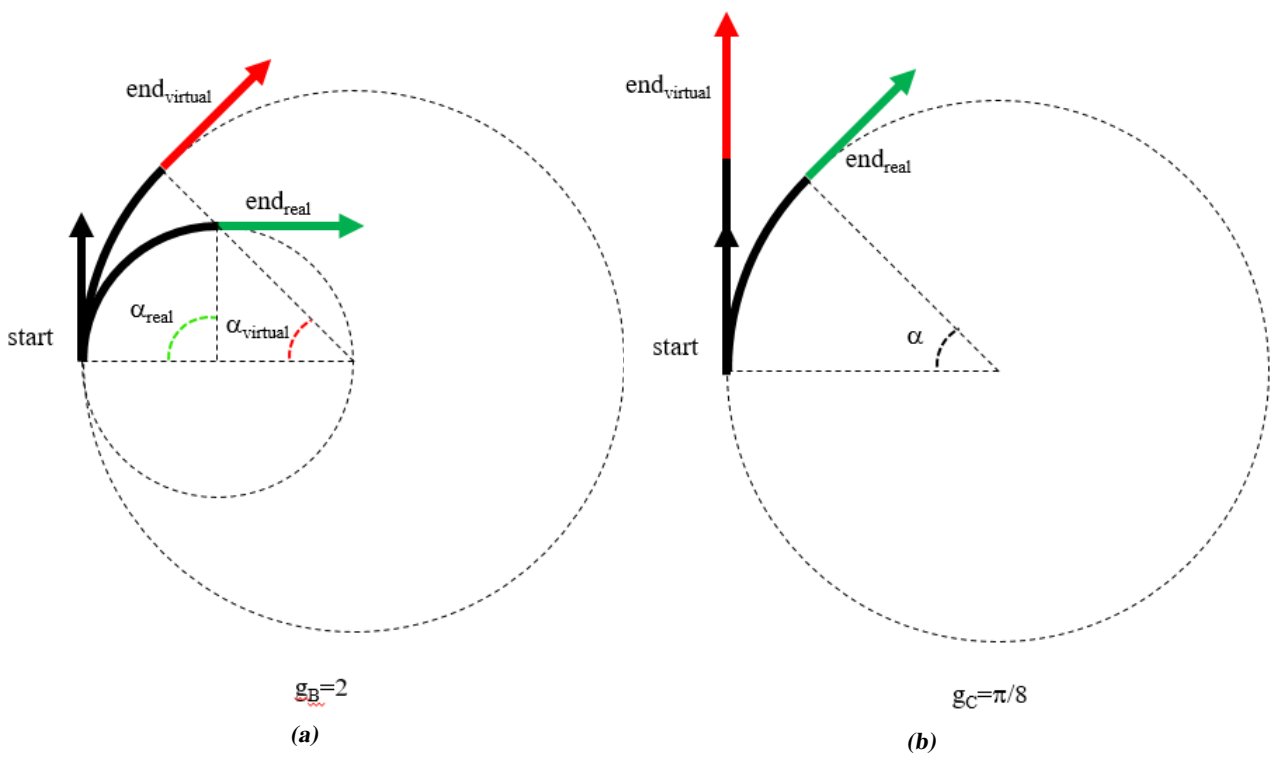
start

α

$g_C{=}\pi/8$

(b)

Figure A.2: *Bending gain $g_B = 2$ with real radius $r_r = \frac{\pi}{4}$ and the equivalent curvature gain*

List of Publications

- A. Nguyen, P. Wüest and A. Kunz,"Human Following Behavior In Virtual Reality", in *ACM Symposium on Virtual Reality Software and Technology 2020*, VRST2020

- A. Nguyen, Y. Rothacher, B. Lenggenhager, P. Brugger, E. Efthymiou, L. Imbach, A. Kunz, "Effect of Cognitive Load on Curvature Redirected Walking Thresholds", in *ACM Symposium on Virtual Reality Software and Technology, 2020*, VRST2020

- A. Nguyen, Y. Rothacher, B. Lenggenhager, P. Brugger, A. Kunz, "Effect of Sense of Embodiment on Curvature Redirected Walking Thresholds", in *ACM Symposium on Applied Perception 2020*, SAP2020

- A. Nguyen, A. Kunz, "Discrete Scene Rotation During Blinks and Its Effect on Redirected Walking Algorithms", in *ACM Symposium on Virtual Reality Software and Technology, 2018*, VRST2018

- A. Nguyen, Y. Rothacher, B. Lenggenhager, P. Brugger, A. Kunz, "Individual differences and impact of gender on curvature redirection thresholds", in *ACM Symposium on Applied Perception, 2018*, SAP2018

- A. Nguyen, M. Inhelder, A. Kunz, "Discrete Rotation during Eye-Blink", in *International Conference on Augmented Reality, Virtual Reality and Computer Graphics, 2018*

- Y. Rothacher, A. Nguyen, B. Lenggenhager, A. Kunz, P. Brugger, "Visual Capture of Gait in Redirected Walking", in *Measuring Behavior, 2018*

- A. Nguyen, Y. Rothacher, A. Kunz, P. Brugger, B. Lenggenhager, "Effect of Environment Size on Curvature Redirected Walking Thresholds", in *IEEE Conference on Virtual Reality and 3D User Interfaces, 2018*, IEEE2018

- A. Nguyen, A. Kunz, Y. Rothacher, P. Brugger, B. Lenggenhager, "Spontaneous Alternation Behavior in Humans", in *ACM Symposium on Virtual Reality Software and Technology, 2017*, VRST2017

- A. Nguyen, F. Cervellati, A. Kunz, "Gain Compensation in Redirected Walking", in *ACM Symposium on Virtual Reality Software and Technology, 2017*, VRST2017

- A. Nguyen, Y. Rothacher, P. Brugger, B. Lenggenhager, A. Kunz, "Estimation of individual redi-

rected walking thresholds using standard perception tests", in *ACM Symposium on Virtual Reality Software and Technology 2016*, VRST2016

- Y. Rothacher, A. Nguyen, B. Lenggenhager, A. Kunz, P. Brugger, "Walking through virtual mazes: Spontaneous alternation behaviour in human adults", Cortex, 2020

- Y. Rothacher, A. Nguyen, B. Lenggenhager, A. Kunz, P. Brugger, "Visual capture of gait during redirected walking", Springer Nature Scientific Reports, 2018

Bülachstrasse 2
8057 Zurich
✆ +41 76 588 11 86
✉ nngoc@ethz.ch

Anh Nguyen

Education

2011–2013 **MSc in Robotics - University of Genova, Italy**, *Average 97.03/100.*
Focus Automation, Robotics, Controller Design.

2004–2008 **BSc in Mechatronics - Nanyang Technological University, Singapore**, *First Class Honours, Top 5%.*

Experience

2019–now **Research Associate**, *Hochschule Luzern.*

2014–now **PhD Candidate**, *ETH Zurich.*
- Researching human perception and behavior in Virtual Reality (VR).
- Implementing VR applications using state-of-the-art VR hardware (HTC Vive, Oculus Rift).
- Writing scientific papers and proposals. Presented at various VR conferences.
- Supervised 3 Bachelor theses, 1 Semester thesis and 1 Master thesis on various VR-related topics.
- Supervised lecture projects for 4 years. Conducted practical courses for groups of up to 8 students.
- Key skills acquired: game development (Unity), modeling (Blender), scientific writing and presentation, supervision skills involving communication, motivation and goal-oriented management.

2010-2011 **Project Officer**, *Advanced Technology Center, Rolls-Royce, Singapore.*
- Performed survey of current finishing technologies for aerospace components. Planned and performed experiments of vibratory finishing for marine impellers and aerospace turbine blades.
- Coordinated meetings and discussions with suppliers and customers.
- Key skills acquired: knowledge of finishing and measurement technologies, cross-team collaboration, customer management and requirement analysis.

2008-2010 **Research Engineer**, *Singapore Institute of Manufacturing Technologies, Singapore.*
- Programmed ABB IRB140 robot for in situ chamfer profile measuring and large blade scanning.
- Perfomed benchmarking survey of current technologies for visual inspection of surface defects on aerospace components.
- Created a method of intuitively teaching robot online using Augmented Reality.
- Programmed humanoid upperbody motion, mobile platform and communication between the two subsystems.
- Key skills acquired: LabVIEW CVI, MATLAB, C#, SolidWorks, VB.NET.

2007 **Intern**, *Sony Precision Engineering Center, Singapore.*
- Designed mechanical parts for precision automatic equipments.
- Key skills acquired: SolidWorks.

Publications

2018 **Virtual Capture of Gaits during Redirected Walking**, *Scientific Reports.*
Yannick Rothacher, Anh Nguyen, Bigna Lenggenhager, Andreas Kunz, Peter Brugger

2018 **Discrete Scene Rotation During Blinks and Its Effect on Redirected Walking Algorithms**, *VRST 2018, Tokyo, Japan.*
Anh Nguyen, Andreas Kunz

2018	**Individual Differences and Impact of Gender on Curvature Redirection Thresholds**, *SAP 2018, Vancouver, Canada*.
	Anh Nguyen, Yannick Rothacher, Peter Brugger, Bigna Lenggenhager, Andreas Kunz

2018 **Effect of Environment Size on Curvature Redirected Walking Thresholds**, *IEEEVR 2018, Reutlingen, Germany*.
Anh Nguyen, Yannick Rothacher, Peter Brugger, Bigna Lenggenhager, Andreas Kunz

2017 **Gain Compensation in Redirected Walking**, *VRST 2017, Gothenburg, Sweden*.
Anh Nguyen, Federico Cervellati, Andreas Kunz

2017 **Spontaneous Alternation Behavior in Humans**, *VRST 2017, Gothenburg,Sweden*.
Anh Nguyen, Yannick Rothacher, Peter Brugger, Bigna Lenggenhager, Andreas Kunz

2016 **Prediction of redirected walking thresholds using standard physical test tools**, *VRST 2016, Munich, Germany*.
Anh Nguyen, Yannick Rothacher, Peter Brugger, Bigna Lenggenhager, Andreas Kunz

Theses

2013 **Controller design for maximized mode observability of switching linear systems**, *Univertity of Genova, Italy*, Master Thesis.
Proposed controller design procedure and simulation of mode identification.

2008 **Using humanoid robot for lion dance performance**, *Nanyang Technological University, Singapore*, Bachelor Thesis.
Programmed humanoid robot and mobile platform.

Awards

2011-2013	Erasmus Mundus Scholarship
2004-2008	ASEAN Scholarship
2001-2004	Best Student Scholarship from Highschool for the Gifted

Other Projects

2012	Designed and implemented basic object localization (MATLAB)
2012	Designed PID controller for a mobile robot for a wall follower application (ROS)
2012	Designed and implemented an algorithm for fall detection using neural networks (MATLAB)
2011	Designed and implemented recognition algorithm for hand-written characters using Naive Bayes Classifier (C++)

Additional Information

Programming Languages	C#, C++, Python
Courses	Model Predictive Control, Recursive Estimation, System Identification, Data Structures and Algorithms
Languages	English, Vietnamese, German (B1-B2)
Interests	circus acrobatics (aerial silks), tango, hiking, skiing, cooking